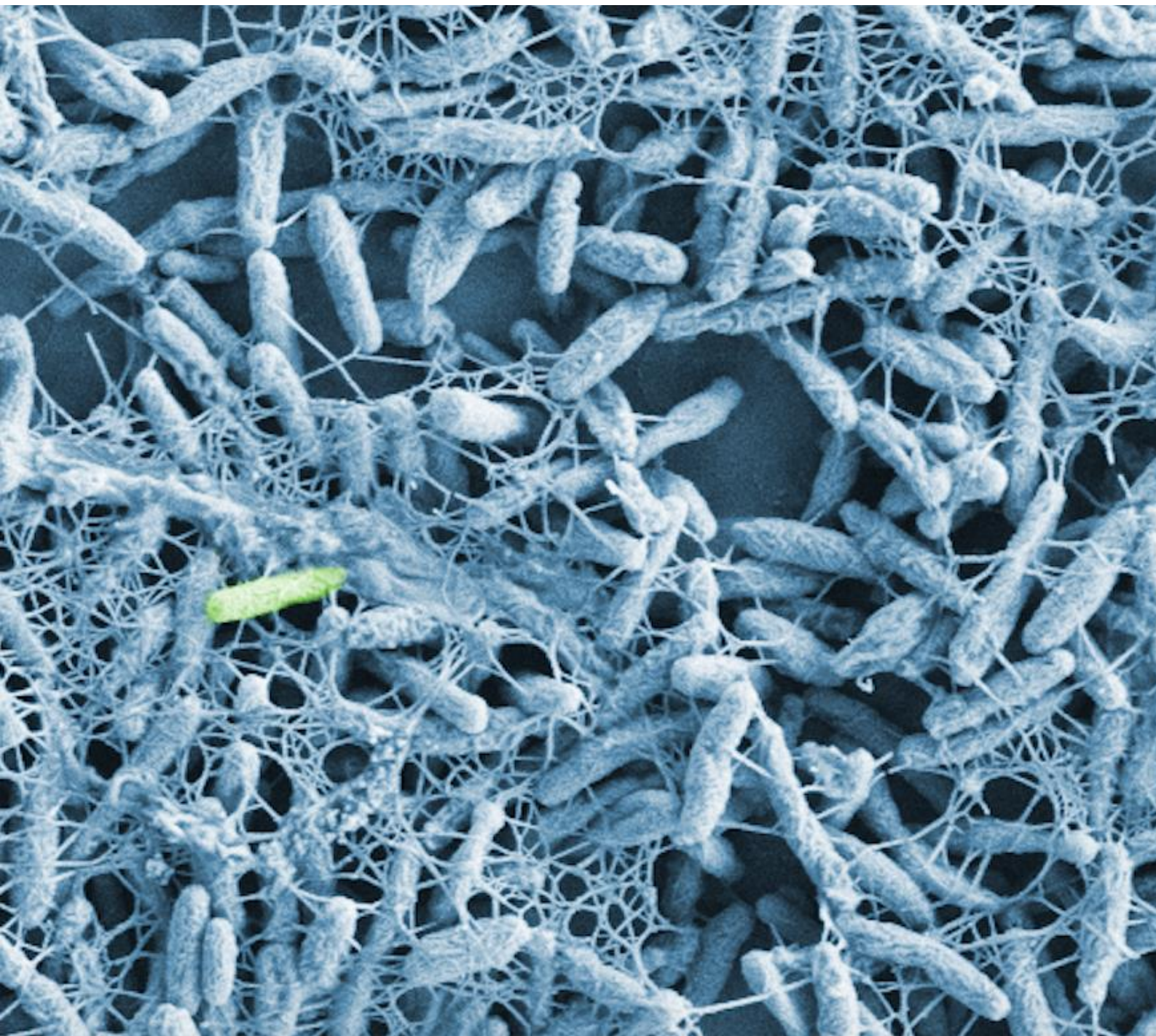


Predicting and managing biofilm growth on flexible polymeric materials in contact with drinking water



Lisa Neu

DISS. ETH NO. 26722

DISS. ETH NO. 26722

**Predicting and managing biofilm growth on flexible polymeric
materials in contact with drinking water**

A thesis submitted to attain the degree of
DOCTOR OF SCIENCES of ETH ZURICH
(Dr. sc. ETH Zurich)

presented by
LISA NEU

MSc Marine Biology, University Rostock
born on 19.02.1989
citizen of Germany

Accepted on the recommendation of
Prof. Dr. Martin Ackermann, examiner
Dr. Frederik Hammes, co-examiner
Dr. Catherine Paul, co-examiner

2020

In every job that must be done

There is an element of fun

You find the fun and ... snap!

The job's a game.

- *Mary Poppins.*

Contents

Summary		3
Zusammenfassung		5
Chapter 1	General introduction	8
Chapter 2	Feeding the building plumbing microbiome: Importance of synthetic polymeric materials for biofilm formation and management	16
Chapter 3	Ugly ducklings – The dark side of plastic materials in contact with potable water	46
Chapter 4	Small-scale heterogeneity in drinking water biofilms	105
Chapter 5	Towards a probiotic approach for building plumbing – Nutrient-based selection during initial biofilm formation on flexible polymeric materials	156
Chapter 6	General conclusions and Future outlook	206
Acknowledgements		223
Curriculum vitae		226

Summary

Building plumbing systems represent a large part of drinking water distribution and their construction and operation considerably influence the microbial ecology therein. Since the vast majority of bacteria reside in biofilms, the overarching goal of this thesis was to identify impacting factors for their growth and to evaluate their importance during initial biofilm formation.

The formation and development of biofilms are susceptible to changes in environmental conditions. Within building plumbing systems, these conditions can vary considerably, which inevitably renders microbial growth unpredictable. As a consequence, neither the water utilities, nor the customers have proper control over the microbial component of building plumbing systems. This is relevant as drinking water biofilms can comprise opportunistic pathogens, such as *Legionella pneumophila* or *Pseudomonas aeruginosa*. To minimize any (hygienic) risk, we need to control and manage biofilm formation, ensuring high quality, safe drinking water until the point of consumption. Flexible polymeric materials (e.g., hoses, sealing rings) were previously identified as components that impact the microbiology of building plumbing systems. Due to the migration of a considerable amount of bioavailable organic carbon from these materials, the growth potential of bacteria increases and biofilms can establish high cell concentrations. It is necessary to link microbiological observations like these with fundamental, ecological principles as this potentially allows for evidence-based management approaches for biofilm formation and growth on building plumbing materials.

This thesis' work comprises (1) observational studies showing that biofilm communities grown on flexible polymeric materials that consumers are exposed to in everyday life (i.e., bath toys) can be very diverse if exposed to different environmental and operational conditions (chapter 3) and (2) that

an individual biofilm shows heterogeneity on μm - to cm -scale, even if grown under supposedly homogeneous conditions (chapter 4). This latter finding is particularly relevant to consider when developing biofilm sampling strategies. Both these studies illustrated that biofilms comprise high bacterial numbers (the material provides nutrients), a very low species diversity (these nutrients select), and that biofilm communities depend on their initially dispersing drinking water communities. This ultimately led to considerations on the importance of initial biofilm formation, addressing both the relevance of initial water-to-surface dispersal (i.e., original bacterial composition of the drinking water) and nutrient-based selection during the early stages of growth (chapter 2, chapter 5). Based on this, a first attempt towards developing a *probiotic approach* for the management of drinking water biofilms on flexible polymeric materials was made (chapter 5). The approach builds on the predictions that the colonization of a new flexible polymeric material will be fast and so will bacterial growth, being supported by the migrating carbon. Bacterial communities, specifically designed for outcompeting others by (1) faster attachment/colonization (space occupation), (2) faster growth (niche occupation), or (3) displacement (elimination), might be selected by or adapted to specific migrating carbon compounds and ultimately be used to pre-colonize a new material prior to installation.

In this thesis, some fundamental aspects of growth on building plumbing materials were examined and the importance of initial biofilm formation processes elucidated, which may ultimately translate into material design and system operation. While several key questions were answered, this study also showed multiple challenges and research opportunities to be explored in future research.

Zusammenfassung

Gebäudeinstallationen machen einen grossen Teil der Trinkwasserverteilung aus und ihre Bauweise wie auch ihr Betrieb haben einen beachtlichen Einfluss auf die Mikrobiologie des Wassers. Die überwiegende Mehrheit der Trinkwasserbakterien befindet sich in Biofilmen auf den Materialoberflächen, welche in direktem Kontakt mit dem Wasser stehen. Aus diesem Grund fokussiert sich die Arbeit dieser Thesis auf die Identifizierung möglicher Einflussfaktoren auf das (anfängliche) Wachstum solcher Biofilme.

Umweltbedingungen verändern sich innerhalb von Gebäudeinstallationen dauerhaft, was einen direkten Einfluss auf die Bildung und Entwicklung von Biofilmen hat. Die hierdurch entstehende Komplexität macht mikrobielles Wachstum für uns unberechenbar, wodurch Wasserversorger wie auch Verbraucher keine ausreichende Kontrolle innerhalb von Gebäudeinstallationen haben. Dies ist von grosser Bedeutung, da Trinkwasserbiofilme opportunistische Krankheitserreger, wie z.B. *Legionella pneumophila* oder *Pseudomonas aeruginosa*, enthalten können. Um jedwedem (Gesundheits-) Risiko minimieren und qualitativ hochwertiges, sicheres Trinkwasser bis zur Verbrauchsstelle garantieren zu können, müssen wir in der Lage sein, Biofilmbildung zu kontrollieren und zu managen. Vorherige Studien haben aufgezeigt, dass flexible Kunststoffe (z.B. Schläuche, Dichtungsringe) die Mikrobiologie des Trinkwassers beeinflussen. Hohe Konzentrationen an biologisch verwertbaren organischen Kohlenstoffen migrieren aus den Materialien und erhöhen das mikrobielle Wachstumspotential des Trinkwassers. Als Folge entwickeln sich Biofilmgemeinschaften mit vergleichsweise hohen Zellkonzentrationen. Wenn es uns gelingt, solche Beobachtungen mit grundlegenden ökologischen Prinzipien zu verknüpfen, könnte dies zur Erarbeitung eines (Evidenz-basierten) Ansatzes beitragen, der das Management von Biofilmbildung und -wachstum auf Materialien in Gebäudeinstallationen erlaubt.

Diese Thesen umfasst Forschungsprojekte die aufzeigen, dass (1) Biofilm-Gemeinschaften, die auf alltäglichen flexiblen Kunststoffen (z.B. Badeenten) wachsen, sehr unterschiedlich zu einander sind, wenn sie unterschiedlichen Umwelt- und Nutzungs-Bedingungen ausgesetzt wurden (Kapitel 3); dass jedoch ein (2) individueller Biofilm Heterogenität auf μm - bis cm -Skala aufzeigt, selbst wenn Bedingungen vermeintlich homogen waren (Kapitel 4). Diese letzte Erkenntnis ist insbesondere bei der Ausarbeitung von Beprobungs-Strategien von Biofilmen relevant. Zudem zeigten beide Studien auf, dass Biofilme auf flexiblen Kunststoffen stets sehr hohe bakterielle Konzentrationen (das Material stellt Nahrung zur Verfügung) und eine sehr niedrige Artenvielfalt (diese Nahrung selektiert) aufweisen und dass Biofilm-Gemeinschaften von ihrer ursprünglichen Trinkwassergemeinschaft abhängig sind. Diese Erkenntnisse führten zu Überlegungen bezüglich der Wichtigkeit anfänglicher Prozesse der Biofilmbildung. Hierbei lag der Fokus insbesondere auf der Relevanz der ersten Besiedlung des Materials durch die Trinkwasserbakterien und auf dem (Nährstoff-basierten) selektiven Wachstum während der ersten Wachstumsphasen (Kapitel 2, Kapitel 5). Daraufhin folgend wurde ein erster Versuch unternommen, einen *probiotischen* Ansatz für das Management von Trinkwasserbiofilmen auf flexiblen Kunststoffen zu formulieren. Dieser Ansatz basiert auf der Vorhersage, dass die Kolonisierung eines neuen Materials schnell vonstattengehen wird und Bakterien durch den zusätzlich zur Verfügung stehenden migrierten Kohlenstoff schnell wachsen werden. Ein neues Material könnte vor dessen Installation mit einer Bakteriengemeinschaft vorbesiedelt werden, welche zuvor durch spezifischen, migrierten Kohlenstoff selektiert oder an diesen in ihrem Wachstum angepasst wurde. Darüber hinaus könnte diese Gemeinschaft so konstruiert werden, dass sie (1) schneller die Oberfläche besiedelt als potentiell konkurrierende Organismen (Raum-Besetzung), (2) schneller wächst als andere (Nischen-Besetzung) oder (3) andere Organismen schlichtweg eliminiert.

Im Zuge dieser Thesis wurden grundsätzliche Aspekte des Biofilmwachstums auf flexiblen Materialien in Gebäudeinstallationen untersucht und die Bedeutung der anfänglichen Schritte der Biofilmbildung eruiert. Dies kann hilfreich sein und Anwendung finden auf Gebieten des Material-Designs oder hinsichtlich des Betriebens solcher Installationen (z.B. Erstbefüllung). Trotz der Beantwortung einiger Schlüsselfragen zu diesem Thema hat diese Arbeit auch zahlreiche Herausforderungen, sowie potentielle Möglichkeiten für zukünftige Forschungsprojekte aufgezeigt.

Chapter 1

General introduction

Our world is becoming more and more complex every day. Because of this, we tend to lose sight for the small but important things. For example, we open our drinking water taps numerous times throughout the day, usually not reflecting at all what journey the water experienced while getting there. We simply enjoy our most precious food. And we can do so because our drinking water is properly treated, distributed, monitored, and microbial growth is controlled. However, behind property lines (i.e., within building plumbing systems) a lot changes as opposed to the main distribution network: various pipe diameters, materials, temperatures, and stagnation times, to name but a few (see chapter 2 for detailed information and literature). Consequently, a highly complex environment is created in which bacteria occupy various different niches, grow, and form biofilms. To be clear, this does not necessarily need to be problematic. However, the complexity emerging from these environmental conditions makes it hard for us (researchers, engineers, operators) to understand and explain microbiological observations within these systems: we create microbiological black boxes. And this, in fact, is problematic because without understanding we cannot manage nor control biofilm formation within building plumbing systems. In uncontrolled scenarios, opportunistic pathogens such as *Legionella pneumophila* or *Mycobacterium avium* were shown to flourish in drinking water biofilms¹, potentially putting the end-user at (health) risk. Consequently, it is important to understand processes that underlie biofilm formation on building plumbing materials, to allow for correct interpretations of microbiological observations and potentially for proactive management strategies on their growth. Based on the complexity of building plumbing systems, the following questions arise:

- How similar are individual biofilm samples despite growing under different environmental conditions?
- Assuming a considerable impact of environmental conditions on biofilm communities, can we expect high similarities between replicate biofilm samples if growth conditions were as homogeneous as possible?
- How does biofilm heterogeneity affect sampling strategies?

For enlightening the microbiological black box, the complexity of conditions needs to be broken down, i.e., we first need to focus on individual factors one by one. In recent years, substantial research in our group was conducted on the importance of polymeric materials in contact with drinking water (e.g., pipes, hoses, sealing rings). The basic outcome was that (low-quality) flexible polymeric materials release high concentrations of bioavailable organic carbon^{2,3}. As drinking water is normally carbon-limited⁴, this additional carbon considerably changes the biological stability of the system. Following up on this, Proctor and colleagues⁵ made more detailed observations on the impact of different flexible hose materials on biofilm communities. Their work highlighted that both carbon quantity and quality impact bacterial cell concentrations and community compositions in developing biofilms. Moreover, a considerable loss in species' diversity was observed, as well as a dependency on the originally introduced drinking water communities⁶. From this, the following questions arise for this thesis' work:

- Can observed biofilm characteristics be explained by basic ecological principles?
- How long does it take for a system to be biofilm dominated?
- Is the composition of a developing biofilm rather determined by the migrating carbon (nutrient-based selection) or by the composition of the initially colonizing drinking water community (water-to-surface dispersal)?

Breaking down the complexity of building plumbing conditions to only flexible polymeric materials allowed for explanations on observed enhanced growth. The next step was to simplify the environment even more, looking at the very small but important things, and to link observations to the biofilm formation theory itself. Despite the variability in fields of biofilm research (e.g., medicine⁷, food industry⁸, or engineering⁹), one biofilm formation theory seems to 'rule them all'¹⁰. Figure 1A illustrates the three common stages of initial biofilm formation (graphic by¹¹). In a simplified scheme: Planktonic cells attach to a new surface (water-to-surface dispersal), which is followed by growth and the

formation of the biofilms' structure. Eventually, biofilm cells detach and return to their planktonic state. The findings by Proctor and others now raise questions on whether this 'common' biofilm formation theory is applicable for biofilms on flexible polymeric materials, amongst others as these communities comprise various bacterial species (Figure 1B). In fact, we propose that the biofilm formation model needs to be adapted in the sense that (1) a more diverse planktonic community is introduced⁶ and (2) that the surface itself supports growth due to carbon migration¹² (Figure 1C). Finally, focusing on the initial colonization of new flexible polymeric materials, the following questions arise:

- Can we select for material-specific biofilm communities?
- Can we identify material-specific pioneer organisms for initial colonization?
- How efficient are pre-selected communities in terms of first colonization?
- Is it feasible to pre-colonize a material? For example, how persistent are these pre-selected communities over time and against invasion?

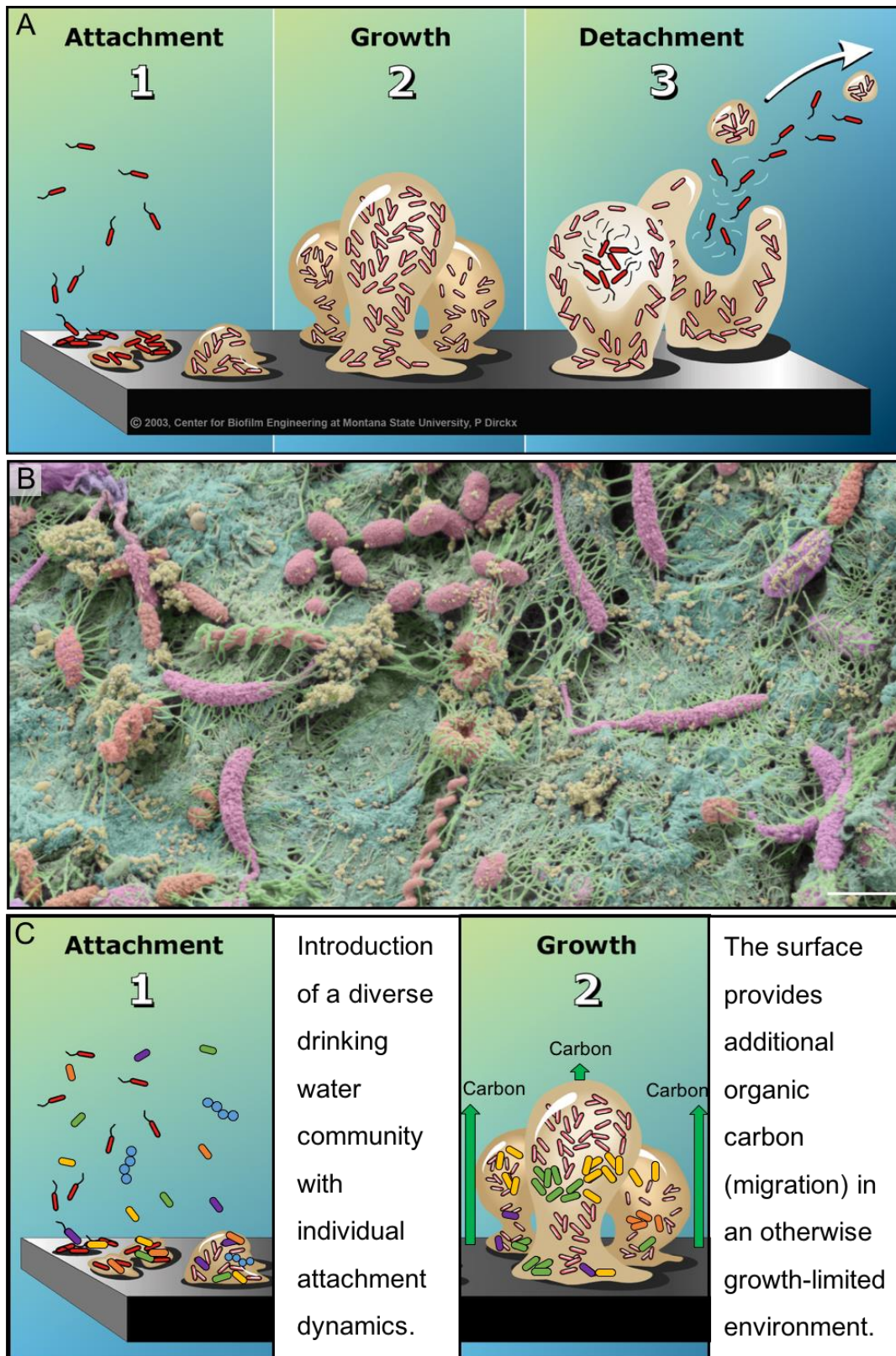


Figure 1 (A) Model on the common biofilm formation theory by Dirckx¹¹. (B) SEM image of a biofilm grown on a flexible polymeric material in contact with drinking water (Image: Center for Microscopy and Image Analysis, University Zurich). Scale bar: 1 μm . (C) Adapted model by Dirckx for biofilm formation on flexible polymeric materials in contact with drinking water.

Thesis overview

This thesis builds on the attempt of linking observational results with fundamental, ecological principles.

Chapter 2 provides an overview on building plumbing microbiology and links current knowledge to perspectives that developed in the course of this thesis' work. The focus is on the impact of material properties on biofilm growth, especially at an early stage (i.e., initial biofilm formation), and how material design can help manage and control biofilms in building plumbing systems.

Chapter 3 provides insight into biofilms that developed on low-quality flexible polymeric materials in contact with drinking (more precisely, bathing) water. The characterization of randomly collected biofilm samples (i.e., inside real bath toys) gave insight into biofilm structures, cell concentrations, and community compositions. This work demonstrated how a variety of factors impacts biofilm growth, resulting in considerable differences amongst biofilms from similar yet conditionally different environments. The characterization of biofilms grown on flexible polymeric materials is important as they can cause drinking water deterioration or even affect the end-user directly, e.g., due to the growth of opportunistic pathogens.

In chapter 4, attention is given to structural and compositional differences within individual biofilms. High-resolution sampling of a supposedly homogeneous biofilm highlighted not only the impact of localized variations in environmental conditions but also a severe selection within developing biofilm communities. The observed low diversity was attributed to the migrating carbon from the flexible hose material, which provided the main carbon for growth. The assessment of small-scale heterogeneity within a very confined environment helps to better evaluate biofilm heterogeneity in more complex systems and to inform sampling and analysis strategies in fundamental research as well as more applied sampling campaigns.

Finally, in chapter 5, the ecological principle of nutrient-based selection was used to explain observations that derived from the previous chapters. The comparison of different original drinking water communities and their corresponding biofilms (grown on flexible EPDM coupons) allowed for an assessment on diversity loss during their formation. Starting with different drinking water communities while supplying the same migrating carbon revealed a severe impact of the migrating carbon on overall growth; however, it also showed that these early-stage biofilm communities were impacted by the initial source water compositions. Linking microbiological observations (chapters 2 and 3) with fundamental, ecological principles allowed for the proposal of a pro-active management strategy for building plumbing biofilms through nutrient-based selection of specific biofilm communities.

Chapter 6 concludes this thesis by linking findings and thoughts of the experimental chapters and completes with an outlook on promising follow-up and future research directions.

References

1. **Falkinham**, J., Pruden, A. & Edwards, M. Opportunistic Premise Plumbing Pathogens: Increasingly Important Pathogens in Drinking Water. *Pathogens* 4, 373–386 (2015).
2. **Koetzsch**, S. & Egli, T. Kunststoffe in Kontakt mit Trinkwasser. *Aqua & Gas* 3, 44–52 (2016).
3. **Koetzsch**, S., Roelli, F. & Hammes, F. Trinkwasserqualität in Gebäuden. *Aqua Gas* 74–78 (2017).
4. **van der Kooij**, D. Assimilable organic carbon as an indicator of bacterial regrowth. *J. / Am. Water Work. Assoc.* 84, 57–65 (1992).
5. **Proctor**, C. R. *et al.* Biofilms in shower hoses - choice of pipe material influences bacterial growth and communities. *Environ. Sci. Water Res. Technol.* 2, 670–682 (2016).
6. **Proctor**, C. R., Reimann, M., Vriens, B. & Hammes, F. Biofilms in shower hoses. *Water Res.* 131, 274–286 (2018).
7. **Anderson**, A. C. *et al.* In-vivo shift of the microbiota in oral biofilm in response to frequent sucrose consumption. *Sci. Rep.* 8, 1–13 (2018).
8. **Zhao**, X., Zhao, F., Wang, J. & Zhong, N. Biofilm formation and control strategies of foodborne pathogens: Food safety perspectives. *RSC Adv.* 7, 36670–36683 (2017).
9. **Salta**, M., Wharton, J. A., Stoodley, P., Wood, R. J. K. & Stokes, K. R. Assessment of marine biofilm attachment and growth for antifouling surfaces under static and controlled hydrodynamic conditions. *Mater. Res. Soc. Symp. Proc.* 1356, 9–15 (2011).
10. **Tolkien**, J. R. . *The Lord of the Rings - The Fellowship of the Ring*. (Allen & Unwin, 1954).
11. **Dirckx**, P. Biofilm Basics: Section 1. (2003). Available at: http://www.biofilm.montana.edu/biofilm-basics/what_are_biofilms.html.
12. **Wen**, G., Kötzsch, S., Vital, M., Egli, T. & Ma, J. BioMig-A Method to Evaluate the Potential Release of Compounds from and the Formation of Biofilms on Polymeric Materials in Contact with Drinking Water. *Environ. Sci. Technol.* 49, 11659–69 (2015).

Chapter 2

Feeding the building plumbing microbiome: The importance of synthetic polymeric materials for biofilm formation and management

This chapter has been submitted in revised form for publication in MDPI Water by L. Neu and F. Hammes.

Abstract

The environmental conditions in building plumbing systems differ considerably from the larger distribution system and, as a consequence, uncontrolled changes in the drinking water microbiome through selective growth can occur. In this regard, synthetic polymeric plumbing materials that are commonly used in new buildings are of particular relevance, since they leach assimilable organic carbon that can be utilized for bacterial growth. Here we discuss the complexity of building plumbing in relation to microbial ecology, especially in the context of low-quality synthetic polymeric materials (i.e., plastics) and highlight the major knowledge gaps in the field. We furthermore show how knowledge on the interaction between material properties (e.g. carbon migration) and microbiology (e.g., growth rate) allows quantification of initial biofilm formation in buildings. Hence, research towards comprehensive understanding of these processes and interactions will enable the implementation of knowledge-based management strategies. We argue that the exclusive use of high-quality materials in new building plumbing systems poses a straightforward strategy towards managing the building plumbing microbiome. This can be achieved through comprehensive material testing and knowledge sharing between all stakeholders including architects, planners, plumbers, material producers, home owners and scientists.

Drinking water microbiology from source to tap

Bacteria are omnipresent in drinking water treatment and distribution systems

Bacteria inhabit nearly every part of drinking water systems¹. Complex microbial communities, comprising thousands of unique taxa, are found at various concentrations ($10^3 - 10^6$ cells/mL)²⁻⁴ from the source water⁵⁻⁷, through different treatment stages⁸⁻¹⁰, through the drinking water distribution system (DWDS)¹¹⁻¹³ and building plumbing system right up to the tap¹⁴⁻¹⁶ (Figure 1). Along the DWDS (i.e., from post-treatment until the property line), the majority of bacteria (~98 %) is present in the form of biofilms and/or attached to particles, while only ~2 % are present as planktonic cells in the water phase¹⁷. Here, typical pipe surface biofilm concentrations range between $10^5 - 10^7$ cells/cm²^{18,19}. The DWDS of the City of Zurich (Switzerland) comprises 1'100 km of main and distribution pipes²⁰. Calculating with an average inner pipe diameter of 100 mm, this translates to 3×10^5 m² pipe surface and 9×10^3 m³ of water. Considering a planktonic bacterial concentration of up to $\sim 1 \times 10^5$ cells/mL after treatment²¹ and a biofilm:water distribution of 98:2 (above), this means an estimated total of 4×10^{16} attached cells and 0.1×10^{16} planktonic cells for the entire DWDS; spectacular numbers indeed.

The microbiology of DWDS is studied, monitored, and regulated

The microbiology of DWDS has been studied intensively (e.g.,^{17,22}) and is routinely monitored by utilities, following defined regulations. Here, several aspects allow for a comparatively controlled, and thus manageable, environment. First, a DWDS is often operated by a single 'owner' (i.e., water utility), which allows for structured planning, operation, management, and monitoring. Second, legal guidelines and regulations are in place and areas of responsibilities are defined, e.g., which pipe materials to use or which water quality variables to monitor (e.g. EU guideline: DWD 98/83/EC²³; USA (EPA) Safe

Drinking Water Act²⁴). Third, DWDS have relatively limited fluctuations in operating conditions. For example, the water in DWDS mains is essentially flowing continuously, resulting in (comparatively) limited changes in flow dynamics and water age at any given point in the system.

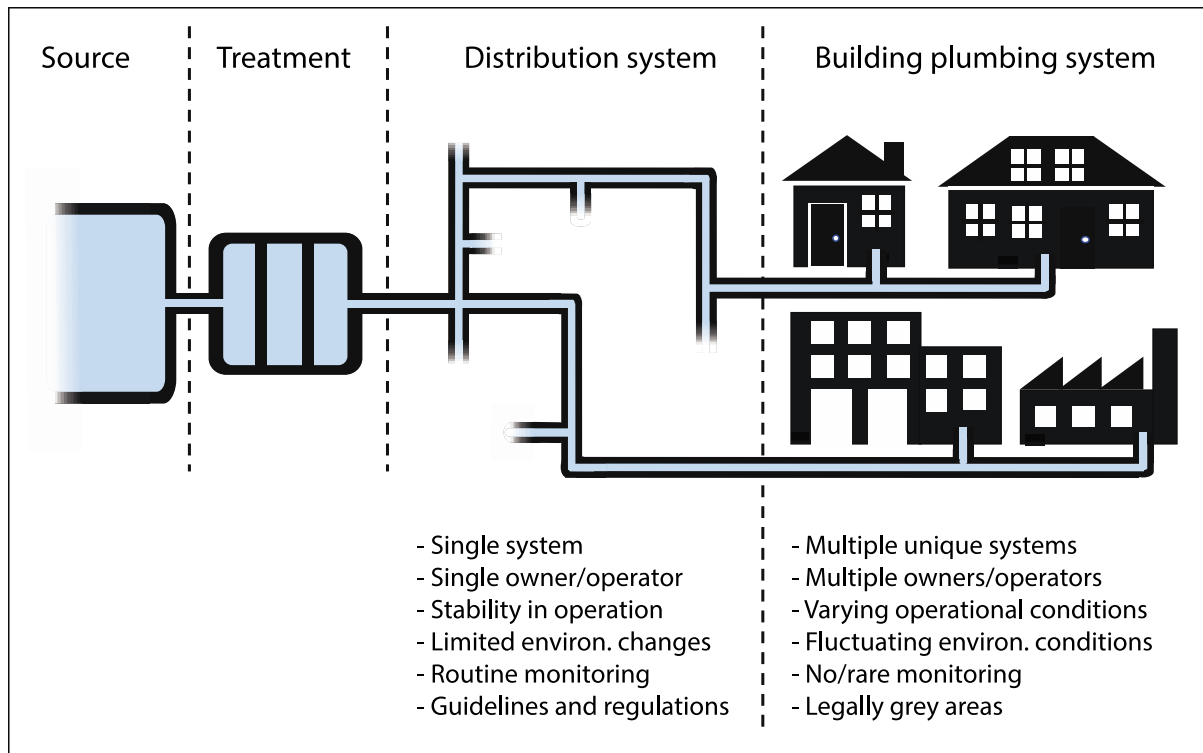


Figure 1 Drinking water from source to tap, highlighting key differences between the main distribution system and building plumbing systems.

The microbiology of DWDS is prone to (environmental) temporal and spatial changes

An ideal DWDS is microbiologically stable, meaning the water quality does not change during distribution (e.g., ²⁵). However, and despite comparatively limited fluctuations, temporal and spatial changes have still been documented. This includes short-term changes in planktonic cell concentrations, which can be attributed to fluctuations in flow velocity, following trends in water consumption throughout the day²⁶, and seasonal changes in both cell concentrations²⁷ and microbiome composition²⁸, presumably linked to changes in environmental conditions. In similar vein,

spatial variations in bacterial concentration and composition resulted for example from increased water age and the depletion of disinfectant residuals throughout the DWDS^{29,30}.

Changes in microbial quality are problematic

From an ecological perspective, understanding the link between changes in environmental conditions and changes in the drinking water microbiome is interesting. Unfortunately, changes like these may also have profoundly adverse consequences for the drinking water quality. For example, the increased detection of *Mycobacterium avium* in a DWDS was linked to water age and the depletion of chlorine during distribution³¹, and seasonal temperature changes within several DWDSs were correlated with the growth of coliforms³². The most dramatic, least understood, and usually uncontrolled changes in environmental conditions occur when water from the DWDS enters building plumbing systems (also referred to as 'premise(s) plumbing'^{33,34} or 'domestic plumbing'^{35,36}) (Figure 1). As discussed below, the environmental conditions between and within building plumbing systems change dramatically relative to the DWDS and relative to each other, and consequently so does the microbiology.

The purpose of this review is (1) to emphasize the complexity of building plumbing in relation to microbial ecology, especially in the context of low-quality synthetic polymeric materials (i.e., plastics) and to (2) highlight major knowledge gaps in the field. This should ultimately (3) highlight the need for more research on the fundamental aspects of biofilm growth in building plumbing systems, (4) allowing for both a better understanding and better options of proactive management of the microbiology in the built environment.

Building plumbing systems change the microbiology

The microbiological black box between the water meter and the tap

A number of studies on building plumbing microbiology emerged during the past decade, for example investigating the impact of temperature on community composition¹⁵, refining adequate building sampling strategies³⁷, monitoring biofilm formation in a new building¹⁶, or evaluating the impact of stagnation on microbiome assemblages¹⁴. Despite this increase in knowledge, building plumbing microbiology still remains considerably less studied than DWDS microbiology, insufficiently monitored, and consequently poorly understood. The two main reasons for this are (1) the severe challenges in sampling and monitoring buildings due to legal restrictions, and (2) the constructional complexity of building plumbing systems.

Legal guidelines in most developed countries cover drinking water safety until the point of use (e.g., Drinking Water Directive, EU²³; TrinkwV, Germany³⁸). While this in theory also renders water utilities responsible for safe water within both private and public buildings, additional interpretations of the legislation allow for the transfer of legal obligations to building owners (e.g., AVBWasserV, Germany³⁹). The consequence is that most buildings, and particularly private homes, are not controlled from a microbiological perspective on a regular basis, if at all.

Apart from legal aspects, additional challenges stem from the complexity of building plumbing systems. Not only are there thousands of unique buildings connected to each DWDS (e.g., >20'000 single-family houses in the City of Zurich (data 2010, ⁴⁰), but each building plumbing system also consists of multiple, different sub-units such as boilers, rising mains and ring mains. In addition, each system typically has warm and cold water outlets (Figure 2), with hoses, taps, and various connected home appliances (e.g., washing

machine); all of which will potentially create unique and very different environments. From a microbiological point of view, bacteria that enter a building plumbing system from the DWDS experience an immediate and considerable change in environmental conditions, and it is common knowledge that a change in environmental conditions will often result in a change in bacterial numbers⁴¹, viability⁴², activity⁴³, and composition⁴⁴.

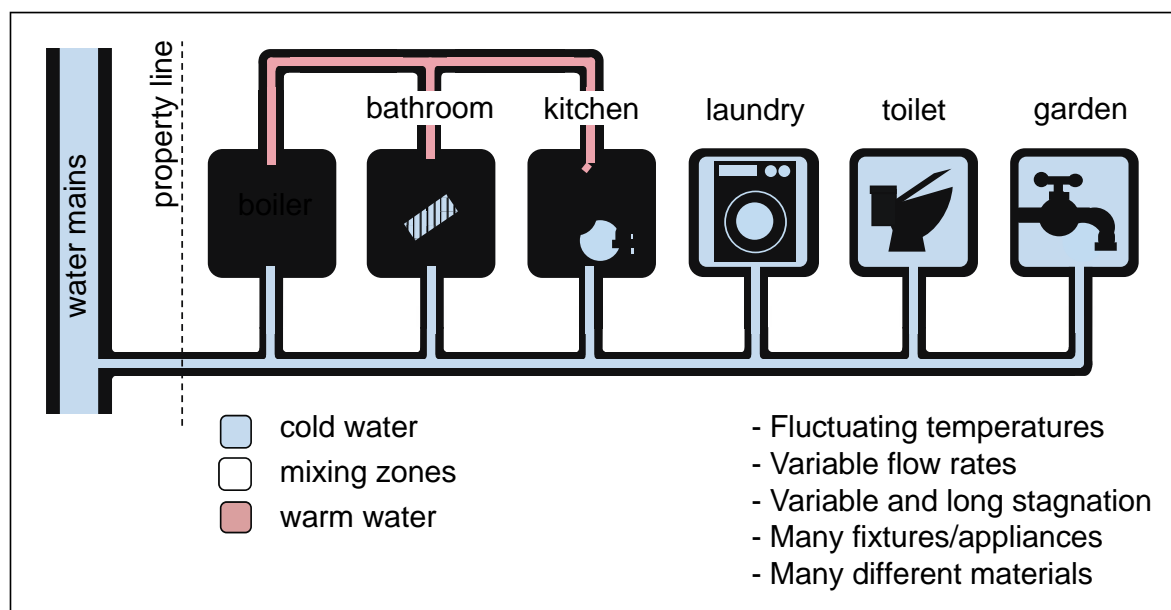


Figure 2 The complexity of building plumbing systems affects environmental conditions and ultimately alters the drinking water microbial composition and quality.

Specific building plumbing system conditions alter microbial water quality

Pipe diameters: Building plumbing pipes have small diameters, ranging between 1 – 2 cm (DN12 – DN20), compared to diameters of 10 – 200 cm (DN100 – DN2000) in the DWDS. This implies that the surface area within building plumbing systems is high compared to the corresponding water volume. For example, DN12 pipes have a surface area to volume (SA/V) ratio of ~3:1, meaning for every 3 cm² of pipe surface there is approximately 1 mL of water (as opposed to the DWDS where 2 mL of water is in contact with 1 cm² of pipe surface). This is particularly relevant, as an increasing SA/V ratio (e.g., from 1:2

in the DWDS to 3:1 in building plumbing systems) translates to a much higher potential impact of the biofilm on the water phase (e.g., due to detachment dynamics). Moreover, pipe diameters directly impact flow velocity and thus shear stress, with both increasing due to decreasing pipe diameters⁴⁵. This is microbiologically relevant, as water dynamics impact both the dominance of specific bacteria⁴⁶ as well as biofilm structure and overall community compositions^{47,48}.

Temperature: Upon entering a building, temperature changes considerably as the water from the DWDS diverges into cold and warm water lines (Figure 2). After entering a building, cold water is subject to gradual warming (e.g., fluctuating between 8 – 20 °C)^{49,50}, potentially favoring increased bacterial growth. Water in the warm water line is subject to a heat shock in the boiler (e.g., 60 – 63 °C)⁴⁹ and to severe temperature gradients along the building plumbing system, e.g., decreasing to below 30 °C within 1 – 3 hours of stagnation³⁷. One study showed that bacterial concentrations can be 20 % higher in the cold water compared to the warm water⁴⁹. Also, dissimilar community compositions have been found in warm and cold water, showing higher diversities at low temperatures and differences in abundant taxa between cold and warm water^{15,51}. Comparing the microbiology of associated cold and warm water in the same system highlights the impact that is introduced by installation design (e.g., pipe isolation) and the choice of operational settings (e.g., boiler temperature).

Stagnation time: In contrast to the DWDS, water stagnates for a significant amount of time in buildings. Here, user habits play an important role. Even though a building usually has a single owner, multiple inhabitants are using the installation, often in a variety of different and uncontrollable ways. For example, in a single family house, multiple people (a) use water for different purposes (e.g., showering, toilet flushing, laundry), (b) at different time points and in different frequencies, and at (c) different spatial locations in the

building (e.g., tap in the bathroom on the upper floor vs. toilet in the basement) (e.g., ⁵²). These variations in operation result in highly irregular and uncontrollable water dynamics within a single building plumbing system and are, without the user's knowledge, inevitably impacting the microbiology thereof. Studies showed that stagnation results in an increase in bacterial cell concentrations in the water phase (e.g., from $\sim 6 \times 10^4$ to $\sim 1 \times 10^5$ cells/mL during overnight stagnation⁵⁰) as well as in community compositional changes, e.g., decreasing richness¹⁴. For some cases, the depletion of disinfectant residuals during stagnation was identified to be a reason for microbial changes⁵³ which ultimately resulted in drinking water deterioration⁵⁴.

Materials: Building plumbing systems consist of numerous types of very different materials. Here, not solely pipes but also components such as sealing rings, hoses, or fixtures are produced from a variety of metals as well as hard and flexible synthetic polymeric materials (Table 1). While this will be discussed in detail in section 3, it is already important to notice that materials significantly impact the microbiology of building plumbing systems, e.g., due to different microbial colonization dynamics, based on surface properties⁵⁵ and nutrient migration^{56,57}.

Importantly, all of the conditions above can be altered/managed either by operational adaptations (e.g., temperature, circulation) or design (e.g., materials, isolation), providing the opportunity to manage building plumbing microbiology proactively. Here, we argue that the selection of good plumbing materials is one of the most straightforward starting points for a good building plumbing management.

Synthetic polymeric materials in building plumbing systems

The variety of materials used in building plumbing systems creates numerous ecological niches

Building plumbing originally consisted almost exclusively of metal-based products (copper, galvanized steel, etc.). However, during the last half-century, synthetic polymeric products were increasingly implemented (Figure 3A). The benefits of the latter are (1) the low cost, (2) an easier installation compared to rigid pipes, (3) high heat resistance, (4) long life-times, (5) corrosion resistance, and (6) better energy conservation due to reduced heat transfer and loss. A large variety of synthetic polymeric materials is used for both pipes and non-pipe components (Table 1). For example, cross-linked polyethylene (PE-X) and unplasticized polyvinyl chloride (PVC-U) are used for pipes. Fittings are often made from polybutylene (PB) and polypropylene (PP). Hoses are made from plasticized PVC (PVC-P), whereas ethylene propylene diene monomer (EPDM) and silicone rubber are typically used for the production of sealing materials. Importantly, there is not only substantially different material types within plumbing systems overall, but also within individual fixtures. For example, one single kitchen tap can comprise numerous different materials in contact with the water (e.g., galvanized steel, copper, PE-X, EPDM, and PVC-P; Figure 3). It is important to realize that every single material potentially poses a unique environment and consequently creates a different niche for bacteria to grow.

Carbon migrates from synthetic polymeric materials

Organic carbon migration (or leaching) from the material to the water is a main reason why synthetic polymeric materials are relevant for microbial growth in buildings. In most cases, the migrating substrates are not the polymers themselves, but rather the so-called *additives* (i.e., flexibilizers,

plasticizers, stabilizers), which are added during production to improve or adapt specific properties of the material⁵⁸. *Stabilizers* include antioxidants that protect the material against thermally introduced oxidation, i.e., increasing heat tolerance⁵⁹. For example, Skjevraak and colleagues detected 2,4-di-tert-butyl-phenol (2,4-DTBP) in water running through HDPE pipes⁵⁹. This compound was previously identified as a degradation by-product of Irgafos 168[®] (BASF, Switzerland⁶⁰), an antioxidant used as an additive in PP pipes⁶¹. *Plasticizers* are added to polymeric materials to increase flexibility⁶². Here, the most commonly used plasticizers are phthalates, such as, di-(2-ethylhexyl) phthalate (DEHP, ⁶³). Due to its structure and polarity, PVC is particularly susceptible to the incorporation of plasticizers. Hence, many flexible hoses such as shower hoses are made from PVC with additional plasticizers. Importantly, these additives are usually low molecular-weight compounds, thus prone to leaching from the material into the water phase. Some of these compounds can serve as primary growth-supporting nutrient sources for bacteria⁶⁴ as they are easily biodegradable⁶⁵, leading to growth, biofilm formation, and ultimately affecting the microbial water quality.

Therefore, European Standards on the 'influence of materials on water for human consumption'⁶⁶ include material testing with respect to both migration potential assays (e.g., KTW guideline, Germany⁶⁷) as well as bacterial growth potential assays. For the latter, three different test methods are recognized⁶⁸, where microbial growth is measured by the *mean dissolved oxygen demand* (MDOD), *volumetric measurements* of total biofilm growth, or the determination of the *biomass production potential* (BPP) based on metabolic activity (i.e., ATP). An alternative method is the Swiss BioMig assay, introduced by Bucheli-Witschel and colleagues⁵⁷, which combines both migration and growth potential assays in a single test. This assay was, for example, used to study the impact of chlorination on the migration potential of biodegradable carbon⁶⁹, but also to evaluate and classify a range of different building plumbing materials⁶⁴.

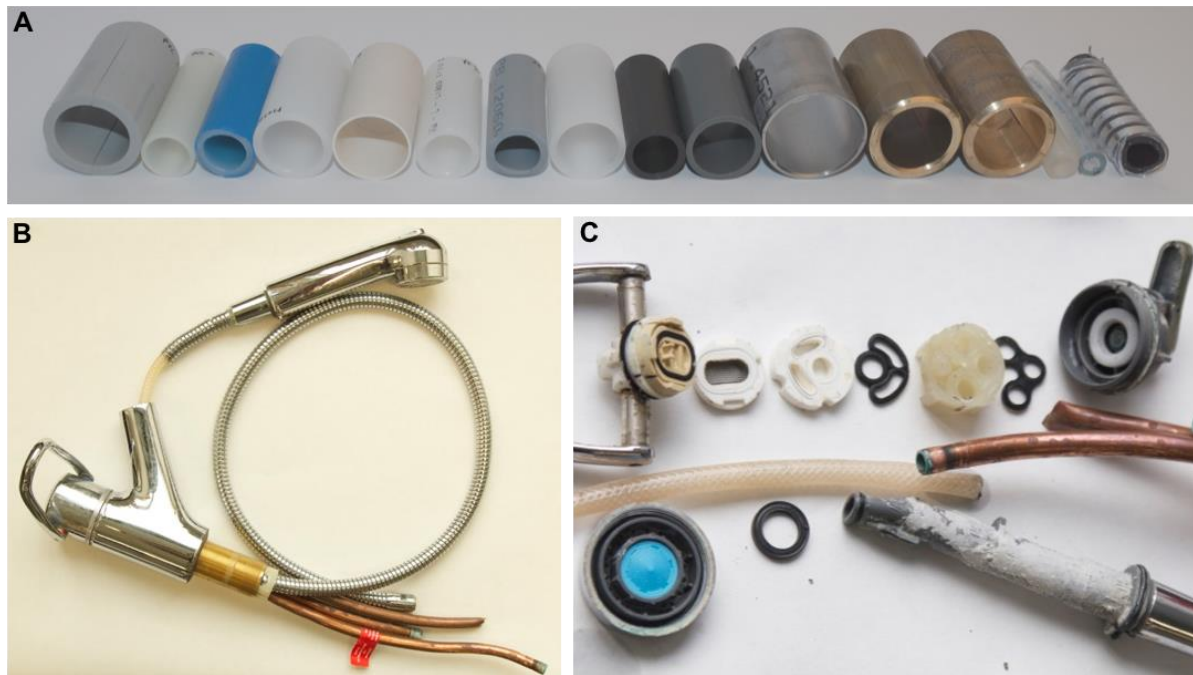


Figure 3 Variety of materials used within building plumbing systems and fixtures. (A) Different pipes and hoses from metals and both hard and flexible synthetic polymeric materials. (B, C) Materials used in a single kitchen tap.

Migrating organic carbon compounds drive biofilm formation and selection

Materials differ considerably in the quantity, composition, and dynamics of carbon migration⁵⁷. For example, a study by Wen and colleagues⁶⁴ found that high-quality PE-X pipe material leaches less (0.3 mg TOC/L/d) total organic carbon (TOC) than flexibilized EPDM (0.7 mg TOC/L/d) or flexible PVC-P (40 mg TOC/L/d) within the first 24 hours of exposure. This study emphasizes the need of quality control of migrating carbon substances from plumbing materials. Especially shower hose materials are mainly made of flexible synthetic polymers (e.g., PVC-P), of which the exact chemical composition is normally not disclosed to the buyer and often not properly regulated by law. Consequently, shower hoses can be purchased in the whole spectrum of qualities: either high-quality and certified for drinking water use or low-quality and thus potentially leaching high carbon concentrations (see, e.g., ⁷⁰). Proctor and colleagues⁷⁰ investigated the growth potential of migrating carbon compounds from five different flexible hose materials (1 x PE-X, 2 x PVC-

P, 1 x silicone, and 1 x unknown). All materials showed different degrees of carbon migration which (mostly) correlated with the actual growth within the corresponding hose. Carbon migration during material testing varied between 0.4 – 10.4 $\mu\text{g C/cm}^2/\text{day}$ and supported growth in a range of 0.5 – 4.8 x 10⁷ cells/cm² in the same assay. Moreover, the diversity in the hose biofilm communities was shown to be at least 10-fold lower than in the corresponding water⁷⁰, highlighting the selectiveness of biofilm growth on flexible synthetic polymeric materials. Selective growth on different materials potentially impacts water quality. For example, several authors showed correlations between carbon migration of different materials, subsequent differences in bacterial growth, and differences in the establishment of *Legionella pneumophila* on those materials^{71,72}. Consequently, we propose that the understanding of nutrient-based selection is essential for understanding and managing biofilm formation in building plumbing systems, particularly during the initial stages (i.e., commissioning of a new building).

Table 1 Materials used in building plumbing systems and their applications.

MATERIAL	APPLICATION
METALS	
Copper and copper alloys	- Pipes & fittings
Brass (copper alloy)	- Taps, valves, pipes & fittings
Galvanized steel (GI)	- Pipes & taps
Stainless steel	- Fittings
Ductile iron	- Pipes & fittings
Malleable iron	- Nipples
Galvanized iron	- Pipes & fittings
SYNTHETIC MATERIALS	
Ethylene propylene diene monomer (EPDM)	- O-rings, seals
Polyvinyl chloride (PVC)	
PVC-U (unplasticized)	- Pipes & fittings
PVC-C (chlorinated)	- Pipes & fittings
PVC-P (plasticized)	- (Shower) hoses
Polyethylene (PE)	
PE-X (crosslinked; a, b, c)	- Pipes (hot water pipes)

	- Multilayer pipes
PE-RT (raised temperature resistant)	- Pipes (hot water pipes)
	- Multilayer pipes
Polybutylene (PB)	- Pipes & fittings
Polypropylene (PP)	
PP-R (random Co-polymer)	- Tubes & fittings
PP-C (Copolymer)	- Tubes & fittings
PP-H (Hologopolymer)	- Tubes & fittings
Polyphenylsulfone (PPSU)	- Fittings
Polyoxymethylen (POM)	- Valve elements
Polyvinylidene fluoride (PVDF)	- Fittings
Polytetrafluorethylen (PTFE; Teflon)	- Valve elements, seals
Silicone rubber	- Seals
Epoxy resin	- Inline coating

Quantifying initial biofilm formation on flexible synthetic polymeric materials

Dispersal and selection as main parameters for initial biofilm formation

Similar to other ecosystems, biofilm formation in building plumbing systems follows known ecological principles such as dispersal, selection, drift, and diversification^{73,74}. This allows the quantification of biofilm formation processes to better understand growth dynamics. In this section, we specifically explore the importance of (1) *water-to-surface dispersal* and (2) *nutrient-based selection* through basic quantification of initial biofilm formation processes. For a theoretical example, we focus on the dynamics that follow the installation of a new shower hose – a common plumbing-maintenance action undertaken by most home owners at some point in time. The purpose of this example is to show that engineering information (e.g., material quality and system operation) can be combined with microbiological knowledge (e.g., attachment and growth data) to develop a quantitative understanding of biofilm formation in buildings. A typical shower hose ($L = 180$ cm, $d_i = 0.8$ cm) is made from flexible PVC-P and has an inner surface area of ~ 450 cm² and a

volume of ~90 mL. Five parameters that will govern the initial biofilm formation are: (1) The inorganic nutrients introduced daily with the drinking water, (2) the organic nutrients that migrate from the shower hose material into the water phase (see section 3), (3) the ability and rate of bacteria to attach to the hose surface (*water-to-surface dispersal*), (4) the metabolic capability of bacteria to utilize the available nutrients and the rate at which they will grow, and (5) selection that occurs within the community due to the specific growth dynamics (*nutrient-based selection*). These parameters are not detached from each other but will, for the sake of clarity, be dealt with separately below.

(1) *Inorganic nutrients from the water*: The water in this example is typical for Zurich (CH), meaning non-chlorinated, biologically stable (i.e., assimilable organic carbon (AOC) < 10 µg/L,⁷⁵), oligotrophic water with approximately 1 mg/L dissolved organic carbon (DOC), 3 mg/L total nitrogen (TN), and 5 µg/L total phosphorous (TP)⁷⁶. This converts to 0.1 mg-TN/hose and 0.5 µg-TP/hose.

(2) *Organics from the material*: Flexible PVC-P leaches up to 4 µg-TOC/cm²/day, of which ~50 % is AOC (i.e., 2 µg-AOC/cm²/day)^{64,70}. This converts to ~900 µg-AOC/hose/day.

(3) *Water-to-surface dispersal*: Zurich tap water comprises ~5 x 10⁴ cells/mL (i.e., 4.5 x 10⁶ cells/hose) and > 5'000 different bacterial taxa⁵¹. Water-to-surface dispersal rates for initial colonization remain poorly characterized for drinking water systems, but it is known that bacterial attachment starts within seconds to minutes of the first exposure^{77,78}. Here, we assume an attachment of 1 % of the total cell concentration (TCC) from the water phase during 1h of stagnation, which means ~1.1 x 10⁶ cells/hose/day in the absence of any growth.

(4) *Bacterial growth*: Based on a conversion factor of 10⁷ cells/µg-AOC^{79,80} and following the rule-of-thumb for growth requirements of bacteria (i.e., a C:N:P ratio of 100:10:1⁸¹), bacterial growth in the water would be carbon-limited (allowing for the growth of ~9 x 10⁶ cells/hose/day). However, this is reversed due to the excessive AOC that migrates continuously from the material,

rendering the shower-hose environment phosphorous-limited. Ultimately, the maximum growth potential of the combined system (i.e., water and hose) is $\sim 1 \times 10^8$ cells/hose/day, assuming that 100 % of the phosphorous is biologically available.

(5) *Nutrient-based selection*: The composition and biodiversity of biofilm communities is influenced by the type of material they grow on⁸². Based on the selection observed in previous studies, we assume for our example that only 10 % of the bacteria present in the water phase and of those dispersing to the material's surface can actually utilize the migrated organic carbon and grow (i.e., 4.5×10^5 cells/hose/day).

Initial colonization, growth, and biofilm formation

In Figure 4, we demonstrate the calculated dynamics of initial biofilm formation on a new material, based on the example discussed above. We calculated planktonic and biofilm growth during the first 72 h of operation with intermittent flushing events occurring every 24 h (Figure 4A). The calculation is based on (1) TP from the water being replenished with every 24-hour flushing event and (2) continuous carbon migration from the material with unutilized compounds being removed with every flushing event (Figure 4B). Within each 24 hour-cycle, (3) a fraction of the planktonic cells will attach to the material's surface (*water-to-surface* dispersal) and (4) some will grow in both the planktonic and biofilm phase. This will (5) benefit growing taxa over others, resulting in a *nutrient-based selection* within the community.

For the calculation of planktonic growth, we used the following equation (Eq. 1):

$$pTCC_t = \left((pTCC_0 * (1 - r)) + ((pTCC_0 * r) * (1 + \mu)^t) \right) - ((pTCC_0 * r) * (1 + \mu)^t) * k_a \quad (\text{Eq.1})$$

with $pTCC_t$ representing the number of planktonic bacteria in the water phase

at a certain time-point t , based on a fraction of growing cells $r = 0.1$ (i.e., 10 % grow) for the originally (i.e., with each flushing event) introduced cells ($pTCC_0$), with a constant growth rate of $\mu = 0.125/h$ and taking a constant attachment into consideration, with the attachment rate coefficient $k_a = 0.01/h$.

For calculating biofilm growth, an adapted equation was used (Eq. 2):

$$sTCC_t = (sTCC_{t-1} * (1 + \mu)) + (((pTCC_0 * r) * (1 + \mu)^t) * k_a) \quad (\text{Eq. 2})$$

with $sTCC_t$ representing the number of bacteria in the biofilm phase at a certain time-point t , based on a fraction of growing cells $r = 0.1$ for the originally introduced cells ($pTCC_0$), with a constant growth rate of $\mu = 0.125/h$ and taking a constant attachment into consideration, with $k_a = 0.01/h$.

Applying this to input variables shows the following (Figure 4C):

(1) During the first stagnation period, i.e., within the first 24 hours of stagnation, planktonic growth dominates the shower hose system, with 1.2×10^7 planktonic (86 %) and 1.8×10^6 attached (14 %) cells/hose. However, in the subsequent day(s) (with daily shower/flushing events), the water phase is exchanged every 24 hours, meaning a replacement of the grown planktonic cells by the source water community, and a replenishment of inorganic nutrients in the otherwise carbon-rich environment. Sessile cells remain in the biofilm and therefore continue growing at the concentration of $sTCC_{24}$ after the first flushing event, subsequently rendering the system biofilm dominated (with 1×10^7 pTCC/hose (26 %) versus 3×10^7 sTCC/hose (74 %) after 48 hours).

(2) Assuming continuous growth in the biofilm, the shower hose system will reach phosphorous-limitation after approximately 70 hours (Figure 4C), limiting further growth until a replenishment of inorganic nutrients.

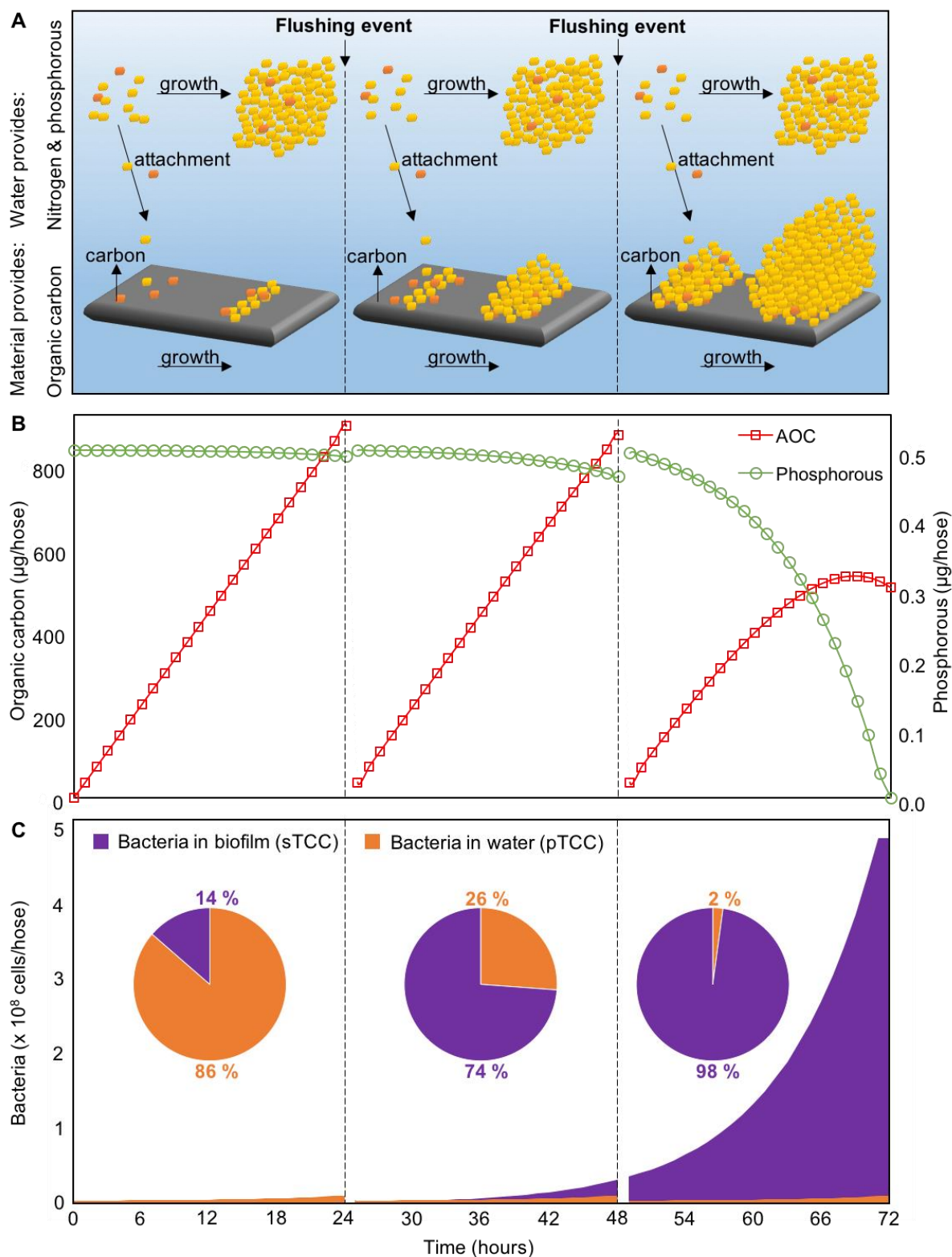


Figure 4 Theoretical example of initial biofilm formation on a new flexible synthetic polymeric material (e.g., PVC-P shower hose). (A) Visualization of the initial stages of biofilm formation, driven by attachment (water-to-surface dispersal) and (nutrient-based selective) growth. (B) Nutrient concentrations with phosphorous deriving from the water and assimilable organic carbon

(AOC) migrating from the material. (C) Quantification of bacterial growth, showing rapid domination of the biofilm in the overall distribution of bacteria.

(3) During the initial stagnation period, the biofilm community is dominated by the initial *water-to-surface dispersal*-driven colonization. However, the continuous growth of adapted cells in the biofilm results in a highly selective growth and biofilm development. More precisely, the original drinking water community of our example comprised around 5'000 different species. Due to the ability of (initially) only 10 % to grow (i.e., 500 species), species heterogeneity in the biofilm inevitably declines. As a result, we can state that *nutrient-based selection* is important for the subsequent development of the biofilm and its microbial community composition.

Details and absolute values of this initial biofilm formation 'model' will certainly vary between locations. However, we argue that the basic concept will be the same. Consequently, these quantitative considerations are important as (1) bacterial/biofilm growth within building plumbing systems (and here especially on low-quality flexible materials) is relevant regarding drinking water quality and (2) knowledge on such ecological factors opens management options.

The relevance and management of building plumbing biofilms

To ensure high-quality drinking water until the point of consumption requires the understanding of basic principles of microbial ecology, as well as the collaboration and interplay between various disciplines and stakeholders (e.g., material producers, plumbers, planners, architects, home owners, and scientists).

Why should we care?

A lack in understanding bacterial growth in building plumbing systems equals a lack of control and can result in aesthetic, operational, and/or hygienic

problems. Aesthetic and operational problems often manifest in customer dissatisfaction involving taste, odor, color, particles, or water pressure; all of which potentially indicate water quality deterioration⁸³. Hygienic problems are particularly relevant, as the number of building plumbing related waterborne disease incidents increased over the last decades. A good example is the worldwide increase in Legionnaires' disease incidents, for example in the US (4.5-fold between 2000 – 2015⁸⁴) and Switzerland (4-fold between 2000 – 2015⁸⁵). The causative organism, *Legionella pneumophila*, is thriving in building plumbing systems, especially in biofilms⁸⁶. Additionally, opportunistic pathogens such as *Pseudomonas aeruginosa* and *Mycobacterium avium* were shown to grow preferably in building plumbing systems⁸⁷. For example, a nationwide German study in 2010 detected *Pseudomonas* sp. above the legal limit (0 CFU/100 mL) in approx. 3 % of all drinking water samples taken (n = 3'468)⁸⁸. The relevance of increasing *Pseudomonas aeruginosa* appearances has been discussed by Bédard and colleagues⁸⁹, highlighting not only their capability of incorporation in building plumbing biofilms but also the emerging health risk for susceptible people, e.g., cystic fibrosis patients. *M. avium* has, for example, been found to colonize shower heads, with 20 % positive samples in a survey study by Feazel and colleagues⁹⁰ (n = 52 samples from 42 different sampling sites). This is critical as *M. avium* is an agent of pulmonary disease, leaving the inhalation of shower water droplets and aerosols as a major transfer route and risk area^{91,92}.

To emphasize this point, all of the opportunistic pathogens mentioned above are commonly detected in building plumbing biofilms³⁴. However, to date, a connection between properties of materials and pathogenic growth is only done sporadically. One example by Wen and colleagues⁹³ used a pathogen growth potential assay⁹⁴, which illustrated the ability of selected pathogens to grow on migrated compounds as sole carbon sources. Also, previous studies showed: (1) that the number of growing bacteria increases with decreasing material quality (e.g., PEX_c < EPDC_{certified} < EPDM_{non-certified}) and (2) that an

increase in bacterial numbers correlates with a higher concentrations of *L. pneumophila*^{71,72}. However, to date no clear correlations between specific materials and specific pathogens have been established.

What can we do?

One straightforward microbial management strategy for new building plumbing systems is to limit the overall use components that are made by default from lower quality materials (e.g., hoses, sealing rings) and only use the highest quality materials for specific applications (Table 1). This strategy depends on (1) proper microbial quality control for all materials in contact with drinking water, (2) knowledge exchange between all stakeholders to raise awareness of microbiological relevance and hygienic issues in building plumbing, and (3) further research to develop a better understanding of the microbial ecology of building plumbing systems.

(1) A quality label for good materials: Important for the widespread use of high-quality materials are sensible and standardized quality control procedures. Irrespective of legal guidelines, assays for the assessment of carbon migration and growth potential exist (section 3; ⁶⁸) and can be used by both material producers and policy makers. The result would be a material-grading system that is ideally freely available to all stakeholders, including plumbers, planners, and architects. This material grading system can, for example, be in form of a quality label, which enables easy identification of high-quality materials for both professional and private costumers. Here the incentive for producers would be the competitive advantage gained over lower quality products from competitors.

(2) Information sharing: To address microbiological challenges requires extensive information sharing between the diverse stakeholders in building plumbing systems. Here, scientists have an opportunity to contribute

knowledge on how the basic principles in microbial ecology relates to different plumbing materials and ultimately water quality. One example can be to incorporate microbiology courses in basic training and teaching modules for plumbers and architects. On a different level, opportunities exist to collaborate with producers of plumbing materials and fixtures on applied research projects focusing on the evaluation of (existing) material properties, their interaction with microorganisms, and their dependency on environmental conditions in buildings. Finally, it is important to engage the public as the end-users who are operating the building plumbing systems and therefore create the conditions that influence material behavior and microbiological growth potential. Elucidating the impact of low-quality materials on drinking water microbial quality will incentivize users to invest in high-quality materials, for example, when purchasing a new shower hose or fixture.

(3) *Further research:* Considerable knowledge gaps exist in our understanding of the microbial ecology of building plumbing systems. There is a clear need for additional pilot- and full-scale experiments dealing with the interplay between existing materials, the developing microbial community, and water quality. More precisely, a better understanding is needed of a materials' behavior in the context of complex building plumbing systems (e.g., fluctuating water temperatures, stagnation, disinfectant residuals, different materials in concert, etc.). Also, it is still completely unclear whether material-specific microbial communities establish when similar plumbing materials are used in different locations, or what exactly the impact of source water differences (e.g., community composition) are on the microbiome development. In similar vein, research is needed on whether specific materials (additives) favor the establishment of specific opportunistic pathogens. Finally, with respect to building plumbing there are clear research opportunities in the field of new material design/development. On the one hand, there is interest in developing anti-microbial strategies focusing on surface-coatings (e.g., copper or silver⁹⁵, or novel anti-microbial compounds). Similarly, there is ongoing research on

materials with anti-adhesive properties to combat fouling⁹⁶. On the other hand, we propose that material design might also move towards exploring the management of a 'good', stable microbial community composition. In this regard, Wang and colleagues⁹³ proposed a *probiotic approach* in which they would introduce specific bacteria into the building plumbing system, potentially coupled with a prebiotic approach of creating favorable conditions for such organisms in building plumbing systems. With respect to the latter, one option would be to tailor the leaching properties of a specific material (nutrient type, rate) to selected *probiotic* microorganisms in order to sustain their presence/dominance in a plumbing system.

Conclusions

- Conditions within building plumbing systems impact and change the microbial community composition of the water, potentially resulting in quality deterioration.
- Flexible synthetic materials leach organic carbon which not only increases the potential for bacterial growth but also drives selection within the establishing biofilm community.
- Ecological principles can be used to understand and quantify microbial growth dynamics and their dependency on engineered components of plumbing systems.
- Gaining and sharing knowledge on the interaction between material properties and microbiology provides stakeholders with the possibility to actively manage building plumbing microbiology through material design, material selection, and operation.
- The exclusive use of high-quality materials in new building plumbing systems poses a straightforward strategy towards managing the building plumbing microbiome.

Acknowledgements

The authors thank Roland Widler (formerly Geberit International AG, Jona, Switzerland) and Marcel Lüscher (formerly: GF JRG AG Sissach, Switzerland) for their professional input on building plumbing materials and their applications (Table 1).

References

1. **Proctor**, C. R. & Hammes, F. Drinking water microbiology - from measurement to management. *Curr. Opin. Biotechnol.* 33, 87–94 (2015).
2. **Hammes**, F. *et al.* Flow-cytometric total bacterial cell counts as a descriptive microbiological parameter for drinking water treatment processes. *Water Res* 42, 269–277 (2008).
3. **Rinta-Kanto**, J. M., Lehtola, M. J., Vartiainen, T. & Martikainen, P. J. Rapid enumeration of virus-like particles in drinking water samples using SYBR green I-staining. *Water Res.* 38, 2614–2618 (2004).
4. **Vital**, M. *et al.* Flow cytometry and adenosine tri-phosphate analysis: Alternative possibilities to evaluate major bacteriological changes in drinking water treatment and distribution systems. *Water Res.* 46, 4665–4676 (2012).
5. **Besmer**, M. D. & Hammes, F. Short-term microbial dynamics in a drinking water plant treating groundwater with occasional high microbial loads. *Water Res.* 107, 11–18 (2016).
6. **Stadler**, H. *et al.* The spectral absorption coefficient at 254nm as a real-time early warning proxy for detecting faecal pollution events at alpine karst water resources. *Water Sci. Technol.* 62, 1898–1906 (2010).
7. **Jung**, A.-V. *et al.* Microbial Contamination Detection in Water Resources : Interest of Current Optical Methods , Trends and Needs in the Context of Climate Change. *Int. J. Environ. Res. Public Heal.* 11, 4292–4310 (2014).
8. **Ma**, X., Vikram, A., Casson, L. & Bibby, K. Centralized Drinking Water Treatment Operations Shape Bacterial and Fungal Community Structure. *Environ. Sci. Technol.* 51, 7648–7657 (2017).
9. **Bruno**, A. *et al.* Changes in the Drinking Water Microbiome: Effects of Water Treatments Along the Flow of Two Drinking Water Treatment Plants in a Urbanized Area, Milan (Italy). *Front. Microbiol.* 9, 1–12 (2018).
10. **Pinto**, A. J., Xi, C. & Raskin, L. Bacterial community structure in the drinking water microbiome is governed by filtration processes. *Env. Sci Technol* 46, 8851–8859 (2012).
11. **Niquette**, P., Servais, P. & Savoiron, R. Bacterial dynamics in the drinking water distribution system of Brussels. *Water Res.* 35, 675–682 (2001).
12. **Henne**, K., Kahlisch, L., Brettar, I. & Höfle, M. G. Analysis of structure and composition of bacterial core communities in mature drinking water biofilms and bulk water of a citywide network in Germany. *Appl Env. Microbiol* 78, 3530–3538 (2012).
13. **Lührig**, K. *et al.* Bacterial Community Analysis of Drinking Water Biofilms in Southern Sweden. *Microbes Environ.* 30, 99–107 (2015).
14. **Ling**, F., Whitaker, R., LeChevallier, M. W. & Liu, W.-T. Drinking water microbiome assembly induced by water stagnation. *ISME J.* 12, 1520–1531 (2018).
15. **Ji**, P., Rhoads, W. J., Edwards, M. A. & Pruden, A. Impact of water heater temperature setting and water use frequency on the building plumbing microbiome. *ISME J.* 11, 1318–1330 (2017).
16. **Inkinen**, J. *et al.* Drinking water quality and formation of biofilms in an

- office building during its first year of operation , a full scale study. *Water Res* 9, 83–91 (2014).
17. **Liu, G. et al.** Pyrosequencing reveals bacterial communities in unchlorinated drinking water distribution system: an integral study of bulk water, suspended solids, loose deposits, and pipe wall biofilm. *Env. Sci Technol* 48, 5467–5476 (2014).
 18. **Wingender, J. & Flemming, H.-C.** Contamination potential of drinking water distribution network biofilms. *Water Sci.* 49, 277–286 (2004).
 19. **Lehtola, M. J. et al.** Microbiology, chemistry and biofilm development in a pilot drinking water distribution system with copper and plastic pipes. *Water Res.* 38, 3769–3779 (2004).
 20. **Departement of Industrial Plants.** Drinking water distribution, City of Zurich. (2019). Available at: <https://www.stadt-zuerich.ch/dib/de/index/wasserversorgung/trinkwasser.html>.
 21. **Hammes, F. et al.** Flow-cytometric total bacterial cell counts as a descriptive microbiological parameter for drinking water treatment processes. *Water Res.* 42, 269–277 (2008).
 22. **Liu, J. et al.** Bacterial community radial-spatial distribution in biofilms along pipe wall in chlorinated drinking water distribution system of East China. *Appl. Microbiol. Biotechnol.* 101, 749–759 (2017).
 23. **EU Comission, D. W. D.** DWD 98/83/EC.
 24. **EPA.** SAFE DRINKING WATER ACT (SDWA). 1–144 (2018).
 25. **Prest, E. I., Hammes, F., van Loosdrecht, M. C. M. & Vrouwenvelder, J. S.** Biological stability of drinking water: Controlling factors, methods, and challenges. *Front. Microbiol.* 7, 1–24 (2016).
 26. **Nescerecka, A., Rubulis, J., Vital, M., Juhna, T. & Hammes, F.** Biological instability in a chlorinated drinking water distribution network. *PLoS One* 9, e96354 (2014).
 27. **Prest, E. I., Weissbrodt, D. G., Hammes, F., Loosdrecht, M. C. M. Van & Vrouwenvelder, J. S.** Long-Term Bacterial Dynamics in a Full-Scale Drinking Water Distribution System. *PLoS One* 1–20 (2016). doi:10.1371/journal.pone.0164445
 28. **McCoy, S. T., Vanbriesen, J. M. & Asce, M.** Temporal Variability of Bacterial Diversity in a Chlorinated Drinking Water Distribution System. *J. Environ. Eng.* 138, 786–795 (2012).
 29. **Stanish, L. F. et al.** Factors Influencing Bacterial Diversity and Community Composition in Municipal Drinking Waters in the Ohio River Basin, USA. *PLoS One* 11, 1–21 (2016).
 30. **Potgieter, S. et al.** Long-term spatial and temporal microbial community dynamics in a large-scale drinking water distribution system with multiple disinfectant regimes. *Water Res.* 139, 406–419 (2018).
 31. **Haig, S., Kotlarz, N., Lipuma, J. J. & Raskin, L.** A High-Throughput Approach for Identification of Nontuberculous Mycobacteria in Drinking Water Reveals Relationship between Water Age and Mycobacterium avium. *MBio* 9, 1–13 (2018).
 32. **LeChevallier, M. W., Welch, N. J. & Smith, D. B.** Full-scale studies of factors related to coliform regrowth in drinking water. *Appl. Environ. Microbiol.*

- 62, 2201–2211 (1996).
33. **Buse**, H. Y., Lu, J., Lu, X., Mou, X. & Ashbolt, N. J. Microbial diversities (16S and 18S rRNA gene pyrosequencing) and environmental pathogens within drinking water biofilms grown on the common premise plumbing materials unplasticized polyvinylchloride and copper. *FEMS Microbiol Ecol* 88, 280–295 (2014).
 34. **Williams**, M. M., Armbruster, C. R. & Arduino, M. J. Plumbing of hospital premises is a reservoir for opportunistically pathogenic microorganisms: a review. *Biofouling* 29, 147–62 (2013).
 35. **Moritz**, M. M., Flemming, H. C. & Wingender, J. Integration of *Pseudomonas aeruginosa* and *Legionella pneumophila* in drinking water biofilms grown on domestic plumbing materials. *Int. J. Hyg. Environ. Health* 213, 190–197 (2010).
 36. **Zlatanovi**, L., Hoek, J. P. Van Der & Vreeburg, J. H. G. An experimental study on the influence of water stagnation and temperature change on water quality in a full-scale domestic drinking water system. 123, 761–772 (2017).
 37. **Bédard**, E., Laferrière, C., Déziel, E. & Prévost, M. Impact of stagnation and sampling volume on water microbial quality monitoring in large buildings. *PLoS One* 1–14 (2018). doi:10.1371/journal.pone.0199429
 38. **Verbraucherschutz**, B. der J. un für & Justiz, B. für. Verordnung über die Qualität von Wasser für den menschlichen Gebrauch (Trinkwasserverordnung - TrinkwV). (2018).
 39. **Bundesministerium für Wirtschaft**. Verordnung über Allgemeine Bedingungen für die Versorgung mit Wasser (AVBWasserV). 1980, (2014).
 40. **Open Data Zürich**. Gebäude und Wohnungen nach Gebäudeart und Stadtquartier seit 2008. (2008). Available at: https://data.stadt-zuerich.ch/dataset/bau_best_geb_whg_bev_gebaeudeart_quartier_seit2008.
 41. **Liu**, G., Van der Mark, E. J., Verberk, J. Q. & Van Dijk, J. C. Flow cytometry total cell counts: a field study assessing microbiological water quality and growth in unchlorinated drinking water distribution systems. *Biomed Res Int* 2013, 1–10 (2013).
 42. **Lin**, S., Wang, X., Chao, Y., He, Y. & Liu, M. Predicting biofilm thickness and biofilm viability based on the concentration of carbon-nitrogen-phosphorus by support vector regression. *Environ. Sci. Pollut. Res.* 23, 418–425 (2016).
 43. **Prévost**, M. *et al.* Suspended bacterial biomass and activity in full-scale drinking water distribution systems: Impact of water treatment. *Water Res.* 32, 1393–1406 (1998).
 44. **Liu**, R. *et al.* Molecular analysis of long-term biofilm formation on PVC and cast iron surfaces in drinking water distribution system. *J. Environ. Sci.* 26, 865–874 (2014).
 45. **Kim**, J. *et al.* Hydrodynamic effects on bacterial biofilm development in a microfluidic environment. *RSC Publ.* 13, 1846–1849 (2013).
 46. **Fang**, H., Chen, Y., Huang, L. & He, G. Analysis of biofilm bacterial communities under different shear stresses using size-fractionated

- sediment. *Sci. Rep.* 7, 1–14 (2017).
47. **Douterelo**, I., Sharpe, R. L. & Boxall, J. B. Influence of hydraulic regimes on bacterial community structure and composition in an experimental drinking water distribution system. *Water Res.* 47, 503–516 (2013).
 48. **Fish**, K., Osborn, A. M. & Boxall, J. B. Biofilm structures (EPS and bacterial communities) in drinking water distribution systems are conditioned by hydraulics and influence discoloration. *Sci. Total Environ.* 593–594, 571–580 (2017).
 49. **Henne**, K., Kahlisch, L., Ho, M. G. & Brettar, I. Seasonal dynamics of bacterial community structure and composition in cold and hot drinking water derived from surface water reservoirs. *Water Res.* 47, 5614–5630 (2013).
 50. **Lautenschlager**, K., Boon, N., Wang, Y., Egli, T. & Hammes, F. Overnight stagnation of drinking water in household taps induces microbial growth and changes in community composition. *Water Res.* 44, 4868–4877 (2010).
 51. **Proctor**, C. R., Reimann, M., Vriens, B. & Hammes, F. Biofilms in shower hoses. *Water Res.* 131, 274–286 (2018).
 52. **Moerman**, A., Blokker, M., Vreeburg, J. & Hoek, J. P. Van Der. Drinking Water Temperature Modelling in Domestic Systems. *Procedia Eng.* 89, 143–150 (2014).
 53. **Nguyen**, C., Elfland, C. & Edwards, M. Impact of advanced water conservation features and new copper pipe on rapid chloramine decay and microbial regrowth. *Water Res.* 46, 611–621 (2011).
 54. **Rhoads**, W. J., Pruden, A. & Edwards, M. A. Survey of green building water systems reveals elevated water age and water quality concerns. *Environ. Sci. Water Res. Technol.* 2, 164–173 (2016).
 55. **Hogt**, A. H., Dankert, J. & Feijen, J. Adhesion of *Staphylococcus epidermidis* and *Staphylococcus saprophyticus* to a Hydrophobic Biomaterial. *J. Gen. Microbiol.* 131, 2485–2491 (1985).
 56. **Connell**, M. *et al.* PEX and PP water pipes: Assimilable carbon, chemicals, and odors. *J. Am. Water Works Assoc.* 108, E192–E204 (2016).
 57. **Bucheli-Witschel**, M., Koetzsch, S., Darr, S., Widler, R. & Egli, T. A new method to assess the influence of migration from polymeric materials on the biostability of drinking water. *Water Res.* 46, 4246–4260 (2012).
 58. **Schiller**, M. *PVC Additives.* (2015).
 59. **Skjevraak**, I., Due, A., Gjerstad, K. O. & Herikstad, H. Volatile organic components migrating from plastic pipes (HDPE, PEX and PVC) into drinking water. *Water Res.* 37, 1912–20 (2003).
 60. **BASF**. Irgafos® 168. 1–2 (2010).
 61. **Löschner**, D. *et al.* Experience with the application of the draft European Standard prEN 15768 to the identification of leachable organic substances from materials in contact with drinking water by GC-MS. *Anal. Methods* 3, 2547–2556 (2011).
 62. **Graham**, P. R. Phthalate Ester Plasticizers-Why and How They Are Used. *Environ. Health Perspect.* 3–12 (1973).
 63. **Erythropel**, H. C., Maric, M., Nicell, J. A., Leask, R. L. & Yargeau, V.

- Leaching of the plasticizer di(2-ethylhexyl)phthalate (DEHP) from plastic containers and the question of human exposure. *Appl. Microbiol. Biotechnol.* 98, 9967–9981 (2014).
64. **Wen**, G., Koetzsch, S., Vital, M., Egli, T. & Ma, J. BioMig - A Method to Evaluate the Potential Release of Compounds from and the Formation of Biofilms on Polymeric Materials in Contact with Drinking Water. *Environ. Sci. Technol.* 49, 11659–11669 (2015).
 65. **Zhang**, L. & Liu, S. Investigation of organic compounds migration from polymeric pipes into drinking water under long retention times. *Procedia Eng.* 70, 1753–1761 (2014).
 66. **EN16421**, D. *Influence of Materials on Water for Human Consumption Enhancement of Microbial Growth (EMG)*. (2014). doi:SS-EN 16421:2014
 67. **Bundesamt**, U. *Leitlinie zur hygienischen Beurteilung von organischen Materialien im Kontakt mit Trinkwasser*. (2016).
 68. **Koetzsch**, S. & Egli, T. Kunststoffe in Kontakt mit Trinkwasser. *Aqua & Gas* 3, 44–52 (2016).
 69. **Mao**, G., Wang, Y. & Hammes, F. Short-term organic carbon migration from polymeric materials in contact with chlorinated drinking water. *Sci. Total Environ.* 613–614, 1220–1227 (2018).
 70. **Proctor**, C. R. *et al.* Biofilms in shower hoses - choice of pipe material influences bacterial growth and communities. *Environ. Sci. Water Res. Technol.* 2, 670–682 (2016).
 71. **Benölken**, J., Dorsch, T., Wichmann, K. & Bendinger, B. Praxisnahe Untersuchungen zur Kontamination von Trinkwasser in halbtechnischen Trinkwasser-Installationen. *IWW Schriftenreihe - Vermeidung und Sanierung von Trinkwasserkontaminationen durch hygienisch relevante Mikroorganismen aus Biofilmen der Hausinstallation* 54, 101–180 (2010).
 72. **van der Kooij**, D. & van der Wielen, P. W. *Microbial Growth in Drinking-Water Supplies*. (2014).
 73. **Nemergut**, D. R. *et al.* Patterns and Processes of Microbial Community Assembly. *MMBR* 77, 342–356 (2013).
 74. **Vellend**, M. Conceptual Synthesis in Community Ecology. (2014). doi:10.1086/652373
 75. **van der Kooij**, D. Assimilable organic carbon as an indicator of bacterial regrowth. *J. / Am. Water Work. Assoc.* 84, 57–65 (1992).
 76. **Stadt Zurich**, W. The Quality of Zurich's Drinking Water. 1–2
 77. **Boks**, N. P., Busscher, H. J., van der Mei, H. C. & Norde, W. Bond-Strengthening in Staphylococcal Adhesion to Hydrophilic and Hydrophobic Surfaces Using Atomic Force Microscopy. *Langmuir* 24, 12990–12994 (2008).
 78. **Schwab**, U., Hu, Y., Wiedmann, M. & Boor, K. J. Alternative sigma factor σ_B is not essential for *Listeria monocytogenes* surface attachment. *J. Food Prot.* 68, 311–317 (2005).
 79. **Kooij**, D. Van Der, Visser, A. & Hijnen, W. A. M. Determining the concentration of easily assimilable organic carbon in drinking. *Am. Water Work. Assoc.* (1982). doi:10.1002/j.1551-8833.1982.tb05000.x
 80. **Hammes**, F. A. & Egli, T. New method for assimilable organic carbon

- determination using flow-cytometric enumeration and a natural microbial consortium as inoculum. *Env. Sci Technol* 39, 3289–3294 (2005).
81. **van der Kooij**, D., Visser, A. & Hijnen, W. Determining the Concentration of Easily Assimilable Organic Carbon in Drinking Water. *J Am Water Work. Assoc* 540–545 (1982).
 82. **Waines**, P. L., Moate, R., Moody, A. J., Allen, M. & Bradley, G. The effect of material choice on biofilm formation in a model warm water distribution system. *Biofouling* 27, 1161–1174 (2011).
 83. **Whelton**, A. J. & Cooney, M. F. We Need Our Customers to Complain. *Opflow* 30, 1–7 (2004).
 84. **Shah**, P. *et al.* Legionnaires' Disease Surveillance Summary Report, United States. *Centers Dis. Control Prev.* (2019).
 85. **Bundesamt für Gesundheit BAG**. Zahlen zu Infektionskrankheiten: Legionellose. (2019).
 86. **Richards**, A. M., Von Dwingelo, J. E., Price, C. T. & Kwaik, Y. A. Cellular microbiology and molecular ecology of Legionella-amoeba interaction. *Virulence* 4, 307–314 (2013).
 87. **Falkinham**, J., Pruden, A. & Edwards, M. Opportunistic Premise Plumbing Pathogens: Increasingly Important Pathogens in Drinking Water. *Pathogens* 4, 373–386 (2015).
 88. **Völker**, S., Schreiber, C. & Kistemann, T. Drinking water quality in household supply infrastructure-A survey of the current situation in Germany. *Int. J. Hyg. Environ. Health* 213, 204–209 (2010).
 89. **Bédard**, E., Prévost, M. & Déziel, E. Pseudomonas aeruginosa in premise plumbing of large buildings. *Microbiologyopen* 5, 937–956 (2016).
 90. **Feazel**, L. M. *et al.* Opportunistic pathogens enriched in showerhead biofilms. *PNAS* 106, 16393–16399 (2009).
 91. **Falkinham**, J. O. Reducing human exposure to mycobacterium avium. *Ann. Am. Thorac. Soc.* 10, 378–382 (2013).
 92. **Gebert**, M. J. *et al.* Ecological Analyses of Mycobacteria in Showerhead Biofilms and Their Relevance to Human Health. *MBio* 9, 1–15 (2018).
 93. **Wen**, G., Kötzsch, S., Vital, M., Egli, T. & Ma, J. BioMig-A Method to Evaluate the Potential Release of Compounds from and the Formation of Biofilms on Polymeric Materials in Contact with Drinking Water. *Environ. Sci. Technol.* 49, 11659–69 (2015).
 94. **Vital**, M., Stucki, D., Egli, T. & Hammes, F. Evaluating the growth potential of pathogenic bacteria in water. *Appl. Environ. Microbiol.* 76, 6477–6484 (2010).
 95. **Stüken**, A. *et al.* Microbial Community Composition of Tap Water and Biofilms Treated with or without Copper-Silver Ionization. *Environ. Sci. Technol.* 52, 3354–3364 (2018).
 96. **Golberg**, K. *et al.* Novel Anti-Adhesive Biomaterial Patches : Preventing Biofilm with Metal Complex Films (MCF) Derived from a Microalgal Polysaccharide. 1–11 (2016). doi:10.1002/admi.201500486

Chapter 3

Ugly ducklings – The dark side of plastic materials in contact with potable water

This chapter has been published in *npj Biofilms and Microbiomes* (2018, 4:7) by L. Neu, C. Bänziger, C.R. Proctor, Y. Zhang, W.-T. Liu, and F. Hammes.

Abstract

Bath toys pose an interesting link between flexible plastic materials, potable water, external microbial and nutrient contamination, and potentially vulnerable end-users. Here, we characterized biofilm communities inside 19 bath toys used under real conditions. In addition, some determinants for biofilm formation were assessed, using six identical bath toys under controlled conditions with either clean water prior to bathing or dirty water after bathing. All examined bath toys revealed notable biofilms on their inner surface, with average total bacterial numbers of 5.5×10^6 cells/cm² (clean water controls), 9.5×10^6 cells/cm² (real bath toys), and 7.3×10^7 cells/cm² (dirty water controls). Bacterial community compositions were diverse, showing many rare taxa in real bath toys and rather distinct communities in control bath toys, with a noticeable difference between clean and dirty water control biofilms. Fungi were identified in 58 % of all real bath toys and in all dirty water control toys. Based on the comparison of clean water and dirty water control bath toys, we argue that bath toy biofilms are influenced by (1) the organic carbon leaching from the flexible plastic material, (2) the chemical and biological tap water quality, (3) additional nutrients by care products and human body fluids in the bath water, as well as, (4) additional bacteria from dirt and/or the end-users' microbiome. The present study gives a detailed characterization of bath toy biofilms and a better understanding of determinants for biofilm formation and development in systems comprising plastic materials in contact with potable water.

Introduction

Unwanted microbial growth in the built environment is frequently reported. Bathroom conditions in particular are known to promote biofilm formation and growth due to moderately high temperatures and increased humidity^{1,2}. In this regard, unwanted microbial growth has been reported, e.g., for basins, bath tubs, and drains^{3,4}, as well as for shower fixtures⁵⁻⁷ and shower curtains⁸. In the same environment, bath toys, best known for so-called 'rubber ducks', present an interesting junction between potentially vulnerable end-users and several determining factors for such growth, namely (1) low quality polymeric material, (2) potable water from the building plumbing, and (3) additional nutrients and microbial contamination by bathing.

Synthetic polymeric materials in contact with potable water not only adsorb some organic matter from the water⁹, but also release substantial amounts of organic carbon through migration, leakage, leaching, and/or permeation, including, e.g., plasticizers, stabilizers and antioxidants¹⁰⁻¹³. A fraction of this organic carbon is biodegradable and offers microorganisms a significant source of assimilable organic carbon (AOC)¹⁴⁻¹⁶. This AOC in turn promotes microbial growth and biofilm formation¹⁶⁻¹⁹ and influences the microbial community composition^{5,20,21}. Flexible polymeric materials, which are typically used in the production of bath toys, are particularly known for excessive carbon leaching and unwanted biofilm formation and growth^{16,20}.

One source of pioneer microorganisms for bath toy biofilms is the tap water microbiome, which differs substantially between different locations^{22,23}. Tap water comprises complex microbial communities and in many cases also opportunistic pathogens such as *Pseudomonas aeruginosa*²⁴⁻²⁶, *Legionella pneumophila*²⁷, and *Mycobacterium avium*²⁸. However, nutrients from tap water typically do not contribute to excessive microbial growth, as it is an oligotrophic environment^{29,30}.

A second, and potentially more dominant, source of microorganisms is the used bath water, which exposes bath toys to microorganisms from both the human microbiome as well as from external/environmental microbial contamination^{22,31}. In addition, bath water is a substantial source of supplementary organic and inorganic nutrients, introduced by care products (soap, shampoo, conditioner) and the human body itself, e.g., in form of urine residuals^{32,33}.

Apart from aesthetic issues, potential problems with contaminated bath toys have been recognized before. Several decades ago, a study by Ruschke² suggested that bath toys not only facilitate microbial growth, but specifically the proliferation of opportunistic pathogens and unwanted organisms, such as *P. aeruginosa* or *Enterococcus* spp.. Approximately 20 years later, a multidrug-resistant *P. aeruginosa* outbreak in a children's hospital was linked to shared bath toys³⁴. That study showed that *Pseudomonas* spp. was only present in the bath toys and not detectable in the bath water itself, making this the first connection between plastic bath toys and children's infections. While scientific studies on the topic are limited, many parents are seemingly well aware of this biofouling phenomenon, which is evidenced by numerous internet blogs and discussion groups on the topic (e.g., www.blogs.babycenter.com or www.welovebeingmoms.blogspot.ch; Table S1).

The aims of the present study were (1) to provide a comprehensive characterization of biofilms grown on the inside of real bath toys to elucidate this phenomenon, and (2) to establish a better understanding of the factors that drive the development of these biofilms. For the first, we studied biofilms from used bath toys that were collected from random households (real bath toys). These were characterized by their appearance, microbial abundance and community composition. For the second, we examined and compared biofilms that were established in new, identical bath toys under controlled

conditions simulating actual use in clean and dirty bath water (control bath toys). The resulting data enabled conclusions on the impact of material composition, water characteristics, and external contamination on biofilm formation in these unique environments, as well as recommendations to mitigate the potential microbial risks for vulnerable users.

Materials and Methods

Bath toy samples

We collected 19 real bath toys (e.g., rubber ducks) from five different Swiss households, where the number of samples was determined by availability. Due to privacy concerns of underage users, no specific information about the age of these bath toys or habits of use was collected. Moreover, no details about the bath toy producers, origin of materials, or water composition were compiled as all bath toys have been used for long time periods. For comparison, six bath toys were used under controlled conditions. These control bath toys were identical, purchased from a single batch, and used in an adult-only household over a period of 11 weeks with baths every second day. The control bath toys were divided into two categories – three bath toys (experimental replicates) were exposed to clean water before bathing, while three were exposed to the used bath water after bathing. The unused bath water was non-chlorinated groundwater and the used bath water was in all cases exposed to one adult using a commercially available soap product. Each control bath toy was filled three times with water, which was immediately squeezed out again, followed by a storage of the bath toys for two days on a shelf in the bathroom prior to reuse. After 11 weeks (equaling 39 exposures) the bath toys were transported to the laboratory, stored at 4 °C, and processed on the same day.

Biofilm visualization

Each bath toy was cleaned on the outside with 70 % ethanol and then dissected in half to access and characterize the biofilms on the inner surface. One half was used for biofilm analysis (below), while the other was photographed and used for further image analysis. The structure and thickness of selected bath toys' biofilms were visualized with optical coherence

tomography (OCT), using a Spectral Domain OCT Imaging System (930nm, OCT System Ganymede, Thorlabs GmbH, Dachau, Germany). Due to the heterogeneous biofilm distribution on the uneven toy surfaces, no data was collected for an overall quantification, but an approximate upper limit for biofilm thickness in analyzed bath toys could be set. For the visualization with scanning electron microscopy (SEM), 1 cm² pieces of some real bath toys were chosen. Samples were fixed with 2.5 % Glutaraldehyde in Cacodylate buffer (0.1 M, pH 7.2) for one hour at room temperature, and thereafter stored in Cacodylate buffer at 4 °C. Final sample preparation and imaging was done by the Center for Microscopy and Image Analysis, University of Zurich.

Biofilm removal

Biofilms were removed from the inner surface of bath toys using an electric toothbrush (Oral-B®, Advanced Power) as follows: one half of each bath toy was put into a sterile beaker and submerged in 100 - 150 mL ultrapure water. The biofilm was then removed by brushing the bath toys' surface for approximately 2 min and this suspension was collected in 50 mL tubes (CellStar® Tube, Greiner Bio-One). The whole procedure was repeated once with fresh ultrapure water to make sure all biofilm was removed. Biofilm clumps and clusters were subsequently dispersed with a sonication needle (Sonopuls HD 2200, Bandelin Sonorex, Rangendingen, Germany) for 30 seconds at 50 % power and 40 % intensity. Thereafter, the biofilm suspensions of one bath toy were combined in a sterile SCHOTT® bottle and the volume was filled up with ultrapure water to a total volume of 500 mL. The toothbrush heads were replaced for each sample to avoid cross contamination.

Flow cytometric cell counting

Flow cytometry (FCM) was used to determine the number of total and intact bacterial cells present in the biofilm suspensions. Measurements and analysis

were performed as described elsewhere ³⁵. In short, biofilm suspensions were diluted 1:100 with ultrapure water. 500 µL of each sample were either stained with 5 µL SYBR[®] Green I (SG, Invitrogen AG, Basel, Switzerland; 100x diluted in Tris buffer, pH 8) to detect the total cell concentration (TCC) or with 5 µL SG with additional propidium iodide (PI; final concentration of 0.3 mM) to quantify the intact cell concentration (ICC). Prior to measurements, samples were incubated for 10 min at 37 °C. A BD Accuri C6[®] flow cytometer (BD Accuri Cytometers, Belgium) was used, applying the same settings and gating strategy as described previously ³⁵. All samples were measured in triplicate.

Next generation sequencing for bacterial and fungal community compositions

MiSeq[®] Sequencing (Illumina, Inc., San Diego, CA) was chosen to study the community compositions of the bath toy biofilms. For that, the biofilm suspensions were concentrated on 0.22 µm polycarbonate Nucleopore[®] membrane filters (Ø 47 mm, Whatman, Kent, UK), using sterile filter units under vacuum pressure. The filtered volume was in all cases 490 mL (± 5 mL). DNA was extracted according to the protocol of the PowerWater DNA Isolation Kit (MoBio Laboratories, Inc., Carlsbad, CA) and quantified with a Qubit[®] 2.0 Fluorometer (Invitrogen, LT Holdings Pte Ltd, Singapore). For each sample, 1 ng of DNA was amplified by polymerase chain reaction (PCR) (for settings see Table S7), using Bakt_341F and Bakt_805R primers ³⁶ for the targeted V3-V5 region of the 16S rDNA (final concentration 0.3 µM). Specific barcoded Nextera XT v2 Index Kit adapters (Illumina) were added to the amplicons via Index PCR (for settings see Table S7). The Agencourt[®] AMPure[®] XP system (Beckman Coulter, Inc., Brea, CA) was performed after both amplification steps for purification. After successful amplification, PCR products were again quantified with a Qubit Fluorometer, followed by a normalization to concentrations of 4 nM (10 mM Tris, pH 8.0). 10 µL of each normalized sample were pooled and thereafter quantified to ensure the final concentration. The sequencing was run at the MiSeq platform, adding 10 % PhiX for quality control.

Data for this community composition analysis was generated in collaboration with the Genetic Diversity Centre (GDC), ETH Zurich.

For DNA analysis, first, primer sites of all sequences were trimmed followed by merging overlapping reads. Second, sequences were filtered according to their quality which was validated in a Quality report (FastQC v0.11.2). Finally, sorted reads were taxonomically assigned using QIIME with phylogenetic analysis for OTU sequences by PyNAST alignment. Here, a 97 % identify cut-off as well as an abundance baseline of 2 was approached for clustering. Even though clustering based on a 97 % similarity allows an identification as specific as genus level, this was not the case for most of the OTUs in this study. Hence, most of the community composition-based analyses focused on the lowest classification level that was common for most of them, which was family. Further data processing was conducted in RStudio (Version 0.99.902) using the packages 'ggplot2' and 'phyloseq'. All samples were scaled to an even minimum depth of 30'133 reads, which correlated to a total of 12'229 OTUs. Here, two real bath toy samples had to be excluded for further analysis due to low numbers of total reads. For DNA analysis of the fungal community composition, the ITS1 region of the extracted DNA was amplified using ITS1-F and ITS2 as described elsewhere ³⁷. Two sets of amplicons from each sample were obtained with primers of different barcode sequences. Owing to the low concentration of genomic DNA, samples that failed to be amplified during the first two rounds were tested with increasing template concentrations in the PCR reaction for another three times. The resulted amplicons were pooled with equal amount (100 ng) after quantification with Qubit. The pool was purified using the Wizard SV Gel and PCR Clean-Up system (Promega, Madison, WI) and sequenced using MiSeq paired-end reads (2 x 250 bp) at the Roy J. Carver Biotechnology Center (University of Illinois at Urbana-Champaign). The paired-end reads were aligned with Mothur ³⁸ and were further analyzed using QIIME with the QIIME/UNITE reference OTUs (alpha version 12_11) and default parameters for demultiplexing, quality filtering, and clustering reads into OTUs.

Conventional plating for specific bacterial groups

As children's infections by opportunistic pathogens pose a big concern regarding bath toys, conventional plating was used as a proof of principle for their potential presence. Here, Compact Dry Plates (HyServe, Germany) were used to detect fecal indicator organisms and opportunistic pathogens; specifically, *Escherichia coli* and Coliforms (EC), *Pseudomonas aeruginosa* (PA), *Listeria* spp. (LS), and Enterococcus spp. (ETC). Special agar plates (Legionella BMP a Selective Medium, PO5035A; Oxoid, Thermo Fisher, Wesel, Germany) were used for the detection of *Legionella pneumophila* (LEG). In this case, the biofilm suspensions were heat shocked (55 °C, 30 min) to eliminate other bacteria prior to plating. One milliliter of the biofilm suspensions was added to each Compact Dry Plate or LEG plate in triplicate. The plates were incubated at 37 °C for either 24 h (EC, ETC), 48 h (PA, LS) or 14 d (LEG), before counting the colony forming units (CFU). Here, colonies of distinct colors were counted following the manual. Only for EC plates, two different colors have been counted as assigned by the producer, distinguishing between coliforms and specifically *E. coli*.

BioMig assay to determine the bioavailability of migrating carbon compounds

A standardized material test ¹⁶ was used to assess the control bath toys for (1) the migration potential (MP) of organic carbon from the plastic material in contact with water and (2) the biomass formation potential (BFP), which relies on the migrated carbon. In short: For the MP, a surface area of 100 cm² from the control bath toys' material was incubated in filtered bottled mineral water (Evian, France), at 60 °C, over a period of 7 d. The water was exchanged every 24 h and the amount of total organic carbon (TOC) was measured after day 1, 3 and 7 (TOC-V_{CPH}, SHIMADZU GmbH, Switzerland). The BFP was determined by incubating 1 cm²-pieces of the material in unfiltered bottled water, at 30 °C, for 14 d, continuously shaking at 90 rpm. The number of planktonic bacteria

(pTCC) was measured with FCM as described above. The same was done for the number of bacteria in the biofilm (bTCC), with an anterior needle sonication to remove the biofilm from the material in 0.2 µm-filtered bottled water. Additionally, a growth-test was conducted to evaluate the general degradability of the released TOC. Therefore, water of the first migration period from the MP assay was used to determine the amount of AOC. The samples were inoculated with the natural microbial community of bottled water and incubated for 7 d at 30 °C, shaking. FCM was used to count the number of bacteria, followed by a re-calculation of the AOC-concentration needed for these cells to grow ^{39,40}.

Results

Visible and dense biofilms inside all bath toys

All bath toys analyzed in this study had dense and slimy biofilms on the inner surface (Figure 1A, Figure S1 for images of all bath toys). While most of the real bath toy biofilms (~70 %) had areas of black discoloration (indicative of mold growth), biofilms inside the control bath toys were transparent. The visual biofilm observation was confirmed by optical coherence tomography (OCT) analysis on selected bath toys, revealing heterogeneous biofilm shapes and thicknesses both within and between individual toys, ranging up to 100 μm (Figure 1B, Figure S2 for additional images). High resolution scanning electron microscopy (SEM) imaging of selected toys showed complex biofilm compositions with what appeared to be diverse microorganisms in a thick layer of extracellular polymeric substances (EPS) (Figure 1C, Figure S3 for additional images).

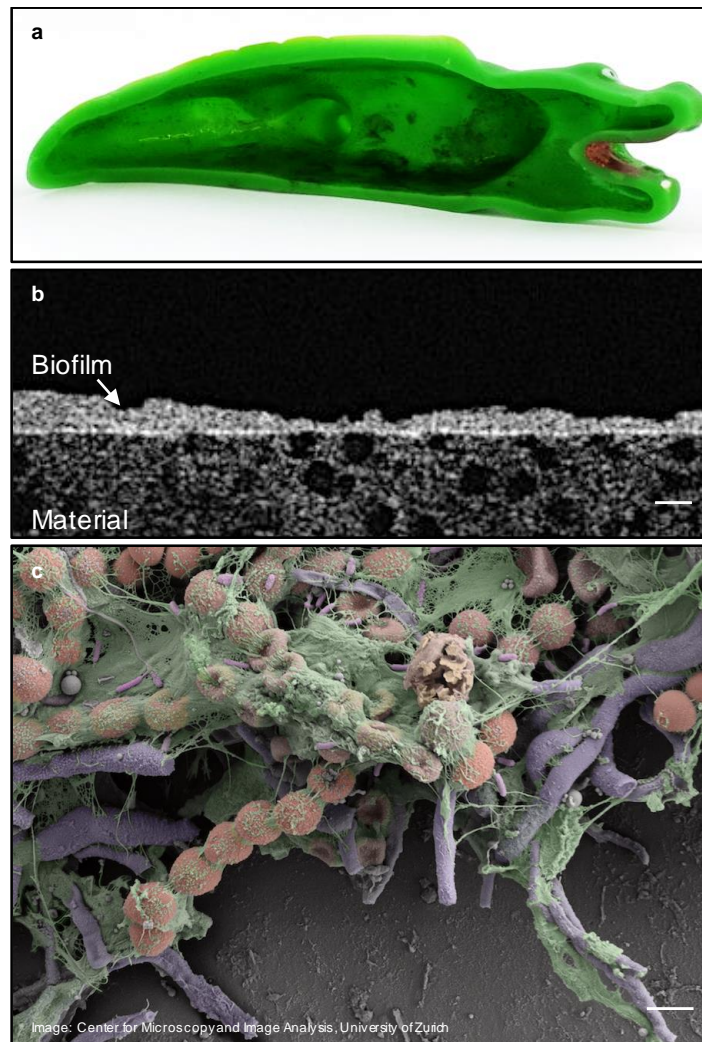


Figure 1 Visualization of biofilms on the inner surface of bath toys. (a) Example for a bath toy used under real conditions. (b) Optical coherence tomography image of the biofilm structure and thickness of the same bath toy (scale bar: 50 μm). (c) Scanning electron microscopy image revealing the complex structure and composition of these bath toy biofilms. Colors were added artificially to draw attention to varied structures (scale bar: 2 μm). For additional images, see supplementary information.

High numbers of bacteria in bath toy biofilms

All bath toy biofilms showed high but variable numbers of bacteria. The real bath toy biofilms had an average coverage of 9.5×10^6 cells/cm² (range: $0.1 - 2 \times 10^7$ cells/cm²), which equals an average of $1.3 \pm 0.07 \times 10^9$ cells/bath toy ($n = 19$) when calculated with the surface area of individual toys (Figure 2, Figure S4). In comparison, clean water controls were on average covered with

approximately half that number of cells ($5.5 \pm 0.08 \times 10^6$ cells/cm²; $n = 3$), which equals $1.2 \pm 0.03 \times 10^9$ cells/bath toy ($n = 3$). The highest coverage was observed on dirty water control toys with an average of $7.3 \pm 1.0 \times 10^7$ cells/cm² ($n = 3$), or $1.3 \pm 0.2 \times 10^{10}$ cells/bath toy ($n = 3$) respectively. Cell numbers in the dirty water controls were shown to be tenfold higher in magnitude than in the clean water controls (ANOVA, F-test, p -value 0.009; Shapiro-Wilk normality test). Viability analysis showed that the percentage of intact cells was on average 62.8 % (± 19.2 %, $n = 19$) in real bath toys, 27.2 % (± 14.2 %, $n = 3$) in clean, and 20.3 % (± 5.7 %, $n = 3$) in dirty water controls (Figure S4). The higher average value for intact cells in real bath toy biofilms was not statistically significant, neither against clean (ANOVA, F-Test, $p = 0.82$) nor against dirty water controls (ANOVA, F-Test, $p = 0.17$).

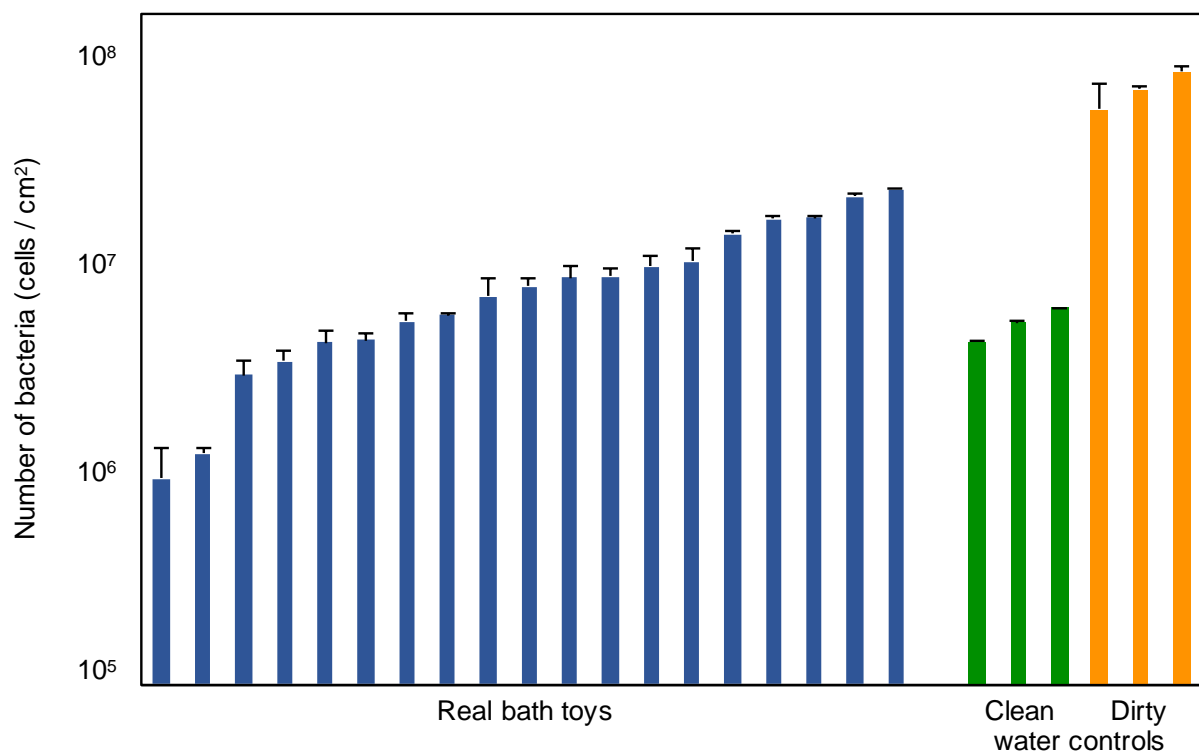


Figure 2 Number of bacteria in biofilms from the inner surface of bath toys. Flow cytometry was used to determine the number of bacterial cells in bath toy biofilms using SYBR® Green I staining following biofilm removal and dispersal. Bath toys were either from real households (real bath toys), or used under controlled conditions with clean water prior to bathing (clean water controls) or with used water after bathing (dirty water controls). Error bars represent standard deviation of triplicate measurements.

Diverse microbial communities in bath toy biofilms

Similarities and differences between biofilm bacterial communities

Overall, bath toy biofilms showed diverse communities. Remarkably, only eight out of a total of 12'229 operational taxonomic units (OTUs) were shared between all bath toys (i.e., control and real bath toys) (Table S2). Four of these OTUs could be classified on genus level, namely *Bradyrhizobium* spp., *Agrobacterium* spp., *Caulobacter* spp., and *Sphingomonas* spp.. The remaining OTUs belonged to the families Methylobacteriaceae, Comamonadaceae, and Microbacteriaceae, but could not be further identified to genus level (for more information see Table S2).

For the comparison of bacterial communities between single bath toys, a non-metric multidimensional scaling (NMDS) plot was used (Figure 3). Distances in this plot correlate with the degree of similarities between the biofilm communities, based on the similarity and frequency of OTUs detected in each of them. Samples that cluster closer to each other have a higher degree of similarity (e.g., Toy05 and Toy10) than samples that cluster further apart (e.g., Toy13 and Toy19; Figure 3).

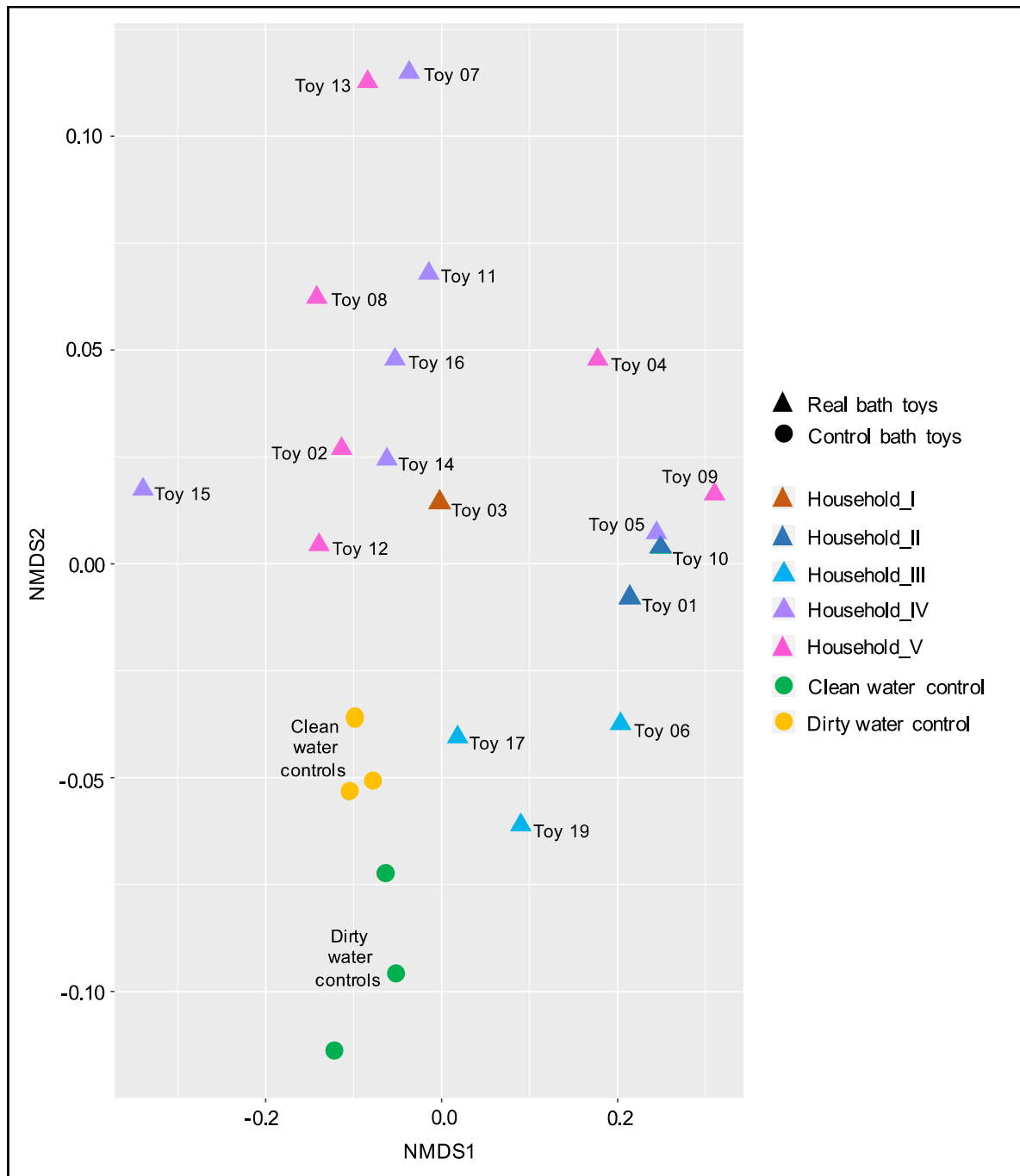


Figure 3 Non-metric multidimensional scaling (NMDS) plot to assess similarities in bacterial community compositions between bath toy biofilms. Filtered OTU sequences, scaled to an even sampling depth, were ordinated with the NMDS method using the Bray-Curtis distance matrix. Triangles represent real bath toy and circles control bath toy biofilm communities. Color codes for real bath toy samples indicate origination from five different Swiss households, while control bath toys are separated into clean and dirty water controls.

Real bath toys showed a diverse clustering, clearly indicating a different community composition in each toy (Figure 3). Yet, biofilm communities from multiple bath toys originating from one household showed variable levels of similarity. For example, the three samples from 'Household_III' clustered closer to each other than the six from 'Household_V', indicating more similarities within samples from 'Household_III'. Shared OTUs within bath toys from the same household varied between 1'445 ('Household_II', n = 2) and 29 ('Household_V', n = 6) (Table S3). Moreover, household-specific core communities could be identified (i.e., OTUs which were found in bath toy biofilms from a single household, but which were not found in other households; Table S3). However, this 'household specific core' represented only about $2.1 \pm 1.4 \%$ (n = 5) of the total number of reads in any given house. This result is inconclusive as the analysis is limited by the low number of samples in each household. Overall, only 13 OTUs were shared between real bath toy biofilms. These included the OTUs shared by all bath toy samples (see above), as well as *Methylobacterium* spp. and *Novosphingobium* spp., and the family Hyphomonadaceae (Table S2).

For the control bath toy biofilms, samples from clean water controls clustered separately from dirty water controls (Figure 3), with smaller distances between clean water control replicates compared to those of the dirty water controls. Forty-seven OTUs were shared amongst all control bath toys (Table S2). However, this number increases when distinguishing between clean and dirty water controls, with 72 shared OTUs in clean and 107 in dirty water controls. Most of the shared OTUs were representatives of the families that were already identified for real bath toys (see above). Additional shared OTUs belonged to diverse taxa within families such as Rhodobacteraceae, Rhodospirillaceae, Pseudomonadaceae, Bdellovibrionaceae, and Flavobacteriaceae. The shared OTUs diverged on closer classification, with, e.g., the genera *Methylobacterium* spp., *Streptococcus* spp., and *Planctomycetes* spp. well represented in clean water controls, and the genera *Rhodobacter* spp.,

Mycobacterium spp., and *Delftia* spp. well represented in dirty water controls (Table S2).

The diversity represented within each type of sample also varied (Table S4). Real bath toys showed on average a higher richness and more variation than control bath toys, ranging from 192 – 6'196 OTUs per bath toy ($1'506 \pm 1'776$, $n = 17$) compared to 188 – 268 (242 ± 33.9 , $n = 6$) in the controls. This is also reflected with higher Shannon-Wiener indices for real bath toys (0.42 ± 0.13 , $n = 17$), compared to both clean (0.22 ± 0.04 , $n = 3$) and dirty water controls (0.28 ± 0.04 , $n = 3$).

Most abundant bacterial OTUs in real and control bath toy biofilms

Due to the variable community compositions throughout real bath toy biofilms and among the controls, communities were characterized in more detail by focusing on the most abundant OTUs in each community. For this, OTUs with the highest number of reads within all bath toys of one category, namely real bath toys, clean water controls, and dirty water controls, were chosen (for a detailed identification of the most abundant OTUs in each individual real bath toy see Figure S5). The phylum *Proteobacteria* was the most abundant in real bath toy biofilms, followed by Bacteroidetes and Cyanobacteria (Figure 4, A). On family level (which was the lowest common level of classification), these most abundant OTUs were representatives of Comamonadaceae, Bradyrhizobiaceae, Caulobacteraceae, Sphingomonadaceae, Cytophagaceae, Rhizobiaceae, and Flavobacteriaceae; which, amongst others, have previously been identified in drinking water systems and corresponding biofilms ⁴¹⁻⁴⁷ or in fresh water systems (Rhodospirillaceae ⁴⁸). Some representatives of the families Comamonadaceae, Bradyrhizobiaceae, Sphingomonadaceae have previously been detected in human microbiota (e.g., gastrointestinal, oral, skin, airways) ⁴⁹⁻⁵¹. It should be noted that the ten most abundant OTUs compiled from the data of all real bath toys were not

necessarily representative of individual biofilms (Figure 4, A). In fact, these OTUs represented on average 33 % of the total number of reads, ranging 6 – 52 % (33 ± 16.5 %, $n = 17$) in individual bath toys, thus highlighting the diversity amongst all real bath toy biofilm communities. Interestingly, most of the identified abundant families in the Proteobacteria clade were identical between real and control bath toys, whereas the abundance of Actinobacteria, in particular the family Mycobacteriaceae, was only identified for control bath toys. In contrast to the real bath toys, the most abundant OTUs in control toys were considerably more representative of their community compositions, representing 73 % (± 7.8 , $n = 6$) of individual communities (Figure 4, B), hence revealing less diversity compared to real bath toy biofilms.

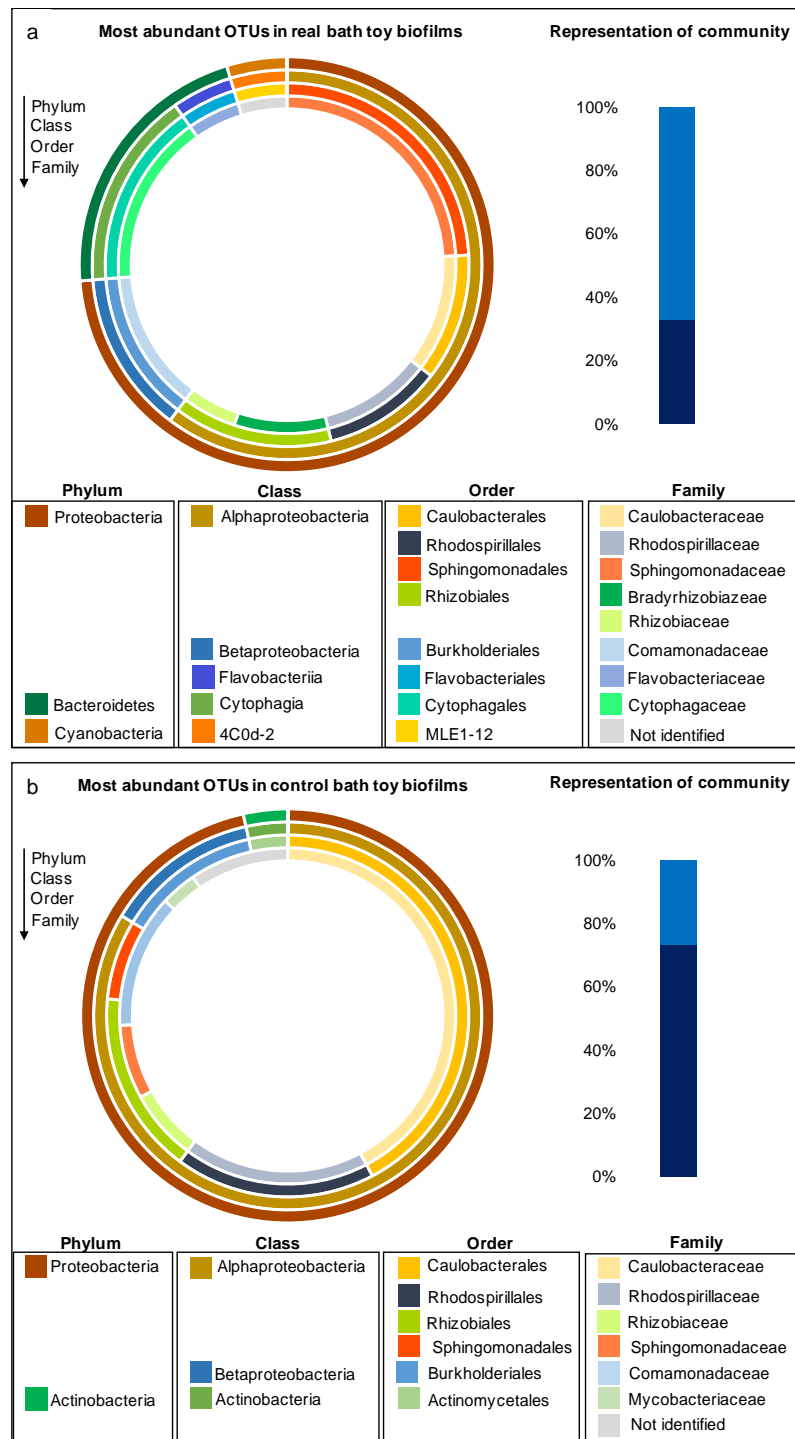


Figure 4 Classification of the ten most abundant operational taxonomic units (OTUs) for biofilm communities grown in real bath toys (a) or control bath toys (b). Outer to inner circles represent classifications from phylum to family level (the lowest common classification level). Bar plots represent the fraction of most abundant OTUs (dark blue bars) in comparison to the rest of the community (light blue bars).

Bathing events affect bacterial community composition in bath toy biofilms

In control bath toy biofilms, the ten most abundant OTUs were representative for the total community composition (see above). For clean water controls, the ten most abundant OTUs covered 87 % (± 2.6 , $n = 3$) of the total community composition, while those for dirty water controls accounted for 79 % (± 9.9 , $n = 3$) (Figure 5). Hence, we compared the most abundant OTUs of clean and dirty water control toys in more detail. Here, comparisons focus on families as this was the lowest common level for most of the OTUs (for deeper classification levels see Table S5).

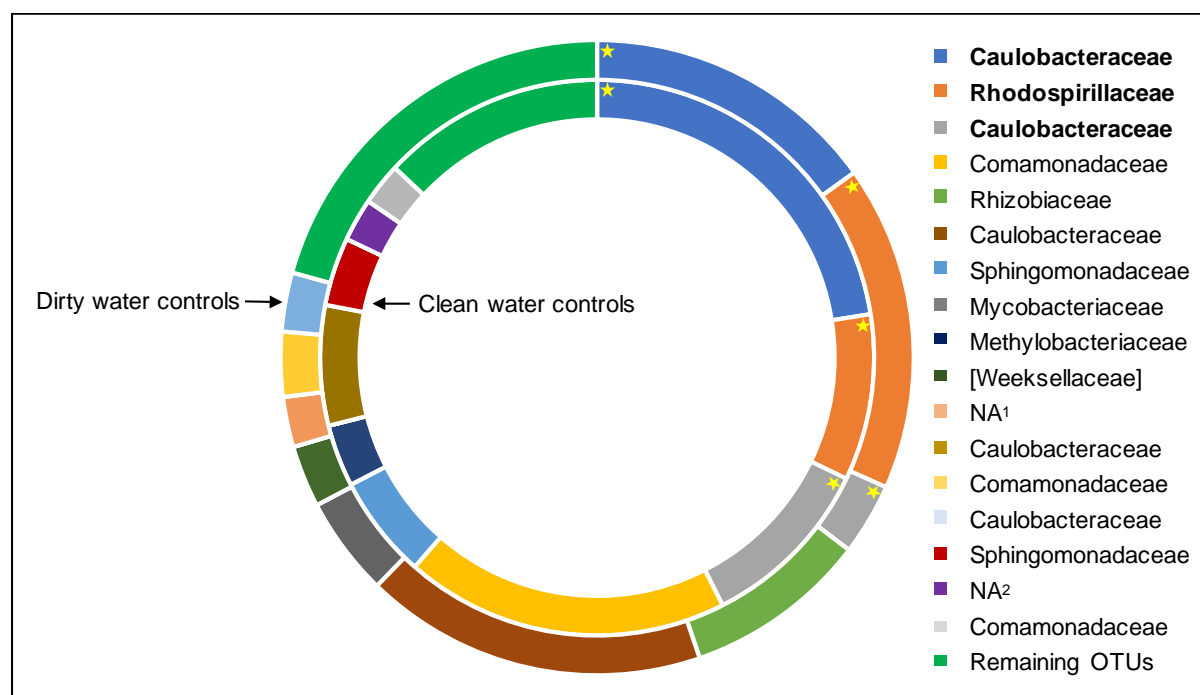


Figure 5 Comparison of the ten most abundant OTUs in control bath toy biofilms classified on family level. The inner circle represents bath toys used with clean water prior to bathing (clean water controls). The outer circle shows their composition in bath toys used with water after bathing (dirty water controls). Asterisks highlight OTUs that were abundant in both clean and dirty water controls. Each section of the plot represents the average relative abundance with the highest number of reads from triplicate bath toys. The portion of remaining OTUs is shown to emphasize the dominance of the ten most abundant OTUs for both clean and dirty water controls. OTUs are listed on family level as lowest common classification level, whereat 'NA' represents OTUs that could only be classified on higher levels: NA¹ – Class of TM7-3, NA² –

Order of Phycisphaerales. For further descriptions on the OTUs' origins see Table S5.

In clean water controls, nine out of the ten most abundant OTUs were members of Proteobacteria and only one belonged to the phylum Planctomycetes. For dirty water controls, the ten most abundant OTUs were more diverse, with seven belonging to Proteobacteria and one each in Bacteroidetes, Actinobacteria, and TM7 respectively (Table S5). Comparing these dominant OTUs of both control groups, only three out of ten were abundant in both clean and dirty water controls; namely members of the families Caulobacteraceae and Rhodospirillaceae (Figure 5). The majority of identified families correlated with ones identified for real bath toy biofilms (Figure 4). Other OTUs belonged to the families Methylobacteriaceae, Mycobacteriaceae, and, on a higher classification level, to the order Phycisphaerales, all of which have been detected in drinking or fresh water systems as well^{28,52-54}. Even amongst these samples with controlled conditions, results varied. To measure reproducibility, standard deviations of the percent community represented by the ten most abundant OTUs for the triplicate control bath toys were calculated. The deviations ranged immense from 0.9 – 157 % in clean water controls and 6.3 – 164 % in dirty water controls (data not shown). These variations between triplicates emphasize differences in the natural assembly of those biofilm communities under even identical conditions.

Fungi identified in studied bath toy biofilms

Fungal species could be identified in 57.9 % of all real bath toy biofilms, in all dirty water controls, and none of the clean water controls (Figure S6). Overall, the fungal communities were dominated by the phylum Ascomycota, the largest phylum of fungi. For real bath toy biofilms, the most abundant OTUs were representatives of the genera *Exophiala* spp., *Phialophora* spp., and *Fusarium* spp.; all of which have previously been detected in drinking water systems⁵⁵⁻⁵⁷. *Verticillium* spp. on the other hand is most commonly found in soil⁵⁸.

For dirty water controls, not only Ascomycota but also the phylum Basidiomycota was represented (Figure S6). For the first, the genus *Scolecobasidium* spp. was abundant in two out of the three dirty water controls. Members of this genus have been identified in soil samples but also in environments like bath rooms⁵⁹. *Cryptococcus* spp., a representative of Basidiomycota, has been detected in spring, surface, and ground waters⁶⁰. Finally, *Polyporales* spp. is known to be an important fungal genus in forest ecosystems⁶¹.

Presence of potentially harmful microorganisms in bath toy biofilms

Presence of culturable indicator bacteria and opportunistic pathogens in bath toy biofilms

Eighty percent of all studied bath toy biofilms showed positive cultivation results for at least one indicator organism or potential opportunistic pathogen (see Table S6 for numbers of CFU/bath toy). The majority of real bath toy biofilms (61 %) was tested positive for *P. aeruginosa*. *Listeria* spp. and *L. pneumophila* were identified in 33 %, while *Enterococci* spp. was present in 22 % of real bath toy biofilms. As for control bath toys, all of the sampled biofilms were tested positive for both *P. aeruginosa* and *Listeria* spp.. Additionally, 66.6 % of the clean and 100 % of the dirty water controls showed positive results for *L. pneumophila*. Interestingly, coliforms (excluding *E. coli*) were only detected in clean water controls, while *E. coli* specifically was only found in dirty water controls. It should be noted that positive colonies were not subjected to additional confirmation tests.

Presence of genera of concern based on sequencing data

Sequencing data was further analyzed for genera of concern, including the bacteria analyzed with cultivation (above). *Pseudomonas* spp. could be

identified on genus-level for all examined bath toys, ranging between 0.007 and 4.8 %. Enterobacteriaceae was detected in 47 % of the real bath toy samples, 67 % of the clean, and 33 % of the dirty water controls (ranging between 0.003 – 2.6 % of total reads). In one real bath toy ('Toy04'), reads for *Klebsiella* spp., a genus of Enterobacteriaceae, made up 4.8 % of the total number of reads of the biofilm community. *Klebsiella* spp. is not only relevant due to its presence in drinking water systems and biofilms, but also as a fecal indicator^{62–64}. Legionellaceae was identified in 94 % of the real bath toy biofilms, in 66.7 % of the clean, and 100 % of the dirty water controls (0.01 – 0.53 % of total reads). Listeriaceae could not be identified from the sequencing data. However, interestingly, the presence of *Staphylococcus* spp., which is a known pathogenic relative of *Listeria* spp., could be detected in 47 % of the real bath toy biofilms and in one of each control bath toys (0.003 – 0.1 % of total reads). Also, *Streptococcus* spp., an indicator for fecal contamination^{65,66}, was identified in 50% of all real bath toys, with 0.01 – 0.64 % of the total number of reads. In addition, *Mycobacterium* spp., known for its presence in potable water and building plumbing installations, as well as for severe diseases^{28,52}, was present in all but one real bath toy biofilm and all dirty control toys, with a wide range of 1.19 ± 2.11 % (n = 18) in real bath toys and 5.26 ± 2.19 % (n = 3) in dirty water controls. Finally, *Chlamydia* spp. as well as *Clostridia* spp. could be identified in five real bath toys with 0.06 or 0.02 %, respectively, with *Clostridia* spp. being an indicator for drinking water contamination⁶⁷, and *Chlamydia* spp. being part of the human, e.g., oral microbiome but also for representatives causing diseases^{68,69}.

Identification of potentially harmful fungal groups based on sequencing data

Regarding the presence of potentially harmful fungal groups, the majority of the real bath toy biofilms showed positive results for *Exophiala*, members of which are potential agents of human and animal mycoses⁷⁰. The genus *Phialophora* spp. was also identified for some real bath toys, being a member

of the 'black yeast and relatives', among which *P. verrucosa* has been reported to cause human infections⁷¹. Finally, infections by *Fusarium* spp. have been reported⁷², with *F. solani* being one of the main pathogenic relatives⁷³. Samples of the dirty water controls showed representatives of *Cryptococcus* spp., which include several important human pathogens, such as *Cryptococcus neoformans*⁷⁴.

Discussion

Almost one decade ago, the potential chemical risks of bath toys were documented in the colorfully titled book 'Slow death by rubber duck'⁷⁵. In contrast, little scientific information is available on microbial colonization and risks in these bath toys, even though related aesthetic and potential hygienic problems have been recognized in social media (Table S1). Therefore, the goals of this study were firstly to characterize biofilms grown on the inner surfaces of real bath toys and secondly to understand factors influencing biofilm growth and community composition using control bath toys. Based on this data we argue that the combination of four main factors impacted the magnitude and composition of bath toy biofilms, namely (1) the flexible plastic material and (2) the bath water quality that is further influenced by (3) chemical additives from washing products and the user, plus (4) biological contamination by the user's microbiome and the environment.

Flexible plastic material supports microbial growth

Bath toys are made from flexible synthetic polymeric materials, mostly polyvinyl chloride (PVC) or silicone rubber⁷⁵ (<https://www.badeenten.de/badeenten-quietscheenten/>; <http://www.toyhalloffame.org/toys/rubber-duck>). Research by Zobell showed that plastic materials adsorb some organic matter, which in turn enables biofilm formation, and which is highly dependent on the type of plastic material⁹. Moreover, flexible polymeric materials are generally known to release a considerable amount of organic carbon compounds, which favor microbial growth and biofilm formation^{16,18,20}. These migrating compounds are typically not the primary polymers, but rather additives such as plasticizers and stabilizers¹⁰⁻¹³. In this study, the material composition of the real bath toys was not determined, nor were they tested for the amount of leaching AOC. The reason was that the real bath toys were all used for extended time periods and most migration evidently occurred prior to our sampling. Therefore, interpreting

the impact of specific materials on biofilm formation and community compositions was not possible for real bath toy biofilms. In contrast, the control bath toys were all identical and their material was tested for both carbon migration potential (MP) and biomass formation potential (BFP) using the BioMig assay proposed by Wen and colleagues¹⁶. This assay revealed a MP of 3.92 ± 0.27 (n = 3) $\mu\text{g TOC}/\text{cm}^2/\text{day}$ (Table S7), and a BFP of $6.6 \pm 1.1 \times 10^8$ (n = 3) cells/cm^2 (Table S7). These values are high and comparable to BFP values measured for materials such as PVC-P (2.7×10^8 cells/cm^2) and 2 % EPDM (8.4×10^8 cells/cm^2)¹⁶, as well as for some flexible shower hoses ($2.9 - 8.3 \times 10^8$ cells/cm^2)⁵. In comparison, other studies showed lower BFP for PE-X_a and PE-X_b materials with values ranging between $3.4 - 4.6 \times 10^7$ cells/cm^2 ^{16,76}. In general, migration is dominant in new materials and diminishes over time^{15,16}, and therefore, it is more relevant in new bath toys (i.e., control toys). However, it should be noted that BioMig assays are carried out under optimal conditions (e.g., with trace nutrient addition) for both carbon migration and biomass formation potential. Therefore, it is not surprising that values for biofilm coverage in the control bath toys ($0.05 - 0.73 \times 10^8$ cells/cm^2) were on average lower than the predicted numbers with the BioMig assays (above). Importantly, the clean water controls showed significantly lower numbers than the dirty water controls (Figure 2). Since the carbon migration by the material was identical in all control toys, we argue that differences in water quality caused the differences in cell numbers and community composition of clean and dirty water controls (discussed further below).

Water quality influences microbial growth

Tap water quality

One seeding source for the microbial community of bath toy biofilms is the microbiome of the tap water. In this study, the real bath toys originated from five different households where water quality was not measured. Nevertheless,

differences in the tap water microbiota can be expected²², potentially causing variations in biofilm community compositions (e.g., Douterelo and colleagues²³), and comprising household specific core communities. These differences occur due to several facts: (1) differences in source waters and treatment procedures dictate potable water communities^{77,78}, (2) spatial and temporal changes result in localized microbial biogeography⁷⁹, (3) differences in water heater temperatures and water usage frequencies influence the potable water microbiome^{80,81}, and finally, (4) the usage of different materials selects for individual microbial communities in the building plumbing system^{82,83}. Besides, several studies showed that microbial communities of potable water systems comprise opportunistic pathogens (e.g., ⁸⁴), such as *L. pneumophila*, *P. aeruginosa*, *Mycobacterium* spp.^{26,85}, or non-tuberculous mycobacteria^{24,28}. Thus, it's not surprising that we recorded positive results for some of these organisms and/or genera to which they belong in several bath toy biofilms (Table S6; Section 2.4.2 above). As for nutrients, tap water poses an oligotrophic environment^{29,30,41,86,87}, with nutrient concentrations insufficient to support the degree of microbial growth observed in the bath toys (Table S8). Similar to the material, the tap water was identical for all control toys, suggesting that observed differences between clean water and dirty water controls (Figure 2 and Figure 3) are attributed to compounds and organisms associated with the dirty bath water.

Additional nutrients support bacterial growth

Under normal use conditions, bath toys are exposed to dirty bath water. This comprises additional organic and inorganic nutrients³², which were shown to be biodegradable⁸⁸ and thus beneficially impacting microbial growth⁸⁹. For example, Blackstock and colleagues showed that not only personal care products, but also body fluids like urine and sweat contribute to the amount of dissolved organic carbon (DOC) in the water³³. Urine in particular is a source for additional nitrogenic compounds in the form of urea, ammonia, or amino

acids^{33,90}. In the control experiment of this study, chemical analysis of the water before and after bathing showed that concentrations in DOC and TOC increased ten-fold, while total nitrogen and phosphorous concentrations were doubled after a bathing event (Table S8). These results explain the higher biofilm coverage in dirty water controls compared to clean water controls (Figure 2), despite the identical growth potential of the plastic material (Table S7) and identical tap water (above). However, it is not possible to conclude from the data whether the growth in the dirty water controls were driven predominantly by the additional organic nutrients or by the inorganic nutrients that enabled optimal use of carbon migrating from the plastic material.

Additional microbial contamination by the human end-user

In addition to the nutrient supply, dirty bath water also serves as a further source of microbial seeding for the bath toys, including both human microbiota and environmental bacteria that are released during bathing^{3,4,22,31,91}. For bacterial numbers, an increase of TCC from $2.1 (\pm 1.1, n = 2) \times 10^5$ to $4.1 (\pm 2.5, n = 2) \times 10^5$ cells/mL could be shown in the tap water after bathing (Table S8). In this study, the microbiome of users and/or their bath tubs were not sampled due to (1) privacy concerns for the children involved and (2) because a single grab sample would only have been representative for one particular time frame and not the period (often multiple years and multiple users) of use/exposure. The human microbiome was previously shown to differ between people. For example, a previous study noted that armpits of different individuals show clear differences in bacterial community compositions, which amongst others could be explained by the use of different care products, e.g., deodorants⁹². The same applies for the microbiome colonizing other parts of the human skin, e.g., forearms^{93,94}, as well as the gut microbiome which depends on peoples age, health, and diet⁹⁵⁻⁹⁷. With this multiplicity, potentially harmful bacteria can get released into the bath water as well. It was previously shown that dirty bath water contains significant amounts of, e.g., *E. coli* or other fecal

coliforms^{31,32,88,98,99}, which supports our cultivation and sequencing data showing organisms/genera of concern in many bath toy biofilms. As for the input of environmental bacteria into the bath water, their origin strongly depends on the activities taken by the person bathing, e.g., soil bacteria after playing in the garden or limnic bacteria after swimming in a lake. It is evident that the pioneer organisms for the biofilm communities in clean water controls were predominantly the microbiome of the tap water and microorganisms potentially present in the clean bath tub, while dirty water controls were additionally influenced by (1) the human microbiome and (2) bacteria from the environment. However, our data did not allow differentiation between the contribution of these two. The points above in turn also explain the low abundance in real bath toy 'household-specific core communities', with different/multiple users, variations in environmental contamination and also variations in patterns (e.g., frequency of use) most likely contributing to the selection in the biofilm communities.

Implications for the end-user

Environmental exposure to bacteria and fungi is not necessarily bad for human health and may indeed even strengthen the immune defense. Nevertheless, two studies have already shown the clinical relevance of bath toy biofilms^{2,34}. While we identified several indicator organisms and genera of concern, the data from both cultivation and sequencing has to be interpreted carefully. Cultivation data can be biased, e.g., due to potential non-selective growth of non-targeted organisms. Similarly, OTUs associated with genera of concern are not necessarily representatives of (opportunistic) pathogens, as strain-level classification was not possible with this approach. Nevertheless, bath toys are typically used by children, who are potentially sensitive and vulnerable users. Squeezing water with chunks of biofilm into their faces (which is not unexpected behavior for these users) may result in eye, ear, wound or even gastro-intestinal tract infections. To assess the real extent of this risk, more

experimental work with specific focus on hygienic aspects is needed. Meanwhile, there are plenty of recommendations for cleaning and storing bath toys (e.g., boiling, removing water after usage) to minimize the risk of infection (Table S1). In addition, one could argue for increased regulations on polymeric materials used for bath toy production. This has already been done with respect to toxic chemical substances^{16,75}, while comprehensive material tests with respect to migration and microbial growth potential are available and increasingly used for building plumbing materials control¹⁰⁰. In fact, the easiest way to prevent children from being exposed to bath toy biofilms is to simply close the hole – but where is the fun in that?

Conclusions

Bath toys from real households are colonized by dense biofilms with complex bacterial and fungal communities. Following the comparison of biofilms grown in clean and dirty water controls, we concluded that the coverage as well as the composition of these biofilm communities depended on the combination of four main factors namely: (1) the flexible plastic material that is releasing AOC and therefore favoring microbial growth; (2) the tap water microbiome that introduces specific microorganisms, including opportunistic pathogens, to the bath toys; (3) additional nutrients in the dirty bath water due to personal care products and human body fluids; and (4) additional bacteria originating from both the user microbiome and environmental contamination. As this was a fundamental characterization study of such bath toy biofilms, further investigations for detailed risk assessment are needed.

Acknowledgements

The authors acknowledge conceptual contributions of Maryna Peter and Stefan Kötzsch, technical support from Franziska Rölli and Romina Sigrist, Teresa Colangelo for assistance with SEM imaging, and all children for the generous donation of their beloved bath toys.

References

1. **Else**, T. A., Pantle, C. R. & Amy, P. S. Boundaries for Biofilm Formation : Humidity and Temperature Boundaries for Biofilm Formation : Humidity and Temperature. *Appl. Environ. Microbiol.* 69, 5006–5010 (2003).
2. **Ruschke**, R. Kunststoff-Schwimmtiere als Biotop für Mikroorganismen und mögliche Infektionsquellen für Kleinkinder. *Zbl. Bakt. Hyg., I.Abt. Orig. B* 163, 556–564 (1976).
3. **Finch**, J. E., Prince, J. & Hawksworth, M. A Bacteriological Survey of the Domestic Environment. *J. Appl. Bacteriol.* 45, 357–364 (1978).
4. **Scott**, E., Bloomfieldt, S. F. & Barlow, C. G. An investigation of microbial contamination in the home. *J. Hyg. Camb.* 89, 279–293 (1982).
5. **Proctor**, C. R. *et al.* Biofilms in shower hoses – choice of pipe material influences bacterial growth and communities. *Environ. Sci. Water Res. Technol.* 2, 8–11 (2016).
6. **Soto-Giron**, M. J. *et al.* Biofilms on hospital shower hoses: Characterization and implications for nosocomial infections. *Appl. Environ. Microbiol.* 82, 2872–2883 (2016).
7. **Feazel**, L. M. *et al.* Opportunistic pathogens enriched in showerhead biofilms. *PNAS* 106, 16393–16399 (2009).
8. **Kelley**, S. T., Theisen, U., Angenent, L. T., St Amand, A. & Pace, N. R. Molecular analysis of shower curtain biofilm microbes. *Appl. Environ. Microbiol.* 70, 4187–92 (2004).
9. **Zobell**, C. E. The effect of solid surfaces upon bacterial activity. *J. Bacteriol.* 46, 39–56 (1943).
10. **Zhang**, L. & Liu, S. Investigation of Organic Compounds Migration from Polymeric Pipes into Drinking Water under Long Retention Times. *Procedia Eng.* 70, 1753–1761 (2014).
11. **Holsen**, T. M., Park, J. K., Jenkins, D. & Selleck, R. E. Contamination of potable water by permeation of plastic pipe. *Am. Water Work. Assoc.* 83, 53–56 (1991).
12. **Skjevrvak**, I., Due, A., Gjerstad, K. O. & Herikstad, H. Volatile organic components migrating from plastic pipes (HDPE, PEX and PVC) into drinking water. *Water Res.* 37, 1912–20 (2003).
13. **Stern**, B. R. & Lagos, G. Are There Health Risks from the Migration of Chemical Substances from Plastic Pipes into Drinking Water ? A Review. *Hum. Ecol. Risk Assess. An Int. J.* 14, 753–779 (2008).
14. **Connell**, M. *et al.* PEX and PP water pipes: Assimilable carbon, chemicals, and odors. *J. Am. Water Works Assoc.* 108, E192–E204 (2016).
15. **Bucheli-Witschel**, M., Koetzsch, S., Darr, S., Widler, R. & Egli, T. A new method to assess the influence of migration from polymeric materials on the biostability of drinking water. *Water Res.* 46, 4246–4260 (2012).
16. **Wen**, G., Kötzsch, S., Vital, M., Egli, T. & Ma, J. BioMig-A Method to Evaluate the Potential Release of Compounds from and the Formation of Biofilms on Polymeric Materials in Contact with Drinking Water. *Environ. Sci. Technol.* 49, 11659–69 (2015).
17. **Schoenen**, D. & Schöler, H. Microbial alterations of drinking water by

- building materials - field observations and laboratory studies. *Am. Water Work. Assoc.* 307–317 (1985).
18. **Lehtola**, M. J. *et al.* Microbiology, chemistry and biofilm development in a pilot drinking water distribution system with copper and plastic pipes. *Water Res.* 38, 3769–3779 (2004).
 19. **Niquette**, P., Servais, P. & Savoie, R. Impacts of pipe materials on densities of fixed bacterial biomass in a drinking water distribution system. *Water Res.* 34, 1952–1956 (2000).
 20. **Yu**, J., Kim, D., Lee, T. & Xx, Y. Microbial diversity in biofilms on water distribution pipes of different materials. *Water Sci. Technol.* 61, 163–171 (2010).
 21. **Kerr**, C. J., Osborn, K. S., Robson, G. D. & Handley, P. S. The relationship between pipe material and biofilm formation in a laboratory model system. *J. Appl. Microbiol.* 85 Suppl 1, 29S–38S (1998).
 22. **Tamames**, J., Abellán, J. J., Pignatelli, M., Camacho, A. & Moya, A. Environmental distribution of prokaryotic taxa. *BMC Microbiol.* 10, 1–14 (2010).
 23. **Doutere**, I., Jackson, M., Solomon, C. & Boxall, J. Spatial and temporal analogies in microbial communities in natural drinking water biofilms. *Sci. Total Environ.* 277–288 (2017). doi:10.1016/j.scitotenv.2016.12.118
 24. **Parsek**, M. R. & Singh, P. K. Bacterial biofilms: an emerging link to disease pathogenesis. *Annu. Rev. Microbiol.* 57, 677–701 (2003).
 25. **Bodey**, G. P., Bolivar, R., Fainstein, V. & Jadeja, L. Infections Caused by *Pseudomonas aeruginosa*. *Rev. Infect. Dis.* 5, 279–313 (1983).
 26. **Falkinham**, J., Pruden, A. & Edwards, M. Opportunistic Premise Plumbing Pathogens: Increasingly Important Pathogens in Drinking Water. *Pathogens* 4, 373–386 (2015).
 27. **Fields**, B. S., Benson, R. F. & Besser, R. E. Legionella and Legionnaire's Disease: 25 Years of Investigation. *Clin. Microbiol. Rev.* 15, 506–526 (2002).
 28. **Falkinham**, J. O. Nontuberculous mycobacteria from household plumbing of patients with nontuberculous mycobacteria disease. *Emerg. Infect. Dis.* 17, 419–424 (2011).
 29. **Boe-Hansen**, R., Martiny, A. C., Arvin, E. & Albrechtsen, H.-J. Monitoring biofilm formation and activity in drinking water distribution networks under oligotrophic conditions. *Water Sci. Technol.* 47, 91–97 (1989).
 30. **Boe-Hansen**, R., Albrechtsen, H.-J., Arvin, E. & Claus, J. Bulk water phase and biofilm growth in drinking water at low nutrient conditions. *Water Res.* 36, 4477–4486 (2002).
 31. **Rose**, J. B., Sun, G. S., Gerba, C. P. & Sinclair, N. A. Microbial quality and persistence of enteric pathogens in graywater from various household sources. *Water Res.* 25, 37–42 (1991).
 32. **Eriksson**, E., Auffarth, K., Henze, M. & Ledin, A. Characteristics of grey wastewater. *Urban Water* 4, 85–104 (2002).
 33. **Blackstock**, L. K., Wang, W., Vemula, S., Jaeger, B. T. & Li, X. Sweetened Swimming Pools and Hot Tubs. *Env. Sci Technol Lett* 4, 149–153 (2017).
 34. **Buttery**, J. P. *et al.* Multiresistant *Pseudomonas aeruginosa* outbreak in a pediatric oncology ward related to bath toys. *Pediatr. Infect. Dis. J.* 17,

- 509–513 (1998).
35. **Prest**, E. I., Hammes, F., Köttsch, S., van Loosdrecht, M. C. M. & Vrouwenvelder, J. S. Monitoring microbiological changes in drinking water systems using a fast and reproducible flow cytometric method. *Water Res.* 47, 7131–7142 (2013).
 36. **Klindworth**, A. *et al.* Evaluation of general 16S ribosomal RNA gene PCR primers for classical and next-generation sequencing-based diversity studies. *Nucleic Acids Res.* 41, 1–11 (2013).
 37. **Walters**, W. *et al.* Improved Bacterial 16S rRNA Gene (V4 and V4-5) and Fungal Internal Transcribed Spacer Marker Gene Primers. *Methods Protoc. Nov. Syst. Biol. Tech.* 1, 1–10 (2015).
 38. **Kozich**, J. J., Westcott, S. L., Baxter, N. T., Highlander, S. K. & Schloss, P. D. Development of a Dual-Index Sequencing Strategy and Curation Pipeline for Analyzing Amplicon Sequence Data on the MiSeq. *Appl. Environ. Microbiol.* 79, 5112–5120 (2013).
 39. **Liu**, W. *et al.* Investigation of assimilable organic carbon (AOC) and bacterial regrowth in drinking water distribution system. *Water Res.* 36, 891–898 (2002).
 40. **Hammes**, F. A. & Egli, T. New method for assimilable organic carbon determination using flow-cytometric enumeration and a natural microbial consortium as inoculum. *Env. Sci Technol* 39, 3289–3294 (2005).
 41. **Martiny**, A. C., Albrechtsen, H., Arvin, E. & Molin, S. Identification of Bacteria in Biofilm and Bulk Water Samples from a Nonchlorinated Model Drinking Water Distribution System : Detection of a Large Nitrite-Oxidizing Population Associated with *Nitrospira* spp . *Appl. Environ. Microbiol.* 71, 8611–8617 (2005).
 42. **Norton**, C. D. & LeChevallier, M. W. A Pilot Study of Bacteriological Population Changes through Potable Water Treatment and Distribution. *Appl. Environ. Microbiol.* 66, 268–276 (2000).
 43. **Williams**, M. M., Domingo, J. W. S., Meckes, M. C., Kelty, C. A. & Rochon, H. S. Phylogenetic diversity of drinking water bacteria in a distribution system simulator. *J. Appl. Microbiol.* 96, 954–964 (2004).
 44. **Zeng**, D.-N. *et al.* Analysis of the bacterial communities associated with different drinking water treatment processes. *World J. Microbiol. Biotechnol.* 29, 1573–1584 (2013).
 45. **Kämpfer**, P., Lodders, N. & Busse, H. J. *Arcicella rosea* sp. nov., isolated from tap water. *Int. J. Syst. Evol. Microbiol.* 59, 341–344 (2009).
 46. **Chao**, Y., Mao, Y., Wang, Z. & Zhang, T. Diversity and functions of bacterial community in drinking water biofilms revealed by high-throughput sequencing. *Sci. Rep.* 5, 10044 (2015).
 47. **Koskinen**, R. *et al.* Characterization of *Sphingomonas* isolates from Finnish and Swedish drinking water distribution systems. *J. Appl. Microbiol.* 89, 687–696 (2000).
 48. **Herbert**, R. Isolation and identification of photosynthetic bacteria (Rhodospirillaceae) from Antarctic marine and freshwater sediments. *J. Appl. Bacteriol.* 41, 75–80 (1976).
 49. **Ursell**, L. K. *et al.* The interpersonal and intrapersonal diversity of human-

- associated microbiota in key body sites. *J Allergy Clin Immunol* 129, 1204–1208 (2012).
50. **Mueller**, N. T., Bakacs, E., Combellick, J., Grigoryan, Z. & Dominguez-Bello, M. G. The infant microbiome development: mom matters. *Trends Mol Med* 21, 109–117 (2015).
 51. **Rudney**, J. D., Xie, H., Rhodus, N. L., Ondrey, F. G. & Griffin, T. J. A Metaproteomic Analysis of the Human Salivary Microbiota by Three-Dimensional Peptide Fractionation and Tandem Mass Spectrometry. *Mol Oral Microbiol* 25, 38–49 (2010).
 52. **Gallego**, V., García, M. T. & Ventosa, A. *Methylobacterium hispanicum* sp. nov. and *Methylobacterium aquaticum* sp. nov., isolated from drinking water. *Int. J. Syst. Evol. Microbiol.* 55, 281–287 (2005).
 53. **Furuhata**, K. *et al.* Isolation and identification of methylobacterium species from the tap water in hospitals in Japan and their antibiotic susceptibility. *Microbiol. Immunol.* 50, 11–17 (2006).
 54. **Vaerewijck**, M. J. M., Huys, G., Palomino, J. C., Swings, J. & Portaels, F. Mycobacteria in drinking water distribution systems: ecology and significance for human health. *FEMS Microbiol. Rev.* 29, 911–934 (2005).
 55. **Göttlich**, E. *et al.* Fungal flora in groundwater-derived public drinking water. *Int. J. Hyg. Environ. Health* 205, 269–279 (2002).
 56. **Nishimura**, K., Miyaji, M., Taguchi, H. & Tanaka, R. Fungi in bathwater and sludge of bathroom drainpipes. *Mycopathologia* 97, 17–23 (1987).
 57. **Lian**, X. & de Hoog, G. S. Indoor wet cells harbour melanized agents of cutaneous infection. *Med. Mycol.* 48, 622–628 (2010).
 58. **Hirsch**, P. R., Atkins, S. D., Mauchline, T. H., Morton, C. O. & G, K. Methods for studying the nematophagous fungus *Verticillium chlamydosporium* in the root environment. *Plant Soil* 232, 21–30 (2001).
 59. **Abe**, N. & Hamada, N. Molecular Characterization and Surfactant Utilization of *Scolecobasidium* Isolates from Detergent-Rich Indoor Environments. *Biocontrol Sci.* 16, 139–147 (2011).
 60. **Pereira**, V. J. *et al.* Occurrence of filamentous fungi and yeasts in three different drinking water sources. *Water Res.* 43, 3813–3819 (2009).
 61. **Zhou**, J., Zhu, L., Chen, H. & Cui, B. Taxonomy and Phylogeny of Polyporus Group *Melanopus* (Polyporales , Basidiomycota) from China. *PLoS One* 1–23 (2016). doi:10.1371/journal.pone.0159495
 62. **Edberg**, S. C., Rice, E. W., Karlin, R. J. & Allen, M. J. *Escherichia coli*: the best biological drinking water indicator for public health protection. *J. Appl. Microbiol.* 88, 106S–116S (2000).
 63. **Jeffrey**, J. B., Xu, H.-S. & Colwell, R. R. Viable but Nonculturable Bacteria in Drinking Water. *Applied* 57, 875–878 (1991).
 64. **Jeffrey**, G. S., Rice, E. W. & Bishop, P. L. Persistence of *Klebsiella pneumoniae* on Simulated Biofilm in a Model Drinking Water System. *Environ. Sci. Technol.* 40, 4996–5002 (2006).
 65. **Spaander**, P. & Roest, A. C. F. The detection of faecal Streptococci in drinking-water. *Antoine van Leeuwenhoek* 25, 169–178 (1958).
 66. **Pinto**, B., Pierotti, R., Canale, G. & Reali, D. Characterization of ' faecal streptococci ' as indicators of faecal pollution and distribution in the

- environment. *Lett. Appl. Microbiol.* 29, 258–263 (1999).
67. **Payment**, P. & Franco, E. Clostridium perfringens and Somatic Coliphages as Indicators of the Efficiency of Drinking Water Treatment for Viruses and Protozoan Cysts. *Appl. Environ. Microbiol.* 59, 2418–2424 (1993).
 68. **Dewhirst**, F. E. *et al.* The Human Oral Microbiome. *J. Bacteriol.* 192, 5002–5017 (2010).
 69. **Miyairi**, I. *et al.* Host Genetics and Chlamydia Disease : Prediction and Validation of Disease Severity Mechanisms. *PLoS* 7, 1–10 (2012).
 70. **Zeng**, J. S. *et al.* Spectrum of Clinically Relevant Exophiala Species in the United States. *J. Clin. Microbiol.* 45, 3713–3720 (2007).
 71. **Li**, Y. *et al.* Biodiversity and human-pathogenicity of Phialophora verrucosa and relatives in Chaetothyriales. *Persoonia* 38, 1–19 (2017).
 72. **Hennequin**, C. *et al.* Identification of Fusarium species involved in human infections by 28S rRNA gene sequencing. *J Clin Microbiol* 37, 3586–3589 (1999).
 73. **Guarro**, J. & Gené, J. Fusarium infections. Criteria for the identification of the responsible species. *Mycoses* 35, 109–114 (1992).
 74. **Vilgalys**, R. & Hester, M. Rapid Genetic Identification and Mapping of Enzymatically Amplified Ribosomal DNA from Several Cryptococcus Species. *J. Bacteriol.* 172, 4238–4246 (1990).
 75. **Smith**, R. & Lourie, B. *Slow death by rubber duck - The secret danger of everyday things.* (2009).
 76. **Koetzsch**, S., Egli, T. & E. E. D. W. Kunststoffe in Kontakt mit Trinkwasser. *Aqua & Gas* 3, 44–52 (2013).
 77. **Pinto**, A. J., Xi, C. & Raskin, L. Bacterial community structure in the drinking water microbiome is governed by filtration processes. *Env. Sci Technol* 46, 8851–8859 (2012).
 78. **Gomez-Smith**, C. K., Tan, D. T. & Shuai, D. Environmental Science water microbiome – from treatment to tap. *Environ. Sci. Water Res. Technol.* 2, 245–249 (2016).
 79. **Roeselers**, G. *et al.* Microbial biogeography of drinking water: Patterns in phylogenetic diversity across space and time. *Environ. Microbiol.* 17, 2505–2514 (2015).
 80. **Ji**, P., Rhoads, W. J., Edwards, M. A. & Pruden, A. Impact of water heater temperature setting and water use frequency on the building plumbing microbiome. *ISME J.* 1–13 (2017). doi:10.1038/ismej.2017.14
 81. **Ji**, P., Parks, J., Edwards, M. A. & Pruden, A. Impact of Water Chemistry, Pipe Material and Stagnation on the Building Plumbing Microbiome. *PLoS One* 10, e0141087 (2015).
 82. **Rozej**, A., Cydzik-Kwiatkowska, A., Kowalska, B. & Kowalski, D. Structure and microbial diversity of biofilms on different pipe materials of a model drinking water distribution systems. *World J Microbiol Biotechnol* 31, 37–47 (2015).
 83. **Lin**, W., Yu, Z., Chen, X., Liu, R. & Zhang, H. Molecular characterization of natural biofilms from household taps with different materials: PVC, stainless steel, and cast iron in drinking water distribution system. *Appl. Microbiol. Biotechnol.* 97, 8393–8401 (2013).

84. **Williams**, M. M., Armbruster, C. R. & Arduino, M. J. Plumbing of hospital premises is a reservoir for opportunistically pathogenic microorganisms: a review. *Biofouling* 29, 147–62 (2013).
85. **Szewzyk**, U., Szewzyk, R., Manz, W. & Schleifer, K. Microbiological Safety of Drinking Water. *Annu.Rev.Microbiol.* 54, 81–127 (2000).
86. **Wingender**, J. & Flemming, H.-C. Biofilms in drinking water and their role as reservoir for pathogens. *Int. J. Hyg. Environ. Health* 214, 417–423 (2011).
87. **van der Wende**, E., Characklis, W. G. & Smith, D. B. Biofilms and bacterial drinking water quality. *Water Res.* 23, 1313–1322 (1989).
88. **Li**, F., Wichmann, K. & Otterpohl, R. Review of the technological approaches for grey water treatment and reuses. *Sci. Total Environ.* 407, 3439–3449 (2009).
89. **Miettinen**, I. T., Vartiainen, T. & Martikainen, P. J. Phosphorus and Bacterial Growth in Drinking Water. *Appl. Environ. Microbiol.* 63, 3242–3245 (1997).
90. **Erdinger**, L., Kirsch, F., Sonntag, H. & Xx, Y. Potassium as an indicator of anthropogenic contamination of swimming pool water. *Zentralblatt fur Hyg. und Umweltmedizin* 200, 297–308 (1997).
91. **Robinson**, C. J., Bohannon, B. J. M. & Young, V. B. From Structure to Function: the Ecology of Host-Associated Microbial Communities. *Microbiol. Mol. Biol. Rev.* 74, 453–476 (2010).
92. **Urban**, J. *et al.* The effect of habitual and experimental antiperspirant and deodorant product use on the armpit microbiome. *PeerJ* 1–20 (2016). doi:10.7717/peerj.1605
93. **Kong**, H. H. Skin microbiome: genomics-based insights into the diversity and role of skin microbes. *Trends Mol Med* 17, 320–328 (2011).
94. **Grice**, E. A. *et al.* A diversity profile of the human skin microbiota. *Genome Res.* 18, 1043–1050 (2008).
95. **Contreras**, M. *et al.* Human gut microbiome viewed across age and geography. *Heal. Hum. Serv. USA* 486, 222–227 (2012).
96. **Lozupone**, C. A., Stombaugh, J. I., Gordon, J. I., Jansson, J. K. & Knight, R. Diversity, stability and resilience of the human gut microbiota. *Nature* 489, 220–230 (2012).
97. **Shreiner**, A. B., Kao, J. K. & Young, V. B. The gut microbiome in health and in disease. *Curr Opin Gastroenterol* 31, 69–75 (2015).
98. **Chaillou**, K., Gérente, C., Andrès, Y. & Wolbert, D. Bathroom greywater characterization and potential treatments for reuse. *Water. Air. Soil Pollut.* 215, 31–42 (2011).
99. **Hourlier**, F. *et al.* Formulation of synthetic greywater as an evaluation tool for wastewater recycling technologies. *Environ. Technol.* 31, 215–223 (2010).
100. **Koetzsch**, S. & Egli, T. Kunststoffe in Kontakt mit Trinkwasser. *Aqua & Gas* 3, (2013).

Chapter 3 – Supplementary Information

Ugly ducklings – The dark side of plastic materials in contact with potable water

Table S1: Exemplary online blog entries on biofouling inside bath toys

Issue - What is the slime?	Link
Rub-a-dub-dub, what's in the tub?	https://www.babble.com/baby/whats-in-the-tub/
What's the black stuff in your squeeze toys?	http://blogs.babycenter.com/momstories/whats-the-black-stuff-in-your-squeeze-toys/
Friday Find: NBC's Today Show segment: Do bath toys carry germs?	http://www.bebravekeepgoing.com/2010/03/friday-find-nbcs-today-show-segment-do.html
Yuck. Yuck. Yuck! (A.K.A. Why my kids no longer have rubber duckies!)	http://www.imperfecthomemaking.com/2012/11/yuck-yuck-yuck-aka-why-my-kids-no.html
Issue – How to prevent or remove it?	Link
How to clean bath toys & prevents mould	http://www.maids.com/blog/how-to-clean-and-prevent-mold-in-bath-toys/
Glue gun the rubber ducky	http://lajollamom.com/glue-gun-the-rubber-ducky/
How to remove mould from bath toys	http://www.howtocleanstuff.net/how-to-remove-mold-from-bath-toys/
Ask Martha: How can I clean my children's bath toys?	http://www.marthastewart.com/1125723/cleaning-childrens-bath-toys
What's the best way to clean bath toys?	http://www.realsimple.com/magazine-more/inside-magazine/ask-real-simple/best-way-clean-bath-toys

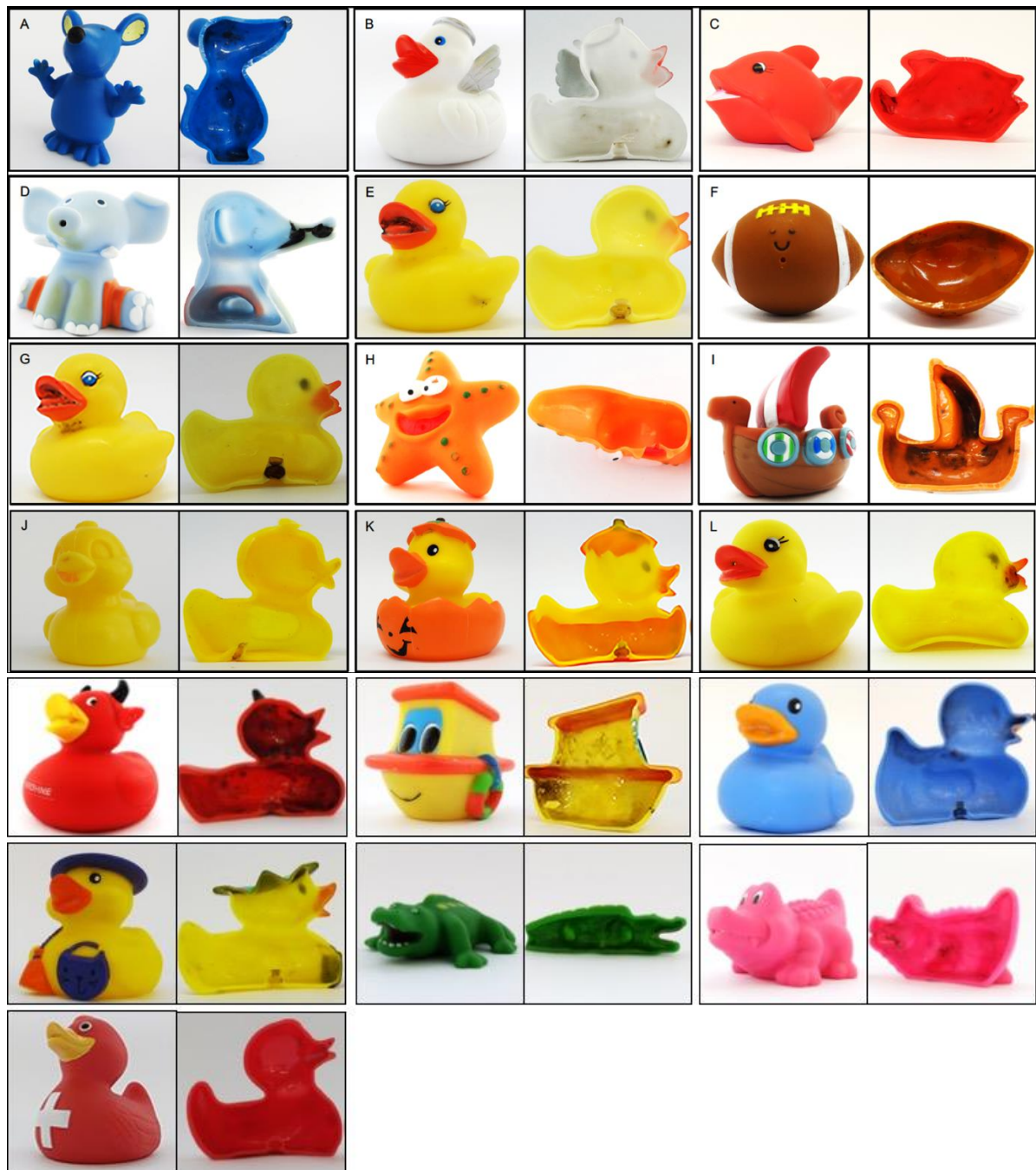


Figure S1-1: Images of all examined real bath toys, both sound and cut open.

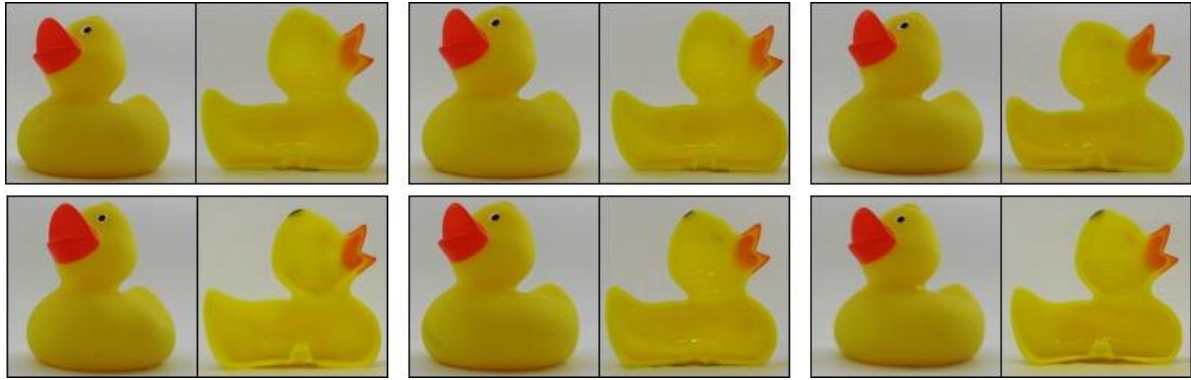


Figure S1-2: Upper row: Control bath toys processed with water prior to bathing (clean water controls). Lower row: control bath toys used with water after bathing (dirty water controls).

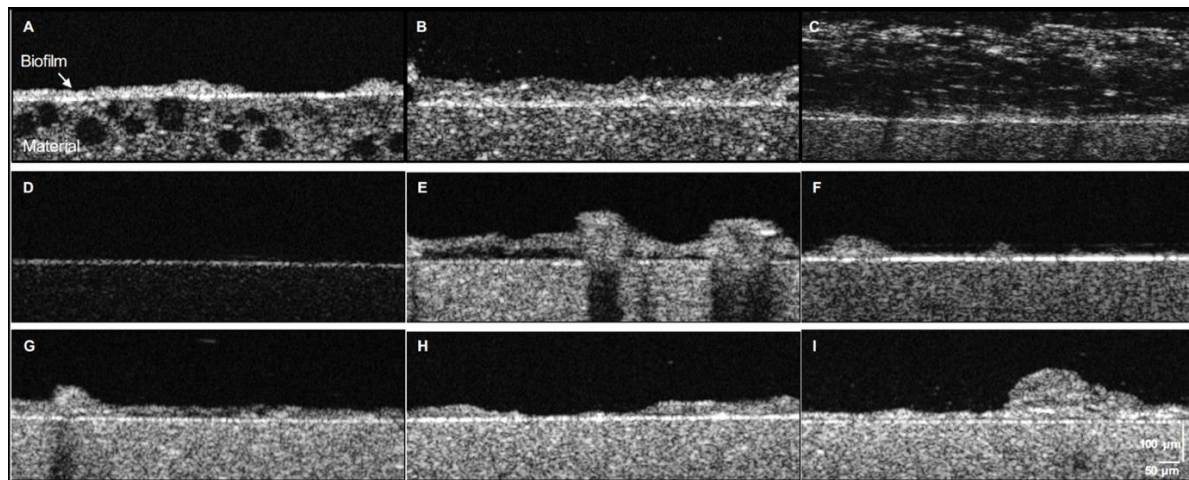


Figure S2: Optical coherence tomography (OCT) was used to image biofilm shape and thickness of selected bath toys. For real bath toys three exemplary biofilms are shown (A-C). Biofilms of clean water controls, which were used with water prior to bathing, are shown in D-F, while biofilms of dirty water controls, processed with water after bathing, are shown in images G-I.

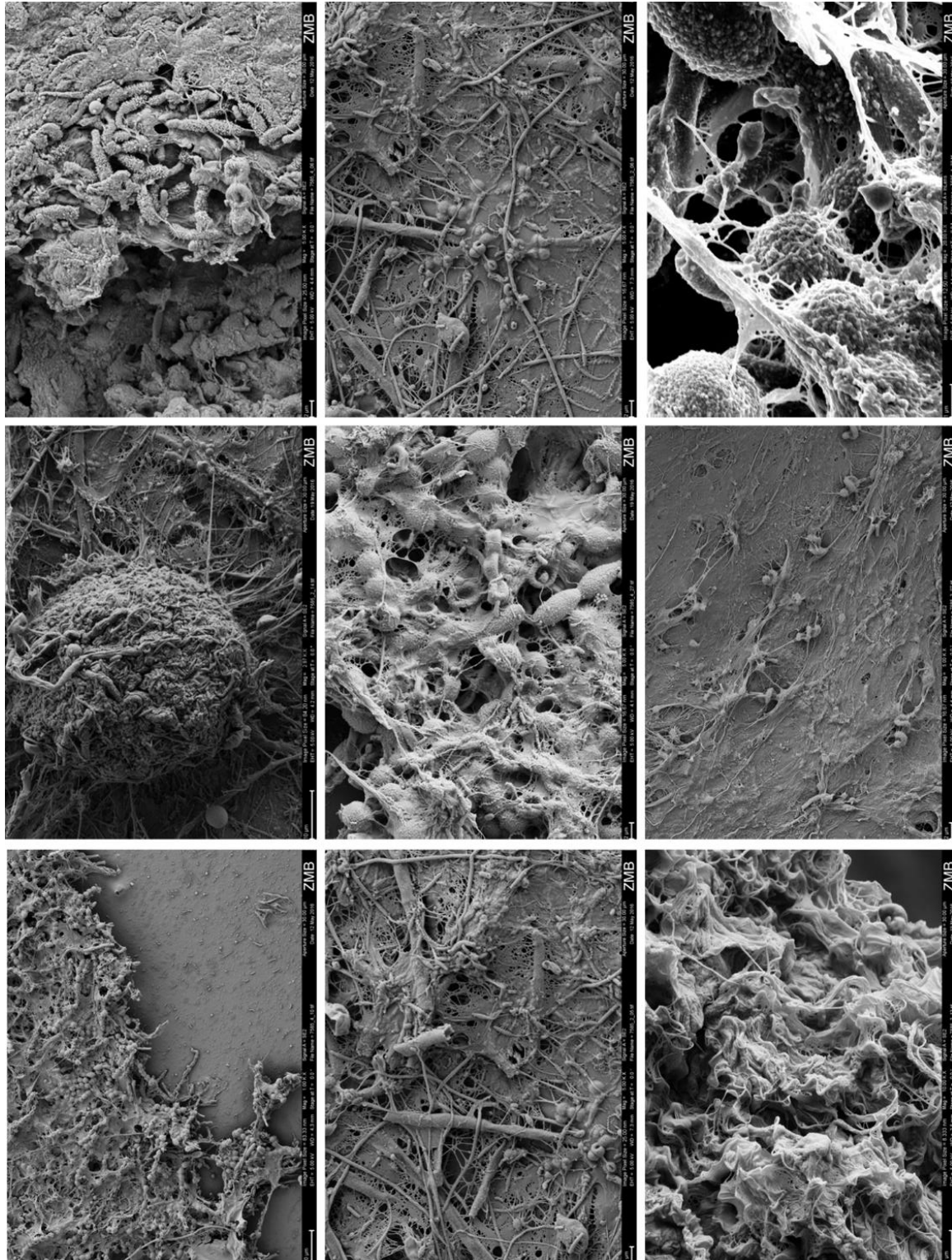


Figure S3 Additional images for biofilm composition by scanning electron microscopy. SEM was used to visualize the microbial community composition in some real bath toy biofilms. Images were taken by the Center for Microscopy and Image Analysis, University Zurich.

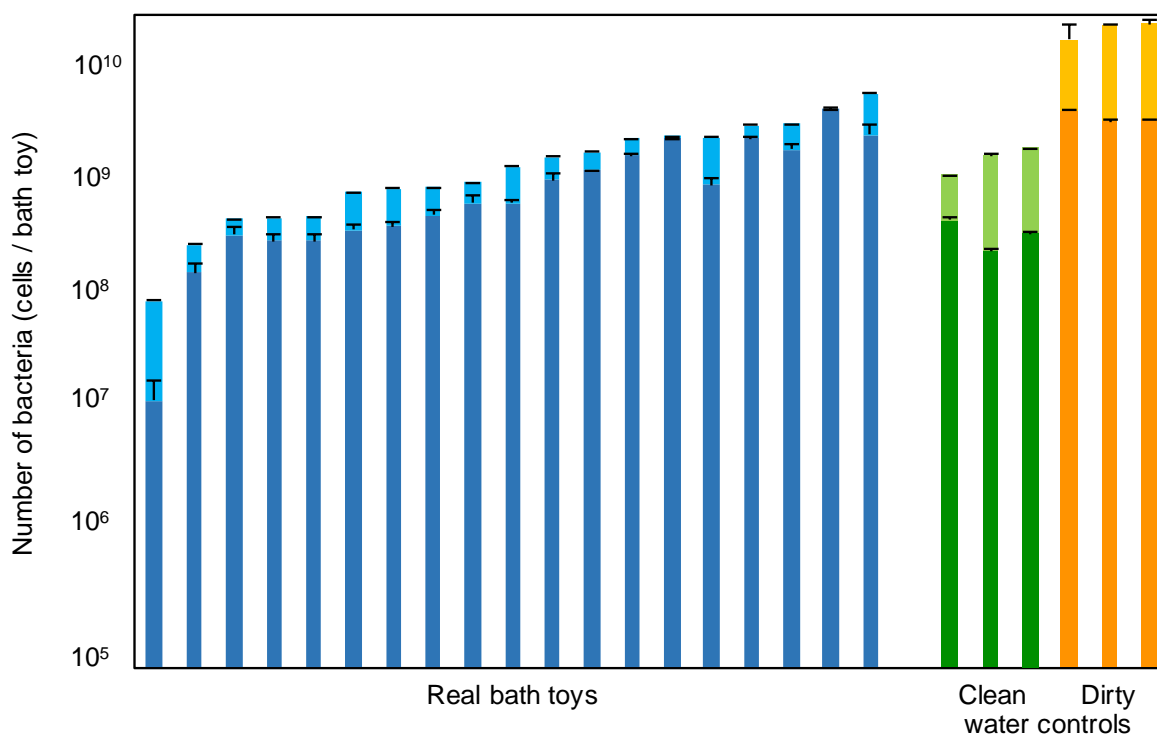


Figure S4: Number of bacteria in bath toy biofilms. Flow cytometry was used to differentiate between the total number of cells (SYBR® Green I staining) and the amount of intact cells (SYBR® Green I and Propidium Iodide staining) in biofilms grown in bath toys from real households or in control bath toys processed with either water prior (clean water controls) or after bathing (dirty water controls). The darker colours represent the number of intact bacteria in each bath toy, the lighter colours the damaged amount of the total number of cells. Error bars represent standard deviations of triplicate measurements.

Table S2 Classification of operational taxonomic units (OTUs) shared by biofilms originating from all bath toys (), all real bath toys (), all control bath toys (), all clean water controls (), or all dirty water controls (). NA indicates that no further classification could be made for that.

	Phylum	Class	Order	Family	Genus
1	Proteobacteria	Betaproteo.	Burkholderiales	Comamonadaceae	NA
2	Proteobacteria	Alphaproteo.	Rhizobiales	Bradyrhizobiaceae	Bradyrhizobium
3	Proteobacteria	Alphaproteo.	Caulobacterales	Caulobacteraceae	Caulobacter
4	Proteobacteria	Alphaproteo.	Rhizobiales	NA	NA
5	Proteobacteria	Alphaproteo.	Sphingomonadales	Sphingomonadaceae	Sphingomonas
6	Proteobacteria	Alphaproteo.	Rhizobiales	Rhizobiaceae	Agrobacterium
7	Proteobacteria	Alphaproteo.	Rhizobiales	Methylobacteriaceae	NA
8	Actinobacteria	Actinobacteria	Actinomycetales	Microbacteriaceae	NA
1	Proteobacteria	Betaproteo.	Burkholderiales	Comamonadaceae	NA
2	Proteobacteria	Alphaproteo.	Rhizobiales	Bradyrhizobiaceae	Bradyrhizobium
3	Proteobacteria	Alphaproteo.	Caulobacterales	Caulobacteraceae	Caulobacter
4	Proteobacteria	Alphaproteo.	Sphingomonadales	Sphingomonadaceae	Novosphingobium
5	Proteobacteria	Alphaproteo.	Rhizobiales	NA	NA
6	Proteobacteria	Alphaproteo.	Sphingomonadales	Sphingomonadaceae	Sphingomonas
7	Proteobacteria	Alphaproteo.	Rhizobiales	Rhizobiaceae	Agrobacterium
8	Proteobacteria	Alphaproteo.	Rhizobiales	Methylobacteriaceae	NA
9	Proteobacteria	Alphaproteo.	Rhodobacterales	Hyphomonadaceae	NA
10	Proteobacteria	Alphaproteo.	Sphingomonadales	Sphingomonadaceae	Sphingomonas
11	Actinobacteria	Actinobacteria	Actinomycetales	Microbacteriaceae	NA
12	Proteobacteria	Alphaproteo.	Rhizobiales	Methylobacteriaceae	Methylobacterium
13	Proteobacteria	Alphaproteo.	Caulobacterales	Caulobacteraceae	NA
1	Proteobacteria	Betaproteo.	Burkholderiales	Comamonadaceae	NA
2	Proteobacteria	Alphaproteo.	Rhizobiales	Bradyrhizobiaceae	Bradyrhizobium
3	Proteobacteria	Alphaproteo.	Caulobacterales	Caulobacteraceae	Caulobacter
4	Proteobacteria	Alphaproteo.	Rhodospirillales	Rhodospirillaceae	NA
5	Proteobacteria	Alphaproteo.	Rhizobiales	NA	NA
6	Proteobacteria	Gammaproteo.	Pseudomonadales	Moraxellaceae	Enhydrobacter
7	Proteobacteria	Alphaproteo.	Sphingomonadales	Sphingomonadaceae	Sphingomonas
8	Proteobacteria	Alphaproteo.	Rhizobiales	Rhizobiaceae	Agrobacterium
9	Proteobacteria	Alphaproteo.	Rhizobiales	Methylobacteriaceae	NA
10	Proteobacteria	Alphaproteo.	Caulobacterales	Caulobacteraceae	Phenylobacterium
11	Bacteroidetes	Flavobacteriia	Flavobacteriales	Flavobacteriaceae	Flavobacterium
12	Proteobacteria	Alphaproteo.	Caulobacterales	Caulobacteraceae	NA
13	Proteobacteria	Betaproteo.	Burkholderiales	Comamonadaceae	Hylemonella
14	Proteobacteria	Gammaproteo.	Pseudomonadales	Pseudomonadaceae	Pseudomonas
15	Actinobacteria	Actinobacteria	Actinomycetales	Brevibacteriaceae	Brevibacterium
16	Actinobacteria	Actinobacteria	Actinomycetales	Microbacteriaceae	NA
17	Planctomycetes	Phycisphaerae	Phycisphaerales	NA	NA
18	TM7	TM7-3	NA	NA	NA
19	Proteobacteria	Gammaproteo.	Pseudomonadales	Moraxellaceae	Acinetobacter
20	Proteobacteria	Alphaproteo.	Rhizobiales	Methylocystaceae	Methylopila
21	Bacteroidetes	Flavobacteriia	Flavobacteriales	[Weeksellaceae]	Chryseobacterium
22	Proteobacteria	Alphaproteo.	Sphingomonadales	Sphingomonadaceae	Sphingobium
23	Proteobacteria	Deltaproteo.	Bdellovibrionales	Bdellovibrionaceae	Bdellovibrio
24	Actinobacteria	Actinobacteria	Actinomycetales	Williamsiaceae	Williamsia
25	Proteobacteria	Alphaproteo.	Caulobacterales	Caulobacteraceae	NA
26	Actinobacteria	Actinobacteria	Actinomycetales	Nocardiaceae	Rhodococcus
27	Proteobacteria	Gammaproteo.	Pseudomonadales	Pseudomonadaceae	Pseudomonas
28	Proteobacteria	Alphaproteo.	Rhodospirillales	Acetobacteraceae	NA

	Phylum	Class	Order	Family	Genus
29	Armatimonadetes	[Fimbriimonadia]	[Fimbriimonadales]	[Fimbriimonadaceae]	Fimbriimonas
30	Bacteroidetes	Flavobacteriia	Flavobacteriales	[Weeksellaceae]	Chryseobacterium
31	Proteobacteria	Alphaproteo.	Rhizobiales	Brucellaceae	Ochrobactrum
32	WPS-2	NA	NA	NA	NA
33	Proteobacteria	Alphaproteo.	Rhizobiales	Rhizobiaceae	Agrobacterium
34	Proteobacteria	Betaproteo.	Burkholderiales	Comamonadaceae	NA
35	Proteobacteria	Alphaproteo.	Rhizobiales	Xanthobacteraceae	Xanthobacter
36	Actinobacteria	Actinobacteria	Actinomycetales	Microbacteriaceae	NA
37	Proteobacteria	Alphaproteo.	Rhizobiales	NA	NA
38	Proteobacteria	Alphaproteo.	Caulobacterales	Caulobacteraceae	Brevundimonas
39	Proteobacteria	Alphaproteo.	Rhodobacterales	Rhodobacteraceae	NA
40	Proteobacteria	Alphaproteo.	Rhizobiales	NA	NA
41	Proteobacteria	Alphaproteo.	Caulobacterales	Caulobacteraceae	NA
42	Proteobacteria	Alphaproteo.	Caulobacterales	Caulobacteraceae	NA
43	Proteobacteria	Alphaproteo.	Caulobacterales	Caulobacteraceae	NA
44	Proteobacteria	Alphaproteo.	Caulobacterales	Caulobacteraceae	NA
45	Proteobacteria	Alphaproteo.	Caulobacterales	Caulobacteraceae	NA
46	Proteobacteria	Alphaproteo.	Caulobacterales	Caulobacteraceae	NA
47	Proteobacteria	Alphaproteo.	Caulobacterales	Caulobacteraceae	NA
1	Proteobacteria	Betaproteo.	Burkholderiales	Comamonadaceae	NA
2	Proteobacteria	Alphaproteo.	Rhizobiales	Bradyrhizobiaceae	Bradyrhizobium
3	Proteobacteria	Alphaproteo.	Caulobacterales	Caulobacteraceae	Caulobacter
4	Proteobacteria	Alphaproteo.	Sphingomonadales	Sphingomonadaceae	Novosphingobium
5	Proteobacteria	Betaproteo.	Burkholderiales	Comamonadaceae	Comamonas
6	Proteobacteria	Alphaproteo.	Rhodospirillales	Rhodospirillaceae	NA
7	Proteobacteria	Alphaproteo.	Rhizobiales	NA	NA
8	Proteobacteria	Gammaproteo.	Pseudomonadales	Moraxellaceae	Enhydrobacter
9	Proteobacteria	Alphaproteo.	Sphingomonadales	Sphingomonadaceae	Sphingomonas
10	Proteobacteria	Alphaproteo.	Rhizobiales	Rhizobiaceae	Agrobacterium
11	Proteobacteria	Alphaproteo.	Rhizobiales	Methylobacteriaceae	NA
12	Proteobacteria	Alphaproteo.	Caulobacterales	Caulobacteraceae	Phenyllobacterium
13	Bacteroidetes	Flavobacteriia	Flavobacteriales	Flavobacteriaceae	Flavobacterium
14	Proteobacteria	Alphaproteo.	Caulobacterales	Caulobacteraceae	NA
15	Proteobacteria	Betaproteo.	Burkholderiales	Comamonadaceae	Hylemonella
16	Proteobacteria	Alphaproteo.	Sphingomonadales	Sphingomonadaceae	Sphingomonas
17	Proteobacteria	Gammaproteo.	Pseudomonadales	Pseudomonadaceae	Pseudomonas
18	Actinobacteria	Actinobacteria	Actinomycetales	Brevibacteriaceae	Brevibacterium
19	Bacteroidetes	Sphingobacteriia	Sphingobacteriales	NA	NA
20	Actinobacteria	Actinobacteria	Actinomycetales	Microbacteriaceae	NA
21	Planctomycetes	Phycisphaerae	Phycisphaerales	NA	NA
22	TM7	TM7-3	NA	NA	NA
23	Proteobacteria	Gammaproteo.	Pseudomonadales	Moraxellaceae	Acinetobacter
24	Proteobacteria	Alphaproteo.	Rhizobiales	Methylocystaceae	Methylopila
25	Bacteroidetes	Flavobacteriia	Flavobacteriales	[Weeksellaceae]	Chryseobacterium
26	WPS-2	NA	NA	NA	NA
27	Proteobacteria	Alphaproteo.	Sphingomonadales	Sphingomonadaceae	Sphingobium
28	Proteobacteria	Deltaproteo.	Bdellovibrionales	Bdellovibrionaceae	Bdellovibrio
29	Actinobacteria	Actinobacteria	Actinomycetales	Williamsiaceae	Williamsia
30	Planctomycetes	Planctomycetia	Planctomycetales	Planctomycetaceae	Planctomyces
31	Proteobacteria	Alphaproteo.	Rhizobiales	Methylobacteriaceae	NA
32	Proteobacteria	Alphaproteo.	Caulobacterales	Caulobacteraceae	NA
33	Proteobacteria	Alphaproteo.	Rhizobiales	Methylobacteriaceae	Methylobacterium
34	Bacteroidetes	Sphingobacteriia	Sphingobacteriales	Sphingobacteriaceae	Pedobacter
35	Actinobacteria	Actinobacteria	Actinomycetales	Nocardiaceae	Rhodococcus
36	Proteobacteria	Gammaproteo.	Pseudomonadales	Pseudomonadaceae	Pseudomonas

	Phylum	Class	Order	Family	Genus
37	Proteobacteria	Alphaproteo.	Rhodospirillales	Acetobacteraceae	NA
38	Bacteroidetes	Cytophagia	Cytophagales	Cytophagaceae	Spirosoma
39	Armatimonadetes	[Fimbriimonadia]	[Fimbriimonadales]	[Fimbriimonadaceae]	Fimbriimonas
40	Firmicutes	Bacilli	Bacillales	Planococcaceae	Lysinibacillus
41	Bacteroidetes	Flavobacteriia	Flavobacteriales	[Weeksellaceae]	Chryseobacterium
42	Proteobacteria	Alphaproteo.	Rhodospirillales	Rhodospirillaceae	Azospirillum
43	Proteobacteria	Alphaproteo.	Rhizobiales	Brucellaceae	Ochrobactrum
44	WPS-2	NA	NA	NA	NA
45	Actinobacteria	Actinobacteria	Actinomycetales	Micrococcaceae	Citricoccus
46	Proteobacteria	Alphaproteo.	Rhizobiales	Rhizobiaceae	Agrobacterium
47	Proteobacteria	Deltaproteo.	Myxococcales	0319-6G20	NA
48	Proteobacteria	Betaproteo.	Burkholderiales	Comamonadaceae	NA
49	Proteobacteria	Alphaproteo.	Rhizobiales	Xanthobacteraceae	Xanthobacter
50	Firmicutes	Bacilli	Lactobacillales	Streptococcaceae	Streptococcus
51	Proteobacteria	Alphaproteo.	Rhizobiales	NA	NA
52	Actinobacteria	Actinobacteria	Actinomycetales	Microbacteriaceae	NA
53	Proteobacteria	Betaproteo.	Burkholderiales	Comamonadaceae	NA
54	Proteobacteria	Gammaproteo.	Pseudomonadales	Pseudomonadaceae	Pseudomonas
55	Proteobacteria	Alphaproteo.	Sphingomonadales	Sphingomonadaceae	NA
56	Proteobacteria	Alphaproteo.	Rhizobiales	NA	NA
57	Proteobacteria	Alphaproteo.	Caulobacterales	Caulobacteraceae	Brevundimonas
58	Proteobacteria	Alphaproteo.	Rhizobiales	Methylobacteriaceae	NA
59	Proteobacteria	Alphaproteo.	Rhodobacterales	Rhodobacteraceae	NA
60	Proteobacteria	Alphaproteo.	Rhizobiales	NA	NA
61	Proteobacteria	Alphaproteo.	Caulobacterales	Caulobacteraceae	NA
62	Proteobacteria	Alphaproteo.	Caulobacterales	Caulobacteraceae	NA
63	Proteobacteria	Alphaproteo.	Caulobacterales	Caulobacteraceae	NA
64	Proteobacteria	Alphaproteo.	Caulobacterales	Caulobacteraceae	NA
65	Proteobacteria	Alphaproteo.	Caulobacterales	Caulobacteraceae	NA
66	Proteobacteria	Alphaproteo.	Rhizobiales	NA	NA
67	Proteobacteria	Alphaproteo.	Caulobacterales	Caulobacteraceae	NA
68	Proteobacteria	Alphaproteo.	Caulobacterales	Caulobacteraceae	NA
69	Proteobacteria	Alphaproteo.	Rhizobiales	Rhizobiaceae	Agrobacterium
70	Proteobacteria	Alphaproteo.	Caulobacterales	Caulobacteraceae	NA
71	Proteobacteria	Alphaproteo.	Caulobacterales	Caulobacteraceae	NA
72	Proteobacteria	Alphaproteo.	Caulobacterales	Caulobacteraceae	NA
1	Proteobacteria	Betaproteo.	Burkholderiales	Comamonadaceae	NA
2	Proteobacteria	Alphaproteo.	Rhizobiales	Bradyrhizobiaceae	Bradyrhizobium
3	Proteobacteria	Alphaproteo.	Caulobacterales	Caulobacteraceae	Caulobacter
4	Proteobacteria	Alphaproteo.	Rhodospirillales	Rhodospirillaceae	NA
5	Proteobacteria	Alphaproteo.	Rhizobiales	NA	NA
6	Proteobacteria	Gammaproteo.	Pseudomonadales	Moraxellaceae	Enhydrobacter
7	TM7	TM7-3	EW055	NA	NA
8	Proteobacteria	Alphaproteo.	Sphingomonadales	Sphingomonadaceae	Sphingomonas
9	Proteobacteria	Alphaproteo.	Rhizobiales	Rhizobiaceae	Agrobacterium
10	Proteobacteria	Alphaproteo.	Rhizobiales	Methylobacteriaceae	NA
11	Proteobacteria	Alphaproteo.	Caulobacterales	Caulobacteraceae	Phenyllobacterium
12	Proteobacteria	Gammaproteo.	Xanthomonadales	Xanthomonadaceae	Pseudoxanthomonas
13	Bacteroidetes	Flavobacteriia	Flavobacteriales	Flavobacteriaceae	Flavobacterium
14	Actinobacteria	Actinobacteria	Actinomycetales	Mycobacteriaceae	Mycobacterium
15	Proteobacteria	Alphaproteo.	Caulobacterales	Caulobacteraceae	NA
16	Proteobacteria	Betaproteo.	Burkholderiales	Comamonadaceae	Hylemonella
17	Proteobacteria	Gammaproteo.	Pseudomonadales	Pseudomonadaceae	Pseudomonas
18	Actinobacteria	Actinobacteria	Actinomycetales	Brevibacteriaceae	Brevibacterium

	Phylum	Class	Order	Family	Genus
19	Actinobacteria	Actinobacteria	Actinomycetales	Microbacteriaceae	NA
20	Bacteroidetes	Flavobacteriia	Flavobacteriales	[Weeksellaceae]	Chryseobacterium
21	Planctomycetes	Phycisphaerae	Phycisphaerales	NA	NA
22	TM7	TM7-3	NA	NA	NA
23	Proteobacteria	Gammaproteo.	Pseudomonadales	Moraxellaceae	Acinetobacter
24	Proteobacteria	Gammaproteo.	Legionellales	Legionellaceae	NA
25	Proteobacteria	Alphaproteo.	Rhizobiales	Methylocystaceae	Methylopila
26	Bacteroidetes	Flavobacteriia	Flavobacteriales	[Weeksellaceae]	Chryseobacterium
27	Proteobacteria	Alphaproteo.	Sphingomonadales	Sphingomonadaceae	Sphingobium
28	Proteobacteria	Deltaproteo.	Bdellovibrionales	Bdellovibrionaceae	Bdellovibrio
29	Verrucomicrobia	Verrucomicrobiae	Verrucomicrobiales	Verrucomicrobiaceae	Prostheco bacter
30	Actinobacteria	Actinobacteria	Actinomycetales	Williamsiaceae	Williamsia
31	Proteobacteria	Alphaproteo.	BD7-3	NA	NA
32	Proteobacteria	Alphaproteo.	Rhodobacterales	Rhodobacteraceae	Rhodobacter
33	Proteobacteria	Alphaproteo.	Caulobacterales	Caulobacteraceae	NA
34	Proteobacteria	Gammaproteo.	Pseudomonadales	Moraxellaceae	Acinetobacter
35	Proteobacteria	Gammaproteo.	Xanthomonadales	Xanthomonadaceae	Dokdonella
36	Actinobacteria	Actinobacteria	Actinomycetales	Nocardiaceae	Rhodococcus
37	Bacteroidetes	Sphingobacteriia	Sphingobacteriales	Sphingobacteriaceae	Pedobacter
38	Proteobacteria	Gammaproteo.	Pseudomonadales	Pseudomonadaceae	Pseudomonas
39	Proteobacteria	Gammaproteo.	Legionellales	Coxiellaceae	Aquicella
40	Proteobacteria	Alphaproteo.	Rhodospirillales	Acetobacteraceae	NA
41	Armatimonadetes	[Fimbriimonadia]	[Fimbriimonadales]	[Fimbriimonadaceae]	Fimbriimonas
42	Bacteroidetes	Flavobacteriia	Flavobacteriales	[Weeksellaceae]	Chryseobacterium
43	Proteobacteria	Alphaproteo.	Rhizobiales	Beijerinckiaceae	NA
44	Proteobacteria	Alphaproteo.	Rhizobiales	Brucellaceae	Ochrobactrum
45	Proteobacteria	Gammaproteo.	Pseudomonadales	Moraxellaceae	Acinetobacter
46	Proteobacteria	Deltaproteo.	Bdellovibrionales	Bdellovibrionaceae	Bdellovibrio
47	Proteobacteria	Gammaproteo.	Xanthomonadales	Xanthomonadaceae	NA
48	WPS-2	NA	NA	NA	NA
49	Bacteroidetes	Flavobacteriia	Flavobacteriales	[Weeksellaceae]	Chryseobacterium
50	Bacteroidetes	[Saprospirae]	[Saprospirales]	Chitinophagaceae	NA
51	Planctomycetes	Planctomycetia	Gemmatales	Isosphaeraceae	NA
52	Proteobacteria	Alphaproteo.	Rhizobiales	Rhizobiaceae	Agrobacterium
53	Actinobacteria	Actinobacteria	Actinomycetales	Gordoniaceae	NA
54	Proteobacteria	Betaproteo.	Burkholderiales	Comamonadaceae	Delftia
55	Proteobacteria	Alphaproteo.	Caulobacterales	Caulobacteraceae	NA
56	Proteobacteria	Betaproteo.	Burkholderiales	Comamonadaceae	NA
57	Proteobacteria	Alphaproteo.	Rhizobiales	Xanthobacteraceae	Xanthobacter
58	Proteobacteria	Betaproteo.	Burkholderiales	Comamonadaceae	NA
59	Proteobacteria	Alphaproteo.	Rhizobiales	Xanthobacteraceae	NA
60	Actinobacteria	Actinobacteria	Actinomycetales	Microbacteriaceae	NA
61	Proteobacteria	Betaproteo.	Burkholderiales	Comamonadaceae	NA
62	Actinobacteria	Actinobacteria	Actinomycetales	Mycobacteriaceae	Mycobacterium
63	Actinobacteria	Actinobacteria	Actinomycetales	Mycobacteriaceae	Mycobacterium
64	Actinobacteria	Actinobacteria	Actinomycetales	Mycobacteriaceae	Mycobacterium
65	Proteobacteria	Betaproteo.	Burkholderiales	Comamonadaceae	Roseateles
66	Proteobacteria	Betaproteo.	Burkholderiales	Comamonadaceae	Roseateles
67	Proteobacteria	Betaproteo.	Burkholderiales	Comamonadaceae	Roseateles
68	Proteobacteria	Betaproteo.	Burkholderiales	Comamonadaceae	Roseateles
69	Proteobacteria	Alphaproteo.	Rhizobiales	NA	NA
70	Proteobacteria	Alphaproteo.	Caulobacterales	Caulobacteraceae	Brevundimonas
71	Proteobacteria	Alphaproteo.	Rhizobiales	NA	NA
72	Proteobacteria	Alphaproteo.	Caulobacterales	Caulobacteraceae	NA

	Phylum	Class	Order	Family	Genus
73	Proteobacteria	Alphaproteo.	Sphingomonadales	Sphingomonadaceae	NA
74	Proteobacteria	Alphaproteo.	Caulobacterales	Caulobacteraceae	NA
75	Proteobacteria	Alphaproteo.	Rhodobacterales	Rhodobacteraceae	NA
76	Proteobacteria	Alphaproteo.	Caulobacterales	Caulobacteraceae	NA
77	Proteobacteria	Alphaproteo.	Caulobacterales	Caulobacteraceae	NA
78	Proteobacteria	Alphaproteo.	Caulobacterales	Caulobacteraceae	NA
79	Proteobacteria	Alphaproteo.	Caulobacterales	Caulobacteraceae	NA
80	Proteobacteria	Alphaproteo.	Rhizobiales	NA	NA
81	Proteobacteria	Alphaproteo.	Caulobacterales	Caulobacteraceae	NA
82	Proteobacteria	Alphaproteo.	Caulobacterales	Caulobacteraceae	NA
83	Proteobacteria	Betaproteo.	Burkholderiales	Comamonadaceae	Roseateles
84	Proteobacteria	Alphaproteo.	Caulobacterales	Caulobacteraceae	NA
85	Proteobacteria	Alphaproteo.	Caulobacterales	Caulobacteraceae	NA
86	Proteobacteria	Alphaproteo.	Caulobacterales	Caulobacteraceae	NA
87	Proteobacteria	Alphaproteo.	Caulobacterales	Caulobacteraceae	NA
88	Proteobacteria	Alphaproteo.	Caulobacterales	Caulobacteraceae	NA
89	Proteobacteria	Alphaproteo.	Caulobacterales	Caulobacteraceae	Phenyllobacterium
90	Proteobacteria	Alphaproteo.	Caulobacterales	Caulobacteraceae	Phenyllobacterium
91	Proteobacteria	Alphaproteo.	Caulobacterales	Caulobacteraceae	NA
92	Proteobacteria	Alphaproteo.	Caulobacterales	Caulobacteraceae	Phenyllobacterium
93	Proteobacteria	Alphaproteo.	Caulobacterales	Caulobacteraceae	NA
94	Proteobacteria	Alphaproteo.	Caulobacterales	Caulobacteraceae	NA
95	Proteobacteria	Alphaproteo.	Caulobacterales	Caulobacteraceae	NA
96	Proteobacteria	Alphaproteo.	Caulobacterales	Caulobacteraceae	NA
97	Proteobacteria	Alphaproteo.	Caulobacterales	Caulobacteraceae	Mycoplana
98	Proteobacteria	Alphaproteo.	Caulobacterales	Caulobacteraceae	NA
99	Proteobacteria	Alphaproteo.	Caulobacterales	Caulobacteraceae	NA
100	Proteobacteria	Alphaproteo.	Caulobacterales	Caulobacteraceae	NA
101	Proteobacteria	Alphaproteo.	Caulobacterales	Caulobacteraceae	NA
102	Proteobacteria	Alphaproteo.	Caulobacterales	Caulobacteraceae	NA
103	Proteobacteria	Alphaproteo.	Caulobacterales	Caulobacteraceae	NA
104	Proteobacteria	Alphaproteo.	Caulobacterales	Caulobacteraceae	NA
105	Proteobacteria	Alphaproteo.	Caulobacterales	Caulobacteraceae	NA
106	Proteobacteria	Alphaproteo.	Caulobacterales	Caulobacteraceae	NA
107	Proteobacteria	Alphaproteo.	Rhodospirillales	Rhodospirillaceae	NA

Table S3 ‘Household-specific core communities’ in real bath toys originated from five different Swiss households, with bath toys provided ranging between 1 – 6 bath toys per household. The OTUs in each core community are (1) present in all samples from the household, and (2) not present in other households; while shared OTUs are (1) present in all samples from the household, but (2) not necessarily exclusively.

	n(bath toys) / household	Sum of reads	n(household specific core OTUs)	% of core-reads / total number of reads w/in household	n(shared OTUs) / household
Household_I	1	30'133	33	0.1	-
Household_II	2	60'266	1'289	2.9	1'445
Household_III	3	90'399	741	2.1	124
Household_IV	5	150'665	1'059	1.1	41
Household_V	6	180'798	3'904	4.2	29

Table S4 Number of operational taxonomic units (OTUs) per individual bath toy and Shannon-Wiener index (H') as a measure of diversity.

Bath toy	Number of observed OTUs	H'
Real bath toy 01	2'826	0.52
Real bath toy 02	239	0.31
Real bath toy 03	597	0.43
Real bath toy 04	3'199	0.62
Real bath toy 05	3'483	0.52
Real bath toy 06	2'483	0.47
Real bath toy 07	281	0.35
Real bath toy 08	192	0.27
Real bath toy 09	6'196	0.71
Real bath toy 10	3'562	0.57
Real bath toy 11	429	0.40
Real bath toy 12	204	0.26
Real bath toy 13	329	0.39
Real bath toy 14	311	0.33
Real bath toy 15	No data available	
Real bath toy 16	335	0.33
Real bath toy 17	527	0.35
Real bath toy 18	No data available	
Real bath toy 19	435	0.32
Clean water control	214	0.26
Clean water control	188	0.23
Clean water control	265	0.17
Dirty water control	269	0.32
Dirty water control	268	0.25
Dirty water control	252	0.25

Figure S5 Classification of abundant OTUs in real bath toy biofilms. The ten most abundant OTUs for each single bath toy (i.e., OTUs with the most numbers of reads with all samples set to an even depth of 30'133 reads), originating from random households, were separated on different classification levels (phylum, class, order) to highlight differences in community compositions.

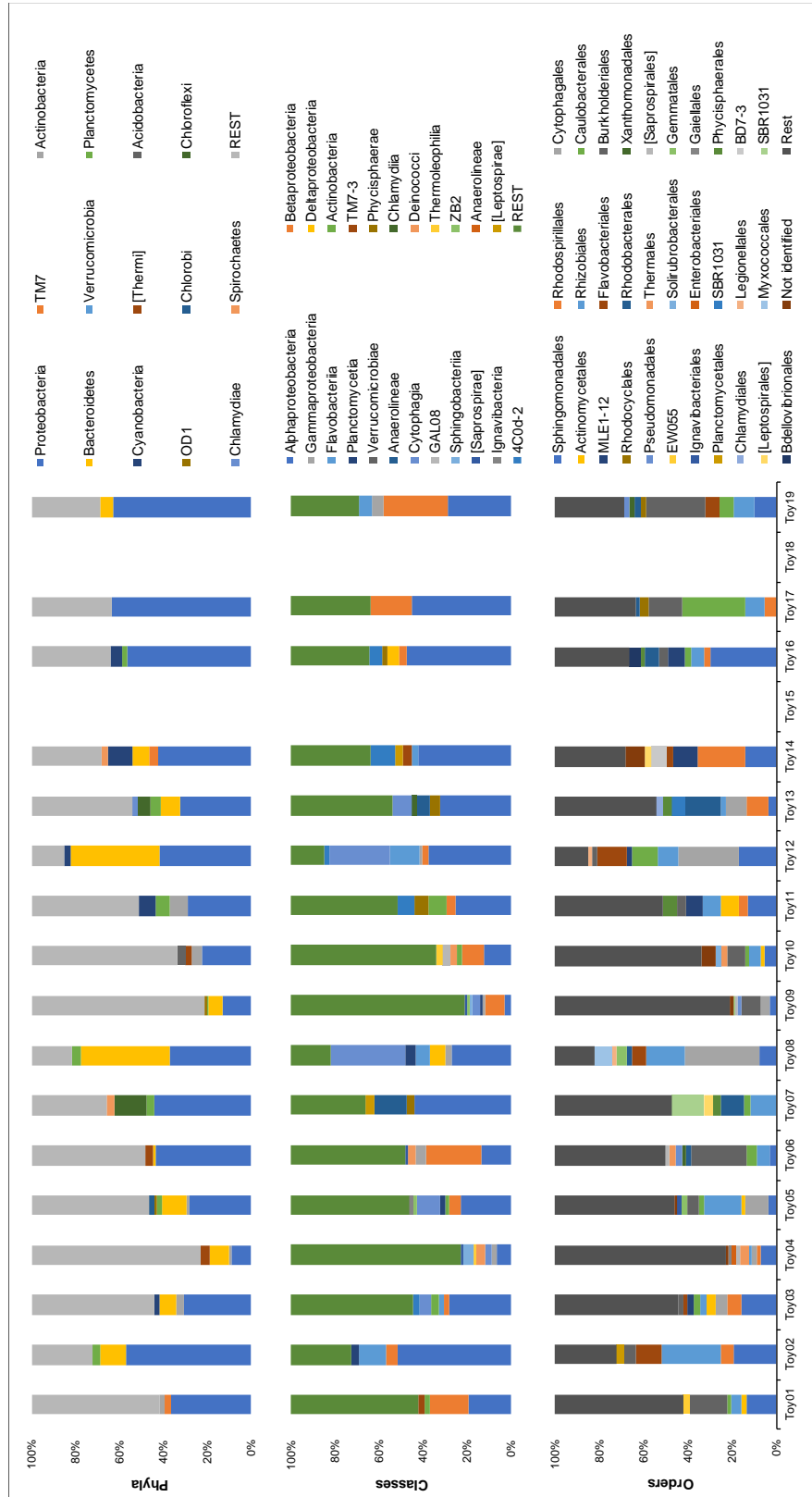


Table S5 Comparison of most abundant operational taxonomic units (OTUs) in control bath toy biofilms. Most abundant OTUs in clean and dirty water control biofilms are specified on different classification levels. Bold highlighted OTUs were dominant in both clean and dirty water controls.

	Phylum	Class	Order	Family	Genus
Clean water controls	Proteobacteria	Alphaproteo.	Caulobacterales	Caulobacteraceae	Caulobacter
	Proteobacteria	Alphaproteo.	Rhodospirillales	Rhodospirillaceae	NA
	Proteobacteria	Alphaproteo.	Caulobacterales	Caulobacteraceae	NA
	Proteobacteria	Betaproteo.	Burkholderiales	Comamonadaceae	NA
	Proteobacteria	Alphaproteo.	Sphingomonadales	Sphingomonadaceae	Sphingomonas
	Proteobacteria	Alphaproteo.	Rhizobiales	Methylobacteriaceae	NA
	Proteobacteria	Alphaproteo.	Caulobacterales	Caulobacteraceae	NA
	Proteobacteria	Alphaproteo.	Sphingomonadales	Sphingomonadaceae	Sphingomonas
	Planctomycetes	Phycisphaerae	Phycisphaerales	NA	NA
	Proteobacteria	Betaproteo.	Burkholderiales	Comamonadaceae	NA
	Rest	/	/	/	/
Dirty water controls	Proteobacteria	Alphaproteo.	Caulobacterales	Caulobacteraceae	Caulobacter
	Proteobacteria	Alphaproteo.	Rhodospirillales	Rhodospirillaceae	NA
	Proteobacteria	Alphaproteo.	Caulobacterales	Caulobacteraceae	NA
	Proteobacteria	Alphaproteo.	Rhizobiales	Rhizobiaceae	Agrobacterium
	Proteobacteria	Alphaproteo.	Caulobacterales	Caulobacteraceae	Phenyllobacterium
	Actinobacteria	Actinobacteria	Actinomycetales	Mycobacteraceae	Mycobacterium
	Bacteroidetes	Flavobacteriia	Flavobacteriales	[Weeksellaceae]	Chryseobacterium
	TM7	TM/-3	NA	NA	NA
	Proteobacteria	Betaproteo.	Burkholderiales	Comamonadaceae	NA
	Proteobacteria	Alphaproteo.	Caulobacterales	Caulobacteraceae	NA
	Rest	/	/	/	/

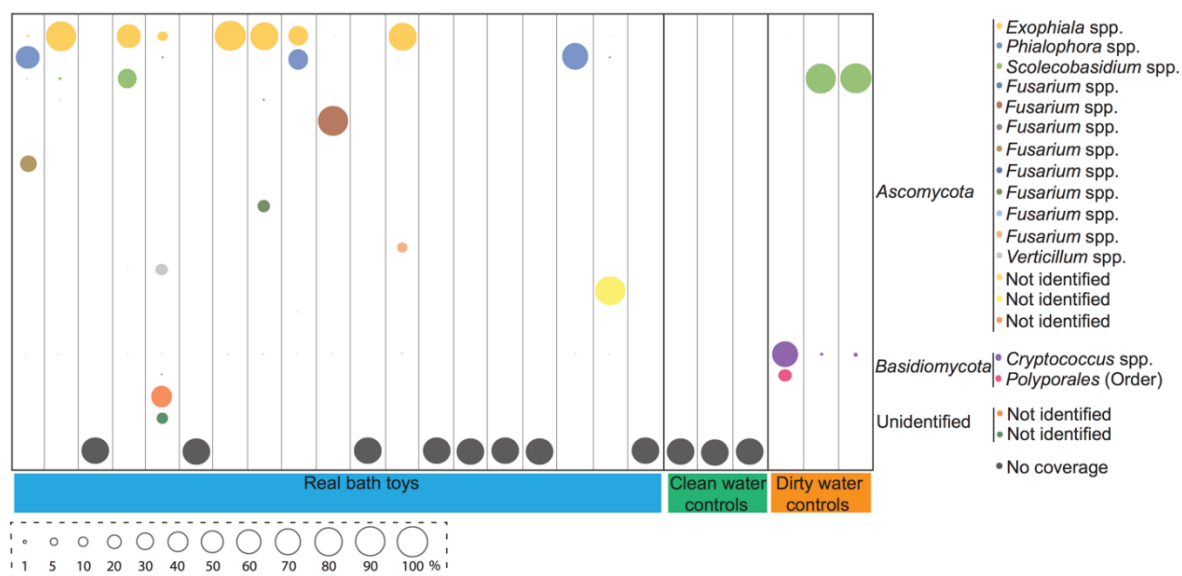


Figure S6 Dominant operational taxonomic units (OTUs) in fungal communities of bath toy biofilms. Colors represent different OTUs on genus level, with the majority belonging to the phylum Ascomycota and the rest either to Basidiomycota or being unidentified. Samples indicated with black circles did not show any results for fungi representatives. In general, the size of the circles indicates the absolute abundance of each OTU, with bigger volumes indicating higher percentages.

Table S6 Conventional plating results testing biofilms from the inner surface of bath toys for several indicator bacteria or groups. Samples were taken from either real bath toys (A) which were used randomly in different households or from control bath toys (B) which were used either with clean water prior to bathing (clean water controls) or with used water after bathing (dirty water controls). Compact Dry Plates were used for testing the presence of *Pseudomonas aeruginosa*, *Listeria* spp., *Enterococci* spp., Coliforms, and *Escherichia coli*. Special agar plates (Legionella BMP a Selective Medium) were used for the detection of *Legionella pneumophila*. Red, empty boxed indicate negative cultivation results. Green boxed indicate positive results including numbers of colony forming units (CFU). The number of CFUs was recalculated to their total presence per bath toy, with a detection limit of 3.3×10^2 CFU/bath toy.

A	Real bath toys																	
<i>P. aeruginosa</i>		3x10 ²		2x10 ⁴		14x10 ⁵		4x10 ⁵		5x10 ⁵	1x10 ⁵	4x10 ⁴		3x10 ³	4x10 ⁵	8x10 ⁵	3x10 ³	
<i>Listeria</i> spp.		3x10 ³				1x10 ⁵	2x10 ⁴								4x10 ²	4x10 ⁵	5x10 ³	
<i>Enterococci</i> spp.		1x10 ³					3x10 ²				3x10 ²					1x10 ⁵		
Coliforms																		
<i>E. coli</i>																		
<i>L. pneumophila</i>		7x10 ⁴	7x10 ⁴					4x10 ⁴						1x10 ⁵		2x10 ⁶	7x10 ³	
B	Clean water controls						Dirty water controls											
<i>P. aeruginosa</i>	2x10 ⁴	1x10 ⁴	1x10 ³	3x10 ⁴	8x10 ⁴	3x10 ⁴												
<i>Listeria</i> spp.	8x10 ³	1x10 ³	1x10 ³	4x10 ⁴	6x10 ⁴	1x10 ⁵												
<i>Enterococci</i> spp.																		
Coliforms	3x10 ³	2x10 ⁴																
<i>E. coli</i>				4x10 ⁴	1x10 ⁵	1x10 ⁵												
<i>L. pneumophila</i>	1x10 ⁴		7x10 ³	2x10 ³	2x10 ³	2x10 ³												

Table S7 Carbon migration potential (MP) and biomass formation potential (BFP) of the control bath toys' plastic material. Carbon migration was measured after 1 (M1), 3 (M3), and 7 (M7) days of incubation (with water renewal on day 2, 4, 5, and 6 without measurement) and values for total organic carbon (TOC), total cell counts/cm² (TCC), as well as the proportion of assimilable organic carbon (AOC) to total organic carbon were summarized afterwards ($\sum_{M1/M3/M7}$). Standard deviations are given for experimental triplicates (*Stdev*). For the BFP, planktonic (pBFP) and biofilm (bBFP) growth after 14 d of incubation was measured.

Carbon migration	TOC [$\mu\text{g}/\text{cm}^2$]	TOC [$\mu\text{g}/\text{cm}^2/\text{day}$]	TCC [cells/cm ²]	AOC/TOC [%]
$\sum_{M1/M3/M7}$	11.8	-	8.7×10^7	73.5
<i>Stdev</i>	0.8	-	1.1×10^6	-
M1	-	5.59		
<i>Stdev</i>	-	0.07		
M3	-	3.59		
<i>Stdev</i>	-	0.62		
M7	-	2.59		
<i>Stdev</i>	-	0.12		
<hr/>				
Biofilm formation	Planktonic cells/cm ²	Biofilm cells/cm ²	\sum BFP [cells/cm ²]	pBFP/bBFP [%]
t ₁₄	3.0×10^8	3.6×10^8	6.6×10^8	82.5
<i>Stdev</i>	5.1×10^7	5.6×10^7	1.1×10^8	-

Characteristics of tap water in the control experiment prior to and after bathing

Method

Water samples were taken before and after bathing in the control experiment. Total cell numbers were analyzed (FCM, SG staining; see above) and the concentrations of dissolved organic carbon (DOC), total organic carbon (TOC), total nitrogen (TN), and total phosphorus (TP) were measured. Chemical measurements were performed in a TOC-L_{CSH} (SHIMADZU GmbH, Switzerland) where carbon dioxide (CO₂) was measured with an infrared (IR) detector after an initial catalytically burning at 720 °C. For differentiating between total and dissolved organic carbon, DOC samples were filtered (0.45 µm) before separate measurement. For the T-N measurement, NO_x was measured with a chemiluminescence detector.

Results

Table S8 Biological and chemical parameters for water before and after bathing. Total cell numbers per milliliter as well as concentrations for dissolved organic carbon (mg DOC/L), total organic carbon (mg TOC/L), total nitrogen (mg TN/L), and total phosphate (µg TP/L) were measured for clean water prior to bathing and dirty water after bathing including dirt and soap. Standard deviations (Stdev) are given for the measurement of three individual samples.

	DOC [mg/L]	TOC [mg/L]	TN [mg/L]	TP [µg/L]	TCC / mL
Before bathing	1.0	1.2	2.6	13.7	2.1 x 10 ⁵
Stdev	0.1	0.1	0.3	6.0	1.1 x 10 ⁵
After bathing	11.3	15.7	4.9	21.2	4.1 x 10 ⁵
Stdev	1.6	1.2	1.0	6.0	2.5 x 10 ⁵

Table S9 Settings for Amplicon PCR and Index PCR.

Amplicon PCR	Temperature	Duration	Cycles
	95°C	5:00 min	
	95°C	0:20 min	29 x
	51°C	0:15 min	
	72°C	0:30 min	
	4°C	hold	
Index PCR	Temperature	Duration	Cycles
	95°C	3:00 min	
	95°C	0:30 min	8 x
	51°C	0:35 min	
	72°C	0:35 min	
	4°C	hold	

Chapter 4

Small-scale heterogeneity in drinking water biofilms

This chapter has been published in *Frontiers in Microbiology* (2019, 10:2446) by L. Neu, C.R. Proctor, J.-C. Walser, and F. Hammes.

Abstract

Biofilm heterogeneity has been characterized on various scales for both natural and engineered ecosystems. This heterogeneity has been attributed to spatial differences in environmental factors. Understanding their impact on localized biofilm heterogeneity in building plumbing systems is important for both management and representative sampling strategies. We assessed heterogeneity within the confined engineered ecosystem of a shower hose by high-resolution sampling (200 individual biofilm sections per hose) on varying scales (μm to m). We postulated that a biofilm grown on a single material under uniform conditions should be homogeneous in its structure, bacterial numbers, and community composition. A biofilm grown for 12 months under controlled laboratory conditions, showed homogeneity on large-scale. However, some small-scale heterogeneity was clearly observed. For example, biofilm thickness of cm-sections varied up to 4-fold, total cell concentrations (TCC) 3-fold, and relative abundance of dominant taxa up to 5-fold. A biofilm grown under real (i.e., uncontrolled) use conditions developed considerably more heterogeneity in all variables which was attributed to more discontinuity in environmental conditions. Interestingly, biofilm communities from both hoses showed comparably low diversity, with < 400 taxa each, and only 3 taxa accounting for 57 % respectively 73 % of the community. This low diversity was attributed to a strong selective pressure, originating in migrating carbon from the flexible hoses as major carbon source. High-resolution sampling strategy enabled detailed analysis of spatial heterogeneity within an individual drinking water biofilm. This study gives insight into biofilm structure and community composition on cm-to m-scale and is useful for decision-making on sampling strategies in biofilm research and monitoring.

Introduction

Microbial biogeography has been documented in diverse aquatic ecosystems and on various spatial scales^{1,2}. Numerous studies revealed a remarkable heterogeneity (i.e., variations) in bacterial abundance^{3,4}, metabolic activities^{5,6}, or microbiomes^{7,8}. Interestingly, this heterogeneity was not attributed to distance per se, but mainly to spatial differences in environmental factors^{9,10}. For example, biogeographical heterogeneity in natural freshwater ecosystems was shown to be driven by localized differences in factors such as temperature¹, alkalinity⁹, and salinity¹¹.

Many environmental factors that enable biogeographical heterogeneity in natural ecosystems are equally relevant in confined engineered aquatic ecosystems, such as drinking water treatment and distribution systems. For example, heterogeneity was ascribed to differences in treatment processes, e.g., treatment units^{12,13}, filtration type^{14,15}, or filtration media¹⁶. Also, changes in the exposure to disinfection and disinfectant residuals^{17,18}, as well as differences in the composition and quantity of nutrients^{19,20}, radial-spatial orientation^{21,22}, and temperatures³ were shown to cause biogeographical heterogeneity. The most dramatic variations in drinking water systems occur in the built environment. Here, several factors shape heterogeneous biofilms within the same connected system, namely: (1) diverse materials that support microbial growth^{23,24} and select for material specific community compositions^{25,26}, (2) variation in surface-to-volume ratios that increase microbial attachment/detachment rates/probabilities²⁷, (3) differences in flow/stagnation regimes^{28,29}, and (4) differences in water temperatures³⁰. These variations do not only occur between different sections of a system, but also within, e.g., one individual pipe or fixture. Considering the clear impact of variable environmental conditions on microbiology, it is reasonable to expect biogeographical heterogeneity within such a connected aquatic system. It is, however, less clear to what degree biogeographical heterogeneity can be

expected when environmental factors are consistent, for example when a single pipe material is exposed to seemingly uniform environmental conditions along its whole length.

The goal of this study was to characterize spatial heterogeneity within a mature drinking water biofilm that grew inside a flexible shower hose. We aimed to identify environmental factors that shape biofilm heterogeneity and elucidate the importance of sample scale in both fundamental and applied biofilm research. Our hypothesis was that a biofilm grown on a single material under uniform conditions would be homogeneously distributed with respect to structure and composition. To test this, a biofilm was grown inside a flexible plastic hose (PVC-P) under defined and controlled laboratory conditions. Small-scale heterogeneity was assessed by comparing (1) biofilm structure and thickness, (2) total cell concentrations, and (3) bacterial community composition of a total of 200 sections of 1.2 cm. Additionally, a biofilm grown in an identical hose under real-use conditions was analyzed in the same way to assess the impact of more variable environmental conditions on biofilm spatial heterogeneity. Our sampling design enabled a high-resolution assessment of drinking water biofilms on small-scale, and the combination of quantitative and qualitative tools for biofilm characterization. This study provides a deeper insight into biofilm formation on building plumbing materials and consequently informs on biofilm sampling strategies.

Materials and Methods

Growing biofilms inside flexible shower hoses under controlled and real-use conditions

Biofilms were grown inside commercially available flexible shower hoses, purchased from the same batch of production. The hoses were made from plasticized polyvinyl chloride (PVC-P), with an inner diameter of 0.8 cm, a total length of 1.80 m, and originally with a metal cover outer sheath.

Biofilm growth under controlled laboratory conditions

In the laboratory setup, the metal sheath was removed and the hose was horizontally aligned in a dark container, preventing any motion or physical disruption (further referred to as 'control hose'). The installation was connected to a warm water tap with automated flushing events realized by a time-controlled magnetic valve. Over the course of one year, the hose was automatically flushed for 15 min with warm water (35 – 42°C) twice per day with consistent stagnation times of 8 and 16 hours, respectively (Figure S1). A flow velocity of 0.3 L/min was provided. The tap water was non-chlorinated drinking water, consisting mostly of pre-treated surface water (78.6 %, Lake Zurich, ozonation, slow sand, activated carbon, and rapid sand filtration) and untreated groundwater (15.0 %), with a small portion of pre-treated spring water (6 %, UV disinfection) (Table S1, A).

Biofilm growth under uncontrolled real-use conditions

Complementary to the control hose, an identical PVC-P hose was installed in a real shower (further referred to as 'real hose'), with the aim to assess the impact of more variable environmental conditions on biofilm heterogeneity. Usage habits (e.g., shower durations, stagnation times, water temperature, and flow rate) varied over the course of one year, with three residents sharing the shower. For showering, mixtures of warm and cold water lines were used

with varying and higher flow velocities compared to the control hose (average use: 8 – 12 L/min), and random stagnation times that went up to 14 days. The water was also non-chlorinated, but originating mostly from untreated groundwater (95 %) with a minor addition of pre-treated spring water (5 %, UV disinfection, slow sand filtration) (Table S1, B).

Sample handling and processing

Both hoses were processed, sampled, and analyzed in the same way (Figure 1). For the control hose, 120 cm from the middle part were sampled for biofilm characterization, while for the real hose, 20 cm from the beginning of the hose (i.e., from the water inlet onwards) were removed and the following 120 cm piece was sampled. The collected 120 cm pieces were each separately dissected into 20 x 6 cm pieces, which were then bisected into top and bottom sections. Optical coherence tomography (OCT) was used for imaging and quantifying biofilm structure and thickness (see below). Following this, each piece was cut into 5 x 1.2 cm sections and biofilms were removed by brushing each of them separately with an electric toothbrush (Oral-B®, Advanced Power) into a total volume of 10 mL of 0.2 µm filtered bottled water (Evian, France). For this, each section was covered with 5 mL of filtered water in a petri dish and brushed for approximately 45 s, depending on the stickiness of the biofilm matrix. The remaining 5 mL were used to remove residuals of biofilm from the toothbrush head and from the surface of the petri dish (approximately 20 s brushing) and transferred to the sample tube. The 10 mL biofilm suspension was then needle sonicated to disrupt cell clusters (Sonopuls HD 2200, Bandelin Sonorex, Rangendingen, Germany). The needle was submerged to the upper third of the sample volume and sonication occurred for 30 s, with 5 x 10 % pulses, and 40 % power. The biofilm suspensions were measured with flow cytometry (FCM) to quantify total cell concentrations (TCC; see below). Finally, biofilm suspensions were filtered for DNA analysis (see below). For all sampling steps, pieces were randomized to minimize the impact of processing errors.

For data analysis, the terminology ‘cm-sections’ refers to the 1.2 cm sections, representing a total of 200 cm-sections per experimental hose. Furthermore, for bacterial cell concentrations and the analysis of sequencing data, units were converted to values per cm^2 to make results more comparable within this study and to other studies.

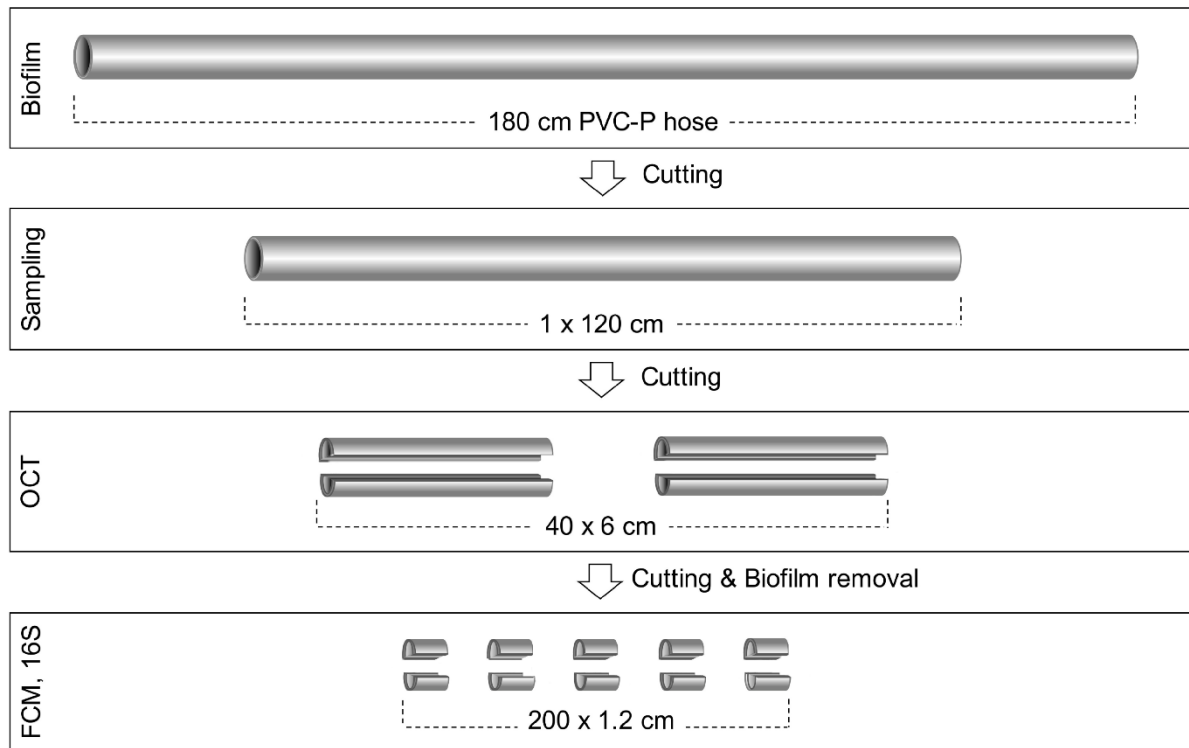


Figure 1: Experimental setup and sample processing. The control hose was horizontally aligned and flushed twice daily. The real hose hung vertically with a bend at the lower end and was used regularly (uncontrolled). The sampling strategy was identical for both hoses. A 120 cm section of each hose was extracted, then cut in 6 cm sections, horizontally bisected and imaged with optical coherence tomography for biofilm thickness. The 6 cm pieces were then cut into 1.2 cm sections followed by biofilm removal, which was then analyzed with flow cytometry for total cell counts and 16S rRNA amplicon sequencing for community analysis.

Biofilm analysis with optical coherence tomography

For characterizing the structure, biofilms were imaged using a Spectral Domain OCT Imaging System (930nm, OCT System Ganymede, Thorlabs GmbH, Dachau, Germany), with an axial detection limit of 4.4 μm . The 6 cm pieces were horizontally aligned and covered with a thin layer of 0.2 μm filtered water for optimal imaging. Along the length of each piece, images of 2 mm (length) x 1 mm (height) were captured, which equals 30 images per piece or 1'200 per hose respectively. The Advanced Positioning Technology (Thorlabs' APT™) Software was used to move the pieces in distinct steps of 2 mm without disrupting the alignment. Biofilm thickness was then determined using an analysis software in MATLAB® (Version R2016b) which has previously been reported by Derlon and colleagues³¹. First, .img files were translated into .tif images. Second, the interface between hose surface and biofilm was detected (grey-scale gradient analysis). In case of inaccurate detection of the interface, a black line was drawn manually using ImageJ (Version 1.50i). Finally, these interfaces were used to create binary images, which were used for further image analysis. Potential problems that arose during image processing where solved as follows: (1) Detached biofilm structures floating around were creating artificially high values for biofilm thickness. For correction, these parts were masked manually with black boxes (ImageJ). (2) If no clear detectable line was indicating the biofilm-water interface, it could result in wrong values for minimal biofilm thickness. For this, white lines were drawn manually indicating the biofilms surface (ImageJ). For better comparison between the different quantitative measurements, average thickness values were used for combined 1.2 cm sections (equals 6 images per section).

Flow cytometry for determining total bacterial cell concentrations

Total bacterial cell concentrations (TCC) were quantified for each 1.2 cm section by flow cytometry (FCM). Sample preparation, measurements, as well

as data analysis were performed as described elsewhere³². First, biofilm suspensions were diluted 1:10 (control hose) or 1:100 (real hose) respectively, with 0.2 µm filtered bottled water. Second, samples were stained with 10 µL/mL SYBR® Green I (SG, Invitrogen AG, Basel, Switzerland; 100x diluted in Tris buffer, pH 8) to detect TCC. Finally, samples were incubated at 37°C for 10 min and then measured using a BD Accuri C6® flow cytometer (BD, Belgium), with an instrumental threshold set at 800 (FL1-H) and a volume of 50 µL measured at a high flow velocity of 66 µL/min. For analysis, one gate was applied for all samples.

Community analysis by 16S rRNA gene sequencing

Prior to DNA extraction, biofilm suspensions were concentrated on 0.22 µm polycarbonate Nucleopore® membrane filters (Ø 47 mm, Whatman, Kent, UK), using sterile bottle top filter units attached to a vacuum pump (vacuubrand 2c, Wertheim, Germany). DNA filters were immediately frozen in liquid nitrogen and stored at -20°C until DNA extraction.

DNA extraction

DNA extraction was performed according to the protocol of the DNeasy PowerWater® Kit (Qiagen, Hilden, Germany). Extracts were stored at -20°C until 16S rRNA gene amplification for sequencing.

16S rRNA gene amplification and MiSeq sequencing

For 16S rRNA gene sequencing, the V3-V5 region of the gene was amplified by polymerase chain reaction (PCR) using the primers Bakt_341F and Bakt_805R³³. First, DNA was quantified with the Qubit™ DNA Broad Range Assay in duplicates, using the Spark® 10M Multimode Microplate Reader (Tecan, Switzerland). The amount of DNA was normalized between all samples (1 ng) and primers were added in a final concentration of 0.3 µM (Table S2, A). After amplification, samples were purified with the Agencort AMPure XO System

(Beckman Coulter, Inc., Brea, CA), followed by the annealing of specific sequencing Nextera XT v2 Index Kit adapters (Illumina) to the generated amplicons via Index PCR (Table S2, B). Purified products were again quantified and the base pair (bp) length was verified with the High Sensitivity D1000 ScreenTape system (Agilent 2200 TapeStation), identifying an average library size of 569 bp. Each sample was normalized to 2 nM (10 mM Tris, pH 8.0), followed by pooling 10 μ L of each, and a last quantification to ensure the final concentration. The Illumina MiSeq platform was used for paired-end 600 cycle sequencing with 10 % PhiX serving as a control in the sequencing run (Illumina: Technical Note on PhiX Control). For amplification and sequencing, a distinct number of samples was processed in duplicates to verify the reliability and reproducibility of sequencing data. Also, a negative control (amplification of PCR grade water) as well as a positive control (Self-made MOCK community: *Burkholderia xenovorans*, *Bacillus subtilus*, *Escherichia coli*, *Micrococcus luteus*, *Pseudomonas protegens*, *Paenibacillus sabinae*, and *Streptomyces violaceoruber*) were incorporated. In the course of sample processing, some biofilm sections needed to be excluded due to low quantities of extracted DNA, poor amplification, or poor number of reads after sequencing. Data on community composition was generated in collaboration with the Genetic Diversity Centre (GDC), ETH Zurich.

Sequencing data processing and analysis

16S rRNA amplicon sequence data were processed following a distinct pipeline. First, data quality was evaluated (Table S3, step A). Second, read ends were trimmed and merged (Table S3, step B). Third, in-silico PCR was performed and primer sites trimmed (Table S3, step C). Then, sequences were filtered based on their quality and size range (Table S3, step D). Finally, amplicon sequence variants (ASV) were established and taxonomically assigned (Table S3, steps E and F). In contrast to the classic 97 % identity clustering method³⁴, sequences were clustered by an ASV approach using UNOISE3³⁵. Unoise3 includes a sequencing error correction and chimaeral

removal. The predicted biological sequences (i.e., ASV) are called zero-radius operational taxonomic units (ZOTUs). Although ZOTUs are valid operational taxonomic units (OTUs) the number is usually inflated. The reason might be the fact that early PCR errors cannot be detected and therefore leading to very similar amplicons. For this reason, we additionally clustered the ZOTUs at different identity levels (99 %, 98 %, and 97 %). For the taxonomic assignment predictions, the Silva 16S database (v128) in combination with the SINTAX classifier was used with a cut-off of 0.9. Attributed classifications for DNA sequences were ultimately verified using the NCBI platform. Data analysis was performed using R (Version 3.3.0) and RStudio (Version 1.1.477) with the R package ggplot2 (Version 2.2.1), vegan (version 2.4.5) and the Bioconductor 'phyloseq' (Version 1.16.2).

Scanning electron microscopy

Ten centimeters from the beginning and end of each hose were immediately prepared for scanning electron microscopy. For this, biofilms were fixed with 2.5 % Glutaraldehyde in Cacodylate buffer (0.1 M, pH 7.2) at room temperature for 60 minutes and stored in Cacodylate buffer at 4°C afterwards. Final preparation and imaging were done by the Center for Microscopy and Image Analysis (University of Zurich).

Results

We analyzed in detail biofilms that formed inside two identical shower hoses under controlled use and real use conditions, with both exposed to non-chlorinated warm water during approximately 12 months. The purpose of this study was to assess the degree of spatial heterogeneity within each individual biofilm by high-resolution sampling, with the communities developing under supposedly uniform (control hose) or more variable (real hose) environmental conditions. In Figure 1, the two longitudinal halves of each hose are categorized as *top* and *bottom*, reflecting the actual spatial orientation of the control hose in the laboratory setup. The real hose was used vertically in a shower, hence the longitudinal *top* and *bottom* do not represent any specific orientation. Data from 200 biofilm sections was analyzed on various scales (from μm – m) for each individual hose. Here, *large-scale* refers to the complete hose (i.e., the 120 cm piece of hose). *Small-scale* refers to the differences between adjacent 1.2 cm-sections.

Biofilm development under controlled conditions

A visibly thick biofilm established on the inner surface of the control hose during 12 months of twice-daily warm water flushing (Figure 2, Figure 3A). The entire biofilm of the 120 cm piece of the hose contained a total of 4.7×10^9 bacteria, at an average distribution of $2.4 \pm 0.5 \times 10^7$ cells/cm² ($n = 200$) (Figure 3B), with the microbial community being dominated by only few taxa (Figure 3C).

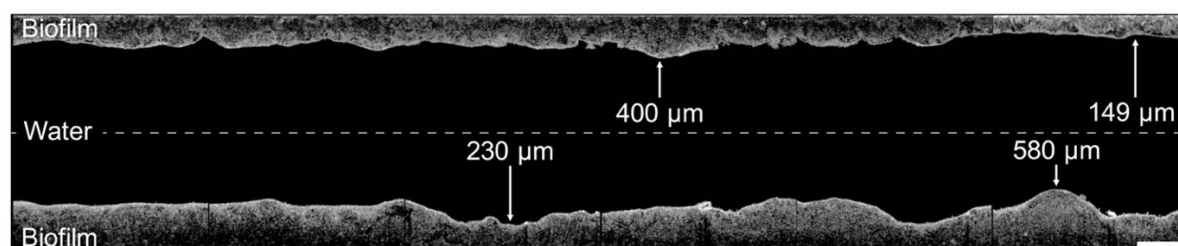


Figure 2: Visualization of the control hose biofilm imaged with optical coherence tomography. Images (2 mm length) were combined to illustrate

the biofilm structure and thickness of 1.2 cm-sections, showing a representative example of the shower hose biofilm. The hose was static and horizontally aligned, thus top and bottom in this image represent the actual orientation of the biofilm. The space between the top and bottom sections is not to scale. Scale bar: 500 μm .

Structure: Thickness varied on μm -scale

The biofilm topography was sinuous, with uneven protrusions and depressions resembling hills/dunes (Figure 2). The averaged thickness of 1.2 cm-sections ranged between 150 – 750 μm with an overall average of $319 \pm 111 \mu\text{m}$ ($n = 200$) (Figure 3A, Figure S2). On large-scale, the biofilm was significantly thicker at the bottom ($386 \pm 117 \mu\text{m}$, $n = 100$) compared to the top ($252 \pm 44 \mu\text{m}$, $n = 100$) (t-test, $p < 0.05$). Moreover, biofilm thickness increased notably over the length of the 120 cm piece following the flow direction; approximately 100 % in the top (linear regression with $R^2 = 0.43$) and 255 % in the bottom (linear regression with $R^2 = 0.40$). This amounts to an average increase of 0.83 $\mu\text{m}/\text{cm}$ (top) and 2.13 $\mu\text{m}/\text{cm}$ (bottom). In addition to the spatial trend, variability in biofilm thickness was already evident on small-scale. Adjacent cm-sections of the top varied $11.7 \pm 8.9 \%$ ($n = 99$), ones in the bottom varied even more with $23.9 \pm 28.5 \%$ ($n = 99$), with the standard deviations suggesting higher variation/heterogeneity throughout the bottom part of the hose. On an even smaller scale (i.e., μm -scale), variations of up to 50 % could be observed (Figure 2). In addition to the assessment of structural heterogeneity, two-dimensional thickness data could be used to roughly reconstruct three-dimensional characteristics. Here, the average biofilm volume, calculated from the average thickness data, was $2.5 \pm 0.4 \times 10^{10} \mu\text{m}^3/\text{cm}^2$ ($n = 100$) in the top and $3.9 \pm 1.2 \times 10^{10} \mu\text{m}^3/\text{cm}^2$ ($n = 100$) in the bottom part of the hose.

Numbers: Bacteria account for only a small fraction of the biofilm volume

Total cell concentrations (TCC) of 1.2 cm-sections ranged between $1.1 - 3.4 \times 10^7$ cells/ cm^2 . Interestingly, average TCC values were the same at the top ($2.3 \pm 0.5 \times 10^7$ cells/ cm^2 , $n = 100$) and at the bottom ($2.4 \pm 0.4 \times 10^7$ cells/ cm^2 , $n = 100$), in stark contrast to the thickness data presented above. Correlations

between TCC and biofilm thickness were weak, but higher for the top ($R^2 = 0.27$; Pearson correlation $r = 0.5$) compared to the bottom biofilm ($R^2 = 0.07$; $r = 0.3$). On large-scale, linear regression suggest an increasing trend in TCC along the length of the hose for both top ($R^2 = 0.36$) and bottom ($R^2 = 0.17$). However, this trend is mainly driven by lower concentrations in the first 30 cm-sections of the control hose, with on average 34 % lower concentrations in the top and 17 % in the bottom part compared to the rest of the hose (Figure 3B). Fluctuations on small-scale, i.e., between adjacent cm-sections, were similar in top (14.9 ± 11.6 %, $n = 99$) and bottom (14.7 ± 13.0 %, $n = 99$). The combination of the TCC data and an estimated average cell volume of $0.3 \mu\text{m}^3$ (calculation based on average cell size from SEM imaging, Figure S3A; comparable to³⁶) allows the calculation of total bacterial cell volume in the biofilm, which was on average $6.8 \pm 1.6 \times 10^6 \mu\text{m}^3/\text{cm}^2$ ($n = 100$) in the top and $7.0 \pm 1.1 \times 10^6 \mu\text{m}^3/\text{cm}^2$ ($n = 100$) in the bottom. This, in turn, allows the calculation of the relative contribution of bacterial cell volume to the overall biofilm volume ($V_{\text{cells}} : V_{\text{biofilm}}$), which was notably small with approximately 0.03 ± 0.01 % ($n = 100$) for the top and 0.02 ± 0.01 % ($n = 100$) for the bottom biofilm.

Microbiome: Biofilm community dominated by only few taxa

The overall biofilm community comprised of 384 ZOTUs (henceforth referred to as taxa). On large-scale, ordination by non-metric multidimensional scaling, based on the Bray-Curtis dissimilarity, showed a clear trend in sample clustering in the control hose (Figure S4A). Here, orientation (i.e., top vs. bottom) accounted for 22 % of community variations (Adonis, $p < 0.001$). Following this, taxa richness (S) was higher in the top ($S = 335$) compared to the bottom ($S = 288$), both with an Evenness index (J') of 0.4. On small-scale, richness ranged from 55 – 92 taxa/cm-section ($J' = 0.5 - 0.6$), with on average 72 ± 6 taxa/cm-section ($n = 95$) in the top and 67 ± 6 taxa/cm-section ($n = 100$) in the bottom. In addition, richness showed variations between adjacent cm-sections of 9 ± 7 % ($n = 92$) in the top and 7 ± 6 % ($n = 99$) in the bottom. Regarding beta-diversity, Bray-Curtis revealed compositional dissimilarities in the communities of

adjacent cm-sections between 0.05 – 0.38 (average 0.15 ± 0.06 , $n = 191$), arguing in favor of a rather similar community composition along the length of the biofilm on small-scale. Interestingly, only few dominant taxa (i.e., taxa with at least 1 % of the total number of reads) made up the majority of the community composition. In fact, the 10 most dominant taxa accounted for 89.3 % of the total biofilm community (Table S4), covering 90.0 % in the top and 89.6 % in the bottom community composition of the hose. Moreover, the three most dominant taxa even made up 56.7 % of the community and were identified as (1) an uncultured genus of the family Cytophagaceae (24.7 %, Figure 3C, green), (2) *Bradyrhizobium* spp. (23.4 %, Figure 3C, red), and (3) an uncultured representative of the phylum TM6_[Dependentiae] (9.6 %, Figure 3C, blue). The remaining seven dominant taxa were identified as *Dechloromonas* spp., *Denitratisoma* spp., *Sediminibacterium* spp., *Brevifollis* spp., *Ohtaekwangia* spp., and *Rhodobacter* spp., as well as another member of the family Rhodobacteraceae which could not be identified further (Table S4). Due to the dominance of similar if not the same taxa in top and bottom, a comprehensive analysis of potential spatial variations over the length of the hose for shared taxa was possible. On large-scale, Cytophagaceae and *Bradyrhizobium* spp. had a negative correlation in both top ($R^2 = 0.67$) and bottom ($R^2 = 0.45$) (Figure S5). Also, repetitive fluctuations along the length of the hose were identified. For example, the detection of Cytophagaceae showed an increase in its relative abundance from 19.9 ± 3.4 % ($n = 11$) to 25.8 ± 3.1 % ($n = 11$) following sections 63 to 84 in the bottom (Figure 3C, green). On small-scale, sections of localized heterogeneity were detected. For example, TM6_[Dependentiae] showed a clear difference in its abundance between sections 70 – 80 and 81 – 91 in the top of the hose; with an increase in relative abundance from 2.5 ± 1.3 % ($n = 11$) to 10.6 ± 2.2 % ($n = 11$) (Figure 3C, blue). Overall, correlations between the relative abundance of specific taxa and (1) thickness ($R^2 < 0.14$), (2) TCC ($R^2 < 0.1$), or (3) richness ($R^2 < 0.2$) were weak.

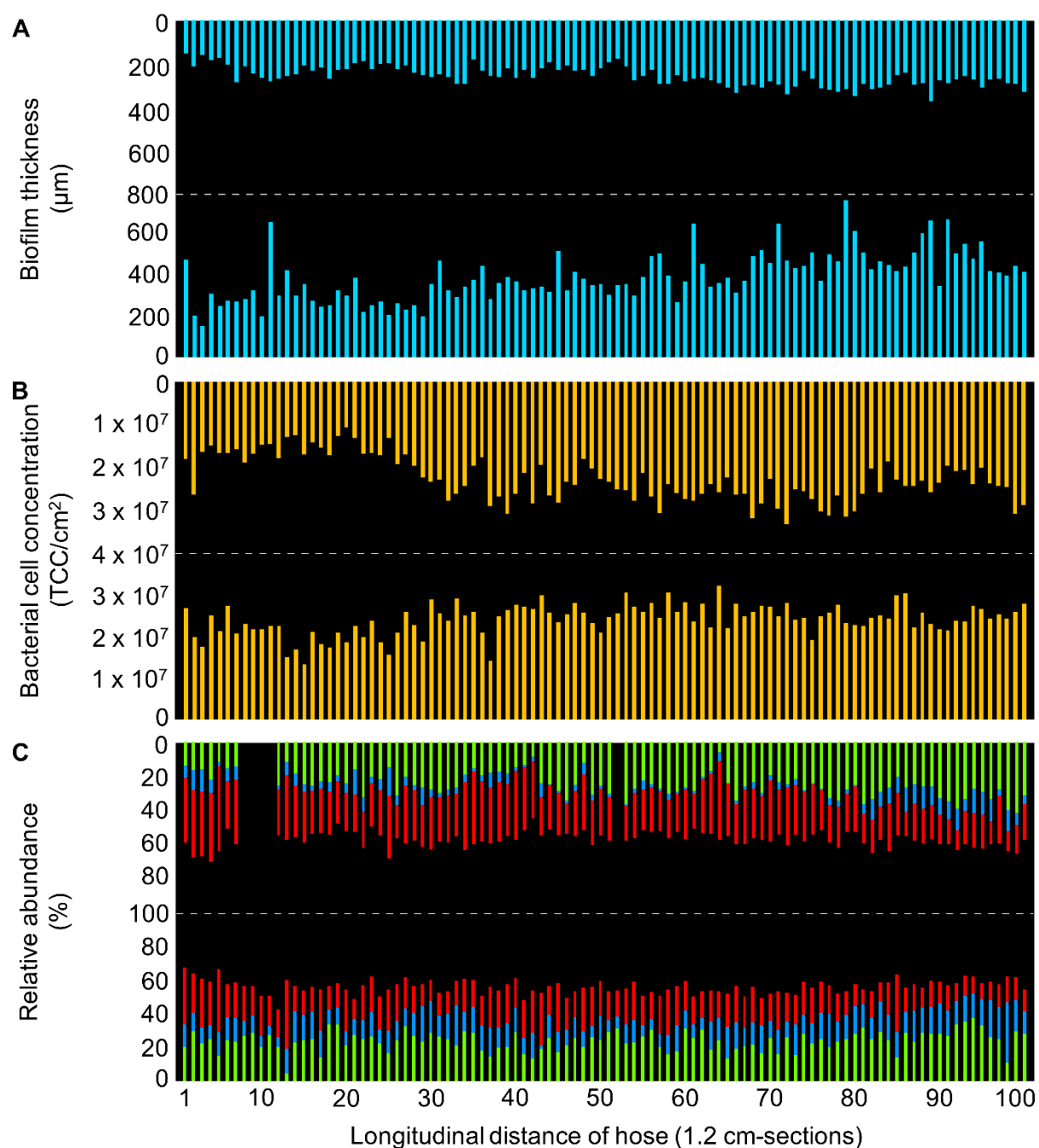


Figure 3: Detailed characterization of the control hose biofilm, with bars representing individual sections of 1.2 cm. (A) Biofilm thickness measured with optical coherence tomography. (B) Bacterial cell concentrations measured with flow cytometry. (C) Community composition measured with 16S rRNA gene sequencing, showing the relative abundance of the three most abundant taxa (green: Cytophagaceae; blue: TM6_[Dependentiae]; red: *Bradyrhizobium* spp.). Data gaps resulted from insufficient DNA amplification.

Biofilm development under real conditions

A comparatively thin biofilm established on the inner surface of the real hose during 12 months of random usage and handling (Figure 4, Figure 5A). The 120 cm piece of hose contained a combined total of 7.6×10^9 bacteria at an average distribution of $3.8 \pm 1.4 \times 10^7$ cells/cm² ($n = 200$) (Figure 5B). The bacterial community composition was also dominated by only few taxa (Figure 5C), comparable to the control hose. While the data is visualized as longitudinal top and bottom (Figure 5) this does not represent the actual orientation of use, but rather two opposite sides of the hose. Therefore, samples of different orientation (*i.e.*, *top* vs. *bottom*) were not analyzed separately.

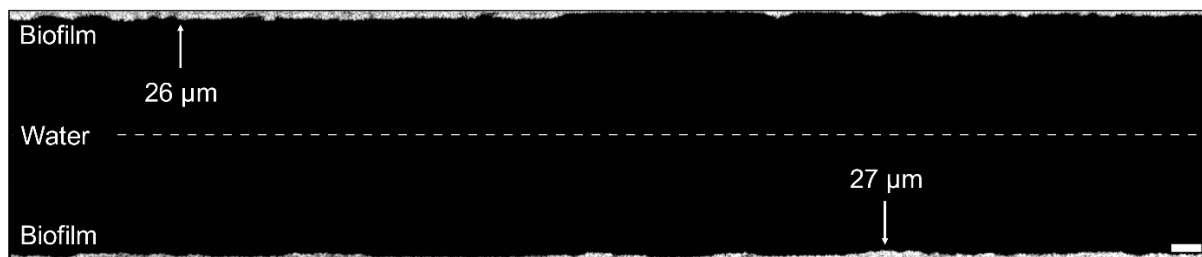


Figure 4: Visualization of the real hose biofilm imaged with optical coherence tomography. Images (2 mm length) were combined to illustrate the biofilm structure and thickness of a mm section, showing a representative example of the shower hose biofilm. Distance between top and bottom sections is not to scale. Scale bar: 200 μ m.

Structure: A comparatively thin biofilm developed inside the real hose

The real hose biofilm was considerably thinner than the control hose biofilm, often below the OCT detection limit ($\sim 4 \mu$ m), but also showing uneven protrusions and depressions throughout (Figure 4). The average thickness per 1.2 cm-section ranged from 4.3μ m up to 35.9μ m with an overall average of $9.8 \pm 4.6 \mu$ m ($n = 200$) (Figure 5A, Figure S6). On large-scale, the biofilm was notably thicker in the first ~ 30 cm-sections ($26.0 \pm 8.9 \mu$ m, $n = 27$) (*i.e.*, lower end of the vertically hanging hose) compared to the rest of the hose ($17.3 \pm 3.8 \mu$ m, $n = 73$). On small-scale, we observed considerable heterogeneity between adjacent cm-sections (average $23.4 \pm 54 \%$, $n = 198$; Figure 5A), with

the average being comparable to those of the control hose biofilm. This structural heterogeneity is evident on even smaller, μm -scale, where variations of up to 74 % in biofilm thickness could be identified (Figure 4). Consistent to the control hose, thickness data was used to calculate the approximate average biofilm volume, which was $9.8 \pm 4.6 \times 10^8 \mu\text{m}^3/\text{cm}^2$ ($n = 200$).

Numbers: Bacterial cell concentrations are in the same magnitude as in the control biofilm

TCC of 1.2 cm-sections ranged between $1.5 - 8.1 \times 10^7$ cells/cm² (Figure 5B), thus being in the same order of magnitude as the control hose biofilm while overall covering a broader range. Interestingly, correlations between TCC and biofilm thickness were higher in the real hose ($R^2 = 0.37$; $r = 0.6$) compared to the control hose biofilm (above). On large-scale, linear regression showed an ongoing decreasing trend over the length of the entire hose ($R^2 = 0.73$). Small-scale heterogeneity between adjacent cm-sections was on average 17.2 ± 15.2 % ($n = 198$), thus comparable to results from the control hose biofilm. The combination of TCC and an average cell volume ($0.3 \mu\text{m}^3$) accounted in this hose biofilm for an average bacterial cell volume of $1.1 \pm 0.4 \times 10^7 \mu\text{m}^3/\text{cm}^2$ ($n = 200$). This in turn allows the calculation of the relative contribution of bacterial cell volume to the overall biofilm volume ($V_{\text{cells}} : V_{\text{biofilm}}$) which was about 1.2 ± 0.5 % ($n = 200$) and therefore considerably higher than in the control hose.

Microbiome: Community dominated by different taxa than the control hose biofilm

On large-scale, no significant heterogeneity in the community composition was caused by the orientation of the hose (Figure S4B), as was expected due to regular movements and re-orientation of the hose during usage. Interestingly, the community compositions of the control and the real hose biofilms showed clear differences when illustrating Bray-Curtis dissimilarities (Figure S4C). Here, the two different experiments (biofilm growth under laboratory conditions vs. under realistic conditions) accounted for 65 % of

community variation (Adonis, $p < 0.001$). It should be noted that input water varied between these two locations, in addition to the differences in operation (Table S1). Regarding alpha-diversity, however, taxa richness was comparable to the control hose biofilm, with 341 taxa and an Evenness index of 0.4. On small-scale, richness ranged from 37 – 119 taxa/cm-section ($J' = 0.3 - 0.6$), with an average of 64 ± 14 taxa/cm-section ($n = 183$). Also, random fluctuations between adjacent cm-sections showed variations in richness, with 15 ± 14 % ($n = 165$). These were less pronounced compared to ones in the control hose. Bray-Curtis dissimilarity showed variations in beta-diversity of adjacent sections, ranging from 0.04 to 0.55 (average: 0.18 ± 0.1 , $n = 169$), and again highlighting a similar pattern in community composition heterogeneity as the control hose biofilm. Moreover, only few taxa dominated the community composition (i.e., covering at least of 1 % of the total number of reads), which was consistent to the control hose biofilm. Here, the 10 most dominant taxa accounted for 90.4 % of the entire community composition (relative abundance; Table S5). Comparable to the control hose biofilm, a comprehensive analysis of potential spatial variations over the length of the hose was conducted for dominant shared taxa. The three most abundant taxa made up for 73.2 % of the community and were identified as (1) *Caulobacter* spp. (34.7 %, Figure 5C, purple), (2) *Bradyrhizobium* spp. (24.2 %, Figure 5C, red), and (3) *Altererythrobacter* spp. (14.2 %, Figure 5C, yellow). The remaining seven dominant taxa were identified as *Brevibacterium* spp., *Bosea* spp., *Bdellovibrio* spp., *Sphingomonas* spp., *Rhodobacter* spp., as well as two members of the family Chitinophagaceae and one representative of the phylum Cyanobacteria (Table S5). Consistent with the analysis of the control hose biofilm data, spatial variations for the three most dominant taxa were analyzed. On large-scale, a negative correlation between *Caulobacter* spp. and *Bradyrhizobium* spp. was identified ($R^2 = 0.34$; Figure S7). Also, repetitive fluctuations in relative abundances were observed. For example, *Caulobacter* spp. increased in its abundance from sections 77 – 88 (27.2 ± 5.9 %, $n = 11$) to the following sections 89 – 99 (54.4 ± 13.0 %, $n = 11$), corresponding to an

increase of 27 % (Figure 5C, purple). On small-scale, obvious localized heterogeneity of *Altererythrobacter* spp. was detectable, which in fact was more pronounced than in the control hose biofilm. Here, the relative abundance of 18.3 ± 4.5 % ($n = 11$) decreased to an average of 8.3 ± 4.2 % ($n = 11$) within the range of sections 79 – 100 (Figure 5C, yellow). Overall, correlations between taxa relative abundance and (1) thickness, (2) TCC and/or (3) richness were mostly poor ($R^2 < 0.2$), with the exception in the relative abundance of *Bradyrhizobium* spp. which positively correlated with TCC ($R^2 = 0.37$).

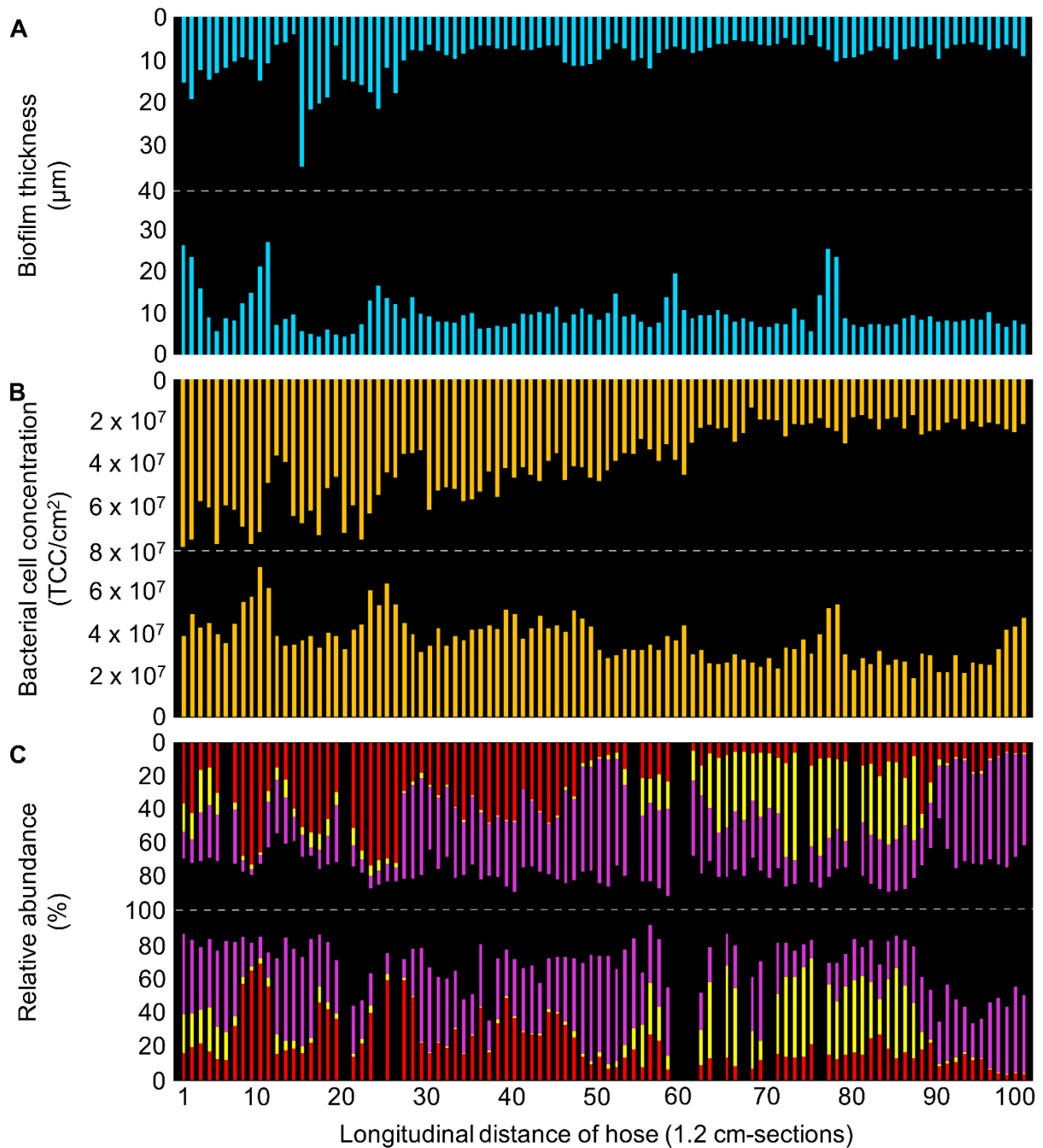


Figure 5: Detailed characterization of the real hose biofilm, with bars representing individual sections of 1.2 cm. (A) Biofilm thickness measured with optical coherence tomography. (B) Bacterial cell concentrations measured with flow cytometry. (C) Community composition measured with 16S rRNA gene sequencing, showing the relative abundance of the three most abundant taxa (red: *Bradyrhizobium* spp.; yellow: *Altererythrobacter* spp.; purple: *Caulobacter* spp.). Data gaps resulted from insufficient DNA amplification.

Discussion

Microbial heterogeneity within large, but connected, ecosystems was previously characterized in both natural^{1,9} and engineered^{2,3} ecosystems. The purpose of this study was to assess spatial heterogeneity within a confined engineered ecosystem (120 cm of flexible shower hose) in detail by characterizing biofilm structure, cell numbers, and microbial community composition on various scales (from μm – m) with high-resolution sampling. Ultimately, this can allow for a better understanding of the driving forces of biofilm formation and localized biofilm heterogeneity in building plumbing systems and the broader implications of such heterogeneity on biofilm sampling and analysis strategies.

Dispersal and selection drive homogenous biofilm assembly under otherwise uniform environmental conditions

Microbial heterogeneity within drinking water pipes was previously ascribed to variations in material properties, e.g., surface structure and adhesion characteristics³⁷, as well as chemical and physical characteristics of the water (e.g., nutrients, pH)³⁸, flow velocity and shear stress^{39,40}. In our study, we presumed uniformity in all these environmental variables along the length of the control hose, and we hypothesized that a biofilm, formed under such spatially uniform environmental conditions, would be homogeneous in terms of structure, cell numbers, and community composition.

Biofilm development was mainly driven by two ecological processes, namely *dispersal* of cells from the source water and *selection* based on growth^{41,42}. The repetitive introduction of the same microbial community along the length of the hose through twice-daily flushing events allowed for a homogeneous dispersal of bacteria from the water to the biofilm, and thus an initially uniform bacterial distribution (numbers and community composition) throughout the

hose. However, we believe that initial dispersal-driven assembly was less important for the final biofilm composition than niche assembly (i.e., selective growth). In fact, dispersal assembly alone did not nearly account for the biofilm TCC measured after one year (on average 2.4×10^7 cells/cm²; Figure 3B), based on the water phase TCC ($\sim 10^5$ cells/mL²⁶). As Swiss tap water is usually carbon limited²⁹, biofilm growth on synthetic polymeric pipe surfaces is primarily driven by the organic carbon migrating from the material^{43,44}. Biodegradable carbon compounds that migrate from flexible plastic materials into the (drinking) water phase (e.g., flexibilizers, plasticizers) were shown to increase microbial growth rates and yields^{45,46}. Several previous studies quantified migrating organic carbon as the main carbon source for microbial growth (e.g.,^{26,44}). Here we assumed, but did not specifically quantify, that the migration of biodegradable carbon compounds is homogenous along the length of a 120 cm shower hose. An assumed uniform migration of these biodegradable carbon compounds should impact biofilm development equally throughout the length of the hose, thus allowing for a homogeneous distribution in cell concentrations but also community compositions (Figure 3B, 3C). In addition, since these migrating compounds are the predominant carbon sources in this environment, a specific niche is created that results in a selective pressure within the developing microbial community⁴⁷. Several studies showed that growth on specific substrates results in the selection of specific taxa even when starting with complex starting communities^{26,48,49}, and also indicated lower richness in biofilms compared to planktonic communities^{23,50}. This selective effect was clearly detectable in our study by a considerable decrease in diversity in the biofilm communities on large-scale. While the initial tap water microbiome was highly diverse with approximately 5'000 different taxa (data not shown), individual biofilms showed a lower total diversity with < 400 taxa. In fact, the three most abundant taxa accounted for the majority of the biofilm communities (Figures 3C, 5C).

Different variability in environmental conditions between similar but disconnected ecosystems result in microbial heterogeneity

Biogeographical heterogeneity is commonly observed in seemingly similar environments that are not physically connected. For example, differences in microbial communities were observed when comparing different drinking water treatment plants, individual water meters², or shower hoses²⁶. Also, on a laboratory scale, biofilms that developed from an identical starting community were dominated by different taxa, which was attributed to the availability of different carbon sources with otherwise identical environmental conditions^{48,51,52}. These examples emphasize that even though environmental conditions are assumed to be similar between two (disconnected) systems (e.g., treatment plants, water meters; ²), already relatively small differences can result in microbial variations, i.e., heterogeneity.

Our study focused on heterogeneity at high spatial resolution within an individual biofilm formed on a single hose (i.e., single environment). The inclusion of a second hose biofilm from an environment with arguably more variability in environmental conditions expanded the broader applicability of the findings to other systems. Both setups comprised identical material but showed differences in usage and incoming water compositions. As a result, the extent of the individual small-scale heterogeneity was different between the two biofilms, but also considerable differences between the two similar but disconnected (i.e., individual) ecosystems were detected. Firstly, the biofilm of the real hose was ten-fold thinner than the one of the control hose (Figures 2, 4). It was shown before that higher flow rates result in thinner biofilm structures compared to slow flow conditions⁵³. As this was the case for the control (0.3 L/min) and the real (10-12 L/min) hose setups, it poses one plausible explanation for the observed difference in biofilm thickness. Despite these differences in thickness, TCC were comparable between the two biofilms, interestingly suggesting a similar growth potential and/or total carrying

capacity. Secondly, the overall biofilm communities of both biofilms (control and real hose) were dissimilar (Figure S4C). One reason for these inter-hose variations is the different source waters. With the installations being located in two cities, water sources, treatment, and distribution were different and therefore resulted in different bacterial community compositions (Table S4, S5; 3,12,15). Also, in the real hose setup, a mixture of hot and cold tap water was used while the control hose was only flushed with water from the hot water line, again providing different community compositions within the waters⁵⁴. Consequently, dispersal-driven assembly was different between the two hoses and allowed for different organisms to settle, attach, and grow.

Comparing the dominant taxa between control and real hose revealed only little consensus between the biofilms. For example, only one out of ten taxa were identical on genus level (*Bradyrhizobium* spp.) and only two were similar on family level (*Bradyrhizobium*, *Chitinophagaceae*) (Tables S4, S5). It was previously shown that the availability of different nutrients enables distinct phylogenetic families to outgrow others in a given ecosystem^{48,51}, based on the ability and efficiency of metabolizing these. In both the control and the real hose setup, migration from the flexible plastic material provided the major carbon source, allowing bacteria that are capable of metabolizing these compounds to outcompete others (niche assembly, ⁴²). The comparison of these two similar but disconnected ecosystems illustrates (1) how environmental conditions shape heterogeneity (e.g., impact of flow rate and dispersal), but also (2) how a dominant carbon source (e.g., migrated from flexible PVC-P) results in comparably low diversity in two otherwise distinct biofilm communities (Figures 3C, 5C). While these differences were obvious on a taxonomic level, no metabolic analyses were performed (e.g., enzyme expressions). In fact, despite a distinct taxonomic assignment, taxa might still perform similar metabolic actions³⁰.

The differences between the control and the real hose were interesting. However, these hoses represent single examples from each environment (laboratory and real-use conditions) and thus provide insufficient replication for (1) representing biofilms of these environments in general and (2) for drawing definitive conclusions on the role of the environment on biofilm formation. Rather, the focus of this study was on the small-scale variations within the biofilms of each hose.

Small-scale differences in environmental variables drive heterogeneity within a connected ecosystem

Heterogeneity in microbial assemblages of connected ecosystems has been widely attributed to localized variations in environmental conditions^{9,10}. Patchiness (i.e., heterogeneity) has even been described within individual biofilms on small-scale, i.e., in systems with apparent uniform conditions^{53,55}. Overall, conditions in the control hose setup were kept as uniform as possible. However, the horizontal alignment introduced a distinct difference between the bottom and the top part as a result of gravity. Gravity was previously identified as a driver for heterogeneity along a radial-spatial orientation due to particle deposition²¹ and the rising of air bubbles⁵⁶. It is probable that the deposition of inorganic particles, which occurred especially during stagnation, over the course of one year of operation contributed to the thicker biofilm in the bottom part of the control hose without significantly affecting the cell concentration (Figures 3A, B). In addition, biofilm sloughing by air bubbles during flow, potentially contributed to a thinner and more variable biofilm structure in the top biofilm compared to the bottom (Figure 3A; ⁵⁶).

In the real hose, which was installed vertically, gravity obviously impacted biofilm thickness differently, with particles likely accumulating in the lower bend (Figure 1B). Here, we observed clear heterogeneity with thicker patches of biofilm in the lower section and a continuously decreasing gradient in TCC

along the length of the hose (Figures 5A, B). In addition, the orientation of the real hose also probably impacted flow dynamics (i.e., with a lower bend). Changes in flow velocity²⁸ and turbulence⁵⁷ were previously shown to impact community composition and biofilm thickness.

In both the control and the real hose biofilm, community composition showed heterogeneity on both large- and small-scale. For example, the relative abundance of some of the most dominant taxa changed on large-scale along the length of the hose, gradually as well as fluctuating (Figures S6, S11). On small-scale, localized heterogeneity was observed for dominant taxa of both control and real hose biofilms (Figures 3C, 5C), being more pronounced in the latter. Previous research showed patchiness (i.e., small-scale heterogeneity) in biofilms due to factors like predation and grazing^{31,58}, successive growth, e.g., based on by-products⁵⁹, oxygen availability and mass transport⁶⁰, variable strategies for colony expansion⁶¹, competition and cooperation^{62,63} and heterogeneity in nutrient gradients and growth dynamics^{64,65}. While any of these could be relevant, our analyses were not designed to untangle any one dominant factor.

Practical implications

The assessment/characterization of small-scale heterogeneity within individual biofilms allows us to draw several conclusions regarding sampling and analysis strategies on a broader scale. Sample size and the required number and spatial distribution of sampling points within a given system are some of the most critical issues when considering biofilm sampling strategies. Across disciplines, biofilm characterization is often limited by the accessibility of the relevant surface which necessarily results in diverse sampling approaches. Consequently, sample sizes in biofilm studies range from microscopic analysis on μm -scale^{66–68} to microbiome studies on single-digit cm-scale^{69,70}, up to specifically designed insertable coupons (e.g., 2.24 cm²; ^{71–73}) as well as whole

pipe/hose sections of, e.g., up to 90 cm in length^{21,74}. Our data highlight the importance of sample size and distribution, as any prevalent spatial heterogeneity influences the representativeness of a sample and therefore impacts conclusions that are drawn.

In the present study, the combination of individual results (i.e., 1.2 cm sections) allowed us to simulate larger sample sizes and to compare these results. For example, the average of ten adjacent samples provides the (theoretical) outcome of sampling the length of 12 cm as one single sample. It is obvious that a sampled biofilm area should be as large as possible to obtain a characterization as close as possible to the average of an entire system (Figure S8). However, while sampling an entire biofilm may well be feasible for shower hoses^{26,74}, this would not be realizable for large pipes or surfaces^{75,76}. As soon as smaller area sizes are sampled, spatial heterogeneity (e.g., top/bottom caused by gravity (²¹; Figure 3A) or longitudinal (¹⁷; Figure 5B)) consequently requires multiple sampling points to capture the heterogeneity within one system, e.g., based on pipe orientation. The data shown in the present study encourages researchers to sample biofilms as representative as possible. Specifically, this means collecting biofilms either from large surface areas or from multiple, distributed small areas, to balance out small-scale heterogeneity. Moreover, we encourage biofilm researchers to both assess and illustrate the representativeness of their sample collection strategy when reporting.

While smaller sampling areas result in large deviations from the overall average (Figure S8) and reduce the representativeness of one sample for an entire system, sampling on small-scale (μm -cm) is particularly valuable if the uniqueness of a system/biofilm is of interest. Our results showed that even if environmental conditions are assumingly uniform, heterogeneity can develop on small-scale in a biofilm. This emphasizes that a biofilm is very unlikely to be homogeneous and thus requires sampling at different locations. Biofilms and

microbial communities have previously been compared to landscapes, i.e., environments consisting of spatial variations and showing complex ecological interactions^{77,78}. Here, variations in environmental conditions can, for example, be introduced by gradients on μm -scale (e.g., oxygen, pH, nutrients), which allow for the establishment of different micro-environments and ecological niches^{60,79}. With limitations in certain resources, bacteria need to adapt, cooperate, and/or compete, which ultimately results in selected bacterial clusters and a distinct spatial organization^{68,80–82}. It is necessary to sample and analyze biofilms on very small scales to allow for the identification of this heterogeneity, and important as processes on such small scale ultimately shape large-scale pattern and effect ecosystem functioning^{83,84}.

Conclusions

- High-resolution sampling of shower hose biofilms (200 samples/120 cm) in addition to detailed analysis on various scales (μm – m), enabled the assessment of small-scale spatial heterogeneity in biofilm structure, bacterial numbers, and community composition.
- A biofilm grown inside a flexible hose under controlled laboratory conditions, was likely uniformly exposed to processes such as dispersal, carbon migration, growth, and selection along its length. Accordingly, the respective biofilm was homogenous on large-scale, but showed notable localized heterogeneity on small-scale.
- A biofilm grown under real (i.e., uncontrolled) use conditions showed considerably more variations in all variables on both large- and small-scale, with particularly clear spatial fluctuations in the relative abundance of dominant taxa.
- The control hose biofilm was different to the real hose biofilm with respect to thickness and community composition, which was most probably influenced by different operational conditions and water sources. However, both hoses showed impressively low biofilm community diversity, which was attributed to the selective force of the migrating carbon from the flexible PVC-P hoses.
- In addition, our results show that the adequate biofilm sample size strongly depends on the research question: whether the small-scale uniqueness of an ecosystem is explored (μm - to cm-scale), or whether an average overview of an entire system is required (cm- to m-scale).

Acknowledgments

Acknowledgments go to Jürg Sigrist for the installation of the laboratory setup, and together with Wen Quin and Dominik Peter for great teamwork during the

sampling days. Nicolas Derlon for guidance and support with OCT analysis and discussions on the topic. Silvia Kobel and Aria Minder Pfyl for support and protocols for library preparations and sequencing. Teresa Colangelo Failla for beautiful SEM imaging.

References

1. **Liu, T. et al.** Integrated biogeography of planktonic and sedimentary bacterial communities in the Yangtze River. *Microbiome* 6, 1–14 (2018).
2. **Roeselers, G. et al.** Microbial biogeography of drinking water: patterns in phylogenetic diversity across space and time. *Environ. Microbiol.* 17, 2505–2514 (2015).
3. **Liu, G., Van der Mark, E. J., Verberk, J. Q. & Van Dijk, J. C.** Flow cytometry total cell counts: a field study assessing microbiological water quality and growth in unchlorinated drinking water distribution systems. *Biomed Res Int* 2013, 1–10 (2013).
4. **Siles, J. A. & Margesin, R.** Abundance and Diversity of Bacterial, Archaeal, and Fungal Communities Along an Altitudinal Gradient in Alpine Forest Soils: What Are the Driving Factors? *Soil Microbiol.* 72, 207–220 (2016).
5. **Chao, Y., Mao, Y., Wang, Z. & Zhang, T.** Diversity and functions of bacterial community in drinking water biofilms revealed by high-throughput sequencing. *Sci. Rep.* 5, 10044 (2015).
6. **Charlop-Powers, Z. et al.** Global biogeographic sampling of bacterial secondary metabolism. *Elife* 1–10 (2015). doi:10.7554/eLife.05048
7. **Stanish, L. F. et al.** Factors Influencing Bacterial Diversity and Community Composition in Municipal Drinking Waters in the Ohio River Basin, USA. *PLoS One* 11, 1–21 (2016).
8. **Boers, S. A. et al.** Monitoring of microbial dynamics in a drinking water distribution system using the culture-free, user- friendly, MYcrobiota platform. *Sci. Rep.* 8, 1–8 (2018).
9. **Langenheder, S. et al.** Bacterial metacommunity organization in a highly connected aquatic system. *FEMS Microbiol. Ecol.* 93, 1–9 (2017).
10. **Hou, D. et al.** Environmental Factors Shape Water Microbial Community Structure and Function in Shrimp Cultural Enclosure Ecosystems. *Front. Microbiol.* 8, 1–12 (2017).
11. **Berga, M., Zha, Y., Székely, A. J. & Langenheder, S.** Functional and Compositional Stability of Bacterial Metacommunities in Response to Salinity Changes. *Front. Microbiol.* 8, 1–11 (2017).
12. **Ma, X., Vikram, A., Casson, L. & Bibby, K.** Centralized Drinking Water Treatment Operations Shape Bacterial and Fungal Community Structure. *Environ. Sci. Technol.* 51, 7648–7657 (2017).
13. **Bruno, A. et al.** Changes in the Drinking Water Microbiome: Effects of Water Treatments Along the Flow of Two Drinking Water Treatment Plants in a Urbanized Area, Milan (Italy). *Front. Microbiol.* 9, 1–12 (2018).
14. **Lautenschlager, K. et al.** Abundance and composition of indigenous bacterial communities in a multi-step biofiltration-based drinking water treatment plant. *Water Res.* 62, 40.42 (2014).
15. **Pinto, A. J., Xi, C. & Raskin, L.** Bacterial community structure in the drinking water microbiome is governed by filtration processes. *Env. Sci Technol* 46, 8851–8859 (2012).
16. **Vignola, M., Werner, D., Wade, M. J., Meynet, P. & Davenport, R. J.** Medium shapes the microbial community of water filters with implications

- for effluent quality. *Water Res.* 129, 499–508 (2018).
17. **Potgieter**, S. *et al.* Long-term spatial and temporal microbial community dynamics in a large-scale drinking water distribution system with multiple disinfectant regimes. *Water Res.* 139, 406–419 (2018).
 18. **Servais**, P., Anzil, A., Gatel, D. & Cavard, J. Biofilm in the Parisian suburbs drinking water distribution system. *J. Water Supply Res. Technol. - AQUA* 53.5, 313–324 (2004).
 19. **Niquette**, P., Servais, P. & Savoie, R. Bacterial dynamics in the drinking water distribution system of Brussels. *Water Res.* 35, 675–682 (2001).
 20. **Bester**, E., Kroukamp, O., Hausner, M., Edwards, E. A. & Wolfaardt, G. M. Biofilm form and function: carbon availability affects biofilm architecture, metabolic activity and planktonic cell yield. *J. Appl. Microbiol.* 110, 387–398 (2010).
 21. **Liu**, J. *et al.* Bacterial community radial-spatial distribution in biofilms along pipe wall in chlorinated drinking water distribution system of East China. *Appl. Microbiol. Biotechnol.* 101, 749–759 (2017).
 22. **Lin**, S., Wang, X., Chao, Y., He, Y. & Liu, M. Predicting biofilm thickness and biofilm viability based on the concentration of carbon-nitrogen-phosphorus by support vector regression. *Environ. Sci. Pollut. Res.* 23, 418–425 (2016).
 23. **Liu**, R. *et al.* Molecular analysis of long-term biofilm formation on PVC and cast iron surfaces in drinking water distribution system. *J. Environ. Sci.* 26, 865–874 (2014).
 24. **Wang**, H., Masters, S., Edwards, M. A., Falkinham, J. O. & Pruden, A. Effect of disinfectant, water age, and pipe materials on bacterial and eukaryotic community structure in drinking water biofilm. *Env. Sci Technol* 48, 1426–1435 (2014).
 25. **Jang**, H.-J., Choi, Y.-J. & Ka, J.-O. Effects of Diverse Water Pipe Materials on Bacterial Communities and Water Quality in the Annular Reactor. *J. Microbiol. Biotechnol.* 21, 115–123 (2011).
 26. **Proctor**, C. R. *et al.* Biofilms in shower hoses – choice of pipe material influences bacterial growth and communities. *Environ. Sci. Water Res. Technol.* 2, 8–11 (2016).
 27. **Ling**, F., Whitaker, R., LeChevallier, M. W. & Liu, W.-T. Drinking water microbiome assembly induced by water stagnation. *ISME J.* 12, 1520–1531 (2018).
 28. **Douterelo**, I., Sharpe, R. L. & Boxall, J. B. Influence of hydraulic regimes on bacterial community structure and composition in an experimental drinking water distribution system. *Water Res.* 47, 503–516 (2013).
 29. **Lautenschlager**, K., Boon, N., Wang, Y., Egli, T. & Hammes, F. Overnight stagnation of drinking water in household taps induces microbial growth and changes in community composition. *Water Res.* 44, 4868–4877 (2010).
 30. **Ji**, P., Rhoads, W. J., Edwards, M. A. & Pruden, A. Impact of water heater temperature setting and water use frequency on the building plumbing microbiome. *ISME J.* 11, 1318–1330 (2017).
 31. **Derlon**, N., Peter-Varbanets, M., Scheidegger, A., Pronk, W. &

- Morgenroth, E. Predation influences the structure of biofilm developed on ultrafiltration membranes. *Water Res.* 46, 3323–3333 (2012).
32. **Prest**, E. I., Hammes, F., Köttsch, S., van Loosdrecht, M. C. M. & Vrouwenvelder, J. S. Monitoring microbiological changes in drinking water systems using a fast and reproducible flow cytometric method. *Water Res.* 47, 7131–7142 (2013).
 33. **Klindworth**, A. *et al.* Evaluation of general 16S ribosomal RNA gene PCR primers for classical and next-generation sequencing-based diversity studies. *Nucleic Acids Res.* 41, 1–11 (2013).
 34. **Schloss**, P. D. & Westcott, S. L. Assessing and Improving Methods Used in Operational Taxonomic Unit-Based Approaches for 16S rRNA Gene Sequence Analysis. *Appl. Environ. Microbiol.* 77, 3219–3226 (2011).
 35. **Edgar**, R. C. Accuracy of microbial community diversity estimated by closed- and open- reference OTUs. *PeerJ* 1–17 (2017). doi:10.7717/peerj.3889
 36. **Heldal**, M., Norland, S., Bratbak, G. & Riemann, B. Determination of bacterial cell number and cell volume by means of flow cytometry, transmission electron microscopy, and epifluorescence microscopy. *J. Microbiol. Methods* 20, 255–263 (1994).
 37. **Pasmore**, M., Todd, P., Pfiefer, B., Rhodes, M. & Bowman, C. N. Effect of polymer surface properties on the reversibility of attachment of *Pseudomonas aeruginosa* in the early stages of biofilm development. *Biofouling* 18, 65–71 (2002).
 38. **Lehtola**, M. J. *et al.* Microbiology, chemistry and biofilm development in a pilot drinking water distribution system with copper and plastic pipes. *Water Res.* 38, 3769–3779 (2004).
 39. **Lehtola**, M. J. *et al.* The effects of changing water flow velocity on the formation of biofilms and water quality in pilot distribution system consisting of copper or polyethylene pipes. *Water Res* 40, 2151–2160 (2006).
 40. **Moreira**, J. *et al.* Influence of flow rate variation on the development of *Escherichia coli* biofilms. *Bioprocess Biosyst Eng* 36, 1787–1796 (2013).
 41. **Kinnunen**, M. *et al.* A conceptual framework for invasion in microbial communities. *ISME J.* 10, 2773–2775 (2016).
 42. **Hubbel**, S. P. Neutral theory and the evolution of ecological equivalence. *Ecology* 87, 1387–1398 (2006).
 43. **Connell**, M. *et al.* PEX and PP water pipes: Assimilable carbon, chemicals, and odors. *J. Am. Water Works Assoc.* 108, E192–E204 (2016).
 44. **Bucheli-Witschel**, M., Koetzsch, S., Darr, S., Widler, R. & Egli, T. A new method to assess the influence of migration from polymeric materials on the biostability of drinking water. *Water Res.* 46, 4246–4260 (2012).
 45. **Zhang**, L. & Liu, S. Investigation of Organic Compounds Migration from Polymeric Pipes into Drinking Water under Long Retention Times. *Procedia Eng.* 70, 1753–1761 (2014).
 46. **Wen**, G., Koetzsch, S., Vital, M., Egli, T. & Ma, J. BioMig - A Method to Evaluate the Potential Release of Compounds from and the Formation of Biofilms on Polymeric Materials in Contact with Drinking Water. *Environ.*

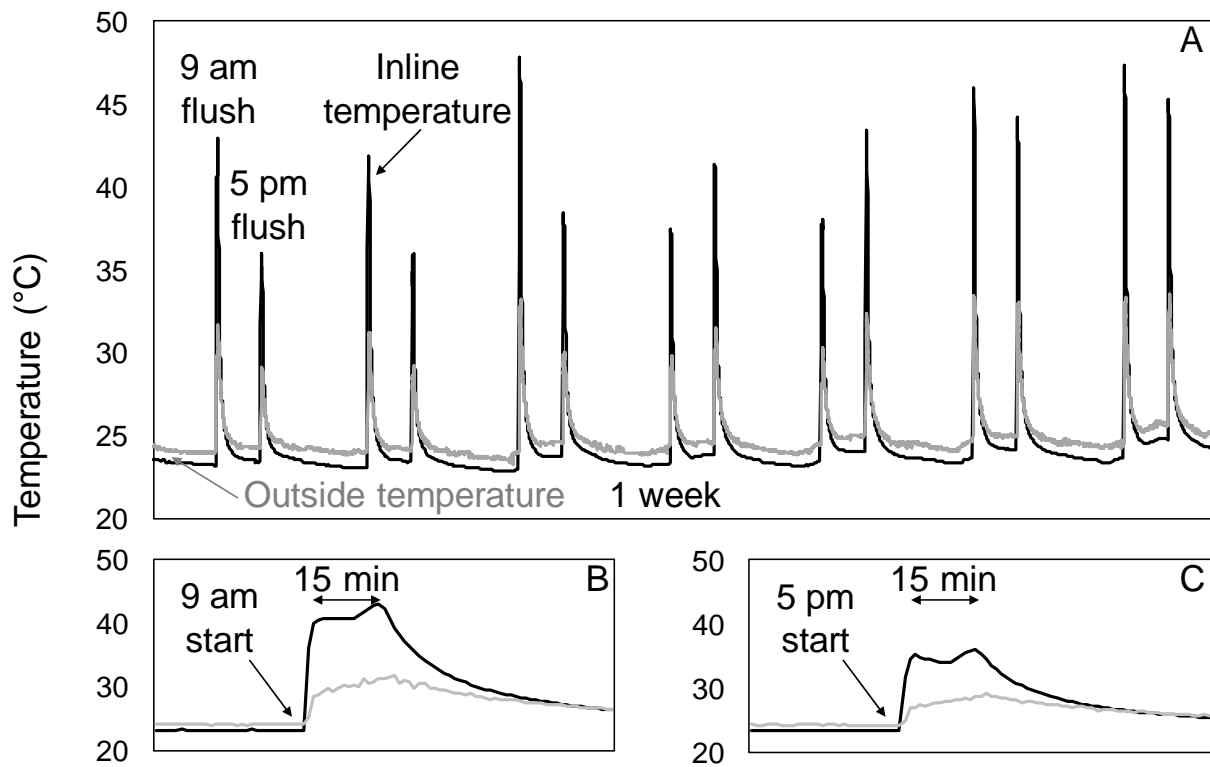
- Sci. Technol.* 49, 11659–11669 (2015).
47. **Vandermeer**, J. H. Niche Theory. *Annu. Rev. Ecol. Syst.* 3, 107–132 (1972).
 48. **Goldford**, J. E. *et al.* Emergent simplicity in microbial community assembly. *Science* (80-.). 361, 469–474 (2018).
 49. **Rivett**, D. W. & Bell, T. Abundance determines the functional role of bacterial phylotypes in complex communities. *Nat. Microbiol. Lett.* 3, 762–772 (2018).
 50. **Henne**, K., Kahlisch, L., Brettar, I. & Höfle, M. G. Analysis of structure and composition of bacterial core communities in mature drinking water biofilms and bulk water of a citywide network in Germany. *Appl. Environ. Microbiol.* 78, 3530–3538 (2012).
 51. **You**, J., Walter, X. A., Greenman, J., Melhuish, C. & Ieropoulos, I. Stability and reliability of anodic biofilms under different feedstock conditions: Towards microbial fuel cell sensors. *Sens. Bio-Sensing Res.* 6, 43–50 (2015).
 52. **Haagensen**, J. A. J., Hansen, S. K., Christensen, B. B., Pamp, S. J. & Molin, S. Development of Spatial Distribution Patterns by Biofilm Cells. *Appl. Environ. Microbiol.* 81, 6120–6128 (2015).
 53. **van Loosdrecht**, M. C. M. *et al.* Biofilm Structures. *Water Sci. Technol.* 8, 35–43 (1995).
 54. **Henne**, K., Kahlisch, L., Ho, M. G. & Brettar, I. Seasonal dynamics of bacterial community structure and composition in cold and hot drinking water derived from surface water reservoirs. *Water Res.* 47, 5614–5630 (2013).
 55. **Lowery**, N. V., McNally, L., Ratcliff, W. C. & Brown, S. P. Division of Labor, Bet Hedging, and the Evolution of Mixed Biofilm Investment Strategies. *MBio* 8, 1–12 (2017).
 56. **Jang**, H., Rusconi, R. & Stocker, R. Biofilm disruption by an air bubble reveals heterogeneous age-dependent detachment patterns dictated by initial extracellular matrix distribution. *npj Biofilms Microbiomes* 3, 1–6 (2017).
 57. **Tsagkari**, E. & Sloan, W. T. Biofilm growth in drinking water systems under stagnant conditions. *E-Proceedings* 707–717 (2018).
 58. **Huws**, S. A., Mcbain, A. J. & Gilbert, P. Protozoan grazing and its impact upon population dynamics in biofilm communities. *J. Appl. Microbiol.* 98, 238–244 (2005).
 59. **Elias**, S. & Banin, E. Multi-species biofilms: living with friendly neighbors. *FEMS Microbiol Rev* 36, 990–1004 (2012).
 60. **de Beer**, D., Stoodley, P., Roe, F. & Lewandowski, Z. Effects of Biofilm Structures on Oxygen Distribution and Mass Transport. *Biotechnol. Bioeng.* 43, 1131–1138 (1994).
 61. **Goldschmidt**, F., Regoes, R. R. & Johnson, D. R. Successive range expansion promotes diversity and accelerates evolution in spatially structured microbial populations. *ISME J.* 11, 2112–2123 (2017).
 62. **Rendueles**, O. & Velicer, G. J. Evolution by flight and fight: diverse mechanisms of adaptation by actively motile microbes. *ISME J.* 11, 555–568 (2016).
 63. **Nadell**, C. D., Drescher, K. & Foster, K. R. Spatial structure, cooperation

- and competition in biofilms. *Nat. Publ. Gr.* 14, 589–600 (2016).
64. **Kreff**, J. & Wimpenny, J. Effect of EPS on biofilm structure and function as revealed by an individual-based model of biofilm growth. *Water Sci. Technol.* 43, 135–141 (2001).
 65. **Sternberg**, C. *et al.* Distribution of Bacterial Growth Activity in Flow-Chamber Biofilms. *Appl. Environ. Microbiol.* 65, 4108–4117 (1999).
 66. **Batté**, M., Mathieu, L., Laurent, P. & Prévost, M. Influence of phosphate and disinfection on the composition of biofilms produced from drinking water, as measured by fluorescence in situ hybridization. *Can. J. Microbiol.* 49, 741–753 (2003).
 67. **Dal Co**, A., van Vliet, S. & Ackermann, M. Emergent microscale gradients give rise to metabolic cross-feeding and antibiotic tolerance in clonal bacterial populations. *bioRxiv Prepr.* 1–16 (2019).
 68. **Mitri**, S., Clarke, E. & Foster, K. R. Resource limitation drives spatial organization in microbial groups. *ISME J.* 10, 1471–1482 (2015).
 69. **Ma**, X. *et al.* Biofilm bacterial community transition under water supply quality changes in drinking water distribution systems. *Environ. Sci. Water Res. Technol.* 4, 644–653 (2018).
 70. **Liu**, R. *et al.* Diversity of bacteria and mycobacteria in biofilms of two urban drinking water distribution systems. *Can. J. Microbiol.* 58, 261–270 (2012).
 71. **Deines**, P. *et al.* A new coupon design for simultaneous analysis of in situ microbial biofilm formation and community structure in drinking water distribution systems. *Appl Microbiol Biotechnol* 87, 749–756 (2010).
 72. **Fish**, K. E., Mark, O. A. & Boxall, J. Characterising and understanding the impact of microbial biofilms and the extracellular polymeric substance (EPS) matrix in drinking water distribution systems. *Environ. Sci. Water Res. Technol.* 2, 614–630 (2016).
 73. **Douterelo**, I., Jackson, M., Solomon, C. & Boxall, J. Spatial and temporal analogies in microbial communities in natural drinking water biofilms. *Sci. Total Environ.* 277–288 (2017). doi:10.1016/j.scitotenv.2016.12.118
 74. **Proctor**, C. R., Reimann, M., Vriens, B. & Hammes, F. Biofilms in shower hoses. *Water Res.* 131, 274–286 (2018).
 75. **Lührig**, K. *et al.* Bacterial Community Analysis of Drinking Water Biofilms in Southern Sweden. *Microbes Environ.* 30, 99–107 (2015).
 76. **Liu**, G. *et al.* Pyrosequencing reveals bacterial communities in unchlorinated drinking water distribution system: an integral study of bulk water, suspended solids, loose deposits, and pipe wall biofilm. *Env. Sci Technol* 48, 5467–5476 (2014).
 77. **Battin**, T. J. *et al.* Microbial landscapes: new paths to biofilm research. *Nat. Rev. Microbiol.* 5, 76–81 (2007).
 78. **Turner**, M. G. Landscape ecology: What is the state of science? *Annu.Rev.Ecol.Evol.Syst.* 36, 319–344 (2005).
 79. **Schramm**, A., de Beer, D., Gieseke, A. & Amann, R. Microenvironments and distribution of nitrifying bacteria in a membrane-bound biofilm. *Environ. Microbiol.* 2, 680–686 (2000).
 80. **van Gestel**, J., Vlamakis, H. & Kolter, R. Division of Labor in Biofilms: the

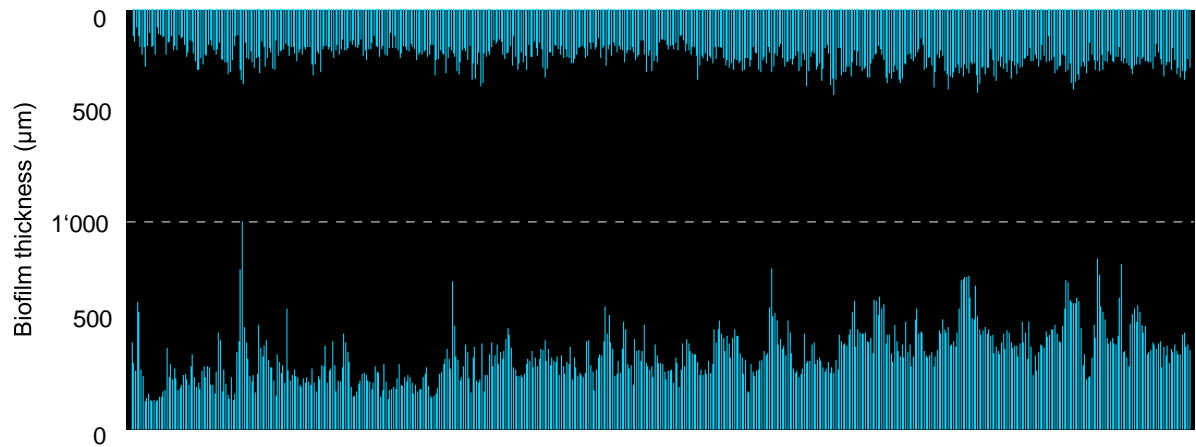
- Ecology of Cell Differentiation. *Microbiol. Spectr.* 3, 1–24 (2015).
81. **Stewart**, P. S. & Franklin, M. J. Physiological heterogeneity in biofilms. *Nat. Rev. Microbiol.* 6, 199–210 (2008).
 82. **Schreiber**, F. *et al.* Phenotypic heterogeneity driven by nutrient limitation promotes growth in fluctuating environments. *Nat. Microbiol.* 1, 1–7 (2016).
 83. **Guichard**, F. & Bourget, E. Topographic heterogeneity, hydrodynamics, and benthic community structure: a scale-dependent cascade. *Mar. Ecol. Prog. Ser.* 171, 59–70 (1998).
 84. **Singer**, G., Besemer, K., Schmitt-Kopplin, P., Hödl, I. & Battin, T. J. Physical Heterogeneity Increases Biofilm Resource Use and Its Molecular Diversity in Stream Mesocosms. *PLoS One* 5, 1–11 (2010).

Chapter 4 – Supplementary Information

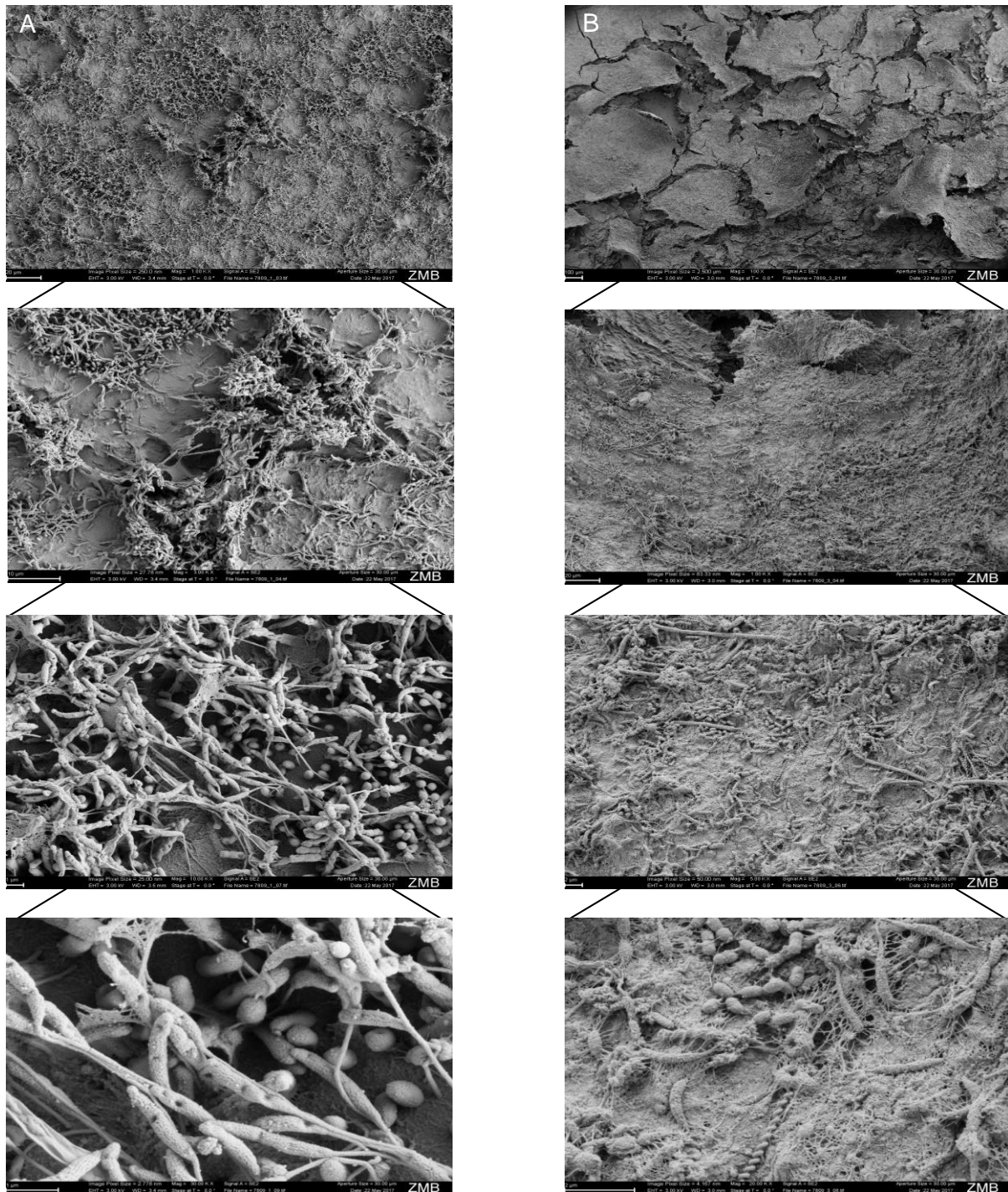
Small-scale heterogeneity in drinking water biofilms



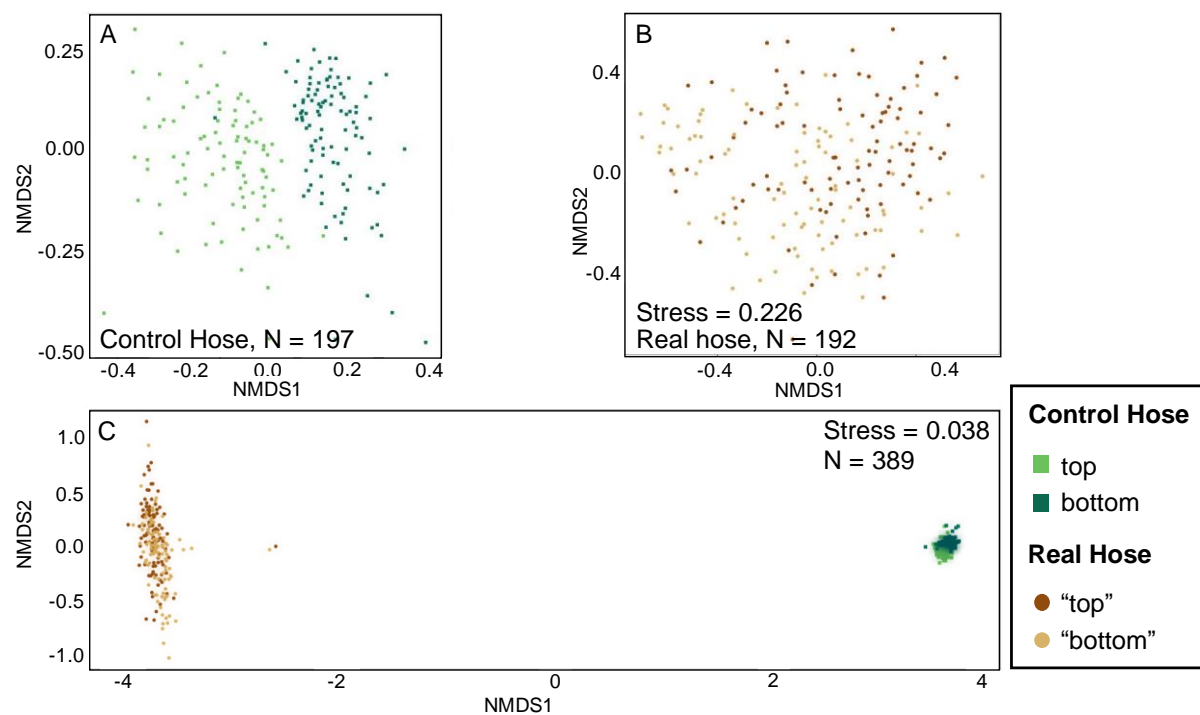
Supplementary Figure S1 Temperature pattern inside PVC-P hose (black) and surrounding temperature inside box (gray). (A) over the course of 1 week; in higher resolution, the (B) 9 am flush and (C) 5 pm flush.



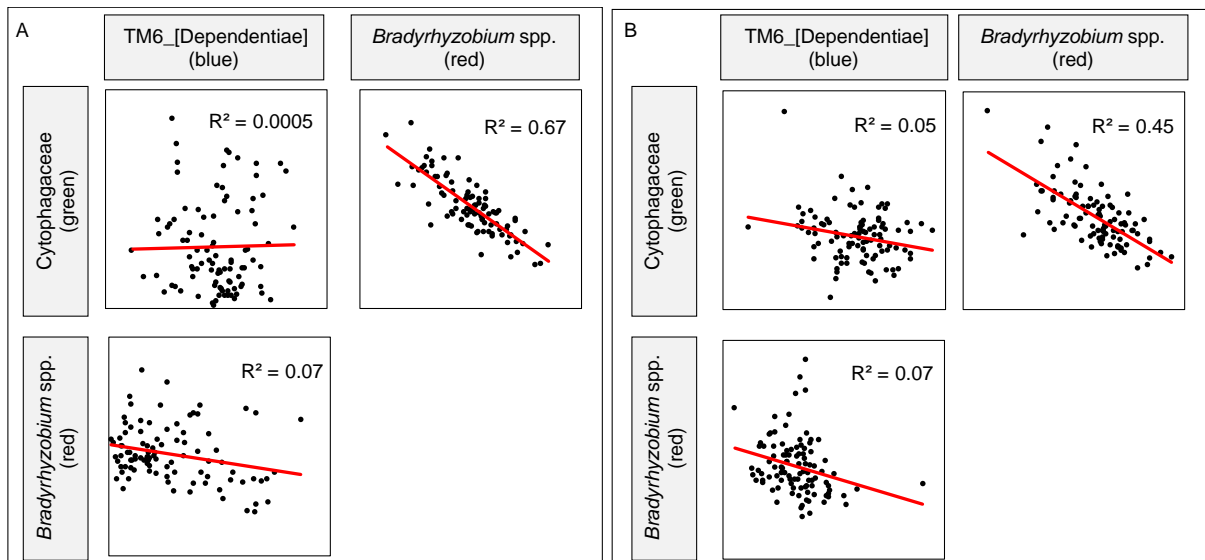
Supplementary Figure S2 Thickness of the control hose biofilm. Optical coherence tomography was used for imaging and analyzing structure and thickness of a biofilm grown inside a flexible PVC-P hose under controlled conditions in the laboratory. Images were taken two-dimensional in 2 mm length and 1 mm in height. Here, each bar represents the average thickness for these 2 mm-sections for 1.20 m hose length.



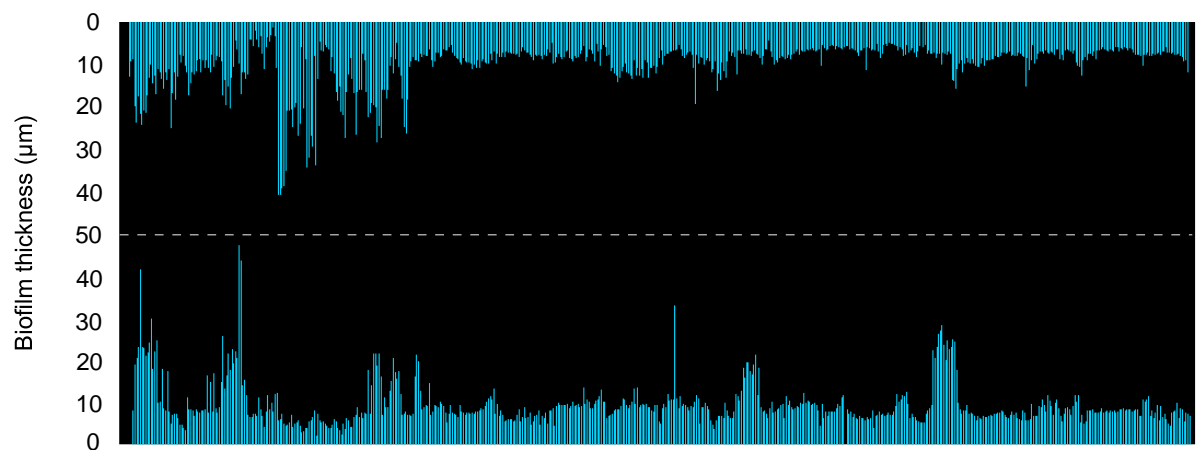
Supplementary Figure S3 Scanning electron microscopic image of biofilms grown under (A) controlled laboratory conditions (Control hose) or (B) real use (i.e., uncontrolled) conditions (Real hose). Images made by the Center for Microscopy and Image Analysis, University of Zurich.



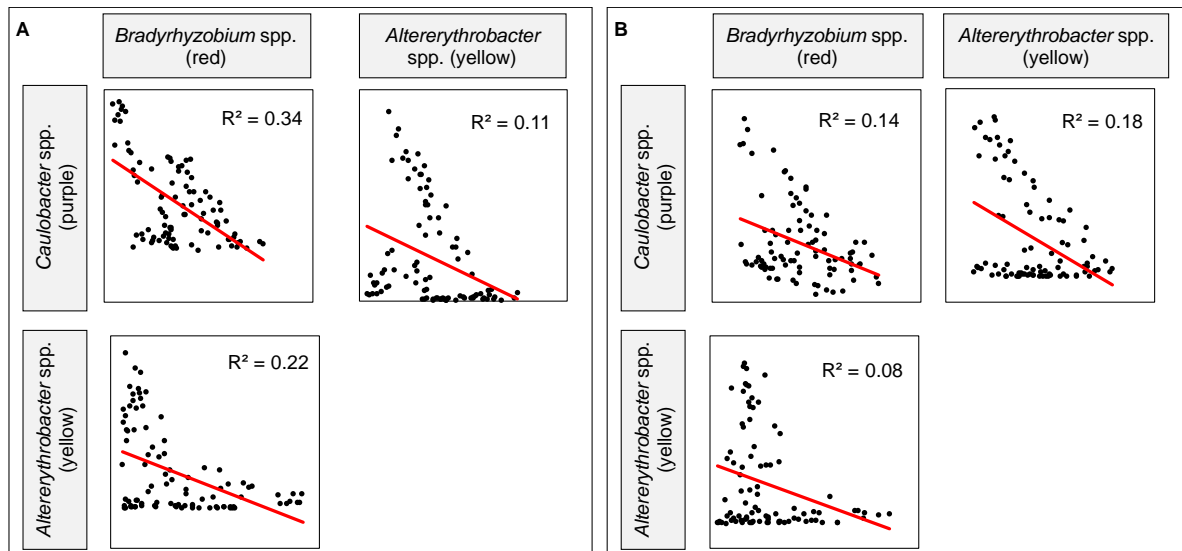
Supplementary Figure S4 Non-metric multidimensional scaling representation of Bray-Curtis dissimilarity between biofilm communities, either grown under controlled laboratory conditions (control hose, A) or under real (i.e., uncontrolled) use conditions (real hose, B). NMDS plots display dissimilarity between subsamples of the control hose biofilm (A), between subsamples of the real hose biofilm (B), and between both biofilms (C).



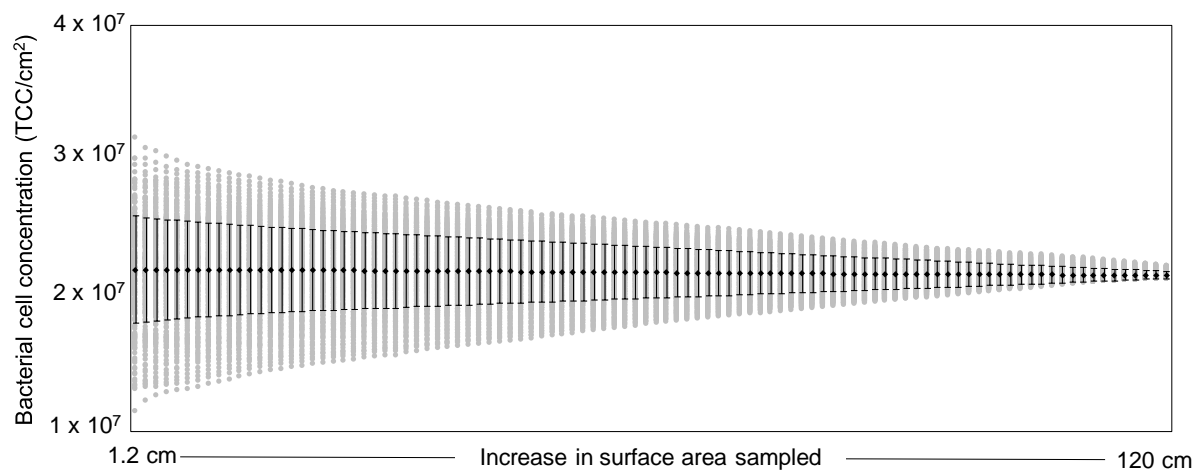
Supplementary Figure S5 Correlations between the relative abundances of the three most dominant taxa in the control hose biofilm. (A) top, (B) bottom part of the hose. Dominant taxa were identified as *Bradyrhizobium* spp., Cytophagaceae, and TM6_(Dependentiae).



Supplementary Figure S6 Thickness of the real hose biofilm. Optical coherence tomography was used for imaging and analyzing structure and thickness of a biofilm grown inside a flexible PVC-P hose under real (i.e., uncontrolled) use conditions. Images were taken two-dimensional in 2 mm length and 1 mm in height. Here, each bar represents the average thickness for these 2 mm-sections for 1.20 m hose length.



Supplementary Figure S7 Correlations between the relative abundances of the three most dominant taxa in the real hose biofilm. (A) top, (B) bottom part of the hose. Dominant taxa were identified as *Bradyrhizobium* spp., *Altererythrobacter* spp., and *Caulobacter* spp.



Supplementary Figure S8 Relevance of sample size. Bacterial cell numbers of the control hose biofilm were exemplarily used to assess the importance of sample size for the representativeness of results. Samples have been created on 1.2 cm-scale. Here, several sections have been combined to illustrate larger sampling sizes. Black dots represent the overall average for the entire shower hose biofilm. Grey dots illustrate the variation of results, decreasing with increasing sample size (i.e., samples cm in length).

Supplementary Table S1 Water characteristics for control and real hose biofilm.

(A) Control hose		(B) Real hose
Origin		
15.0 %	Groundwater	96%
6.4 %	Spring water	4%
78.6 %	Lake water	-
Physico-chemical parameters		
95 mg/L	Calcium	100 mg/L
12 mg/L	Sodium	5 mg/L
14.7 mg/L	Magnesium	15 mg/L
14.3 mg/L	Nitrate	21 mg/L
1.9 mg/L	Potassium	-
15.6 mg/L	Chloride	14 mg/L
16.7 mg/L	Sulfate	20 mg/L
0.05 mg/L	Fluoride	< 0.1 mg/L
-	Manganese	> 0.01 mg/L
-	Hydrogen carbonate	31 mg/L
-	Iron	< 0.01 mg/L
pH		
-	pH	7.3
Hardness		
26.8 °fH	Hardness	34°fH
Temperature		
13.2 °C	Temperature	12°C

Supplementary Table S2 Detailed information on PCR reactions.

(A) Amplicon PCR		
		<i>Volume (25 μL reaction)</i>
2xKAPA HiFi HotStart ReadyMix		12.5 μ L
Forward primer (10 μ M)		0.75 μ L
Reverse primer (10 μ M)		0.75 μ L
Template DNA (adjusted to 1 ng / reaction with DNase free water)		11.0 μ L
<i>Temperature</i>	<i>Duration</i>	<i>Cycles</i>
95 $^{\circ}$ C	5:00 min	
95 $^{\circ}$ C	0:20 min	29 x
51 $^{\circ}$ C	0:15 min	
72 $^{\circ}$ C	0:30 min	
4 $^{\circ}$ C	hold	
(B) Index PCR		
		<i>Volume (50 μL reaction)</i>
2xKAPA HotStart ReadyMix		25.0 μ L
Nextera XT Index 1 primer		5.0 μ L
Nextera XT Index 2 primer		5.0 μ L
Template DNA		15.0 μ L
<i>Temperature</i>	<i>Duration</i>	<i>Cycles</i>
95 $^{\circ}$ C	3:00 min	
95 $^{\circ}$ C	0:30 min	8 x
51 $^{\circ}$ C	0:35 min	
72 $^{\circ}$ C	0:35 min	
4 $^{\circ}$ C	hold	

Supplementary Table S3 Processing of 16S rRNA gene sequences.

(A) Quality control		
	FastQC V0.11.4	
(B) Trimming and merging of primers		
	usearch	v10.0.240_i86linux64
	Trim R1	20
	Trim R2	50
	Flash	v1.2.11
	Minimal overlap	15
	Maximal overlap	300
	Maximal mismatch density	0.25
(C) Primer site trimming		
	Usearch	v10.0.240 i86linux64
	Coverage	full-length
	Allowed number of mismatches	1
	Amplicon size range	50 - 600
(D) Filtering based on quality and size		
	Size range	200 - 500
	GC range	30 - 70
	Minimal Q mean	200 - 500
	Number of Ns	1
	Low complexity	dust / 30

Supplementary Table S4 List of all dominant taxa (i.e., with at least 1 % of the total number of reads) in the control hose biofilm. (*) Portion of total community (%).

%(*)	Phylum	Class	Order	Family	Genus
24.7	Bacteroidetes	Cytophagia	Cytophagales	Cytophagaceae	uncultured
23.4	Proteobacteria	Alphaproteo.	Rhizobiales	Bradyrhizobiaceae	Bradyrhizobium
9.6	TM6_[Dependentiae]	uncultured_bacterium	uncultured_bacterium	uncultured_bacterium	uncultured_bacterium
8.6	Proteobacteria	Alphaproteo.	Rhodobacterales	Rhodobacteraceae	NA
6.3	Proteobacteria	Alphaproteo.	Rhodobacterales	Rhodobacteraceae	Rhodobacter
6.2	Bacteroidetes	Sphingobacteriia	Sphingobacteriales	Chitinophagaceae	Sediminibacterium
5.7	Verrucomicrobia	Verrucomicrobiae	Verrucomicrobiales	Verrucomicrobiaceae	Brevifollis
1.9	Bacteroidetes	Cytophagia	Cytophagales	Cytophagaceae	Ohtaekwangia
1.5	Proteobacteria	Betaproteo.	Rhodocyclales	Rhodocyclaceae	Dechloromonas
1.4	Proteobacteria	Alphaproteo.	Caulobacterales	Caulobacteraceae	Phenylobacterium
1.3	Proteobacteria	Betaproteo.	Rhodocyclales	Rhodocyclaceae	Denitratisoma

Supplementary Table S5 List of all dominant taxa (i.e., with at least 1 % of the total number of reads) in the real hose biofilm. (*) Portion of total community (%).

%(*)	Phylum	Class	Order	Family	Genus
34.7	Proteobacteria	Alphaproteo.	Caulobacterales	Caulobacteraceae	Caulobacter
24.2	Proteobacteria	Alphaproteo.	Rhizobiales	Bradyrhizobiaceae	Bradyrhizobium
14.2	Proteobacteria	Alphaproteo.	Sphingomonadales	Erythrobacteraceae	Altererythrobacter
5.4	Actinobacteria	Actinobacteria	Micrococcales	Brevibacteriaceae	Brevibacterium
4.8	Proteobacteria	Alphaproteo.	Rhizobiales	Bradyrhizobiales	Bosea
2.0	Bacteroidetes	Sphingobacteriia	Sphingobacteriales	Chitinophagaceae	NA
1.4	Proteobacteria	Deltaproteo.	Bdellovibrionales	Bdellovibrionaceae	Bdellovibrio
1.4	Bacteroidetes	Sphingobacteriia	Sphingobacteriales	Chitinophagaceae	uncultured
1.2	Proteobacteria	Alphaproteo.	Sphingomonadales	Sphingomonadaceae	Sphingomonas
1.2	Cyanobacteria	ML635J-21	NA	NA	NA
1.1	Proteobacteria	Alphaproteo.	Rhodobacterales	Rhodobacteraceae	Rhodobacter

Chapter 5

Towards a probiotic approach for building plumbing – Nutrient-based selection during initial biofilm formation on flexible polymeric materials

This chapter has been submitted in revised form for publication in *npj Biofilms and Microbiomes* by L. Neu, L. Cossu, and F. Hammes.

Abstract

Upon entering building plumbing systems, drinking water bacteria experience considerable changes in environmental conditions. For example, some flexible polymeric materials leach organic carbon, which increases bacterial growth and reduces diversity. Here we show that the carbon supply by a flexible polymeric material drives nutrient-based selection within establishing biofilm communities. We found that migrating carbon from EPDM coupons resulted in considerable growth for different drinking water communities ($0.2 - 3.3 \times 10^8$ cells/cm²). All established biofilm communities showed low diversity (29 – 50 taxa/biofilm), with communities dominated by even fewer taxa (e.g., 5 taxa accounting for 94 ± 5 % relative abundance, $n = 15$). Interestingly, biofilm communities shared some taxa (e.g., *Methylobacterium* spp.) and families (e.g., Comamonadaceae), despite the difference in starting communities. Moreover, selected biofilm communities performed better than their original communities regarding maximum attachment (91 ± 5 vs. 69 ± 23 %, $n = 15$) and attachment rate ($5.0 \pm 1.7 \times 10^4$ vs. $2.4 \pm 1.2 \times 10^4$ cells/cm²/h, $n = 15$) when exposed to new EPDM coupons. Our results demonstrate nutrient-based selection during initial biofilm formation on a flexible polymeric material and a resulting benefit to selected communities. We anticipate our findings to help connecting observational microbiological findings with their underlying ecological principles. Regarding initial biofilm formation, attachment dynamics, growth, and selection thereof are important for the management of microbial communities. In fact, managing initial colonization by supplying specific carbon and/or introducing consciously chosen/designed communities potentially paves the way for a probiotic approach for building plumbing materials.

Introduction

Uncontrolled microbial growth in building plumbing systems is generally undesirable as it can lead to operational and/or hygienic problems^{1,2}. Such growth is caused by changes in environmental conditions, which is what drinking water bacteria experience as soon as they enter a building plumbing system. For example, water temperature increases and fluctuates spatially and temporally, which was shown to alter community composition^{3,4}. Also, pipe diameters are considerably smaller (e.g., < 2 cm) compared to main distribution pipes (e.g., ≥ 10 cm), which provides more surface area per water volume⁵, and increases the impact of biofilms on the water phase. Regarding operation, flow pattern and rates have been shown to impact biofilm structure and community composition^{6,7}. Finally, diverse materials are used for pipes and non-pipe components⁸, and some of these support microbial growth by leaching biodegradable substances⁹, which is especially critical under long stagnation times of the water¹⁰. The bottom line is that building plumbing systems often provide more favorable environmental conditions for bacterial growth than the main distribution network and that it is important to understand and control not only their individual but also their combined impact on the drinking water microbiome.

Several previous studies investigated the impact of building plumbing conditions on its microbiome. Overall, microbial community compositions tend to change considerably, e.g., (1) during stagnation¹¹, (2) while forming biofilms inside flexible shower hoses¹², or (3) due to the combined impact of material, temperature, and stagnation¹³. Considering one of the above in more detail, studies in our research group that were addressing biofilm formation on flexible polymeric materials revealed (1) high bacterial numbers (i.e., growth) and (2) a considerable loss in species diversity (i.e., selection)^{12,14}. Also, Proctor and colleagues¹⁵ observed the development of dissimilar biofilm community compositions when exposing the same drinking water community to different

polymeric hose materials. Thereupon, they reasoned for considerable impact of migrating organic carbon on both growth and selection.

In this study, we investigated nutrient-based selection during initial biofilm formation, using a microcosm set up for the simulation of new flexible polymeric material (EPDM) in contact with drinking water. Our hypotheses were: (1) EPDM coupons release biodegradable organic carbon, which increases the potential of bacteria to grow in an otherwise carbon-limited environment. (2) Selection occurs within establishing biofilm communities, irrespective of the initial drinking water community composition. (3) Due to the common carbon supply, biofilm communities will show a certain degree of similarity in their compositions. (4) The selection process will bring advantages for initial biofilm formation, e.g., attachment, growth, etc.. We finally argue that this information provides an opportunity for the development of new, proactive approaches for the management of biofilms that form on polymeric building plumbing materials.

Materials and Methods

Selection of coupon material and water

The interplay between one flexible polymeric material and five different drinking waters was tested regarding biofilm formation and community selection (Figure 1A). Coupons of ethylene-propylene-diene monomer (EPDM) rubber (Angst+Pfister AG, Switzerland) with an ethylene fraction of 2 % (w/w) was used as experimental material throughout this study. EPDM is approved for the use in contact with drinking water^{16,17}, e.g. as rubber seals within building plumbing systems. Two bottled waters and three non-chlorinated tap waters were selected as water matrices, namely: Evian (France; *B1*), Aproz (Switzerland; *B2*), tapped groundwater Dübendorf (Switzerland; *T1*), tap water Dübendorf (Switzerland; *T2*), and tap water Oerlikon (Switzerland; *T3*). The five waters differed in their chemical and biological composition. However, all waters were oligotrophic with low organic carbon and phosphorous concentrations and total bacterial concentrations in the same order of magnitude ($1 - 3 \times 10^5$ cells/mL; Table S1).

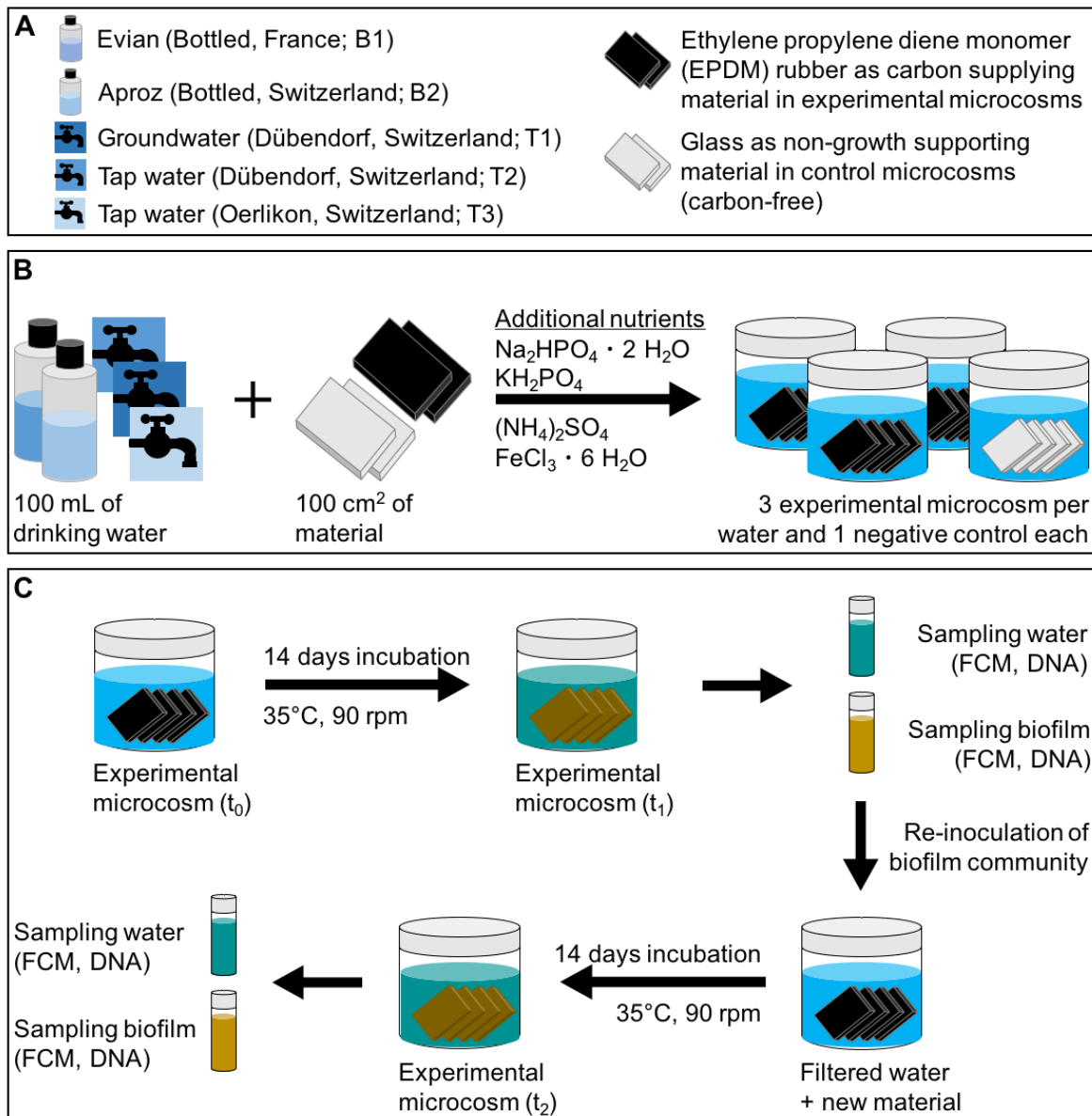


Figure 1 Experimental design. (A) Water and coupon materials. (B) Microcosms contained 100 mL water and 100 cm² of coupons. To exclude growth limitation, phosphorous, nitrogen, and iron were added to each microcosm. (C) Microcosms were incubated for 14 days (35 °C, 90 rpm). Biofilms and water were analyzed using flow cytometry for total cell concentrations and 16S rRNA gene sequencing for the community compositions (t_1). New microcosms were set up using filtered water which was spiked with individual biofilm communities. After another 14 days, biofilms and water phases were again sampled and analyzed (t_2).

Microcosm design

Microcosms consisted of 240 mL glass jars (74 x 89 mm) with polypropylene lids including a PTFE lined inlet (Infochroma AG, Zug, Switzerland) (Figure 1). All glassware was cleaned with 1% (0.33 M) hydrochloric acid (HCl, 32%; Fluka, Sigma-Aldrich, Buchs, Switzerland), rinsed with nanopure water, and air dried. The clean glassware was muffled in a furnace (Nabertherm Schweiz AG, Hägendorf, Switzerland) (4.5 h; 500°C). EPDM flat sheets were cut into coupons of 0.2 x 2.6 x 4.3 cm (25 cm²). Prior to use, coupons were cleaned with a 0.1% (v/v) sodium hypochlorite solution (Sigma-Aldrich, Buchs, Switzerland) and rinsed with nanopure water. Glass was used as the control material. Microscope slides (Menzel-Gläser, 1 mm, ThermoScientific) were cut to the same coupon size as the EPDM and cleaned following the same procedure as for the glass jars (above). For each microcosm, four coupons or slides (i.e., 100 cm²) were stacked (Figure 1), separated by stainless steel springs. The springs and the jar lids were cleaned (60°C, 1 h) in a 100 g/L sodium persulfate solution (Na₂S₂O₈, Sigma-Aldrich, Buchs, Switzerland), then rinsed with nanopure water, and air dried. Before use, the bottled drinking water was inverted 3-4 times for uniform mixing, while cold tap water was flushed for 5 min before filling into muffled 1 L SCHOTT Duran® bottles (SCHOTT AG, Mainz, Germany). Each microcosm was subsequently filled with 100 mL water. To ensure unlimited growth conditions, additional nitrogen, phosphorous, and iron were added to the microcosms. The nitrogen/phosphorous buffer contained sodium phosphate dibasic dehydrate (Na₂HPO₄ · 2H₂O, 1.28 g/L), potassium phosphate monobasic (KH₂PO₄, 0.3 g/L), and ammonium sulfate ((NH₄)₂SO₄, 1.77 g/L) and 3.4 mL of buffer was added to each microcosm. Iron was supplemented in the form of iron (III) chloride hexahydrate (FeCl₃ · 6 H₂O, 2.7 g/L), with 50 µL per microcosm. All chemicals were purchased from Sigma-Aldrich (Buchs, Switzerland).

Migration and growth potential assays

For the assessment of carbon migration from the experimental material (EPDM) and the resulting consequences for bacterial growth, the material BioMig testing method was applied¹⁸. This method comprises a migration assay and a growth potential assay. In short: for the migration assay, 100 cm² of EPDM was incubated (60°C, 24h, without shaking) with 100 mL bottled water (Evian). Over the course of seven days, the EPDM material was transferred into a new microcosm with fresh water every day. After the 1st, 3rd, and 7th day of incubation, the water was sampled and the migrated total organic carbon (TOC) was quantified (see below). In addition, the growth of bacteria in the migration water was assessed. For this, 1 mL of fresh Evian bottled water was inoculated into 20 mL of migration water, with the addition of 690 µL phosphate/nitrogen buffer and 10 µL FeCl₃. This test was performed in sterile, muffled 40 mL glass vials with screw caps lined with a PTFE septum (Supelco, Sigma-Aldrich Chemie GmbH, Buchs, Switzerland). Incubation (30°C, 120 rpm, 6 d) was followed by the quantification of the total cell concentration (TCC) using flow cytometry (FCM) (see below). For the growth potential assay, 100 cm² of new EPDM material was incubated (30°C, 14 d) with 100 mL of fresh bottled water (Evian) and additional nutrients (see above). After 14 d of incubation, the water and biofilm phases were sampled for TCC, allowing for the determination of the bacterial growth potential within the experimental microcosms due to migrating carbon compounds (in direct comparison to a glass control set up without additional carbon)¹⁸.

Selection experiment

For all five water samples, triplicate microcosms were assembled with the testing material (EPDM) and an additional one containing glass as a control set up (Figure 1, B), as described above. After assembly (t_0), the microcosms were incubated (14 d, 35°C, 90 rpm) (Figure 1, C). After 14 days (t_1), biofilms

were removed from the material surface (EPDM and glass; see below) and both the biofilm and water phase of each microcosm were sampled for TCC (see below) and community composition by 16S rRNA gene sequencing (see below). For a second selection step, biofilm samples were re-inoculated into new microcosms. For this, the corresponding drinking water matrix was filtered using sterile bottle top filter units and membrane filters (Whatman® Nucleopore™ Track-Etched Membranes, 47 mm, 0.2 µm, Sigma Aldrich). New material was cleaned and stacked, additional nutrients added, and selected biofilm communities were added in a final concentration of 1×10^7 cells/microcosm (i.e., 1×10^5 cells/mL). After another 14d incubation, biofilms and water phases of all microcosms were again sampled (t_2), following the same procedure. Regarding terminology, in the course of this study, initial drinking water communities are referred to as *original drinking water communities* and the biofilm communities of t_1 and t_2 as *selected biofilm communities*.

Attachment experiment

Here we compared attachment dynamics of selected biofilm communities with the original drinking water communities. The same microcosm set up was used as described above, with triplicate experimental microcosms (EPDM coupons) and single control microcosms (glass slides). The starting concentration of bacteria in the water phase (TCC, t_0) was adjusted to be the same by diluting the biofilm communities relative to the drinking water TCC. The microcosms were incubated (35°C, 90 rpm) and the TCC in the water phase was measured for all at 30 min intervals over the course of 5 h ($t_1 - t_{10}$).

Sampling and analysis

Chemical water analysis

Total organic carbon (TOC) was measured using a TOC-V_{CPH} Analyzer (Shimadzu Schweiz GmbH, Reinach, Switzerland). The minimum detection limit of the instrument is 0.1 mg/L. For total phosphorous, samples were chemically digested with potassium peroxodisulfate at 121°C, followed by a reaction to a phosphorous-molybdenum-blue complex and the determination of ortho-phosphate with spectrophotometry. The minimum detection limit of this method was 3.0 µg/L. Total nitrogen concentrations were measured via chemiluminescence using a Shimadzu TOC-L_{CSH} instrument. The minimum detection was 0.5 mg/L.

Biofilm removal

All biofilms were removed with an electrical toothbrush (Oral-B®, Advanced Power) and toothbrush heads were replaced after each use to prevent cross-contamination. In short: EPDM or glass coupons were placed into muffled glass petri dishes and covered with filtered (0.2 µm) water. The water volume was always 25 mL per coupon (i.e., a total of 100 mL per microcosm). The coupons were brushed one by one, for approximately 90 sec each (including both coupon sides and the edges). During biofilm removal, 10 mL were saved and after the biofilm removal from all four coupons of a microcosm. This volume was ultimately used to recover biofilm residuals in the petri dish and on the brush head, by pouring the 10 mL filtered water into the petri dish and brushing without any coupon. The biofilm suspensions of the microcosms were collected in individual, sterile 100 mL SCHOTT Duran® bottles. 10 mL of the biofilm suspension was used for flow cytometry (below). The rest of the biofilm suspension was used for the re-inoculation in the selection experiment (see

above), for further steps on community analysis (see below), or for the attachment experiments (see above).

Flow cytometry for the quantification of total cell concentrations

FCM was used for the determination of total cell concentrations (TCC) in all biofilm and water samples. For biofilms, a 10 mL subsample of the biofilm suspension (see above) was collected and needle-sonicated in a round-bottom glass tube (DURAN®; Faust Laborbedarf AG, Schaffhausen, Switzerland) using the Sonopuls HD 2200 instrument (Bandelin Sonorex, Rangendingen, Germany) and the Sonotrode Sonopuls MS 73 (tip diameter 3 mm, Bandelin). Sonication settings were: 30 sec at 50% power, and 40% amplitude intensity, with the pulse amplitude of the needle being 308 μm . The sonicated biofilm samples were then diluted 10-100x using 0.1 μm filtered Evian water (Millex®-VV, Merck-Millipore), while the water samples were measured undiluted. For the detection of TCC, samples were stained with 10 $\mu\text{L}/\text{mL}$ SYBR® Green I (SG, Invitrogen AG, Basel, Switzerland; 100x diluted in 10mM Tris buffer, pH 8). Stained samples were incubated (37°C, 10 min) and measured using a BD Accuri C6® flow cytometer (BD, Belgium) or a CytoFLEX Flow Cytometer (Beckman Coulter International SA, Nyon, Switzerland). Gates and settings were kept the same within experiments. For more detailed information on data analysis and gating strategies see¹⁹.

16S rRNA gene-based community analysis

For sequencing, samples of (1) all original drinking waters (t_0), (2) all selected biofilms (t_1 , t_2), and the water phase of the microcosms (t_1 , t_2) were concentrated onto 0.2 μm polycarbonate Nucleopore® membrane filters (\varnothing 47 mm, Whatman, Kent, United Kingdom) by vacuum filtration, using sterile bottle top filter units. Filters were immediately frozen in liquid nitrogen and stored at -20°C.

DNA extraction

The DNeasy PowerWater® Kit (Qiagen, Hilden, Germany) was used for DNA extraction and performed according to the provided protocol. Extracted DNA was frozen and stored at -20°C until further processing.

Library preparation and sequencing

For analyses on bacterial community compositions, the V3-V5 region of the 16S rRNA gene was amplified via polymerase chain reaction (PCR), using the primers Bakt_341F and Bakt_805R²⁰. For library preparation, extracted DNA was quantified in duplicates using a Spark® 10M Multimode Microplate Reader (Tecan, Switzerland; Qubit™DNA Broad Range Assay). DNA concentrations were normalized between samples prior to amplification (1 ng DNA / 11 µL). For the PCR, normalized DNA was mixed with 2xKAPA HiFi HotStart Ready Mix (Kapa Biosystems, Roche Holding AG). Primers were added in a final concentration of 0.3 µM (details see Table S2, A). In addition to experimental samples, a negative control (i.e., amplification of sterile water instead of sample-DNA) and a positive control (self-made MOCK community: pure DNA of *Burkholderia xenovorans*, *Bacillus subtilus*, *Escherichia coli*, *Micrococcus luteus*, *Pseudomonas protegens*, *Paenibacillus sabiniae*, and *Streptomyces violaceoruber*) were amplified. Additionally, some experimental samples were amplified in replicates. For this PCR, all samples were amplified in duplicates (2 x 25 µL reactions), which were combined prior to clean up. Amplified products were purified using the Agencourt AMPure XO System (Beckman Coulter, Inc., Brea, CA, United States). For this, products were attached to magnetic beads, washed with 80% EtOH, and re-suspended in 10 mM Tris, pH 8.0. To enable pooling and re-identification of individual samples, specific sequencing Nextera XT v2 Index Kit adapters (Illumina) were annealed to the amplicons via Index PCR (Table S2, B). Products were again cleaned using the AMPure approach, quantified, and quality was checked using the High Sensitivity

D1000 ScreenTape system (Agilent 2200 Tape Station). All samples were normalized to a concordant concentration followed by the pooling of 5 μ L per sample. This pool was adapted to a final concentration of 2 mM and the base-pair (bp) length of the product determined with the Tape Station (627 bp). Sequencing was performed using the MiSeq platform. For this, 0.1M NaOH was added to the pool, centrifuged (300 g, 60 s) and incubated for 5 min (room temperature) prior to the addition of the hybridization buffer HT1. This step was to (1) generate single stranded DNA and to (2) prevent unspecific bindings to the flow cell during sequencing. As a final step, 10% PhiX was added as a sequencing run control (Illumina: Technical Note on PhiX Control). The MiSeq run was a paired-end 600 cycle sequencing run. Data on community composition was generated in collaboration with the Genetic Diversity Center (GDC), ETH Zurich.

Processing of sequencing data

Data processing followed a distinct pipeline. First, data quality was controlled using FastQC (Table S2, A). Then, read ends were trimmed and merged (Table S2, B), which was followed by an *in silico*-PCR and the trimming of the primer sites (Table S2, C). Finally, sequences were filtered (based on quality and size range) (Table S2, D) and amplicon sequence variants (ASV) were generated and taxonomically assigned. The clustering of sequences was performed as presented in a previous study¹⁴. It is based on an amplicon sequence variant (ASV) approach using UNOISE3, proposed by Edgar and colleagues²¹, and includes a correction for sequencing errors and a chimaeral removal. Clustered sequences are called zero-radius operational taxonomic units (ZOTUs). Due to a potential overestimation of the actual number of ZOTUs, an additionally clustering was performed at different identity levels of 99, 98, and 97%. For predictions on taxonomic assignments, the Silva 16S database (v128) and the SINTAX classifier were used (cut-off 0.9).

Results

Migration and growth potential assays

Applying an established material testing package (BioMig¹⁸) revealed that a considerable amount of organic carbon migrates from the experimental EPDM coupons and that a substantial fraction of the migrating carbon can be used by drinking water bacteria to grow. The migration assay (60 °C) showed that organic carbon migrated in high concentrations from new EPDM coupons and that it increased the TOC concentration of the water 5-fold (average: 1.1 µg TOC/mL, n = 2) within the first 24 h of migration (Figure 2A). The extent of migration diminished over time. However, even after 7 d of sequential migrations, the TOC concentration of the water with EPDM coupons still increased 3-fold (0.43 ± 0.03 µg TOC/mL, n = 2), equivalent to a rate of 0.3 µg TOC/cm²/d. These values are typical for flexible materials in contact with drinking water (e.g., in general^{14,22}, or specifically for EPDM^{23,24}). A separate growth potential assay at 30 °C showed that $2.3 \pm 0.09 \times 10^7$ cells/mL (n = 3) were able to grow on migrating carbon from EPDM coupons during 14 days, which is 30x more compared to growth in the absence of EPDM (Figure 2B). Given that the carbon-source for growth was the EPDM coupons, this translated to the growth of 2.3×10^7 cells/cm² coupon. Of these cells, 57 % (i.e., 1.3×10^7 cells/cm²) were recovered directly from the surface of the EPDM coupons. To summarize, results show that the EPDM coupons favor biofilm formation by (1) providing a surface for colonization and by (2) adding biodegradable organic carbon to the water. Therefore, this material was deemed suitable for the further experiments on biofilm growth and the selection within growing communities (below).

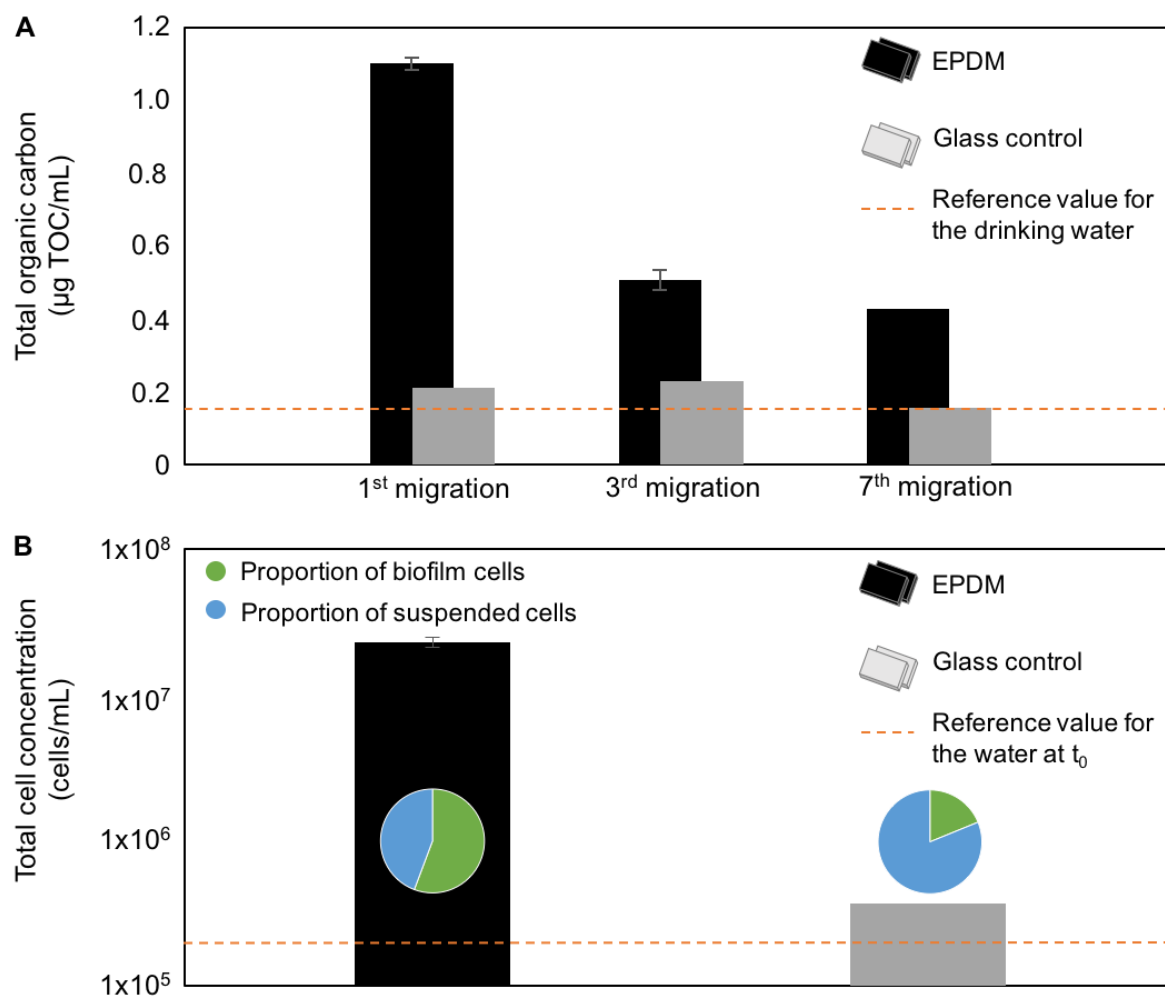


Figure 2 Assessment of carbon migration from EPDM and the resulting potential for bacterial growth. (A) Migration assay for the quantification of total organic carbon (TOC) in microcosms with EPDM or glass coupons. Material was transferred into fresh microcosms every 24 h, with measurements after the 1st, 3rd, and 7th migration. (B) Bacterial growth potential based on EPDM, or glass as control. Total cell concentrations (TCC) are shown per mL for total growth of both suspended and biofilm cells. The conversion of cm⁻² for biofilm cells to mL⁻¹ was based on the water volume to material surface area ratio of 1:1 in the microcosm set up. Proportions of biofilm and suspended cells are indicated via pie charts. Error bars represent the range between duplicate microcosms in (A) and standard deviations for triplicate microcosms in (B).

Selection experiment

The basic concept and design of the growth potential assay was used to test the growth of five different drinking water communities on identical EPDM coupons (Figure 1). All communities showed (1) intensive growth and (2) a considerable loss in taxa diversity (apart from B2), with (3) the development of different biofilm communities involving shared taxa.

Considerable growth for different original drinking water communities

Figure 3 shows that after two sequential 14-day cycles of inoculation and incubation (Figure 1), substantial growth was measured for all five waters in the presence of EPDM coupons, ranging within one order of magnitude ($0.2 - 3.3 \times 10^8$ cells/mL). These final concentrations represent both the planktonic and biofilm phases. The proportion of cells recovered directly from the biofilm ranged between 59 – 86 %, equivalent to $0.2 - 2 \times 10^8$ cells/cm². While experimental microcosms had considerable growth, differences were identified. Growth in the absence of EPDM coupons (i.e., in the glass controls) highlighted the impact of the migrating carbon, showing that TCC concentrations were 93 – 99 % lower without the additional carbon source. The proportion of cells in the biofilm was still high with 30 – 93 %, which translates to $1.4 \pm 0.5 \times 10^6$ cells/cm² ($n = 5$). These findings confirm our results from Figure 2 on the carbon migration and growth potential based on EPDM coupons. The results show that the growth is high for different drinking water communities and that there was substantial biofilm growth, irrespective of the starting community.

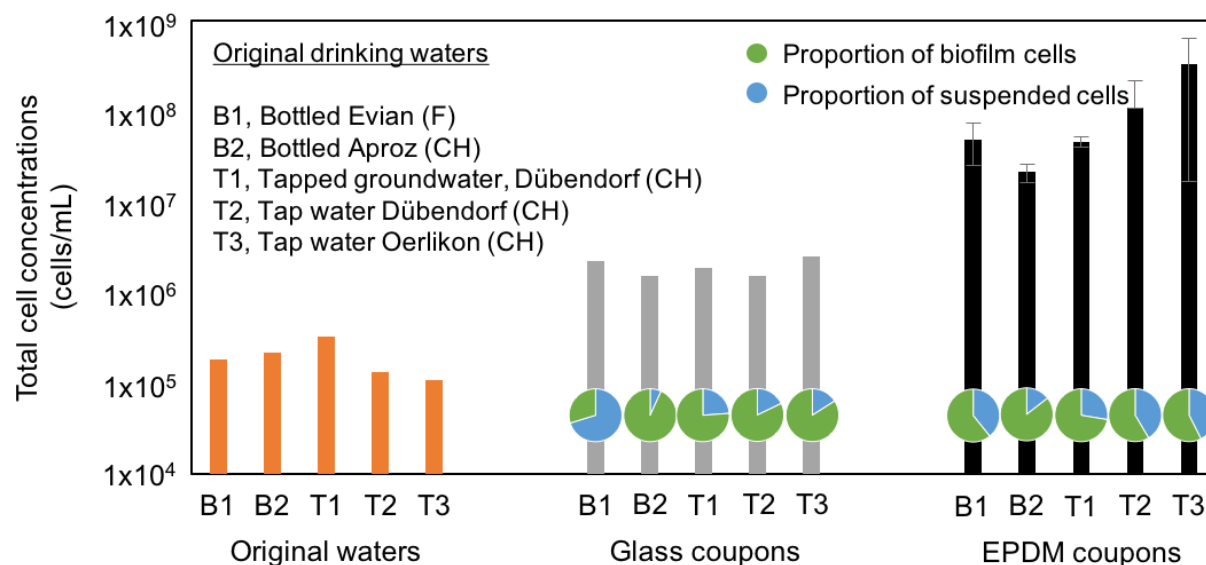


Figure 3 Total cell concentrations in the original drinking waters (t_0) and in microcosms at the end of the experiment (t_2), i.e., 2 x 14 d of incubation with an intermediate re-inoculation of biofilms grown at t_1 . For growth in microcosms with glass and EPDM coupons, total cell concentrations (TCC) are shown per mL for the total growth of both suspended and biofilm cells. The conversion of cm^{-2} for biofilm cells to mL^{-1} was based on the water volume to material surface area ratio of 1:1 in the microcosm set up. Proportions of biofilm and suspended cells are indicated via pie charts. Error bars represent standard deviations for triplicate microcosms in the EPDM coupon set up.

Comparatively low taxa diversity detected in biofilm communities

A comparison of the original drinking water communities with the biofilm communities at the conclusion of the experiment revealed a notable loss in diversity (apart from B2, see below). Richness, i.e., the number of different taxa, decreased and became more comparable between the different waters. Figure 4A shows the richness values for the five original drinking water communities. Interestingly, tapped waters showed considerably more taxa ($2'178 \pm 131$, $n = 9$) than the bottled waters, with the original water B2 comprising strikingly few taxa (54 ± 0 , $n = 3$) compared to B1 (270 ± 15 , $n = 3$). Overall, biofilm communities comprised comparatively few taxa (29 – 50 taxa), which corresponded to a diversity loss of 46 – 98 % from the original waters. This

impressive loss of up to 2'000 individual taxa (tap waters) highlights the relevance of nutrient-based selection within establishing biofilm communities. As a consequence to this loss in diversity (through growth and selection), the similarity between the biofilm communities increased (with respect to diversity), with only 21 % variation in richness between biofilms as opposed to 73 % between the original drinking water communities. Shannon diversity followed a similar trend. Figure 4B shows a comparable dissimilarity between the original tapped water communities (5.9 ± 0.7 , $n = 9$) and bottled water communities (2.3 ± 0.03 , $n = 3$ for B1; 1.1 ± 0.01 , $n = 3$ for B2). The relation between the Shannon Index (H') and its maximum value (H'_{\max}) is important for drawing conclusions on diversity, i.e., the closer H' to H'_{\max} , the higher the diversity within the community. Here, the relation was 1:1.3 for the tapped waters, 1:2.5 for B1, and 1:3.7 for B2 respectively, indicating a higher diversity in the tapped waters. This difference decreased with biofilm formation, resulting in a comparable degree of diversity. Here, the ratio between H' and H'_{\max} is close to 1:3 for all samples. This shows that (1) diversity decreased for (almost) all communities and (2) that biofilm communities are more similar to each other compared to the original drinking water communities. As indicated above, bottled water B2 was the misfit amongst the original water communities with a particularly low initial richness and diversity. Interestingly, this community also grew the least during the selection experiment (Figure 3). This suggests that the initially low diversity did not allow the community to metabolize as many nutrients as for the other more diverse communities. Results on richness and Shannon diversity allowed for the calculation of Evenness. Evenness indices were low for the bottled waters (0.34 ± 0.07 , $n = 6$) and did not change much during the growth experiment (0.35 ± 0.09 , $n = 6$). For the original tapped waters, Evenness was high (0.77 ± 0.08 , $n = 9$), indicating a rather equal distribution of taxa. For the tapped water biofilms, indices decreased approx. 50 % which resulted in comparable Evenness indices for all samples (0.37 ± 0.1 , $n = 15$).

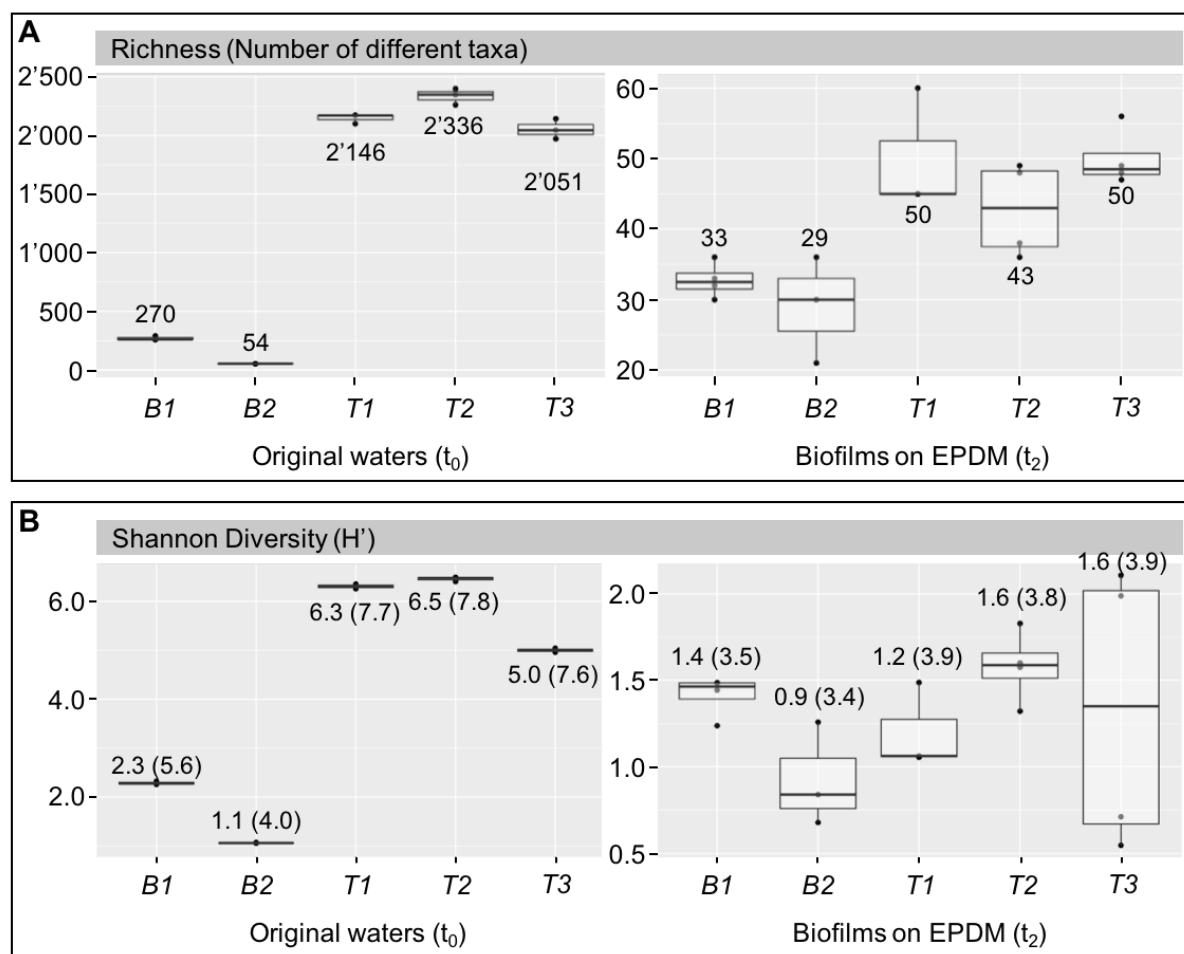


Figure 4 Diversity between microbial communities following growth on EPDM coupons. Alpha-diversity indices richness (A) and Shannon diversity (B) of the original drinking water communities (B1, B2, T1, T2, and T3) and the selected biofilm communities grown on EPDM (t_2) for each experimental water. Results are presented as averaged numbers for richness (A) and averaged Shannon indices with additional information on (H'_{max}). Original drinking waters were sequenced in triplicates and biofilms were sampled from triplicate experimental microcosms (additional sampling points in plot are due to replicate sampling of selected biofilms).

What is particularly interesting is that, involving already severe loss in taxa diversity and richness (i.e., a strong selection), the low degree of evenness within biofilm communities indicated a dominance of an even smaller number of taxa. This was, in fact, the case with the five most abundant taxa accounting for $95 \pm 5\%$ ($n = 15$) of the individual biofilm community compositions (Table S4). These results highlight that (1) the bottled waters had low diversities from the start, (2) the number of different taxa decreased during biofilm formation

and so did (3) the equality of their distribution. This rendered all biofilm communities more similar, with comparably low diversity and (4) only few taxa dominating the entire biofilm communities.

Biofilm growth alters community composition

The decrease in taxa diversity came along with a change in community composition from the original drinking water to the selected biofilm communities. Figure 5 illustrates the dissimilarities between the bacterial communities of the original drinking waters (t_0 , triangles) and their corresponding biofilm communities that grew on EPDM coupons (t_2 , circles). The distance between original and biofilm communities was large for the tapped waters (e.g., highlighted for T3, Figure 5).

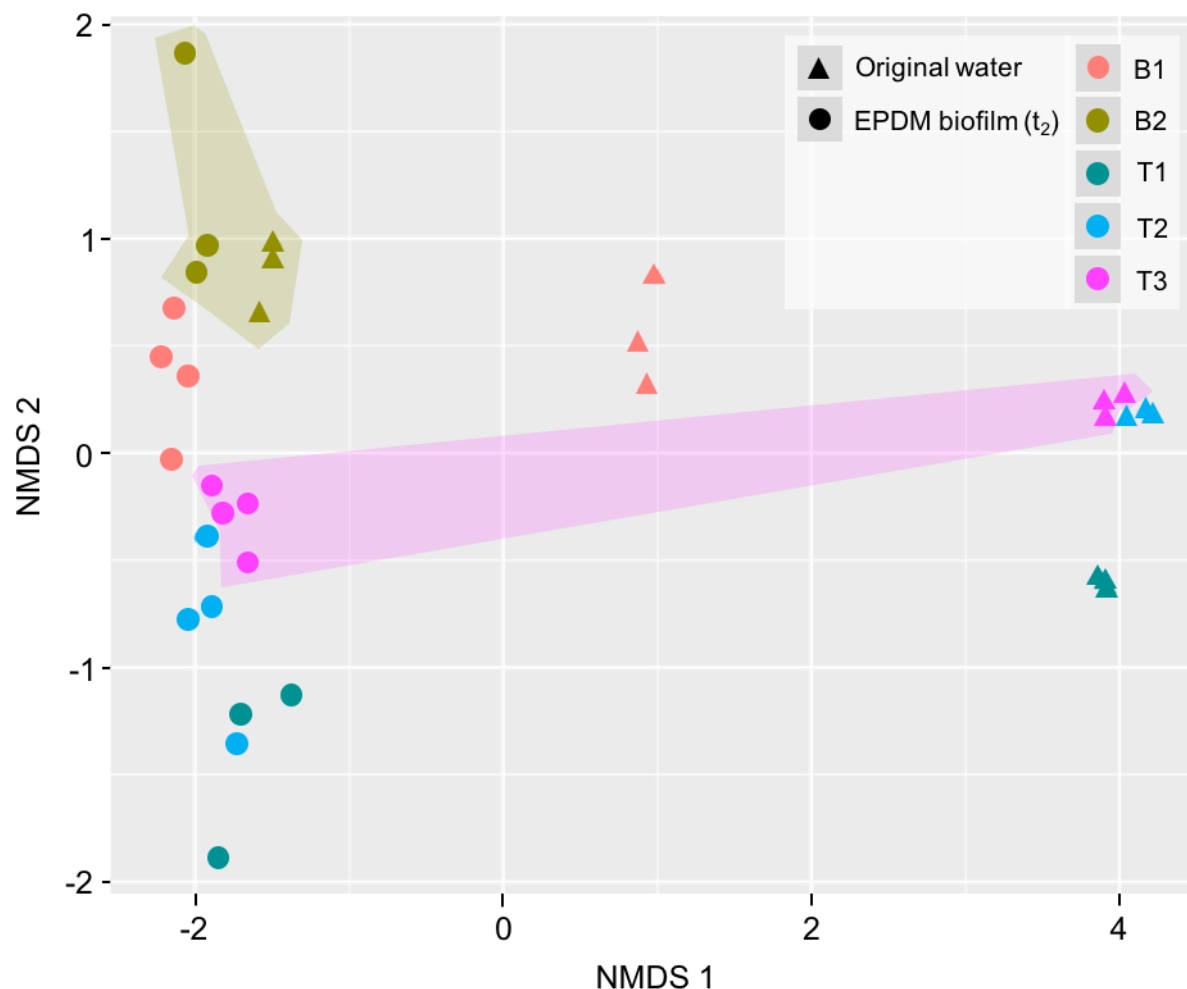


Figure 5 NMDS ordination plot based on Bray-Curtis Dissimilarity. Comparison of five different original drinking water communities (B1, B2, T1, T2, and T3) and their corresponding biofilms that formed on EPDM (t_2). Original drinking waters were sequenced in triplicates and biofilms were sampled from triplicate experimental microcosms (additional sampling points in plot are due to replicate sequencing of selected biofilm samples). Highlighted areas were added manually to emphasize differences between samples.

In accordance with the degree of diversity loss, these community compositions changed considerably more compared to the bottled waters, which was attributed to the higher loss in taxa richness. Here, Bray-Curtis (BC) indices indicated a dissimilarity of 100 % between original and biofilm communities on taxa level ($BC\ 1.0 \pm 0.0$, $n = 3$). In comparison, the dissimilarity was smaller for communities of B2 (highlighted in Figure 5), with BC indicating a dissimilarity of 89 %. The higher degree of similarity for B2 indicated that (1) the community composition changed comparatively little during biofilm formation. This

indicates, in combination with the low growth, that diversity in the original B2 did not cover enough metabolic functions to exploit the full growth potential provided by migrating carbon. To emphasize this, 83 % of the most abundant taxa of B2 biofilms (i.e., the 5 most abundant taxa amongst triplicate microcosms) were also detected in the original water community (Table S5), which is high compared to B1 (56 %) or the tapped waters (38 – 50 %). Interestingly, when comparing samples of different origin (i.e., with different starting communities), biofilms were more similar to each other compared to the original drinking water communities. Here, Bray-Curtis dissimilarity between original drinking water communities was 0.94 ± 0.1 ($n = 5$) and resulted in a BC of 0.83 ± 0.16 ($n = 5$) between biofilms. In summary, accompanying the reduction in taxa diversity, the community compositions of the original waters changed during biofilm formation and become more similar to each other. What remains unclear is whether the loss in diversity and compositional changes necessarily involved the growth of identical taxa.

Similarities in biofilm communities

Biofilm communities that developed from different (original drinking water) starting communities comprised shared taxa and families. Out of 29 ± 12 taxa/biofilm community ($n = 15$; including taxa with ≥ 0.01 % relative abundance), only two taxa were present in all biofilms that grew on EPDM coupons (Table S4). These taxa were identified as (1) *Methylobacterium* spp. (0.3 ± 0.1 %, $n = 15$; ZOTU7) and as a (2) not further identified member of the family Bradyrhizobiaceae (0.5 ± 0.6 %, $n = 15$; ZOTU23). Taxa that were detected in at least one of the experimental triplicates per set up were (1) a member of Bacilliaceae (0.04 ± 0.05 %, $n = 13$; ZOTU148), (2) *Aquabacterium* spp. (23 ± 29 %, $n = 13$; ZOTU1024), and (3) a member of the family Comamonadaceae (10 ± 16 %, $n = 14$; ZOTU5147). Here, ZOTU5147 was very abundant in the biofilms of B1 (35 ± 14 %, $n = 3$) and ZOTU1024 in the biofilms of T1 (70 ± 9 %, $n = 3$) and T2 (49 ± 8 %, $n = 3$). Out of 16 ± 6 families/biofilm community ($n = 15$), four families

were present in all EPDM biofilms, namely (1) Bradyrhizobiaceae (0.6 ± 0.6 %, $n = 15$), (2) Comamonadaceae (43 ± 28 %, $n = 15$), (3) Methylobacteriaceae (0.3 ± 0.1 %, $n = 15$), and (4) Sphingomonadaceae (3 ± 7 %, $n = 15$) (Table S6). In addition, the families (1) Bacillaceae (0.05 ± 0.05 %, $n = 13$), (2) Brucellaceae (0.03 ± 0.02 %, $n = 13$), (3) Burkholderiaceae (22 ± 30 %, $n = 13$), (4) Caulobacteraceae (4 ± 6 %, $n = 13$), and (5) Xanthomonadaceae (8 ± 13 %, $n = 13$) were present in at least one triplicate per experimental set up. Of these, Comamonadaceae was highly abundant in the biofilm communities of T1 (71 ± 10 %, $n = 3$) and T2 (61 ± 14 %, $n = 3$). For the bottled waters, Burkholderiaceae was dominant in B2 (71 ± 15 %, $n = 3$) and Xanthomonadaceae showed a high abundance in the biofilm communities of B1, with a relative abundance of up to 18 %. This result highlights that biofilm communities had a certain consistency in their compositions, despite clear differences in their starting communities. The selective pressure during biofilm formation and growth was not only demonstrated by the loss of taxa but also by the dominance of originally rare taxa. Within individual biofilm communities, the five most abundant taxa accounted for 94 ± 5 % ($n = 15$) (Table S4). From these individual abundant taxa, 53 ± 17 % ($n = 5$) were detectable in the corresponding original drinking water communities (i.e., the rest was below detection limit of the method). Interestingly, the chance of dominant biofilm taxa also being abundant in the original drinking water community was associated with the degree of initial diversity. For example, a highly abundant taxon in T1 biofilms (70 ± 10 %, $n = 3$; ZOTU1024) was rarely detected in the original water with a relative abundance of only 0.03 ± 0.01 % ($n = 3$) (Table S5). Bottled water B2 had the lowest taxa richness and diversity. Here, the most abundant biofilm taxa (71 ± 15 %, $n = 3$; ZOTU46) was already very abundant in the original water (8 ± 0.4 %, $n = 3$; ZOTU46). These results show that biofilm formation on carbon supplying EPDM coupons was highly selective and resulted in a considerable loss in taxa richness and diversity. As a result, the composition of biofilm communities differed from their original drinking water communities. Individual biofilms showed, however, similarities regarding dominant organisms, which indicated

that, irrespective of starting communities, the environment (i.e., additional carbon supply) was selective for specific taxa and families, which was potentially linked to metabolic functions (see, e.g., ²⁵).

Attachment experiment

The selected biofilm communities attached more and much faster to new surfaces compared to the original water communities (Figure 6).

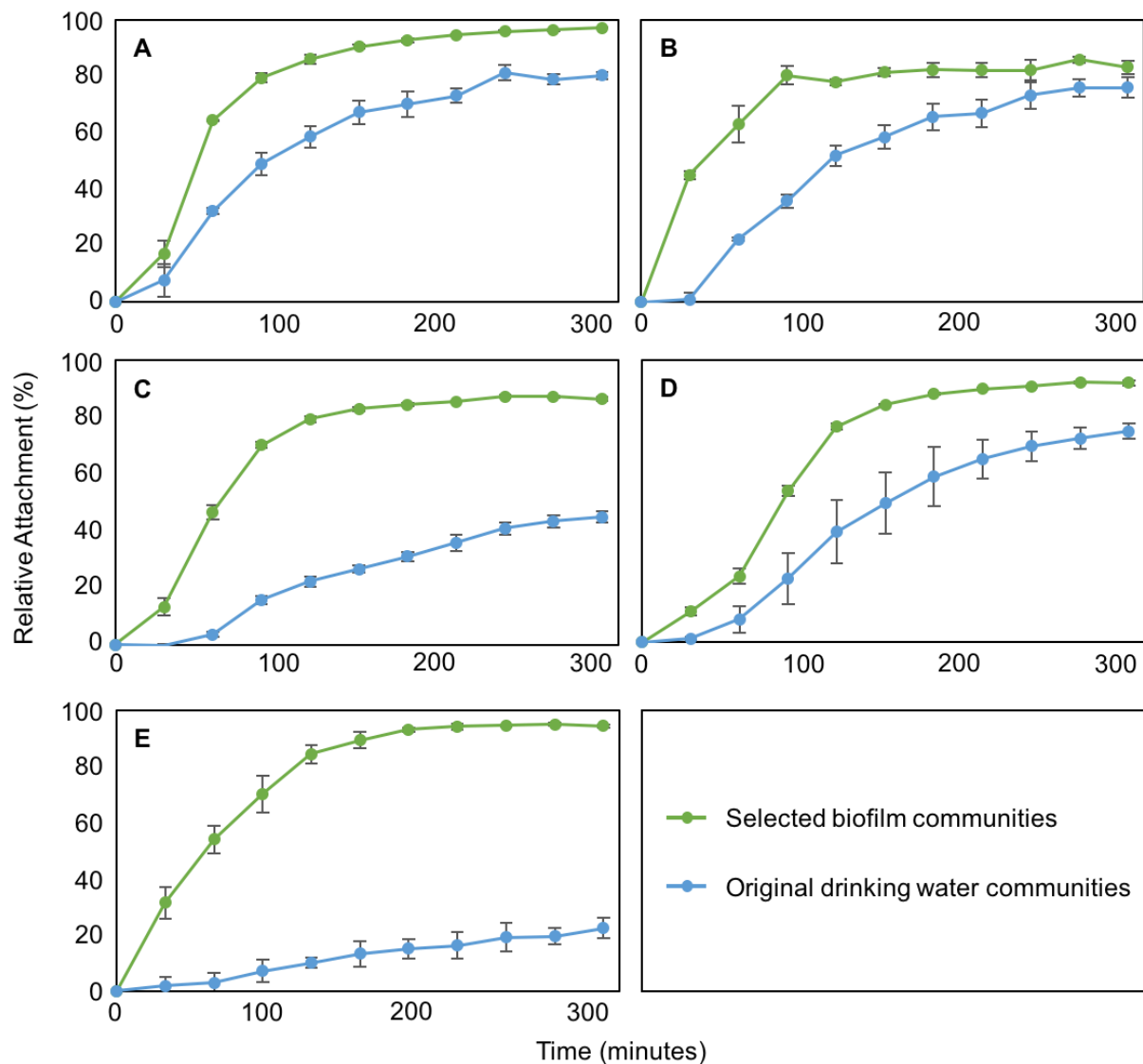


Figure 6 Attachment of selected biofilm and original drinking water communities to EPDM coupons. (A) B1 (bottled Evian; F), (B) B2 (bottled Aproz; CH), (C) T1 (tapped groundwater, Dübendorf; CH) (D) T2 (tap water, Dübendorf; CH) (E) T3 (tap water, Oerlikon; CH). Data points show average values and standard deviations for triplicate experiments.

For the selected communities, $91 \pm 5\%$ ($n = 15$) of the cells attached within the first 5 hours after exposing freshly suspended cells to new EPDM coupons. This was approx. 30% more than for the original water communities ($69 \pm 23\%$, $n = 15$). Between the original communities, strong differences were measured in maximum attachment. For example, cells from original water B1 attached to $80 \pm 1\%$ ($n = 3$) within 5 hours as opposed to T1 with only $45 \pm 2\%$ ($n = 3$). The direct comparison between original and selected communities showed a clear advantage for the selected cells. For example, after 5 hours of incubation one tapped water (T3) showed a relative attachment of $94 \pm 1\%$ ($n = 3$) for the selected community, but only $22 \pm 4\%$ ($n = 3$) for the original community (Figure 6E). In absolute numbers, this percentage translates to a maximum attachment of $6.7 \pm 0.1 \times 10^4$ cells/cm² ($n = 3$) for the selected community and $1.4 \pm 0.3 \times 10^4$ cells/cm² ($n = 3$) for the original community (Table S6). In addition to the high maximum attachment, maximum attachment rates were on average $5.0 \pm 1.7 \times 10^4$ cells/cm²/h ($n = 15$) in selected communities and $2.4 \pm 1.2 \times 10^4$ cells/cm²/h ($n = 15$) in original communities. Regarding T3, maximum attachment rate for selected cells was almost 10-fold higher with $3.9 \pm 0.4 \times 10^4$ cells/cm²/h ($n = 3$) as opposed to $4.6 \pm 0.9 \times 10^3$ cells/cm²/h ($n = 3$). The comparison of the relative attachment between selected and original communities of all waters showed a 1- to 4-times higher maximum attachment and a 1- to 7-times higher maximum attachment rate for the selected communities. Interestingly, the attachment dynamics were similar with glass coupons as surface (Figure S1). Maximum attachment rates were almost identical between EPDM and glass coupons. Maximum attachment after 5 hours was, however, 6-fold higher on EPDM coupons (Table S7). In summary, a considerably large proportion of planktonic cells attached to the coupons (both EPDM and glass) within a short time. The selected communities attached faster and showed higher absolute values for attachment compared to the original drinking water communities.

Discussion

We analyzed biofilm growth on flexible EPDM coupons for five different drinking water communities (Figure 1). The purpose was to study the amount of growth due to biodegradable carbon migrating from the EPDM (Figure 2) and to assess selection within the developing biofilm communities due to this carbon. In the course of biofilm growth (Figure 3), all samples showed a significant loss in species diversity (Figure 4) with, however, the development of different community compositions (Figure 5). The selected communities were in turn more likely to form new biofilms on clean coupons (Figure 6).

Nutrient-based selection within microbial communities

Community composition in complex biofilms is governed by known ecological principles such as dispersal, selection, drift, and diversification²⁶. In the presence of sufficient nutrients, selection within microbial communities is (at least partially) driven by the metabolic potential and growth physiology of individual members. The supply of different/new substrates to an established community allows the growth of different bacterial species based on their metabolic capabilities, resulting in a change in the community composition. For example, Eilers and colleagues²⁷ (soil communities) and Reintjes and colleagues²⁸ (marine communities) demonstrated that the addition of particular carbon substrates resulted in bacterial growth, a loss in diversity, and considerable changes in community compositions. Reintjes and colleagues²⁸ also showed that initially abundant taxa were not abundant in the grown communities anymore. Finally, Wawrik and colleagues²⁹ showed that carbon sources that differ in their complexity select for different bacterial communities, with 70 % dissimilarities between communities grown on different substrates. This happened quickly, e.g., with a developing community growing on acetate being 70 % dissimilar within 18 h of incubation. The establishment of similar communities, relative to the complexity of supplied carbon substrate,

indicated that metabolic capabilities (biochemical pathways) are similar amongst growing cells²⁹. Our results mirrored many of these findings, in that richness decreased dramatically (Figure 4) and the dominating bacteria after growth on EPDM were completely different to the dominating bacteria in each original water (Figure 5). However, it is noted that even when microorganisms are capable of using the same substrates, growth physiology (i.e., growth rate and yield) allows some species to outcompete others. This so called *competitive exclusion principle*³⁰ was demonstrated by Friedman and colleagues³¹ and Christensen and colleagues³² who correlated the ability to outcompete others to a species' growth rate and yield. Our data (e.g., Figure 5) does not allow separation between selection caused by metabolic capabilities and growth physiology. However, this may be an explanation why some taxa dominated in the microcosms.

The arguments above explain selection during growth, but may lead to an erroneous conclusion that growth on the EPDM coupons should by default result in similar communities being selected. Here, our data clearly showed that all five original water samples resulted in completely different final communities following growth (Figure 5). This is explained by the fact that many different bacterial species can have the same carbon-degrading functions, i.e., identity does not equal functionality. In this regard, Burke and colleagues³³ showed that communities that are dissimilar in their taxonomical composition (e.g., 15 % similarity) can be very similar regarding their functional composition (with, e.g., 70 % similarity). Recent work by Goldford and colleagues²⁵ showed that growth on additional carbon sources increased the dissimilarity between developing communities on taxonomic level, however, revealed carbon source specific analogies on family level²⁵.

Understanding building plumbing microbiomes

One very practical relevance of biofilm growth and selection discussed above is the first colonization of drinking water plumbing systems during the commissioning of new buildings. Here, a wide variety of synthetic plumbing materials^{34,35} provides biodegradable organic carbon^{36,37} to complex drinking water microbial communities^{38,39}. The consequence is biofilm formation and development in the plumbing system, which ultimately affects the microbiological quality of the drinking water^{34,40}. Observations in recent years from several pilot-scale and full-scale studies reported considerable changes in drinking water microbial communities after passage through building plumbing systems. For example, Ling and colleagues¹¹ showed that the community composition of the drinking water changes during stagnation within building plumbing systems compared to the composition within the distribution network. Work from our own group specifically compared tap water, stagnated water, and biofilm communities in shower hoses and showed distinct changes in the microbiome due to the biofilms growing in the hoses¹². These findings are further supported by data from Ji and colleagues¹³ and Dai and colleagues⁴¹ showing that material, temperature, and stagnation time change the microbiology compared to the water community flowing into the rig installations, with, e.g., stagnation resulting in a diversity loss within the drinking water community⁴¹.

It is clear that building plumbing systems are per se complex environments, with multiple confounding factors (e.g., temperature, hydraulics, nutrients) affecting bacterial colonization, growth, and microbiome composition. Previous studies suggested that the choice of plumbing material plays a critical role, particularly when the material supplies nutrients for growth^{15,24,42}. For example, Rogers and colleagues⁴³ studied biofilm development on different materials with different extents of growth supporting properties (and their ability to resist invading *Legionella*). Proctor and colleagues¹⁵ studied different

shower hose materials and found differences in growth community composition. Along the same lines, we demonstrated in a previous study considerable selection in biofilm communities forming within shower hoses, with differences in the microbiome measurable on small-scale¹⁴. In the present study, we show an example for EPDM, which is commonly used for drinking water applications^{16,24,44,45} (Figures 3, 4, 5). We demonstrated selection, but also showed that selection differed based on the source water (Figure 5). While there is an obvious need and scope for larger observational studies on drinking water microbiomes⁴⁶, there is also a clear need for basic laboratory-scale ecological studies that can help to inform on interpretations from complex building plumbing data. Moreover, understanding the basic ecology of building plumbing systems will provide a basis for proactive management of the microbiomes in these systems.

Managing colonization of building plumbing materials

Better knowledge on growth-dependent selection within biofilm communities can be used to design building plumbing systems where the microbiology is controlled or even specifically tailored to the system. Microbial colonization and growth on building plumbing materials is currently not (properly) controlled. Upon commissioning of a building, all new plumbing material is exposed to complex drinking water communities during the first use. In fact, there is essentially no control over the identity and composition of bacteria that attach and proliferate in the new system, irrespective of the location, source water, disinfectant use, building type, or plumbing materials. To date, there are surprisingly few studies looking at this initial colonization of building plumbing materials, both full- and pilot-scale. A notable exception is the study by Salehi and colleagues³⁴, where they monitored changes in water chemistry and bacterial growth during the first days/weeks of building occupation. Also, a study by Douterelo and colleagues⁴⁷, showed that specific bacteria are dominant during the initial colonization (7 – 28 d) of distribution pipe materials.

The fact is, in current practice the owners/operators have effectively no control over the communities that colonize their building plumbing systems.

Smart use of material properties can control microbial growth (and thus biofilm communities). For example, the use of high-quality materials and the avoidance of low-quality ones (e.g., flexible hoses) reduces the potential of bacteria to actually grow. For this, standards for material quality requirements have already been implemented in Europe (e.g., ⁴⁸) and official tests on carbon migration and corresponding growth potentials have been established (e.g., ^{17,49}) (e.g., Figure 2). Using such tests to qualify the use of individual materials in new buildings should be a must for the industry. A more expensive but sensible approach is to use materials that do not leach any carbon (e.g., stainless steel plumbing). For example, Van der Koi and colleagues⁵⁰ showed that biofilm growth and the incorporation of *Legionella* spp. was less on stainless steel compared to polymeric PE-X pipes. It is, however, important to take into account that high quality polymeric materials can perform as good as metal piping with regard to microbial growth (see, e.g., ⁵¹). As another possibility, some studies suggested developing and using plumbing materials with anti-microbial properties for minimizing microbial growth and the proliferation of pathogens. For example, Saleh and colleagues⁵² showed that a coating containing copper and silver ions resulted in less bacterial attachment and biofilm growth when exposing a *Pseudomonas aeruginosa* isolate ($10^5 - 10^6$ CFU/mL) to coated glass slides for 2 h, shaking.

An alternative approach could be to embrace the microbiology of building plumbing systems instead of resisting it. Carbon migration from building plumbing materials can theoretically be used to select and maintain preferred communities. Wang and colleagues⁵³ provocatively suggested that systems may be redesigned in a pre/probiotic approach to favor certain communities of choice. One way to approach this addresses the concept of niche occupation, which is especially important during the colonization of new

surfaces, e.g., during the commissioning of a new building. Niche occupation can result in the exclusion of species due to a more efficient spatial expansion of a competitor or due to better growth physiologies⁵⁴. For the first, Schluter and colleagues⁵⁵ emphasized the importance of adhesion during initial attachment for the *evolutionary fate of microbes in biofilms*. For the second, Freilich and colleagues⁵⁶ defined the competition for identical nutrient sources as a *win-lose relationship*, which will ultimately allow organisms with better growth yields/rates to outcompete others. This pre/probiotic approach can be taken a step further by introducing, selecting, and maintaining specific antagonistic bacteria that challenge unwanted organisms. For example, several studies showed that a range of aquatic isolates, especially *Pseudomonas* spp., produce *bacteriocin-like substances* that have an antagonistic effect on the establishment of *Legionella* spp. in biofilms⁵⁷⁻⁵⁹, which can potentially be exploited as probiotic communities against *Legionella pneumophila*.

Here we propose a combination of the approaches above. We argue for the use of plumbing materials that provide specific substrates and for the targeted colonization of these materials of a benign microbial community. The approach foresees the use of a materials that migrate organic carbon in such a quality and quantity that it allows bacteria to grow and to sustain their existence in the developing biofilm. We furthermore propose colonizing these materials with bacteria from a safe source (e.g., bottled water), pre-selected on the substances migrating from the material (e.g., Figure 5). This adaption to the nutrients ultimately allows for a rapid colonization (e.g., Figure 6), growth and long-term persistence. A further expansion of the approach could be the use of purposefully designed synthetic communities that specifically include antagonists to specific building plumbing pathogens⁵⁷⁻⁵⁹. Combining both niche occupancy capabilities and powerful antagonistic functions within a pre-conditioned/pre-selected community is an unconventional but exciting

approach towards the future management of biofilm formation on polymeric materials in contact with drinking water.

Conclusions

- The use of a flexible polymeric plumbing material (here EPDM) increased the biodegradable organic carbon concentration of drinking water, which resulted in substantial growth for bacterial communities of different origin.
- The migrating carbon drove nutrient-based selection within the original drinking water communities, which resulted in (1) a dramatic decrease in taxa richness and diversity, (2) compositional changes in communities, and (3) an increase in similarity amongst growing biofilm communities, i.e., similarities in abundant taxa.
- Selected biofilm bacteria showed better attachment performances to new material surfaces, with more attachment and higher attachment rates.
- This work is a step towards pro-active managing of building plumbing biofilms through nutrient-based selection of specific communities of choice.

Acknowledgements

The authors thank Silvia Kobel and Aria Minder-Pfyl for support and protocols for library preparation and sequencing, Jean-Claude Walser for support with data processing, and Caitlin Proctor for preliminary discussions on the topic.

References

1. **Gaylarde**, C., Ribas Silva, M. & Warscheid, T. Microbial impact on building materials: an overview. *Mater. Struct.* 36, 342–352 (2003).
2. **Williams**, M. M., Armbruster, C. R. & Arduino, M. J. Plumbing of hospital premises is a reservoir for opportunistically pathogenic microorganisms: a review. *Biofouling* 29, 147–62 (2013).
3. **Ji**, P., Rhoads, W. J., Edwards, M. A. & Pruden, A. Impact of water heater temperature setting and water use frequency on the building plumbing microbiome. *ISME J.* 1–13 (2017). doi:10.1038/ismej.2017.14
4. **Henne**, K., Kahlisch, L., Ho, M. G. & Brettar, I. Seasonal dynamics of bacterial community structure and composition in cold and hot drinking water derived from surface water reservoirs. *Water Res.* 47, 5614–5630 (2013).
5. **Brazos**, B. J., O'Conner, J. T. & Abcouwer, S. Kinetics of Chlorine Depletion and Microbial Growth. (1985).
6. **Kim**, J. *et al.* Hydrodynamic effects on bacterial biofilm development in a microfluidic environment. *RSC Publ.* 13, 1846–1849 (2013).
7. **Fish**, K., Osborn, A. M. & Boxall, J. B. Biofilm structures (EPS and bacterial communities) in drinking water distribution systems are conditioned by hydraulics and influence discoloration. *Sci. Total Environ.* 593–594, 571–580 (2017).
8. **WHO**. *Standards for materials used in plumbing systems.* (2011).
9. Holsen, T. M., Park, J. K., Jenkins, D. & Selleck, R. E. Contamination of potable water by permeation of plastic pipe. *Am. Water Work. Assoc.* 83, 53–56 (1991).
10. **Zhang**, L. & Liu, S. Investigation of organic compounds migration from polymeric pipes into drinking water under long retention times. *Procedia Eng.* 70, 1753–1761 (2014).
11. **Ling**, F., Whitaker, R., LeChevallier, M. W. & Liu, W.-T. Drinking water microbiome assembly induced by water stagnation. *ISME J.* 12, 1520–1531 (2018).
12. **Proctor**, C. R., Reimann, M., Vriens, B. & Hammes, F. Biofilms in shower hoses. *Water Res.* 131, 274–286 (2018).
13. **Ji**, P., Parks, J., Edwards, M. A. & Pruden, A. Impact of Water Chemistry, Pipe Material and Stagnation on the Building Plumbing Microbiome. *PLoS One* 10, e0141087 (2015).
14. **Neu**, L., Proctor, C. R., Walser, J.-C. & Hammes, F. Small-scale heterogeneity in drinking water biofilms. *Front. Microbiol.* 10, 1–14 (2019).
15. **Proctor**, C. R. *et al.* Biofilms in shower hoses - choice of pipe material influences bacterial growth and communities. *Environ. Sci. Water Res. Technol.* 2, 670–682 (2016).
16. **Moritz**, M. M., Flemming, H. C. & Wingender, J. Integration of *Pseudomonas aeruginosa* and *Legionella pneumophila* in drinking water biofilms grown on domestic plumbing materials. *Int. J. Hyg. Environ. Health* 213, 190–197 (2010).
17. **Koetzsch**, S. & Egli, T. Kunststoffe in Kontakt mit Trinkwasser. *Aqua & Gas*

- 3, 44–52 (2016).
18. **Wen**, G., Koetzsch, S., Vital, M., Egli, T. & Ma, J. BioMig - A Method to Evaluate the Potential Release of Compounds from and the Formation of Biofilms on Polymeric Materials in Contact with Drinking Water. *Environ. Sci. Technol.* 49, 11659–11669 (2015).
 19. **Prest**, E. I., Hammes, F., Kötzsch, S., van Loosdrecht, M. C. M. & Vrouwenvelder, J. S. Monitoring microbiological changes in drinking water systems using a fast and reproducible flow cytometric method. *Water Res.* 47, 7131–7142 (2013).
 20. **Klindworth**, A. *et al.* Evaluation of general 16S ribosomal RNA gene PCR primers for classical and next-generation sequencing-based diversity studies. *Nucleic Acids Res.* 41, 1–11 (2013).
 21. **Edgar**, R. C. Accuracy of microbial community diversity estimated by closed- and open- reference OTUs. *PeerJ* 1–17 (2017). doi:10.7717/peerj.3889
 22. **Neu**, L. *et al.* Ugly ducklings - The dark side of plastic materials in contact with potable water. *npj Biofilms Microbiomes* 4, (2018).
 23. **Mao**, G., Wang, Y. & Hammes, F. Short-term organic carbon migration from polymeric materials in contact with chlorinated drinking water. *Sci. Total Environ.* 613–614, 1220–1227 (2018).
 24. **Park**, J. W. *et al.* Evaluation of organic migration and biomass formation on polymeric components in a point-of-use water dispenser. *Water Res.* 165, (2019).
 25. **Goldford**, J. E. *et al.* Emergent simplicity in microbial community assembly. *Science (80-.)*. 361, 469–474 (2018).
 26. **Kinnunen**, M. *et al.* A conceptual framework for invasion in microbial communities. *ISME J.* 10, 2773–2775 (2016).
 27. **Eilers**, K. G., Lauber, C. L., Knight, R. & Fierer, N. Shifts in bacterial community structure associated with inputs of low molecular weight carbon compounds to soil. *Soil Biol. Biochem.* 42, 896–903 (2010).
 28. **Reintjes**, G., Arnosti, C., Fuchs, B. & Amann, R. Selfish, sharing and scavenging bacteria in the Atlantic Ocean: a biogeographical study of bacterial substrate utilisation. *ISME J.* 13, 1119–1132 (2019).
 29. **Wawrik**, B., Kerkhof, L., Kukor, J. & Zylstra, G. Effect of different carbon sources on community composition of bacterial enrichments from soil. *Appl. Environ. Microbiol.* 71, 6776–6783 (2005).
 30. **Hardin**, G. The Competitive Exclusion Principle Published by : American Association for the Advancement of Science Linked references are available on JSTOR for this article : The Competitive Exclusion Principle. *Science (80-.)*. 131, 1292–1297 (1960).
 31. **Friedman**, J., Higgins, L. M. & Gore, J. Community structure follows simple assembly rules in microbial microcosms. *Nat. Ecol. Evol.* 1, 1–7 (2017).
 32. **Christensen**, B. B., Haagenen, J. A. J., Heydorn, A. & Molin, S. Metabolic commensalism and competition in a two-species microbial consortium. *Appl. Environ. Microbiol.* 68, 2495–2502 (2002).
 33. **Burke**, C., Steinberg, P., Rusch, D., Kjelleberg, S. & Thomas, T. Bacterial community assembly based on functional genes rather than species.

- Proc. Natl. Acad. Sci. U. S. A.* 108, 14288–14293 (2011).
34. **Salehi**, M. *et al.* Case study: Fixture water use and drinking water quality in a new residential green building. *Chemosphere* 195, 80–89 (2018).
 35. **Koetzsch**, S. & Egli, T. Kunststoffe in Kontakt mit Trinkwasser. *Aqua & Gas* 3, (2013).
 36. **Schoenen**, D. & Schöler, H. Microbial alterations of drinking water by building materials - field observations and laboratory studies. *Am. Water Work. Assoc.* 307–317 (1985).
 37. **Connell**, M. *et al.* PEX and PP water pipes: Assimilable carbon, chemicals, and odors. *J. Am. Water Works Assoc.* 108, E192–E204 (2016).
 38. **Ma**, X., Vikram, A., Casson, L. & Bibby, K. Centralized Drinking Water Treatment Operations Shape Bacterial and Fungal Community Structure. *Environ. Sci. Technol.* 51, 7648–7657 (2017).
 39. **Henne**, K., Kahlisch, L., Brettar, I. & Höfle, M. G. Analysis of structure and composition of bacterial core communities in mature drinking water biofilms and bulk water of a citywide network in Germany. *Appl. Environ. Microbiol.* 78, 3530–3538 (2012).
 40. **Inkinen**, J. *et al.* Drinking water quality and formation of biofilms in an office building during its first year of operation, a full scale study. *Water Res.* 48, 83–91 (2014).
 41. **Dai**, D., Rhoads, W. J., Edwards, M. A. & Pruden, A. Shotgun Metagenomics Reveals Taxonomic and Functional Shifts in Hot water microbiome due to temperature setting and stagnation. *Front. Microbiol.* 9, 1–17 (2018).
 42. **Rogers**, J., Dowsett, A. B., Dennis, P. J., Lee, J. V. & Keevil, C. W. Influence of plumbing materials on biofilm formation and growth of *Legionella pneumophila* in potable water systems. *Appl. Environ. Microbiol.* 60, 1842–1851 (1994).
 43. **Rogers**, J., Dowsett, A. B., Dennis, P. J., Lee, J. V. & Keevil, C. W. Influence of plumbing materials on biofilm formation and growth of *Legionella pneumophila* in potable water systems. *Appl. Environ. Microbiol.* 60, 1842–1851 (1994).
 44. **Kilb**, B., Lange, B., Schaule, G., Flemming, H. C. & Wingender, J. Contamination of drinking water by coliforms from biofilms grown on rubber-coated valves. *Int. J. Hyg. Environ. Health* 206, 563–573 (2003).
 45. **Meier**, T. & Bendinger, B. Survival of pathogens in drinking water plumbing systems: impact factors and sanitation options. *Water Sci. Technol. Water Supply* 16, 931–941 (2016).
 46. **Hull**, N. M. *et al.* Drinking Water Microbiome Project: Is it Time? *Trends Microbiol.* 27, 670–677 (2019).
 47. **Doutere**, I., Sharpe, R. & Boxall, J. Bacterial community dynamics during the early stages of biofilm formation in a chlorinated experimental drinking water distribution system: Implications for drinking water discoloration. *J. Appl. Microbiol.* 117, 286–301 (2014).
 48. **EN16421**, D. *Influence of Materials on Water for Human Consumption Enhancement of Microbial Growth (EMG)*. (2014). doi:SS-EN 16421:2014
 49. **Bundesamt**, U. *Leitlinie zur hygienischen Beurteilung von organischen*

- Materialien im Kontakt mit Trinkwasser.* (2016).
50. **Van Der Kooij**, D., Veenendaal, H. R. & Scheffer, W. J. H. Biofilm formation and multiplication of *Legionella* in a model warm water system with pipes of copper, stainless steel and cross-linked polyethylene. *Water Res.* 39, 2789–2798 (2005).
 51. **Lehtola**, M. J. *et al.* Microbiology, chemistry and biofilm development in a pilot drinking water distribution system with copper and plastic pipes. *Water Res.* 38, 3769–3779 (2004).
 52. **Saleh**, S., Sweileh, B., Taha, S. O., Mahmoud, R. & Taha, M. O. Preparation of polyester-based metal-cross linked polymeric composites as novel materials resistant to bacterial adhesion and biofilm formation. *Molecules* 16, 933–950 (2011).
 53. **Wang**, H., Edwards, M. A., Falkinham 3rd, J. O. & Pruden, A. Probiotic approach to pathogen control in premise plumbing systems? A review. *Env. Sci Technol* 47, 10117–10128 (2013).
 54. **Lloyd**, D. P. & Allen, R. J. Competition for space during bacterial colonization of a surface. *J. R. Soc. Interface* 12, (2015).
 55. **Schluter**, J., Nadell, C. D., Bassler, B. L. & Foster, K. R. Adhesion as a weapon in microbial competition. *ISME J.* 9, 139–149 (2015).
 56. **Freilich**, S. *et al.* Competitive and cooperative metabolic interactions in bacterial communities. *Nat. Commun.* 2, (2011).
 57. **Corre**, M. H., Delafont, V., Legrand, A., Berjeaud, J. M. & Verdon, J. Exploiting the richness of environmental waterborne bacterial species to find natural legionella pneumophila competitors. *Front. Microbiol.* 10, 1–11 (2019).
 58. **Héchar**, Y., Ferraz, S., Bruneteau, E., Steinert, M. & Berjeaud, J. M. Isolation and characterization of a *Staphylococcus warneri* strain producing an anti-*Legionella* peptide. *FEMS Microbiol. Lett.* 252, 19–23 (2005).
 59. **Guerrieri**, E. *et al.* Effect of bacterial interference on biofilm development by *Legionella pneumophila*. *Curr. Microbiol.* 57, 532–536 (2008).

Chapter 5 – Supplementary Information

Towards a probiotic approach for building plumbing – Nutrient-based selection during initial biofilm formation on flexible polymeric materials

Table S1 Chemical and biological composition of different drinking waters used in this study. Total phosphorous, total nitrogen, total organic carbon, and total bacterial numbers are displayed for (1) Bottled Evian (France, B1), (2) Bottled Aproz (Switzerland, B2), (3) tapped Groundwater Dübendorf (Switzerland, T1), (4) Tap water Dübendorf (Switzerland, T2), and (5) Tap water Oerlikon (Switzerland, T3).

	Total phosphorous (µg/mL)	Total nitrogen (mg/mL)	Total carbon organic (mg/mL)	Bacterial numbers (TCC/mL)
Evian (Bottled, F)	2.4	0.9	0.08	1.8 x 10 ⁵
Aproz (Bottled (CH))	5.3	<0.5	0.19	2.2 x 10 ⁵
Groundwater (Dübendorf, CH)	23.5	3.0	1.09	3.3 x 10 ⁵
Tap water (Dübendorf, CH)	7.8	1.8	0.44	1.4 x 10 ⁵
Tap water (Oerlikon, CH)	6.9	0.7	0.37	1.1 x 10 ⁵

Table S2 Information on volumes for amplifications and on settings of (A) amplification PCR and (B) Index PCR reactions.

(A) Amplicon PCR		
		<i>Volume (25 μL reaction)</i>
2xKAPA HiFi HotStart ReadyMix		12.5 μ L
Forward primer (10 μ M)		0.75 μ L
Reverse primer (10 μ M)		0.75 μ L
Template DNA (adjusted to 1 ng / reaction with DNase free water)		11.0 μ L
<i>Temperature</i>	<i>Duration</i>	<i>Cycles</i>
95 °C	5:00 min	
95 °C	0:20 min	29 x
51 °C	0:15 min	
72 °C	0:30 min	
4°C	hold	
(B) Index PCR		
		<i>Volume (50 μL reaction)</i>
2xKAPA HotStart ReadyMix		25.0 μ L
Nextera XT Index 1 primer		5.0 μ L
Nextera XT Index 2 primer		5.0 μ L
Template DNA		15.0 μ L
<i>Temperature</i>	<i>Duration</i>	<i>Cycles</i>
95 °C	3:00 min	
95 °C	0:30 min	8 x
51 °C	0:35 min	
72 °C	0:30 min	
4°C	hold	

Table S3 Report information of data processing.

(A) Quality control		
	FastQC	
(B) Trimming and merging of primers		
	usearch	v11.0.667_i86linux64
	Trim R1	20
	Trim R2	40
	Flash	v1.2.11
	Minimal overlap	15
	Maximal overlap	300
	Maximal mismatch density	0.25
(C) Primer site trimming		
	Usearch	v11.0.667_i86linux64
	Coverage	full-length
	Allowed number of mismatches	3
	Amplicon size range	100 - 600
(D) Filtering based on quality and size		
	Size range	200 - 500
	GC range	30 - 70
	Minimal Q mean	20
	Number of Ns	0
	Low complexity	dust / 30

Table S4 Relative abundances of ZOTUs (taxa) within biofilm communities that formed on EPDM coupons and with different original starting communities (B1, B2, T1, T2, T3).

	Biofilm 1		Biofilm 2		Biofilm 3	
	Rel %	ZOTU	Rel %	ZOTU	Rel %	ZOTU
B1	49.6	ZOTU10	42.2	ZOTU1024	51.6	ZOTU5147
	29.3	ZOTU46	36.8	ZOTU5147	14.2	ZOTU35
	16.6	ZOTU5147	6.4	ZOTU35	12.4	ZOTU10
	1.6	ZOTU61	4.2	ZOTU2255	10.8	ZOTU46
	0.8	ZOTU9849	3.5	ZOTU21	8.1	ZOTU2255
	0.4	ZOTU5674	2.2	ZOTU10	0.7	ZOTU61
	0.3	ZOTU1816	1.4	ZOTU115	0.7	ZOTU141
	0.3	ZOTU141	1.2	ZOTU444	0.6	ZOTU77
	0.3	ZOTU77	0.6	ZOTU11	0.3	ZOTU7
	0.2	ZOTU729	0.5	ZOTU141	0.2	ZOTU115
	0.2	ZOTU7	0.3	ZOTU46	0.1	ZOTU1816
	0.1	ZOTU23	0.2	ZOTU11189	0.1	ZOTU23
	0.08	ZOTU421	0.2	ZOTU7	0.06	ZOTU11380
	0.04	ZOTU148	0.07	ZOTU23	0.04	ZOTU142
	0.03	ZOTU42	0.07	ZOTU61	0.03	ZOTU148
	0.03	ZOTU22	0.04	ZOTU142	0.03	ZOTU5674
	0.03	ZOTU2436	0.04	ZOTU77	0.02	ZOTU13679
	0.02	ZOTU35	0.03	ZOTU4844	0.02	ZOTU4
	0.02	ZOTU3965	0.02	ZOTU1816	0.01	ZOTU42
	0.01	ZOTU13679	0.02	ZOTU2436	0.01	ZOTU113
0.01	ZOTU113	0.02	ZOTU5674	0.01	ZOTU2436	
0.01	ZOTU6380	0.02	ZOTU4	0.01	ZOTU6380	
0.01	ZOTU7519	0.02	ZOTU148	0.01	ZOTU5438	
0.01	ZOTU21	0.01	ZOTU6380	0.01	ZOTU3965	
		0.01	ZOTU42	0.01	ZOTU1024	
		0.01	ZOTU113	0.01	ZOTU21	
		0.01	ZOTU4269			
		0.01	ZOTU11380			
		0.01	ZOTU144			
		0.01	ZOTU778			
B2	84.6	ZOTU46	78.5	ZOTU46	49.3	ZOTU46
	5.5	ZOTU21	9.0	ZOTU5438	32.8	ZOTU5438
	4.3	ZOTU31	5.7	ZOTU21	10.2	ZOTU21
	2.6	ZOTU5438	3.2	ZOTU31	4.0	ZOTU5138
	1.3	ZOTU5138	1.8	ZOTU77	1.5	ZOTU77
	0.4	ZOTU7	1.3	ZOTU5138	1.0	ZOTU421
	0.3	ZOTU77	0.1	ZOTU421	0.6	ZOTU31
	0.3	ZOTU5674	0.1	ZOTU7	0.2	ZOTU7
	0.2	ZOTU87	0.05	ZOTU2052	0.2	ZOTU2052
	0.1	ZOTU23	0.05	ZOTU23	0.09	ZOTU23
	0.07	ZOTU2207	0.02	ZOTU5725	0.07	ZOTU5147
	0.03	ZOTU148	0.02	ZOTU5674	0.02	ZOTU42
	0.02	ZOTU421	0.02	ZOTU113	0.02	ZOTU2436
	0.02	ZOTU42	0.01	ZOTU4	0.02	ZOTU148
	0.02	ZOTU113	0.01	ZOTU1024	0.01	ZOTU6117
	0.02	ZOTU2436	0.01	ZOTU87	0.01	ZOTU3965
	0.02	ZOTU4311			0.01	ZOTU5
	0.02	ZOTU4498			0.01	ZOTU20
0.01	ZOTU4295			0.01	ZOTU113	
0.01	ZOTU6117			0.01	ZOTU28	

	Biofilm 1		Biofilm 2		Biofilm 3	
	Rel %	ZOTU	Rel %	ZOTU	Rel %	ZOTU
	0.01	ZOTU2052			0.01	ZOTU7365
	0.01	ZOTU9847			0.01	ZOTU10
	0.01	ZOTU35			0.01	ZOTU6049
	0.01	ZOTU4599			0.01	ZOTU4599
	0.01	ZOTU4				
	0.01	ZOTU11702				
	0.01	ZOTU7365				
	0.01	ZOTU2605				
	0.01	ZOTU165				
T1	56.7	ZOTU1024	76.9	ZOTU1024	76.8	ZOTU1024
	15.2	ZOTU34	5.0	ZOTU25	5.3	ZOTU13
	13.5	ZOTU9139	4.0	ZOTU94	4.3	ZOTU25
	3.9	ZOTU13	3.5	ZOTU185	3.2	ZOTU4295
	3.1	ZOTU4295	3.4	ZOTU4295	2.6	ZOTU94
	1.5	ZOTU2448	2.0	ZOTU13	1.8	ZOTU64
	1.4	ZOTU64	1.3	ZOTU5147	1.3	ZOTU185
	1.1	ZOTU23	1.0	ZOTU23	1.1	ZOTU32
	0.7	ZOTU25	0.5	ZOTU12603	0.9	ZOTU2448
	0.5	ZOTU32	0.5	ZOTU7874	0.9	ZOTU23
	0.5	ZOTU185	0.4	ZOTU5	0.8	ZOTU157
	0.4	ZOTU7	0.2	ZOTU2448	0.2	ZOTU7874
	0.2	ZOTU12603	0.2	ZOTU32	0.2	ZOTU7
	0.2	ZOTU157	0.2	ZOTU7	0.1	ZOTU12603
	0.2	ZOTU7874	0.1	ZOTU151	0.06	ZOTU160
	0.2	ZOTU151	0.1	ZOTU444	0.04	ZOTU151
	0.1	ZOTU2881	0.1	ZOTU5329	0.04	ZOTU13720
	0.1	ZOTU160	0.08	ZOTU10854	0.03	ZOTU2436
	0.09	ZOTU5147	0.07	ZOTU160	0.03	ZOTU5329
	0.08	ZOTU94	0.05	ZOTU13720	0.02	ZOTU148
	0.07	ZOTU5329	0.03	ZOTU578	0.02	ZOTU43
	0.07	ZOTU148	0.03	ZOTU2881	0.02	ZOTU5147
	0.04	ZOTU220	0.03	ZOTU141	0.02	ZOTU2881
	0.03	ZOTU42	0.02	ZOTU220	0.01	ZOTU220
	0.02	ZOTU578	0.02	ZOTU113	0.01	ZOTU5725
	0.02	ZOTU7300	0.01	ZOTU7300	0.01	ZOTU42
	0.02	ZOTU13720	0.01	ZOTU145	0.01	ZOTU10854
	0.02	ZOTU2436	0.01	ZOTU7347	0.01	ZOTU113
	0.01	ZOTU3179	0.01	ZOTU43	0.01	ZOTU13584
	0.01	ZOTU444	0.01	ZOTU64	0.01	ZOTU5
	0.01	ZOTU113	0.01	ZOTU6119	0.01	ZOTU4918
	0.01	ZOTU5892	0.01	ZOTU11348	0.01	ZOTU11348
	0.01	ZOTU10854	0.01	ZOTU10190	0.01	ZOTU5892
	0.01	ZOTU4498	0.01	ZOTU5892	0.01	ZOTU578
	0.01	ZOTU43	0.01	ZOTU307	0.01	ZOTU7745
	0.01	ZOTU3344	0.01	ZOTU5725	0.01	ZOTU9139
	0.01	ZOTU4546	0.01	ZOTU933	0.01	ZOTU125
	0.01	ZOTU144	0.01	ZOTU31		
	0.01	ZOTU3802	0.01	ZOTU2628		
	0.01	ZOTU82				
0.01	ZOTU3949					
0.01	ZOTU146					
0.01	ZOTU202					
0.01	ZOTU46					
0.01	ZOTU1682					

	Biofilm 1		Biofilm 2		Biofilm 3	
	Rel %	ZOTU	Rel %	ZOTU	Rel %	ZOTU
T2	0.01	ZOTU49				
	0.01	ZOTU3965				
	0.01	ZOTU638				
	0.01	ZOTU4599				
	37.8	ZOTU1024	58.0	ZOTU1024	51.0	ZOTU1024
	29.6	ZOTU32	21.0	ZOTU5147	23.0	ZOTU11
	7.7	ZOTU1581	11.2	ZOTU5	10.5	ZOTU5
	4.0	ZOTU11	3.2	ZOTU32	3.4	ZOTU4295
	4.0	ZOTU5	1.4	ZOTU4295	3.2	ZOTU6340
	3.9	ZOTU2448	1.2	ZOTU23	2.8	ZOTU32
	3.6	ZOTU145	1.0	ZOTU274	1.5	ZOTU103
	2.3	ZOTU23	0.6	ZOTU185	0.8	ZOTU2448
	2.1	ZOTU141	0.6	ZOTU7	0.7	ZOTU185
	2.0	ZOTU4295	0.4	ZOTU444	0.5	ZOTU23
	1.7	ZOTU185	0.2	ZOTU141	0.4	ZOTU2071
	0.3	ZOTU7	0.2	ZOTU148	0.4	ZOTU43
	0.2	ZOTU5147	0.2	ZOTU2448	0.2	ZOTU39
	0.2	ZOTU444	0.1	ZOTU42	0.2	ZOTU7874
	0.1	ZOTU39	0.1	ZOTU2436	0.2	ZOTU142
	0.09	ZOTU7874	0.09	ZOTU394	0.2	ZOTU7
	0.09	ZOTU421	0.09	ZOTU113	0.2	ZOTU290
	0.06	ZOTU94	0.06	ZOTU489	0.2	ZOTU4868
	0.04	ZOTU43	0.05	ZOTU11702	0.1	ZOTU2355
	0.04	ZOTU148	0.04	ZOTU13720	0.1	ZOTU145
	0.04	ZOTU13720	0.04	ZOTU5438	0.1	ZOTU94
	0.03	ZOTU113	0.04	ZOTU3965	0.08	ZOTU13720
	0.02	ZOTU2436	0.03	ZOTU46	0.07	ZOTU141
	0.02	ZOTU42	0.03	ZOTU7874	0.05	ZOTU5147
	0.01	ZOTU46	0.02	ZOTU401	0.04	ZOTU113
	0.01	ZOTU2628	0.01	ZOTU13630	0.04	ZOTU3965
	0.01	ZOTU6340	0.01	ZOTU4937	0.03	ZOTU148
	0.01	ZOTU10313	0.01	ZOTU10002	0.02	ZOTU444
	0.01	ZOTU142	0.01	ZOTU4	0.02	ZOTU42
	0.01	ZOTU2881	0.01	ZOTU5725	0.02	ZOTU2436
	0.01	ZOTU99			0.02	ZOTU31
	0.01	ZOTU1053			0.01	ZOTU274
	0.01	ZOTU125			0.01	ZOTU5725
					0.01	ZOTU10854
					0.01	ZOTU10313
					0.01	ZOTU74
				0.01	ZOTU223	
				0.01	ZOTU951	
				0.01	ZOTU13071	
				0.01	ZOTU165	
	90.3	ZOTU4	86.5	ZOTU4	34.5	ZOTU46
	2.1	ZOTU25	3.0	ZOTU5147	21.5	ZOTU1024
	2.0	ZOTU28	2.9	ZOTU25	14.9	ZOTU4
	1.6	ZOTU5147	2.0	ZOTU1581	6.0	ZOTU20
	1.1	ZOTU1581	1.5	ZOTU28	5.2	ZOTU5147
	0.6	ZOTU27	1.1	ZOTU27	5.2	ZOTU6049
	0.3	ZOTU7	0.5	ZOTU69	3.0	ZOTU3965
	0.3	ZOTU11702	0.3	ZOTU7	2.7	ZOTU27
	0.3	ZOTU69	0.3	ZOTU11702	2.4	ZOTU2448
	0.2	ZOTU214	0.3	ZOTU214	1.8	ZOTU11702

	Biofilm 1		Biofilm 2		Biofilm 3	
	Rel %	ZOTU	Rel %	ZOTU	Rel %	ZOTU
T3	0.1	ZOTU4295	0.2	ZOTU3965	0.5	ZOTU77
	0.1	ZOTU23	0.2	ZOTU20	0.4	ZOTU69
	0.1	ZOTU176	0.1	ZOTU187	0.4	ZOTU274
	0.1	ZOTU187	0.1	ZOTU176	0.3	ZOTU7
	0.1	ZOTU3965	0.1	ZOTU4295	0.2	ZOTU23
	0.09	ZOTU13679	0.1	ZOTU23	0.2	ZOTU185
	0.08	ZOTU20	0.1	ZOTU13679	0.1	ZOTU444
	0.05	ZOTU5	0.08	ZOTU2189	0.09	ZOTU5
	0.05	ZOTU148	0.08	ZOTU4844	0.09	ZOTU4295
	0.05	ZOTU6049	0.08	ZOTU6049	0.09	ZOTU141
	0.04	ZOTU1024	0.06	ZOTU11380	0.08	ZOTU11189
	0.04	ZOTU11380	0.06	ZOTU5	0.07	ZOTU12758
	0.04	ZOTU12603	0.06	ZOTU1024	0.04	ZOTU39
	0.03	ZOTU113	0.05	ZOTU274	0.04	ZOTU155
	0.03	ZOTU4844	0.04	ZOTU42	0.04	ZOTU113
	0.02	ZOTU2189	0.04	ZOTU141	0.03	ZOTU1816
	0.02	ZOTU49	0.03	ZOTU148	0.03	ZOTU148
	0.02	ZOTU2436	0.03	ZOTU12603	0.03	ZOTU28
	0.02	ZOTU274	0.03	ZOTU809	0.03	ZOTU5725
	0.01	ZOTU207	0.02	ZOTU46	0.03	ZOTU4945
	0.01	ZOTU42	0.02	ZOTU5138	0.02	ZOTU13679
	0.01	ZOTU141	0.02	ZOTU113	0.02	ZOTU421
	0.01	ZOTU155	0.02	ZOTU2436	0.02	ZOTU2436
	0.01	ZOTU3774	0.02	ZOTU155	0.02	ZOTU42
	0.01	ZOTU46	0.01	ZOTU43	0.02	ZOTU4844
	0.01	ZOTU43	0.01	ZOTU615	0.02	ZOTU51
	0.01	ZOTU11704	0.01	ZOTU5438	0.01	ZOTU43
	0.01	ZOTU809	0.01	ZOTU12758	0.01	ZOTU144
	0.01	ZOTU165	0.01	ZOTU3774	0.01	ZOTU165
	0.01	ZOTU5138	0.01	ZOTU110	0.01	ZOTU74
		0.01	ZOTU1682	0.01	ZOTU1581	
		0.01	ZOTU32	0.01	ZOTU11380	
		0.01	ZOTU49	0.01	ZOTU6560	
		0.01	ZOTU1804	0.01	ZOTU49	
		0.01	ZOTU4599	0.01	ZOTU151	

Table S5 Shared taxa between biofilm communities and their initial original drinking water communities. Biofilms were grown on EPDM coupons in triplicate microcosm set ups. Original drinking water communities were different (B1, B2, T1, T2, T3). Colored rows highlight taxa that were present in both biofilm and original water.

	Biofilm communities					Original drinking water communities					
	1 (Rel%)	2 (Rel%)	3 (Rel%)	Average (Rel%)	Deviation (Rel%)	1 (Rel%)	2 (Rel%)	3 (Rel%)	Average (Rel%)	Deviation (Rel%)	
B1	ZOTU5147	16.6	36.8	51.6	35.0	14.3	0.1	0.08	0.1	0.1	0.02
	ZOTU10	49.6	0	12.4	20.7	21.1	0	0	0	0	0
	ZOTU1024	0	42.2	0	14.1	19.9	0.2	0.01	0.16	0.1	0.08
	ZOTU46	29.3	0	10.8	13.4	12.1	3.1	3.6	4.1	3.6	0.4
	ZOTU35	0	6.4	14.2	6.9	5.8	0.01	0	0	0	0
	ZOTU2255	0	4.2	8.1	4.1	3.3	0.05	0.01	0.05	0.04	0.02
	ZOTU21	0	3.5	0	1.2	1.6	0	0	0	0	0
	ZOTU61	1.6	0	0	0.5	0.7	0.01	0	0	0	0
	ZOTU9849	0.8	0	0	0.3	0.4	30.9	31.7	26.7	29.8	2.2
B2	ZOTU46	84.6	78.5	49.3	70.8	15.4	8.1	8.8	7.8	8.2	0.4
	ZOTU5438	2.6	9.0	32.8	14.8	13.0	0.3	0.2	0.24	0.2	0.01
	ZOTU21	5.5	5.7	10.2	7.1	2.2	0	0.01	0	0.01	0.01
	ZOTU31	4.3	3.2	0	2.5	1.8	0	0	0	0	0
	ZOTU5138	1.3	0	4	1.8	1.7	8.0	8.5	7.6	8.0	0.4
	ZOTU77	0	1.8	1.5	1.1	0.8	0.05	0.08	0.09	0.07	0.02
T1	ZOTU1024	56.7	76.9	76.8	70.2	9.5	0.03	0.03	0.04	0.03	0.01
	ZOTU34	15.2	0	0	5.1	7.2	0	0	0	0	0
	ZOTU9139	13.5	0	0	4.5	6.4	0.06	0.04	0.01	0.04	0.02
	ZOTU4295	3.1	3.4	3.2	3.2	0.2	0.02	0.01	0	0.01	0.01
	ZOTU25	0	5.0	4.3	3.1	2.2	0.01	0.04	0.03	0.02	0.01
	ZOTU13	3.9	0	5.3	3.1	2.2	0	0	0.01	0	0
	ZOTU94	0	4.0	2.6	2.2	1.7	0	0	0	0	0
	ZOTU185	0	3.5	0	1.2	1.6	0	0	0.01	0	0
T2	ZOTU1024	37.8	58.0	51.0	48.9	8.4	0.1	0.02	0.01	0.05	0.05
	ZOTU32	29.6	3.2	0	10.9	13.3	0	0.01	0	0	0
	ZOTU11	4.0	0	23.0	9.0	10.0	0.01	0	0	0	0
	ZOTU5	4.0	11.2	10.5	8.6	3.2	0	0	0	0	0
	ZOTU5147	0	21.0	0	7.0	9.9	0.06	0.00	0.01	0.02	0.02
	ZOTU1581	7.7	0	0	2.6	3.6	0	0	0.01	0	0
	ZOTU4295	0	1.4	3.4	1.6	1.4	0	0.01	0	0	0
	ZOTU6340	0	0	3.2	1.1	1.5	0.02	0.01	0	0.01	0.01
T3	ZOTU4	90.3	86.5	14.9	63.9	34.7	0	0.01	0	0	0
	ZOTU46	0	0	34.5	11.5	16.2	0.02	0.01	0	0.01	0.01
	ZOTU1024	0	0	21.5	7.2	10.1	0.2	0.01	0.01	0.07	0.08
	ZOTU5147	1.6	3.0	5.2	3.3	1.5	0.03	0.00	0	0.01	0.01
	ZOTU20	0	0	6.0	2.0	2.8	0	0	0	0	0
	ZOTU25	2.1	2.9	0	1.7	1.2	0	0	0	0	0
	ZOTU28	2.0	1.5	0	1.2	0.8	0	0	0	0	0
	ZOTU1581	1.1	2.0	0	1.0	0.8	0	0	0.01	0	0

Table S6 Relative abundances of taxonomically assigned families within biofilm communities that formed on EPDM coupons and with different original starting communities (B1, B2, T1, T2, T3).

	Biofilm 1		Biofilm 2		Biofilm 3	
	Rel %	Family	Rel %	Family	Rel %	Family
B1	49.6	Xanthomonadaceae	80.9	Comamonadaceae	52.4	Comamonadaceae
	29.3	Burkholderiaceae	6.4	Rhizobiaceae	14.2	Rhizobiaceae
	18.2	Comamonadaceae	4.2	Moraxellaceae	12.4	Xanthomonadaceae
	1.6	Phyllobacteriaceae	3.5	Hyphomonadaceae	10.8	Burkholderiaceae
	0.6	NA	2.2	Xanthomonadaceae	8.1	Moraxellaceae
	0.2	Uncultured_bacterium	1.4	Nocardiodaceae	0.8	NA
	0.2	Methylobacteriaceae	0.6	Caulobacteraceae	0.7	Phyllobacteriaceae
	0.1	Bradyrhizobiaceae	0.3	Burkholderiaceae	0.3	Methylobacteriaceae
	0.04	Bacillaceae	0.2	Methylobacteriaceae	0.2	Nocardiodaceae
	0.03	Caulobacteraceae	0.1	Bradyrhizobiaceae	0.2	Bradyrhizobiaceae
	0.03	Brucellaceae	0.07	NA	0.04	Bacillaceae
	0.02	Rhizobiaceae	0.07	Phyllobacteriaceae	0.01	Brucellaceae
	0.02	Sphingomonadaceae	0.02	Brucellaceae	0.01	Sphingomonadaceae
	0.01	Hyphomonadaceae	0.02	Bacillaceae	0.01	Hyphomonadaceae
		0.01	Sphingomonadaceae			
B2	84.6	Burkholderiaceae	78.5	Burkholderiaceae	49.3	Burkholderiaceae
	5.6	Hyphomonadaceae	10.5	Comamonadaceae	38.0	Comamonadaceae
	4.3	Caulobacteraceae	5.7	Hyphomonadaceae	10.2	Hyphomonadaceae
	4.3	Comamonadaceae	3.2	Caulobacteraceae	1.6	NA
	0.4	Methylobacteriaceae	1.8	NA	0.6	Caulobacteraceae
	0.3	NA	0.1	Methylobacteriaceae	0.2	Methylobacteriaceae
	0.2	Cytophagaceae	0.05	Bradyrhizobiaceae	0.09	Bradyrhizobiaceae
	0.1	Bradyrhizobiaceae	0.02	Sphingomonadaceae	0.02	Bacillaceae
	0.05	Sphingomonadaceae	0.01	Cytophagaceae	0.02	Brucellaceae
	0.03	Bacillaceae			0.01	Xanthomonadaceae
	0.02	Brucellaceae			0.01	Sphingomonadaceae
	0.01	Rhodocyclaceae			0.01	Chitinophagaceae
	0.01	Oxalobacteraceae			0.01	Flavobacteriaceae
	0.01	Rhizobiaceae				
0.01	Microbacteriaceae					
T1	56.9	Comamonadaceae	78.4	Comamonadaceae	76.9	Comamonadaceae
	15.3	Xanthomonadaceae	5.0	Caulobacteraceae	5.3	Chitinophagaceae
	13.5	Leptospiraceae	4.0	Xanthomonadaceae	4.3	Caulobacteraceae
	3.9	Chitinophagaceae	3.5	Rhodocyclaceae	3.2	Rhodocyclaceae
	3.1	Rhodocyclaceae	3.5	Rhodobacteraceae	3.1	Rhodobacteraceae
	1.8	Rhodobacteraceae	2.5	Chitinophagaceae	2.6	Xanthomonadaceae
	1.5	Rhodospirillales_Incertae_Sedis	1.2	NA	1.3	NA
	1.1	Bradyrhizobiaceae	1.0	Bradyrhizobiaceae	1.1	Sphingomonadaceae
	0.9	NA	0.2	Rhodospirillales_Incertae_Sedis	1.0	Rhodospirillales_Incertae_Sedis
	0.7	Caulobacteraceae	0.2	Sphingomonadaceae	0.9	Bradyrhizobiaceae
	0.5	Sphingomonadaceae	0.2	Methylobacteriaceae	0.2	Methylobacteriaceae
	0.4	Methylobacteriaceae	0.1	Microbacteriaceae	0.04	Microbacteriaceae
0.2	Microbacteriaceae	0.1	Nitrosomonadaceae	0.03	Brucellaceae	
0.1	Xanthobacteraceae	0.04	uncultured_bacterium	0.03	Nitrosomonadaceae	

	Biofilm 1		Biofilm 2		Biofilm 3	
	Rel %	Family	Rel %	Family	Rel %	Family
T1	0.07	Bacillaceae	0.03	Thermaceae	0.03	Bacillaceae
	0.07	Nitrosomonadaceae	0.03	Xanthobacteraceae	0.02	uncultured_bacterium
	0.07	uncultured_bacterium	0.01	Propionibacteriaceae	0.02	Xanthobacteraceae
	0.02	Thermaceae			0.01	Burkholderiaceae
	0.02	Brucellaceae			0.01	Leptospiraceae
	0.01	Burkholderiaceae			0.01	Thermaceae
	0.01	Anaerolineaceae				
	0.01	Nanoarchaeota_archaeon_SCGC_AAA011-D5				
T2	48.3	Comamonadaceae	79.8	Comamonadaceae	54.6	Comamonadaceae
	29.6	Sphingomonadaceae	11.2	Chitinophagaceae	23.0	Caulobacteraceae
	4.0	Caulobacteraceae	3.2	Sphingomonadaceae	10.5	Chitinophagaceae
	4.0	Chitinophagaceae	1.4	Rhodocyclaceae	3.4	Rhodocyclaceae
	3.9	Rhodospirillales_Incertae_Sedis	1.2	Bradyrhizobiaceae	2.8	Sphingomonadaceae
	3.7	Xanthomonadaceae	1.0	Rhizobiales_Incertae_Sedis	1.8	NA
	2.3	Bradyrhizobiaceae	0.6	Rhodobacteraceae	1.1	Rhodospirillales_Incertae_Sedis
	2.0	Rhodocyclaceae	0.6	Methylobacteriaceae	0.7	Bradyrhizobiaceae
	1.7	Rhodobacteraceae	0.2	Bacillaceae	0.7	Rhodobacteraceae
	0.3	Methylobacteriaceae	0.2	Rhodospirillales_Incertae_Sedis	0.4	TK34
	0.1	NA	0.1	NA	0.2	Xanthomonadaceae
	0.05	Bacillaceae	0.1	I-10	0.2	Methylobacteriaceae
	0.02	Brucellaceae	0.1	Brucellaceae	0.2	MNG7
	0.01	Burkholderiaceae	0.06	Rhodospirillaceae	0.2	Legionellaceae
	0.01	Propionibacteriaceae	0.03	Burkholderiaceae	0.1	Parviterribacteraceae
	0.01	uncultured	0.02	Oxalobacteraceae	0.03	Bacillaceae
	0.01	Xanthobacteraceae	0.01	uncultured_bacterium	0.02	Brucellaceae
					0.01	Rhizobiales_Incertae_Sedis
				0.01	Microbacteriaceae	
				0.01	uncultured_bacterium	
T3	90.4	NA	86.8	NA	34.5	Burkholderiaceae
	3.2	Comamonadaceae	5.6	Comamonadaceae	29.0	Comamonadaceae
	2.1	Caulobacteraceae	3.0	Caulobacteraceae	18.4	NA
	2.0	Flavobacteriaceae	1.5	Flavobacteriaceae	6.0	Xanthomonadaceae
	0.6	Sphingomonadaceae	1.1	Sphingomonadaceae	5.2	Caulobacteraceae
	0.3	Methylobacteriaceae	0.5	ODP1230B8.23	2.7	Sphingomonadaceae
	0.3	ODP1230B8.23	0.3	Methylobacteriaceae	2.4	Rhodospirillales_Incertae_Sedis
	0.2	env.OPS_17	0.3	env.OPS_17	0.4	ODP1230B8.23
	0.2	I-10	0.3	I-10	0.4	Rhizobiales_Incertae_Sedis
	0.1	Rhodocyclaceae	0.2	Xanthomonadaceae	0.3	Methylobacteriaceae
	0.1	Bradyrhizobiaceae	0.1	Rhodocyclaceae	0.3	Rhodobacteraceae
	0.08	Xanthomonadaceae	0.1	Bradyrhizobiaceae	0.2	Bradyrhizobiaceae
	0.05	Chitinophagaceae	0.08	Phycisphaeraceae	0.09	Chitinophagaceae
	0.05	Bacillaceae	0.06	Chitinophagaceae	0.09	Rhodocyclaceae

	Biofilm 1		Biofilm 2		Biofilm 3	
	Rel %	Family	Rel %	Family	Rel%	Family
	0.03	Opitutaceae	0.05	Rhizobiales_Incertae_Sedis	0.04	Hyphomicrobiaceae
	0.02	Phycisphaeraceae	0.04	Bacillaceae	0.03	Bacillaceae
	0.02	Brucellaceae	0.04	Opitutaceae	0.03	Flavobacteriaceae
	0.02	Rhizobiales_Incertae_Sedis	0.02	Burkholderiaceae	0.02	Brucellaceae
	0.01	Burkholderiaceae	0.02	Brucellaceae	0.02	Microbacteriaceae
	0.01	Hyphomicrobiaceae	0.02	Hyphomicrobiaceae	0.01	uncultured_bacterium
	0.01	Microbacteriaceae	0.01	Rhodospirillales_Incertae_Sedis		
	0.01	Rhodospirillales_Incertae_Sedis	0.01	Rhodobacteraceae		
			0.01	Rhodospirillaceae		

Table S7 Attachment performances for selected biofilm and original drinking water communities. B1 (bottled water), B2 (bottled water), T1 (tapped groundwater), T2 (tap water), T3 (tap water). Experiments on EPDM were performed in experimental triplicates, glass controls were done in singletons.

Maximum attachment rate (TCC/cm ² /h)				
	EPDM		Glass	
	Original	Selected	Original	Selected
B1	3.3±0.6 x 10 ⁴ (n = 3)	5.4±0.1 x 10 ⁴ (n = 3)	2.8 x 10 ⁴	5.3 x 10 ⁴
B2	3.3±0.4 x 10 ⁴ (n = 3)	5.0±0.7 x 10 ⁴ (n = 3)	3.2 x 10 ⁴	4.3 x 10 ⁴
T1	3.1±0.3 x 10 ⁴ (n = 3)	7.8±0.5 x 10 ⁴ (n = 3)	3.0 x 10 ⁴	6.5 x 10 ⁴
T2	1.7±0.3 x 10 ⁴ (n = 3)	2.9±0.1 x 10 ⁴ (n = 3)	1.6 x 10 ⁴	2.3 x 10 ⁴
T3	4.6±0.8 x 10 ³ (n = 3)	3.9±0.4 x 10 ⁴ (n = 3)	3.4 x 10 ³	3.1 x 10 ⁴
Maximum attachment (TCC/cm ²)				
	EPDM		Glass	
	Original	Selected	Original	Selected
B1	6.3±0.1 x 10 ⁴ (n = 3) (80±1%)	8.1±0.2 x 10 ⁴ (n = 3) (97±0%)	1.4x 10 ⁴ (81%)	4.8 x 10 ³ (92%)
B2	7.1±0.2 x 10 ⁴ (n = 3) (76±4%)	6.5±0.1 x 10 ⁴ (n = 3) (83±2%)	3.0 x 10 ⁴ (66%)	1.1 x 10 ⁴ (87%)
T1	7.4±0.3 x 10 ⁴ (n = 3) (45±2%)	1.2±0.0 x 10 ⁵ (n = 3) (87±1%)	9.6 x 10 ⁴ (41%)	3.2 x 10 ⁴ (76%)
T2	4.0±0.1 x 10 ⁴ (n = 3) (75±3%)	5.0±0.0 x 10 ⁴ (n = 3) (92±1%)	1.8 x 10 ⁴ (67%)	7.7 x 10 ³ (86%)
T3	1.4±0.3 x 10 ⁴ (n = 3) (24±4%)	6.7±0.1 x 10 ⁴ (n = 3) (94±1%)	5.3 x 10 ⁴ (12%)	5.4 x 10 ³ (92%)

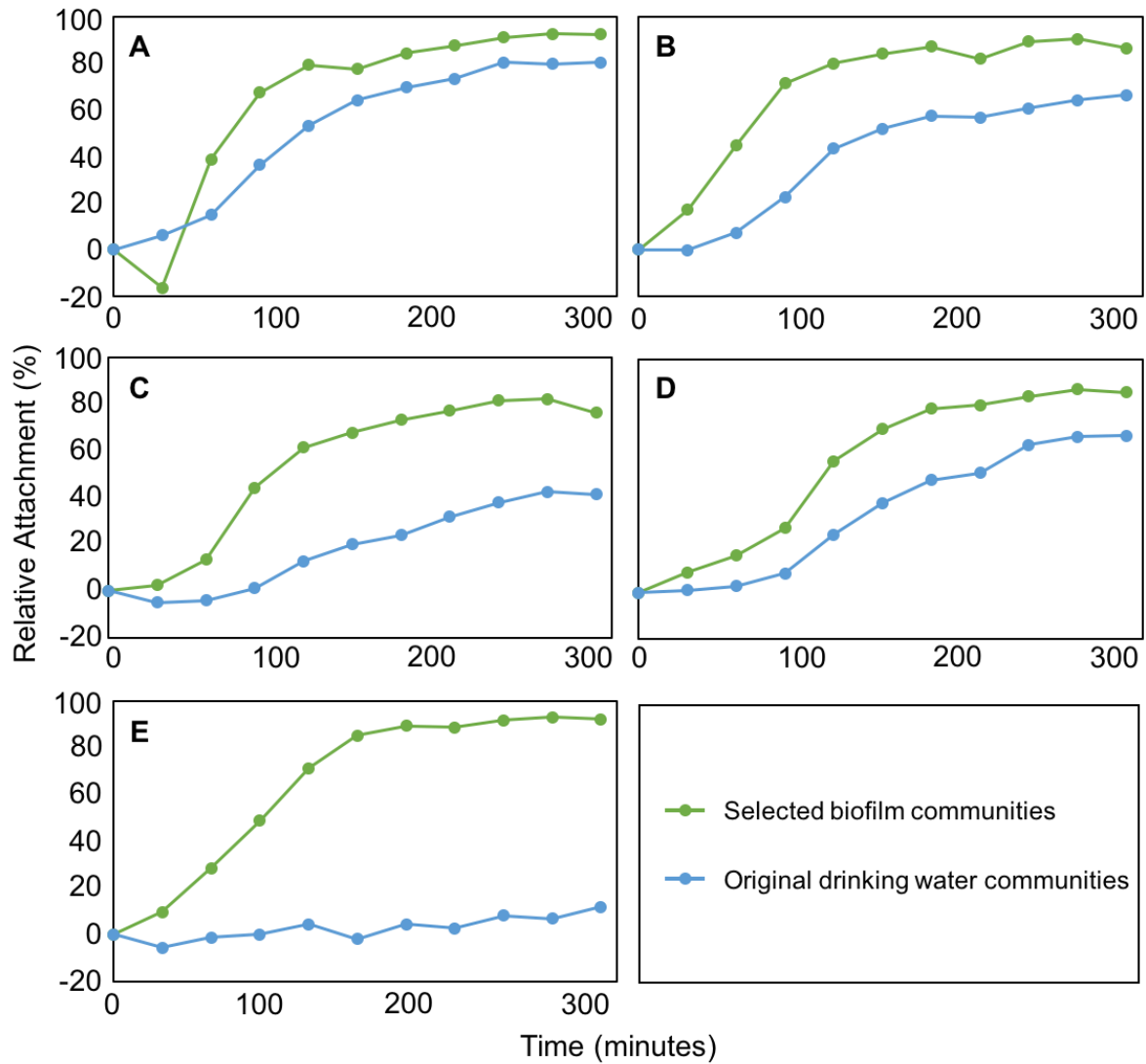


Figure S1 Attachment performances of selected biofilm and original drinking water communities (initial colonization) on glass coupons. (A) bottled water *B1*, (B) bottled water *B2*, (C) tapped groundwater *T1*, (D) tap water *T2*, and (E) tap water *T3*. Starting concentrations between selected and original communities were adapted to be similar within set ups.

Chapter 6

General conclusions and Future outlook

General conclusions

The goal of this thesis was to improve our abilities to predict and manage biofilm growth on flexible polymeric materials in contact with drinking water. For this, we characterized biofilms that developed under different environmental conditions, identified universal/concordant characteristics, and tried to explain these by using fundamental ecological principles.

The first approach was to characterize biofilms on flexible polymeric materials from different households to assess the degree of (dis-)similarity between biofilms that developed under different environmental conditions (chapter 3). We found considerable differences/heterogeneity regarding biofilm structure, bacterial numbers, and community compositions between individual samples. These differences were attributed to heterogeneous conditions, addressing mainly material properties, drinking water composition (biological and chemical), differences in additional nutrients, biofilm age, and usage habits. While this heterogeneity between biofilm samples was expected, we were less certain whether an individual biofilm, grown under supposedly identical conditions, would be homogeneous in its structure and composition.

A biofilm that grew on one material, exposed to one drinking water, for a fixed time, and operated under steady conditions showed homogeneous trends and fluctuations on large-scale (i.e., 1.20 m; chapter 4). However, high-resolution subsampling revealed heterogeneity on small-scale (μm – cm) in biofilm structure and thickness, bacterial numbers, and community composition. This spatial heterogeneity is relevant as it influences the representativeness of individual biofilm subsamples and potentially biases conclusions that we draw when extrapolating findings. Therefore, we determined biofilm sample size and the number of spatially distributed subsamples to be critical when considering biofilm sampling strategies.

Moreover, questions on the origin of this small-scale heterogeneity arose, especially regarding community composition.

At this juncture, a first attempt was done to try and explain observed biofilm characteristics by basic ecological principles. Consequently, the final study of this thesis addressed two (what we believe are) driving processes of initial biofilm development, namely: water-to-surface dispersal and nutrient-based selection (i.e., growth). More precisely, the question was whether the composition of a developing biofilm was rather determined by the composition of the initially colonizing drinking water community (water-to-surface dispersal) or by the migrating carbon (nutrient-based selection). The incubation of one flexible polymeric material with different drinking water communities under otherwise identical environmental conditions resulted in biofilm communities that followed similar trends in their formation yet were different in their compositions (chapter 5). In compliance, migrating carbon increased growth for all drinking water communities as opposed to an incubation without an additional carbon supply. Moreover, all biofilms had low species diversities and were dominated by an astonishingly small number of individual species. Differentiating was the development of distinct community compositions, following the dispersal of different drinking water communities. This different development in composition indicated that not one specific migrating carbon was selecting for one specific taxon. Consequently, this implies that migrating carbon compounds were versatile and/or that different bacterial species performed the same metabolic functions, i.e., that the environment potentially selected for functionality rather than identity. Independent of the underlying mechanism of selection, the dominance of only few species in the developing biofilms was remarkable. Based on this dominance, we propose to invest in the design of material-specific biofilm communities that might be introduced as first colonizers to stand up against the invasion of, e.g., opportunistic pathogens.

This thesis work (in particular chapter 5) poses a first step towards the development of a *probiotic approach* for the management of building plumbing biofilms. In contrast to other, mostly anti-microbial/anti-biofilm, approaches, we propose the introduction of pre-selected “good” bacterial communities that are able to either (1) occupy surface space and prevent first-colonizers to settle in the first place or to (2) select for bacteria or bacterial communities that compete with unwanted organisms and extinguish them by, e.g., the excretion of specific enzymes. For a successful implementation of such an approach, however, more studies are needed to design suitable communities and to test whether these can resist the invasion of other (normal) drinking water communities and/or specifically pathogens over time.

In conclusion, this thesis' work shows that biofilms on flexible polymeric materials (1) establish fast, (2) develop high bacterial concentrations, with (3) low species diversities, indicating (4) a high selective pressure during growth, which (5) considerably depends on the initially introduced drinking water community. All of this allows for (6) a connection between applied questions on, e.g., material design with fundamental ecological principles, ultimately allowing for (7) the development of management approaches for ensuring safe drinking water until the point of consumption.

Future outlook

This thesis builds on microbial observations for biofilms on flexible polymeric materials (i.e., high bacterial concentrations, low species diversity), explores these under more controlled conditions, and links them to ecological principles of initial biofilm formation. In the course of this work, multiple challenges and potential future research opportunities were identified. Promising future research includes (1) the identification of factors that are responsible for the observed small-scale heterogeneity in the community composition of one, individual biofilm and (2) to explore factors accountable for the substantial selectiveness during this early stage biofilm development. To address these, it is (1) essential to better understand carbon migration as major driver for the observed (selective) growth, (2) important to assess bacterial growth and biofilm development under fluctuating nutrient conditions, and (3) necessary to include microbial interactions as they will without any question impact the establishing biofilm community ultimately after initial colonization.

Carbon migration

In the course of this thesis, migrating carbon was solely quantified as total organic carbon (TOC) at a specific high temperature (60 °C) and, at its best, the bioavailable portion was determined in a growth potential assay (30 °C). What remains unclear is (1) the dependency of carbon migration on prevailing environmental conditions in a building plumbing system (e.g., temperature), (2) the identity of migrating carbon compounds, and (3) analysis on which of these are actually degraded and metabolized by drinking water bacteria.

Building plumbing materials are exposed to varying temperatures, which will ultimately impact carbon migration dynamics and subsequently microbial growth. Thus, it is important to include these variations in biofilm formation models and considerations on material design. Previous studies showed that

temperature influences carbon migration¹. Figure 1A shows that considerably more TOC migrates from a new flexible polymeric material when exposed to 60 °C as opposed to 30 °C. Interestingly, differences in migrating TOC concentrations diminish over time, i.e., with periodical water exchanges, and so does the proportion of bioavailable carbon that supports bacterial growth (AOC). This is important, as (1) materials in building plumbing systems experience fluctuations in water temperature (e.g., within a shower hose; Figure 1B) and (2) water is periodically replenished. Consequently, studies on migration dynamics following temperature fluctuations might be linked to fluctuations in bacterial growth or potentially explain a decrease in growth over time as carbon migration diminishes. Also, such information would be valuable for material designer and producers as it allows them to assess the long-term impact of their products on the drinking water microbiology.

In this thesis, the migrating carbon is only quantified as TOC. This TOC comprises numerous different carbon fractions, out of which some are more accessible for bacteria to consume than others. Identifying the migrating fractions in more detail could, e.g., be useful for controlled growth experiments based on specific migrating carbon compounds. Liquid chromatography (LC) is a common technique that is used to differentiate constituents of organic matter². The approach of organic carbon detection (OCD) is based on a molecule size-dependent separation and allows for the distinction between complex fractions such as biopolymers, intermediate products like building blocks, or simple molecules such as low molecular weight (LMW) acids³. Figure 1C shows LC-OCD chromatograms of (1) a drinking water (Evian, France) and (2) the same water after the incubation with a flexible polymeric material (EPDM, 17h, 60 °C). The result demonstrates an increase in organic carbon compounds, e.g., LMW-Neutrals, which can be simple sugars or amino acids and thus are easily available for bacterial to grow⁴. Consequently, techniques such as LC-OCD (or other spectrometric methods) seem to be useful for a better identification of migrating organic compounds.

Following the identification of additional, migrating carbon would also allow for the monitoring of their bacterial degradation. A hereby suggested experimental approach combines the above with bacterial growth (Figure 1D). Based on the differences in growth potentials from different original drinking water communities (chapter 4) it would be interesting to compare LC-OCD chromatographs of the original waters after their incubation with the flexible polymeric material. Differences in these fingerprints potentially indicate different dependencies/interactions between the material and the water's chemistry. Ultimately, these migration waters could be inoculated with bacterial pure cultures or complex drinking water communities to (1) analyze the bacterial growth potential but especially to (2) compare the chromatograms after growth to the original ones and ultimately identify metabolized fractions of the migrated carbon. Such an approach could also help understand whether the growth potential declines with periodical flushing events as easily accessible compounds (e.g., LMW-Neutrals) potentially migrate pre-dominantly in the beginning.

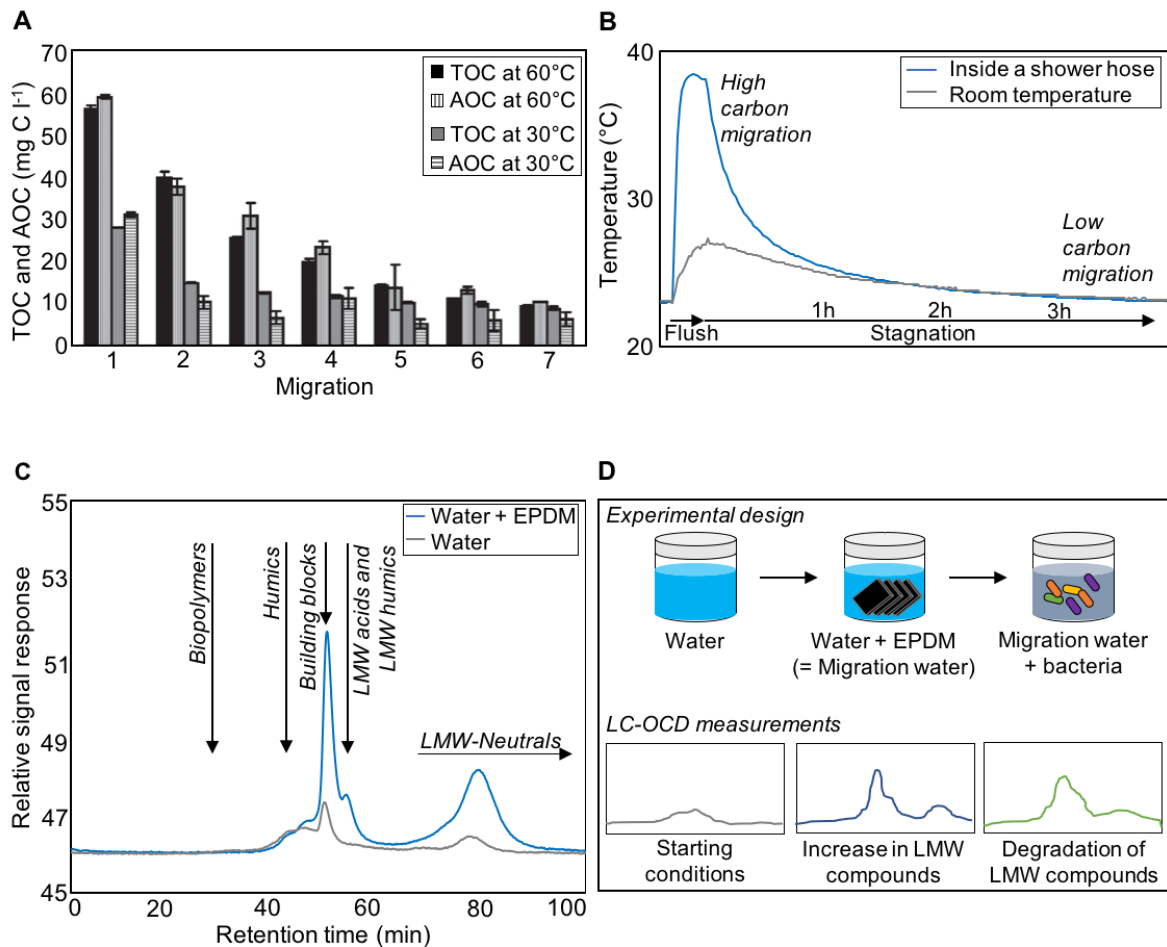


Figure 1 (A) Migration of total organic carbon from flexible PVC-P material at 60 °C or 30 °C for 7 consecutive migration periods of 24 h, with the corresponding proportion of assimilable organic carbon¹. (B) Exemplary environmental condition that fluctuates temporally: water temperature inside a shower hose following a shower event, with higher temperatures potentially resulting in higher carbon migration compared to low temperatures. (C) Liquid-chromatographic organic carbon detection (LC-OCD). Chromatograms of drinking water (0.2 µm filtered bottled Evian, France) and the same water incubated with flexible EPDM coupons (17 h, 60 °C). LMW = low molecular weight. Measurements and integration by Jacqueline Traber. (D) Experimental design and hypothetical outcome for studying bacterial degradation of migrating carbon compounds.

Growth dynamics under fluctuating nutrient conditions

It was discussed earlier that building plumbing systems are microbiological black boxes. One reason for this are fluctuations (e.g., flow, temperature). Particularly interesting for this thesis are fluctuations in nutrient concentrations during stagnation periods, e.g., inside a shower hose. Carbon will continuously migrate, but phosphorous will eventually be used up, limiting growth until the next flushing event (chapter 2). In this context, it is interesting to study bacterial behavior under nutrient fluctuations.

Under variable and fluctuating conditions, bacteria need to adapt periodically and potentially need to switch fast between metabolic pathways. For this, New and colleagues⁵ demonstrated the principle of catabolic repression. In such a case, only genes are expressed that are needed for metabolizing the preferred available carbon compound (e.g., glucose). Following a switch in carbon supply (e.g., to maltose), the unnecessary gene for glucose fermentation will be repressed and the catabolic gene responsible for maltose degradation will be activated. Figure 2A shows the adaption phases of different strains following this switch, highlighting that some strains will ultimately outcompete others⁵. Importantly, adapting slower than others does not necessarily need to be a disadvantage. For example, Acar and colleagues⁶ studied the impact of fluctuation rates on the success of fast- vs. slow-switching populations, revealing that slow-switching can in fact be beneficial if the environmental conditions fluctuate fast (Figure 2B). These findings are particularly relevant for follow up research on this thesis as this opens questions on (1) the minimal nutrient concentrations that cells need to grow (When does limitation start during stagnation?), (2) the duration of a potential adaption period after replenishing the nutrients, (3) whether all bacteria succeed in adapting their metabolism and growth to the fluctuations, and, finally, (4) whether these fluctuations might be a cause for the observed

low diversity and/or the observed small-scale heterogeneity within biofilm communities.

For the investigation of such fundamental research questions, we propose the application of a microfluidic device. Microfluidics is commonly used for studying microbial ecology on single-cell level⁷. In this case, it would allow us to create a beautiful link between fundamental single-cell approaches and applied research questions. The use of a microfluidic device allows us to mimic growth within a building plumbing system on single-cell level and under very controlled conditions (Figure 2C). The proposed device includes a main channel that supplies nutrient solutions via a continuous flow and numerous diverging small channels that hold single cells. Over time, these cells eventually grow and push themselves out of the small and into the main channel, ultimately being washed out. Performing real-time microscopy allows to image the growth process and to later track the growth of individual cells. For our purposes, the fed nutritious solution would be a migration water and continuously supplied. Fluctuations would we introduced for phosphorous, declining when simulating stagnation. A first step was already done, by evaluating growth of a pure culture strain (here *E. coli*) in migration water of flexible EPDM (Figure 2C).

Especially for biofilm communities, not only temporal fluctuations but also gradients are important. Dal Co and colleagues⁸ studied the growth dynamics of an *E. coli* population using a modified microfluidic device. The experimental set up did not provide fluctuations in nutrient concentrations per se, however, the microbial response to gradients in carbon supply (glucose) was studied (Figure 2D). They showed that growth rate declines rapidly, essentially not allowing for growth on the provided carbon substrate anywhere after 30 μm in depth. This is particularly interesting, considering that in our system carbon migrates from the bottom up and might therefore eventually not reach newly attaching cells at the top layer of the biofilm anymore, thus not contributing to

their growth. In addition to the reduction in growth, Dal Co indicated that cells in the back of the experimental chambers started to express genes that allow for the degradation of acetate (a glucose derivative) and with this, identified the initiation of a glucose-acetate cross-feeding interaction (Figure 2D).

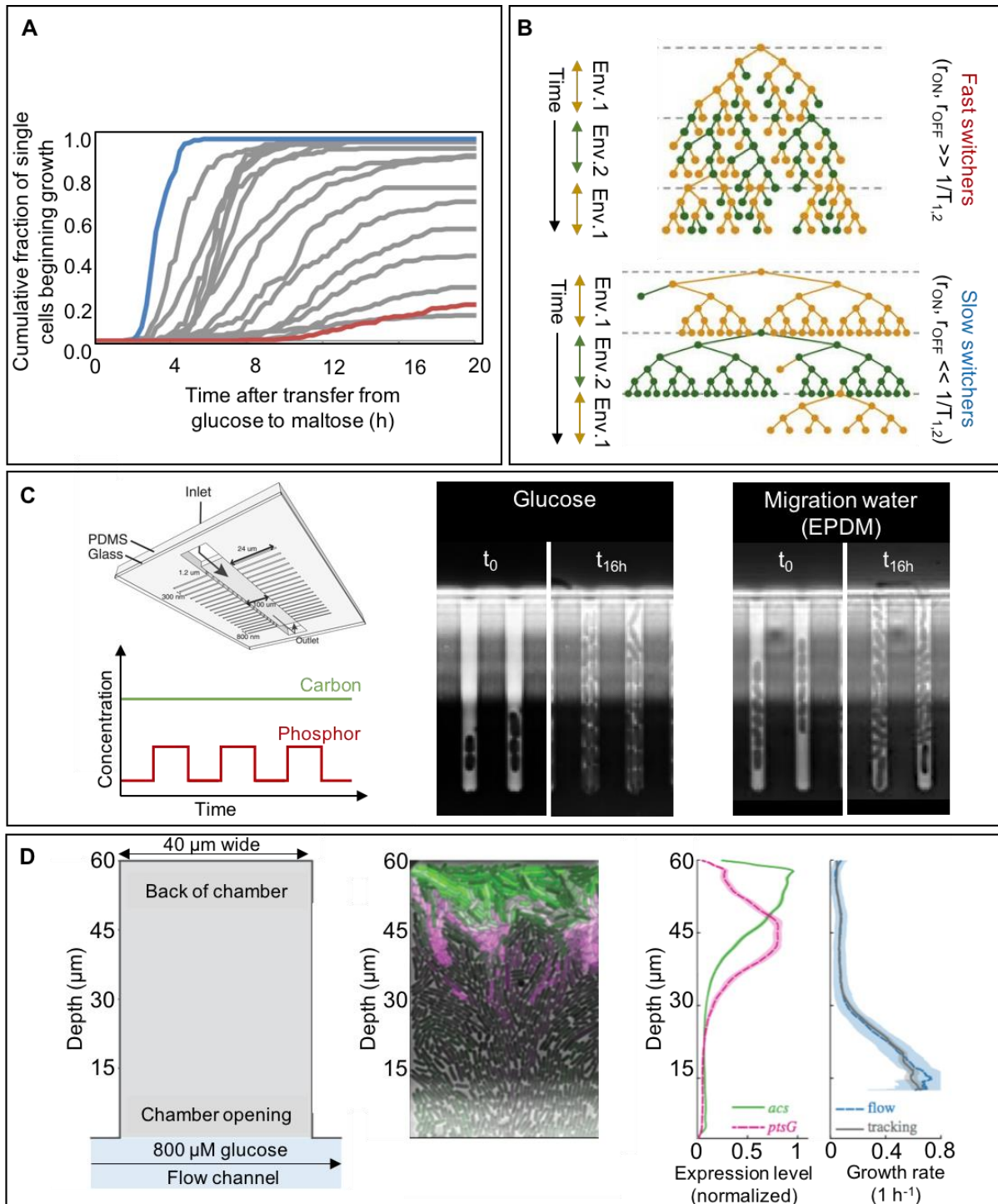


Figure 2 (A) Growth curves of different bacterial strains after a switch in carbon source indicating differences in lag phases before starting to grow again

(adapted from⁵). (B) Scheme of fast and slow switching cell lineages in an alternating environment (adapted from⁶). (C) Exemplary microfluidic chip (image from TU Delft-Leiden, Project, Microfluidics http://2014.igem.org/Team:TU_Delft-Leiden/Project/Microfluidics) made from PDMS, with an in- and an outlet for nutritious solutions. Plot on nutrient concentrations as an example for fluctuation regimes, here: constant carbon supply with fluctuating phosphorous to mimic a stagnation period. Microscopic images generated in the course of preliminary experiments, for testing growth abilities of *E. coli* on migrating carbon. These experiments were performed in cooperation with Kim Schlegel. (D) Impact of a nutrient gradient on growth of and interactions between individual *E. coli* cells (adapted from⁸).

Microbial interactions during initial colonization

Microbial interactions have not been addressed in this thesis, thus it remains unclear how individual bacteria interact in these biofilms, i.e., during initial colonization and biofilm growth. However, microbial interactions might be relevant for explaining the observed small-scale heterogeneity in community composition (chapter 4), as these interactions would allow different species to grow (based on cooperation or competition) and thus locally alternate the communities' composition.

Assuming the implementation of a new flexible polymeric material, a new environment is created and the first bacteria to be introduced will colonize the new surface (chapter 2). Connell and Slatyer⁹ defined three alternative scenarios that are possible for the establishment of a community: (1) Not all bacteria colonize the new surface, but those that do create an environment that is favorable for others to colonize at a later stage. (2) All bacteria colonize and they do not change the environment in any positive or negative way for others to colonize at a later stage. (3) All bacteria colonize and they make the environment unfavorable for others to follow. Biological principles that underlie such interactions are, e.g., competition for nutrients¹⁰, a mutualistic relationship¹¹, or commensalism¹² (see also Figure 3A). Consequently, some bacteria will either outcompete others, co-exist, or cooperate.

The interaction between bacteria was previously shown to depend on environmental conditions. This might be important for the early-stage development in biofilm growth on flexible polymeric materials as conditions change continuously, spatially and temporally (chapter 2). In the shower hose example from above, environmental conditions such as temperature but also carbon supply will fluctuate over time (i.e., with flushing events and stagnation periods). Differences in such conditions were shown to impact the type of microbial interaction between species. For example, Rodríguez-Verdugo and

colleagues¹³ studied the dependency of ecological interactions on fluctuations in carbon supply. Figure 3B shows how two individual species do either interact positively (commensalism) or negatively (competition) when supplied with different carbon sources. This result emphasizes the importance of (1) potential localized variations in carbon migration dynamics but also (2) how microbial interactions might change over time as migrating carbon compounds potentially change.

For the current example of a new shower hose, it would be interesting to understand how two bacterial species behave when colonizing right in each other's sphere of action. More precisely, will one species expand faster and outcompete the other, and will this reduce diversity within the establishing biofilm? Range expansion experiments are often used to study the impact of different species or phenotypes onto each other. Figure 3C shows exemplary microscopic images of simultaneous and successive range expansions¹⁴. In these, a co-culture either comprises two organisms that can degrade the provided nutrient independently from each other (simultaneous expansion) or comprises a producer and a consumer that depend on each other in their metabolism (successive expansion). Interestingly, the study revealed that simultaneous growth expansion locally resulted in a loss of diversity. This is particularly interesting for studies on initial colonization of flexible polymeric materials as severe reductions in species diversities have been recorded. A straightforward approach might be the creation of agar plates containing migrated carbon as major carbon source. Monitoring the range expansion of two (potentially previously isolated) strains would help understanding potential interactions of competing or cooperating species during early biofilm formation.

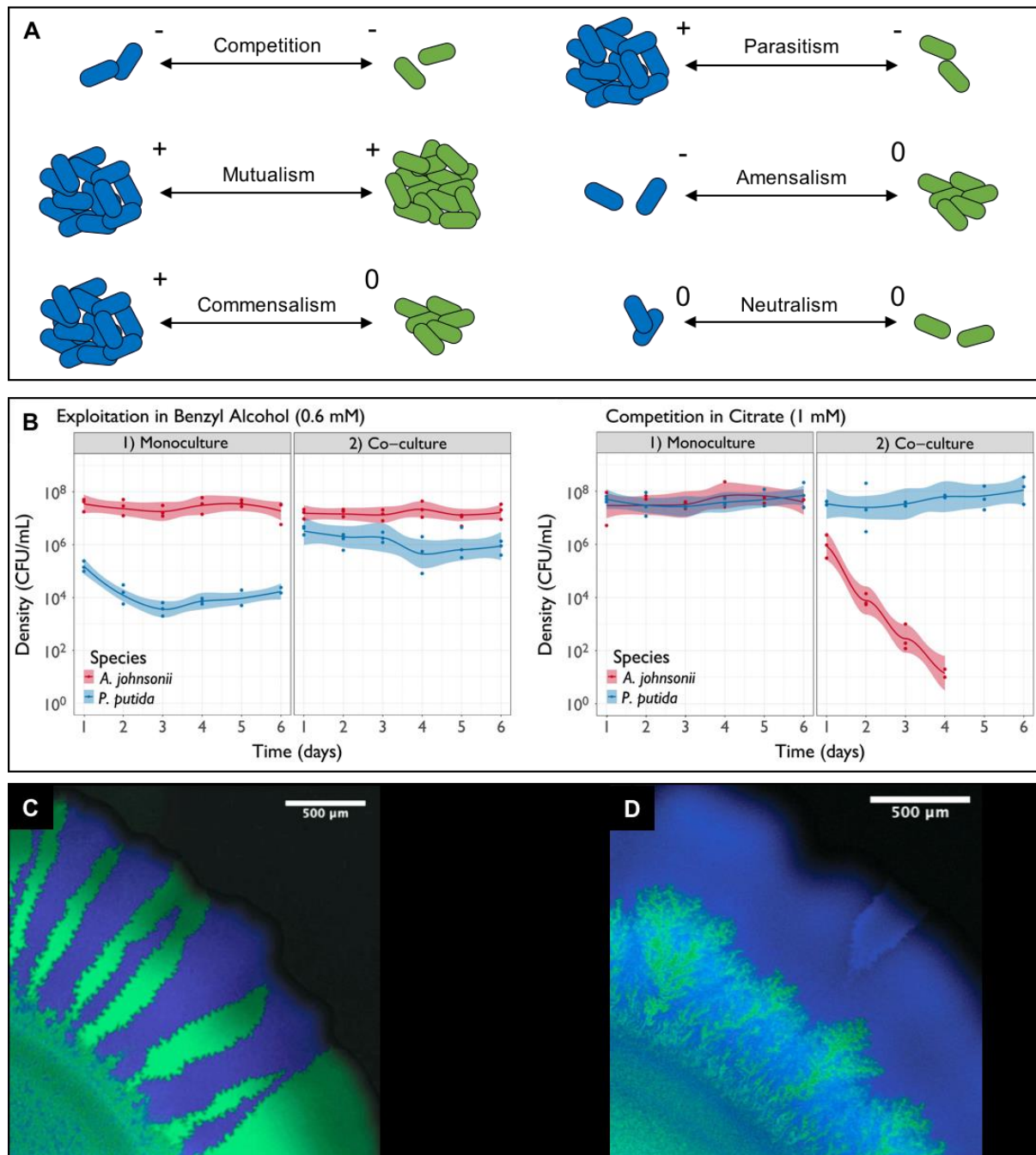


Figure 3 (A) Microbial interactions (adapted from¹⁵). (B) Differences in bacterial interactions depending on environmental conditions, here carbon supply¹³. (C, D) Microscopic images of colonies during a range expansion experiment¹⁴. (C) shows simultaneous growth and (D) successive growth expansion of two bacterial strains that either grow independent from each other (C) or comprising a producer and a consumer, depending on each other (D).

References

1. **Bucheli-Witschel**, M., Koetzsch, S., Darr, S., Widler, R. & Egli, T. A new method to assess the influence of migration from polymeric materials on the biostability of drinking water. *Water Res.* 46, 4246–4260 (2012).
2. **Villacorte**, L. O. *et al.* Characterisation of algal organic matter produced by bloom-forming marine and freshwater algae. *Water Res.* 73, 216–230 (2015).
3. **Huber**, S. A., Balz, A., Abert, M. & Pronk, W. Characterisation of aquatic humic and non-humic matter with size-exclusion chromatography - organic carbon detection - organic nitrogen detection (LC-OCD-OND). *Water Res.* 45, 879–885 (2011).
4. **Gunina**, A., Smith, A. R., Kuzyakov, Y. & Jones, D. L. Microbial uptake and utilization of low molecular weight organic substrates in soil depend on carbon oxidation state. *Biogeochemistry* 133, 89–100 (2017).
5. **New**, A. M. *et al.* Different Levels of Catabolite Repression Optimize Growth in Stable and Variable Environments. *PLoS Biol.* 12, 17–20 (2014).
6. **Acar**, M., Mettetal, J. T. & Van Oudenaarden, A. Stochastic switching as a survival strategy in fluctuating environments. *Nat. Genet.* 40, 471–475 (2008).
7. **Rusconi**, R., Garren, M. & Stocker, R. Microfluidics Expanding the Frontiers of Microbial Ecology. *Annu Rev Biophys* 43, 65–91 (2014).
8. **Dal Co**, A., Van Vliet, S. & Ackermann, M. Emergent microscale gradients give rise to metabolic cross-feeding and antibiotic tolerance in clonal bacterial populations. *Philos. Trans. R. Soc. B Biol. Sci.* 374, (2019).
9. **Connell**, J. H. & Slatyer, R. O. Mechanisms of Succession in Natural Communities and Their Role in Community Stability and Organization. *Am. Nat.* 111, 1119–1144 (1977).
10. **Coyte**, K. Z., Schluter, J. & Foster, K. R. The ecology of the microbiome: Networks, competition, and stability. *Science (80-.)*. 350, 663–666 (2015).
11. **Liu**, W. *et al.* Interspecific bacterial interactions are reflected in multispecies biofilm spatial organization. *Front. Microbiol.* 7, 1–8 (2016).
12. **Christensen**, B. B., Haagensen, J. A. J., Heydorn, A. & Molin, S. Metabolic commensalism and competition in a two-species microbial consortium. *Appl. Environ. Microbiol.* 68, 2495–2502 (2002).
13. **Rodríguez-Verdugo**, A., Vulin, C. & Ackermann, M. The rate of environmental fluctuations shapes ecological dynamics in a two-species microbial system. *Ecol. Lett.* 22, 838–846 (2019).
14. **Goldschmidt**, F., Regoes, R. R. & Johnson, D. R. Successive range expansion promotes diversity and accelerates evolution in spatially structured microbial populations. *ISME J.* 11, 2112–2123 (2017).
15. **Perez-Garcia**, O., Lear, G. & Singhal, N. Metabolic network modeling of microbial interactions in natural and engineered environmental systems. *Front. Microbiol.* 7, (2016).

Acknowledgements

Frederik, thank you so much for making this PhD such an exciting adventure. I can say, from the bottom of my heart, that you are an incredible supervisor, and I am super grateful for all your patience (must have been hard sometimes) and enthusiasm throughout these 4 years.

Martin, I am thankful for all our inspiring discussions and for your everlasting interest in my work and well-being. It was a pleasure having you as my *Doktorvater*.

Jürg, all the work in the lab and mental strength would not have been possible without you. Thank you so much for your technical support and just as much for all the coffee breaks, conversations, and unfunny comments from your side. Only one last thing to say: muhahaha.

Caitlin, you were my companion, tutor, and friend for almost my entire PhD and beyond that. Thanks to you I had a great start in the lab but also on dance floors and in concert halls all around Zurich – one could not ask for more.

Franziska R. and **Stefan**, both of you accompanied me throughout my PhD, even if from different locations. What can I say? It's been a blast. Thanks for all the great conversations, for introducing me to the *Sanitärbereich*, and for all the motivation and enthusiasm that you bring along.

DrinkMic-Group over the years, many people joined and left our group, and I would like to say a big THANK YOU to **Michael, Romina, Franziska B., Franziska G., Isabelle, Marja** for creating such a great working atmosphere and so many nice memories.

Special thanks go to **Carola**, you made it possible for me to step right into it when I started. Thanks for the funny times in the lab (scalping innocent bath toys) and your continuous interest in my work over all these years.

Laura, it was such a pleasure working with you, discussing, trying to do the math ... and chemical solutions. Your thesis was one of the best times during my PhD – thank you!

I'd like to thank all people from the department, **Umik**, for the inspiring working atmosphere. Particularly also **Bettina** and **Annette**, thanks for all your help over the years.

Not to be forgotten, **Iris** and **Caroline**, thanks for all the burrito-lunches and coffee breaks, and of course joyful activities outside of work.

Elyse and **Jordi**, I am grateful for the time you invested in proof-reading parts of this thesis. Your critical feedback improved these a lot. To me, both of you are inspiring as people and researchers and I am thankful for our time together, be it in meetings, espressi breaks, or on the weekends.

Davide, thanks for always driving me nuts 😊

Thanks to **Lea**, **Thomas**, **Teresa**, and **Kim** for all the support in the lab and nice conversations over the years.

Nico, thank you for all the discussions on biofilms and OCT, for reminding me to take care of myself, and for great Christmas party-dancing.

From the *dark side of campus*, Empa, I thank **Emma** and **Léo** for such great times.

Mom, **Dad**, **Scott**, thanks for all your love and support throughout the years. You always believe that I can achieve anything, so I believed it too.

Max, you are without question the one person who witnessed it all – ups, downs, distress, excitement, fatigue, enthusiasm, no mood, bad mood, good mood ... too many different moods, but you handled them all. You were and are my anchor and I am truly thankful for that.

Curriculum vitae

Lisa Neu

born 19 February 1989

in Neunkirchen (Saar), Germany

Education

03.2016 – 04.2020 **PhD student Drinking Water Microbiology**

ETH Zurich, Department of Environmental System Sciences
Eawag, Dübendorf, Department of Environmental
Microbiology

10.2012 – 10.2014 **M.Sc. Marine Biology**

University of Rostock, Germany

10.2009 – 09.2012 **B.Sc. Biology**

Julius-Maximilians-University of Würzburg, Germany

09.1999 – 06.2008 **Abitur**

Gymnasium Ottweiler, Germany

Research experiences

03.2016 – 04.2020 **PhD Student**

ETH Zurich and Eawag Dübendorf, Switzerland
(Prof. Dr. Martin Ackermann, Dr. Frederik Hammes)

10.2014 **Research Cruise Assistant (Marine Chemistry)**

Leibniz Institute for Baltic Sea Research Warnemünde,
Germany

Scientific cruise aboard Elisabeth Mann Borgese (EMB-087)

03.2014 – 09.2014 **Master Thesis for M.Sc. Marine Biology**

Identification of aquatic methyl-halide degrading bacteria

Leibniz Institute for Baltic Sea Research Warnemünde,
Germany

Department Biological Oceanography – Microbial Ecology
(Prof. Dr. Klaus Jürgens, Dr. Christian Stolle)

12.2013

Student Research Assistant (Molecular Biology)

Leibniz Institute for Baltic Sea Research Warnemünde,
Germany

Department Biological Oceanography – Microbial Ecology

05.2013 – 08.2013 **Student Research Assistant (Literature Research)**

Leibniz Institute for Baltic Sea Research Warnemünde,
Germany

Department Marine Chemistry

03.2012 – 09.2012 **Bachelor Thesis for B.Sc. Biology**

The dynamics of nematocysts in *Hydra oligactis* and their
fate in the turbellarian *Microstomum lineare*

Julius-Maximilians-University of Würzburg, Germany

Department for Cell and Developmental Biology

(Prof. Dr. Georg Krohne)

Supervision of students

10.2018 – 04.2019 **M.Sc. thesis Laura Cossu**

Probiotic drinking water biofilms – A first approach for
designing biofilm communities based on material-selection

Environmental Sciences, ETH Zurich

Scientific outreach

- 01.2019 **Swiss microbial ecology meeting** (Lausanne, Switzerland)
Oral presentation: Biofilms on flexible plastics – from measurement to management
- 11.2018 **Water Quality and Technology Conference** (Toronto, Canada)
Oral presentation: Heterogeneity in drinking water biofilms
- 05.2018 **Biofilms8** (Aarhus, Denmark)
Poster presentation: Small-scale heterogeneity in drinking water biofilms
- 09.2017 **How Dead is Dead V** (Vienna, Austria)
Poster presentation: Bacterial viability assessment – advantages and challenges of using different methods
- 05.2017 **Swiss society for biomaterials and regenerative medicine**
(St. Gallen, Switzerland)
Poster presentation: Stable water until the point of use – towards a probiotic approach for plastic materials
- 09.2016 **MEWE and Biofilms IWA Specialists Conference** (Copenhagen, Denmark)
Poster presentation: Ugly ducklings – the dark side of materials in contact with potable water

Public outreach

- 11.2018 **Zukunftstag Eawag** (*Dübendorf, Switzerland*)
Open doors for children (10 – 13 years) at Eawag

- 02.2017 **Rendez-vous Forschung: A scientist-public speed-dating event**
(Bern, Switzerland)
Ask and Tell event as part of the Biology17 Conference
Title: Bakterien in Badeentchen

Knowledge transfer outside academia

- 10.2019 **Sanitärtag – Kompetenz Trinkwasserinstallation** (Bern, Switzerland)
Organizer: Suissetec
Oral presentation: Trinkwassermikrobiologie – Biofilme in
Gebäudeinstallationen
- 06.2019 **SVG Hygienetagung** (Zurich, Switzerland)
Organizer: Schweizer Vereinigung für Gesundheitsschutz und
Umwelttechnik
Oral presentation: Biofilme und ihre Bedeutung für die
Trinkwasserqualität in Gebäuden
- 02.2019 **Schweizer Planertag (Warmwasserforum)** (Brugg, Switzerland)
Organizer: Euroforum Schweiz
Oral presentation: Biofilme und ihre Bedeutung für die
Trinkwasserqualität in Gebäuden
- 01.2019 **5. Schweizer Hygienetagung** (Lucerne, Switzerland)
Organizer: Schweizerischer Verein des Gas- und Wasserfaches
Oral presentation: Biofilme in Gebäudeinstallationen – Wo
kommen sie her, wo gehen sie hin?

